

NASA Contractor Report 181841

**AN EXPERIMENTAL INVESTIGATION OF THE
GROUND VORTEX CREATED BY A MOVING JET**

V.R.Stewart
Aerodynamic Consultant
Columbus, Ohio

July 1989

**(NASA-CR-181841) AN EXPERIMENTAL
INVESTIGATION OF THE GROUND VORTEX CREATED
BY A MOVING JET (Stewart (V. R.)) 124 p
CSSL 01A**

N89-268 15

**Unclas
G3/02 0224015**

Prepared for
NASA Langley Research Center
under L-29341C

NASA

National Aeronautics and
Space Administration

Langley Research Center
Hampton, Virginia 23665-5225

SUMMARY

The impingement of a vertical jet on the ground creates a ground vortex which can cause significant effects on a STOL airplane. The ground vortex can have large effects on the aerodynamics of the airplane and can result in significant inlet distortions in temperature and in flow quality. An experimental investigation of the ground vortex has been made in NASA's Langley Vortex Research Facility (VRF) with a moving jet over a stationary ground board. Data showing the ground pressures resulting from the ground vortex created by the jet moving over a fixed ground board at various speeds have been gathered. These ground board pressures have been analyzed and the results are compared to several existing studies with fixed jets over fixed ground boards and to previous tests of a jet moving over the ground.

The results of this comparison show that the penetration of the vortex created by the moving jet is diminished when compared to that created by a stationary jet. This reduction is shown to be approximately a 30% reduction in the centerline penetration into the opposing air stream and a reduction in the lateral penetration of approximately 50%. These significant reductions are believed to be the result of the elimination of the ground boundary layer inherent in the fixed jet and ground board of the majority of the existing data.

Just how much the reduction in the vortex size will affect the aerodynamic characteristics can not be determined from the current data base. The data give some indication that even

though the vortex penetration is seen to be reduced, the vortex appears to be stronger. This indicated may result in a somewhat delayed onset of the forces associated with the ground vortex but the force change due to the vortex may be more severe.

Additional data must be obtained with a moving model test to provide model forces in addition to the ground vortex position and strength.

TABLE OF CONTENTS

SECTION	PAGE
SUMMARY.....	i
TABLE OF CONTENTS.....	iii
LIST OF FIGURES.....	v
LIST OF TABLES.....	vii
SYMBOLS.....	viii
INTRODUCTION.....	1
REVIEW OF EXISTING DATA	4
Centerline Vortex Penetration	4
Lateral Penetration of the Ground Vortex	8
GROUND VORTEX OF MOVING JET	10
TEST PROCEDURES.....	10
Test Facility.....	10
Instrumentation.....	11
Model.....	11
Test Program.....	12
DATA ANALYSIS	13
Pressure Distribution.....	14
Forward Extent.....	17
Lateral Shape.....	18
COMPARISON WITH PREVIOUS DATA.....	19
NOZZLE SURVEYS	20
DATA BASE REQUIREMENTS.....	23
CONCLUSIONS.....	23
REFERENCES.....	24

TABLE OF CONTENTS (CONT.)

APPENDIX	TITLE	PAGE
A	BASIC DATA FOR THE 1.0 INCH JET NOZZLE	A1
B	BASIC DATA FOR THE 0.6 INCH NOZZLE CONFIGURATION	B1
C	NOZZLE SURVEY DATA	C1

LIST OF FIGURES

FIGURE	TITLE	PAGE
1	Formation of the Ground Vortex	27
2	Typical Vortex Ground Pressure Distribution.....	27
3	Variation of Jet Free Air Path with velocity Ratio	28
4	Correlation of the Ground Vortex from Existing Stationary Model Data	28
5	Comparison of Ground Vortex from Existing Stationary and Moving Model Data	29
6	Lateral Ground Vortex Shape, Ref. 6	29
7	Comparison of Lateral Vortex Shape, Existing Data Base, Refs. 1, 5, and 6	30
8	Correlation of Lateral Vortex Shape, Existing Data Base, Refs. 1, 5, and 6	30
9	Correlation of Lateral Vortex Shape, Additional Stationary Model Data	31
10	Facility, Model, and Ground Simulation	32
11	Ground Board Pressure Instrumentation, 1" Jet ..	33
12	One Inch Jet Nozzle	33
13	Jet Nozzle Installation	34
14	One Inch Jet Nozzle Geometry	34
15	Test Conditions for One Inch Nozzle	35
16	Ground Board Pressure Instrumentation, .6" Jet .	35
17	0.6 Inch Jet Nozzle	36
18	Time History of Ground Board Pressures	36
19	Ground Pressure Distribution, 1.0" Jet, Ve=0.042	37
20	Ground Pressure Distribution, 1.0" Jet, Ve=0.052	39
21	Ground Pressure Distribution, 1.0" Jet, Ve=0.090	41

LIST OF FIGURES (CONT.)

FIGURE	TITLE	PAGE
22	Ground Pressure Distribution, 0.6" Jet	42
23	Ground Pressure Field, Position C, Run 22, $V_e=0.042$	43
24	Ground Pressure Field, Position C, $V_e=0.90$	43
25	Ground Vortex Forward Penetration, NASA Moving Model	44
26	Ground Vortex Forward Penetration, Correlation of Stationary and Moving Model	44
27	Ground Vortex Lateral Extent, $V_e=0.042$	45
28	Ground Vortex Lateral Extent, $V_e=0.052$	45
29	Ground Vortex Lateral Extent, $V_e=0.090$	46
30	Lateral Shape of the Ground Vortex, Comparison of Stationary and Moving Models	46
31	Correlation of Lateral Vortex Shape for Stationary and Moving Jets, $k=1.03$,	47
32	Correlation of Lateral Vortex Shape for Stationary, $k=1.03$, and Moving Jets, $k=0.50$, ..	47
33	Lateral Penetration of the Ground Vortex at $x/d = 0.0$	48
34	Jet Cross Section Pressure Distribution, $d=1.0"$, $h/d=3.0$, $Q_j = 935$ psf	49
35	Jet Cross Section Pressure Distribution, $d=0.6"$, $h/d=3.0$, $Q_j = 1054$ psf	50
36	Comparison of Jet Cross Section Pressure Distribution $h/d=3.0$, $y/d=0.0$	51
37	Comparison of Jet Expansion	51
38	Comparison of Average Jet Pressure Coefficient Along Jet Centerline	52
39	Comparison of Jet Shapes at $y/d=0.0$	52
40	Effect of Jet Dynamic Pressure on Jet Pressure Ratio for the One Inch Jet	53

LIST OF FIGURES (CONT.)

FIGURE	TITLE	PAGE
41	Comparison of One Inch Jet Pressure Ratio at Various Jet Dynamic Pressures	53

LIST OF TABLES

TABLE	TITLE	PAGE
1	One Inch Jet Run Schedule and Test Program	13

SYMBOLS

C_p	Pressure Coefficient
d	Nozzle Diameter
F.S.	Fuselage Station
h	Height Above Ground
NPR	Nozzle Pressure Ratio
Q_j	Jet Dynamic Pressure
Q_o	Free Stream Dynamic Pressure
T	Temperature
V_e	Velocity Ratio - V_o/V_j
V_j	Jet Velocity
V_m	Model Velocity
V_o or V	Free Stream Velocity
$(W/l)_j$	Nozzle Aspect Ratio
x	Longitudinal Distance
x'	Vortex Penetration
y	Lateral Distances
z	Vertical Distances
ΔP	Local Pressure Coefficient
\ominus	Jet deflection

INTRODUCTION

The operation of STOL vehicles will be enhanced if the engine thrust is utilized to develop lift or stopping force. This vectoring of the engine thrust often results in the jet impinging on the ground during the terminal phases of the flight. This can generate flow fields under the airplane which, in turn, can result in large changes in the aerodynamic loads. In addition the resulting gas cloud can cause hot gas reingestion and possible FOD to the jet engine.

The primary flow characteristic effecting the aerodynamics is called the ground vortex. When a jet strikes the ground perpendicularly, a wall jet radiates symmetrically about the point of impact. That portion flowing into the oncoming free stream is retarded by the free stream and turned back onto itself as the ground vortex. The ground vortex penetration is controlled by the relative energies in the wall jet and the freestream air flow. The wall jet is a thin sheet of air along the ground and the retarding of this wall jet will be affected by any ground boundary layer present. The presence of a low energy ground boundary allows the wall jet to penetrate unrealistically far into the free stream. The testing procedures used will determine if a ground boundary layer is present under the free stream air flow. Testing in a wind tunnel with its moving air will create a ground boundary while in actual flight the airplane moves through still air without a ground boundary layer.

Figure 1 shows the formation of the ground vortex. The ground vortex created by an isolated jet is a horseshoe shaped

flow field about the jet. The vortex, at least in the region to the side of the jet, is not a true vortex in that the flow is simply redirected aft and then continues along and parallel to the free stream. In the region directly upstream of the jet the flow within the vortex is most likely split to the sides of the jet and flows aft around the high energy jet path. These characteristics will hold for the concentrated jets discussed in this study, but, in the case of the distributed jets such as jet flaps and large aspect ratio nozzles, the vortex flow may be trapped ahead of the jet and may roll into a very strong vortex. The vortex from the jet flap will be entrained by the nozzle jet and will appear as a more classic vortex. The present study is limited to the concentrated circular jet configurations exhausting at ninety degrees, perpendicular, to the ground board.

Figure 2 presents a definition of terms for the vortex and the ground board pressures along the jet centerline. In the profile view the jet will be bent aft somewhat by the free stream velocity and will impinge on the ground at a point downstream of the nozzle centerline. This jet bending will be of concern only because of the various methods of data taking in the moving model tests and will be discussed later as appropriate. The impinging jet creates a large positive ground board pressure region as seen in Figure 2. The positive pressure decreases as the distance from the nozzle centerline increases and returns to ambient downstream of the jet. The data from the moving model tests to be discussed later indicate that the downstream centerline pressures become negative along the jet centerline. The earlier

data did not show this characteristic. Upstream of the jet the ground board pressures become negative in the region of the vortex, and, as the forward velocity of the wall jet slows the ground pressures slowly return to ambient. In fact, the data show a slightly positive pressure ahead of the vortex. For vortex definition, the point at which the negative pressures under the vortex return to ambient is picked as the most forward travel of the ground vortex. This definition appears to agree well with that extent determined from the flow visualization used for some of the data.

The moving model data taken during this study does not provide correlation of model position to ground board pressures. The ground vortex positioning is therefore measured from the point of maximum positive pressure. This maximum positive pressure is slightly aft of the nozzle centerline as the nozzle passes over the pressure recorder. Figure 3 shows the bending of the jet due to the free stream air flow. The data from Reference 1 show that at a height of three nozzle diameters above the ground the bending of the jet is relatively insignificant. At a velocity ratio of 0.10 the bending is approximately 0.125 jet diameters along the centerline. The forward penetration for this condition is approximately 7.5 jet diameters, also from Reference 1. The effect of the bending of the jet at a height above the ground board of 3 diameters would result in an error of less than 2% of the indicated vortex penetration at the highest velocity ratio tested (0.17) and less at lower velocities. These possible errors are well within the data accuracy of the system and can be

dismissed.

The existing data base consists primarily of stationary jets over stationary ground boards. One early study by Abbott, Reference 2, provided an interesting insight into the possible effects of a moving jet. Also, a previous study of a moving jet over the ground in the NASA Vortex Research Facility is presented in this review. These data are reviewed in the following section.

REVIEW OF EXISTING DATA

There have been several previous experimental studies of the ground vortex due to deflected jets. The majority of these studies have used a fixed jet exiting over a stationary ground board in a cross flow. The ground in this case has a boundary layer built up due to the moving free stream. This boundary layer has less energy than the free stream and allows the ground vortex to penetrate farther up stream. The results of the previous studies are summarized in the following sections of this report.

Centerline Vortex Penetration: Schwanties, Reference 3, is an experimental investigation of the vortex centerline penetration into the oncoming free stream air. In this study, Schwanties was mainly concerned with the reingestion effects of the ground jet and the effect of the flow variables on the reingestion. One experiment is described which yields some important characteristics of the ground vortex and the effect of

some basic parameters on that ground vortex. The effect of temperature on the vortex was investigated and Schwanties states that no consistent effect of jet temperature can be seen. The separation point was measured by light pictures of the jet and free stream and are defined by Schwanties as being the most forward projection of the wall jet developed by the nozzle. This definition is different than that used by Weber and Gay and presented in Reference 4. Weber and Gay defined separation point as the point at which the wall jet began to leave the wall and the maximum forward travel was shown to be as much as 20% forward of the initial separation point.

Schwanties also presented ground vortex penetration for one temperature (400 degrees centigrade) at several jet velocities and at different forward speeds also variations of nozzle pressure ratio were presented. This is the only known data which has systematically varied jet pressure ratio. The pressure ratio does not appear to have a significant effect on the vortex penetration. These data indicate that the dynamic pressure ratio is a reliable correlating parameter. The data from Reference 3 are compared to the vortex penetration with other stationary model data in Figure 4.

Stewart and Kuhn, conducted a study of the ground vortex with a generic configuration, Reference 1. A jet model was tested in several fixed positions over a fixed ground board. The study included several nozzle shapes and configurations with single and multiple nozzle arrangements. The single circular nozzle projected 90 degrees to the ground is used in this

comparison.

In Reference 1, the jet was tested at a variety of heights ranging from 25 diameters to a minimum of one nozzle diameter for certain conditions. Velocity ratios of 0.1, 0.2, and 0.3 were tested and the vortex penetration was determined as the point at which the ground pressure distribution returned to zero as discussed in the previous sections. Ground board pressures were available for the jet centerline and three lateral positions.

Although it is beyond the scope of the present comparison this data source provided a look at the effect of the vortex on the aerodynamic characteristics through the force balance installed on the model shell. Some wing position effects are available on the wing-fuselage combination.

Weber and Gay, Reference 4, presented the results of a deflected jet in ground effect with an oncoming air stream. Vortex shape characteristics were determined by side view photographs. The initial separation as well as the maximum penetration could also be determined from the photographs. The photographs show a gas cloud which penetrates about 20% ahead of the separation point and rises to a height of approximately 50% of the forward travel. The maximum forward vortex penetration, 120% of the separation point, is compared to the stationary model penetration data base in Figure 4.

Cimbala, Reference 5, describes a series of tests done by Pennsylvania State University. Data consisted of ground board

pressures and flow visualization of the ground vortex with a smoke screen setup. Center line ground board pressures and several lateral rows of pressures were obtained as a function of height and velocity ratio. The centerline penetration of the ground vortex from the Reference 5 tests appear to agree fairly well with other data for stationary nozzle tests as seen in Figure 4. It appears that the centerline penetration may be slightly reduced over the majority of the data at the lower Velocity ratios. This may be due, in part, to a possible side wall interference.

Colin and Olivari, Reference 6, present the results of another ground vortex study. Again, the data were obtained the jet nozzle exiting 90 degrees to a fixed ground board at varying velocities and heights over the ground board. Ground board pressure instrumentation as well as flow visualization were used to determine the vortex position. The vortex penetration at the centerline and the lateral vortex shape were determined. Figure 4 presents the centerline penetration for several V_e conditions and are compared to the stationary model data base.

The available data showing the vortex penetration created by a moving jet indicates a reduced penetration into the freestream. Abbott, Reference 2, utilized photographs of the dust cloud created when the jet crossed over a chalk line on the ground to determine the penetration. Abbott's data are compared to the stationary model penetration results in Figure 5. The comparison shows that a reduction of approximately 30 percent of the penetration is experienced due to the elimination of the ground

boundary layer.

A second source of vortex data with a moving jet was briefly discussed in Reference 7. The tests were conducted by NASA, also in the Vortex Research Facility and were of a 0.6 inch jet moving over the ground. These data and model are similar to that of the present study and are discussed to a greater extent in a later section. The data from the 0.6 inch jet appear to favorably agree with Abbott's results.

Lateral Penetration of the Ground Vortex. To date, the only data describing the lateral shape of the ground vortex were given in References 1, 5, and 6. These data were all for stationary jets. The previous investigations of moving jets, References 2 and 7, did not provide an insight into the character of the lateral vortex characteristics. The earliest known lateral vortex data was presented by Colin and Olivari, Reference 6. Colin and Olivari utilized an oil visualization technique to determine the lateral shape shown in Figure 6 and discussed in the referenced study. Colin and Olivari also developed a theoretical prediction equation based on the relative energy of the forward and lateral wall jets and the oncoming free stream jet energy. That equation apparently would predict the lateral shaping of the ground vortex for the data base generated by Colin and Olivari. The correlating equation were;

$$x/d = k * (1/Ve)^{.9}$$
$$D * k * (1/Ve)^{.9} * \arctan y/x - y = 0$$

These equations appear to work well for the data of Reference 6, but, do not appear to adequately predict the penetration in the plane of symmetry for the data in References 1 and 5. This is likely to be the result of the various other causes such as wall effects possible in Reference 5 or to different ground boundary layers created by test facility configurations. Figure 7 presents the lateral vortex shape from each of the references at approximately the same velocity ratio. If a simple expression of the ratio of forward penetration to the penetration at $y=0$ is used a better lateral match of the several sets of data are shown as can be seen in Figure 8.

Several other test conditions are available from the data discussed in Reference 5 which were not included in the published analysis. The data included several heights and velocity ratios. It was suspected that the data may have been influenced by the tunnel side walls. The lateral vortex shapes of these data are presented in Figure 9. The results indicate considerable data scatter, but, as can be seen in Figure 9a, the penetration appears to fall off at extremes of the lateral extent parameters. Figure 9a uses a energy factor of $k=1.03$, the same as Colin and Olivari. Reducing this factor to $k=0.75$, Figure 9b, and to $k=0.68$ in Figure 9c show that a better correlation with base data is realized. Whether this is an energy change or a wall effect can not be determined from the existing data base. The composite data from all tests, Figure 8, indicate that the vortex for the fixed model could extend as much as 13 nozzle diameters to the side for a test condition of $Ve=0.10$ with no wall interference.

The tunnel wall for the Penn State tests was only 8 nozzle diameters from the jet center line. It is impossible from the data currently available to determine if the side walls would indeed suppress the centerline vortex penetration or if there is any affect of the walls on the vortex characteristics. No data have been found to determine if there is any effect but, it would be expected that the overall effect might be one of simulating a higher relative speed.

GROUND VORTEX OF MOVING JET

An experimental study of the effects of a moving jet on the ground vortex has been completed. This experimental study performed in the Vortex Research Facility at NASA Langley Research Center has shown that the vortex is affected by the reduction of the ground boundary layer characteristic in wind tunnel testing. The following sections discuss the experiment. The analysis of the results are compared to the vortex created by a stationary jet impacting on a fixed ground board.

TEST PROCEDURES

Test Facility. The ground effect testing of the moving jet was done in the Vortex Research Facility at the NASA Langley Research Center. The facility was modified for ground effect studies by installing a 150 foot long ground plane assembly approximately in the center of the test section (Figure 10). The ground board consisted of two parts, a ramp of 100 feet length at a slope of 4 degrees and a 50 foot horizontal section. The model to be tested is attached to a moving cart at a fixed vertical

position in the tunnel. As the cart carrying the model accelerates and moves through the test section the model approaches the ground board at a simulated sink rate (rate of descent) which is dependent upon the velocity as given by the equation:

$$\dot{h} = V_0 \tan 4^\circ.$$

After passing over the ramp, the model moves over the horizontal section to simulate constant altitude flight (see Figure 10. See Reference 8 for a discussion of the test facility and test variable definition.

Instrumentation: The data recorded during this test was ground board pressure distribution. The pressures were recorded by nine Endevco time sensitive pressure transducers located in three rows along the model path. Figure 11 shows the location of the pressure transducers. The rows of transducers were located at (A) 2.5 inches upstream of the junction of the ramp and the horizontal section, (B) 10 inches downstream of the junction, and (C) 25 feet downstream of that junction. Row A is on the simulated glide slope while rows B and C are on the flat portion of the ground board. Continuous strip time histories of the transducer output were recorded as the jet approached and passed over each row. In addition the model speed and the jet nozzle conditions were recorded. These data were used to compute the distances along the model path and the exit velocity of the jet.

Model. The model for this series of tests was a one inch

diameter nozzle suspended from the support sting of the moving cart. Figure 12 shows the model and figure 13 presents the model and sting installation. As can be seen the nozzle was mounted to the sting and directed toward the ground by a series of bends. Figure 14 presents the nozzle geometry. The nozzle is formed by inserting a constriction with a 15 degree contraction at the exit, The outside nozzle shape was contoured by a 45 degree slope to an approximately 0.01 inch thick edge at the exit of the one inch jet nozzle. The NASA nozzle was fabricated to duplicate the nozzle used in the Reference 1 tests, however, the NASA jet nozzle was one inch in diameter while the jet in the reference had a diameter of two inches.

Test Program. The tests for the ground vortex study was a series of model passes over the ground board. Table 1 presents the conditions of the tests. The data points are shown graphically in Figure 15. Model speed and nozzle pressure ratio were varied resulting in velocity ratios ($V_e = \sqrt{Q_o/Q_j}$) of 0.18, 0.09, 0.05, and 0.04. All data were recorded for a height over the horizontal section of three inches or a height to nozzle diameter ratio (h/d) of three. The height of position A (on the slope) was actually 3.17 nozzle diameters above the ground board while the positions B and C were 3.00 nozzle diameters above the ground board. Since previous data has indicated that below h/d of approximately 4 the vortex characteristics are relatively unchanged, the slight differences between the heights at position A and that at positions B and C can be ignored.

Similar data were obtained earlier with a test of a moving

jet over the same ground board. The earlier data was obtained with a 0.6 inch nozzle diameter and a different transducer placement. Figure 16 shows the location of the pressure transducers for the 0.6 inch jet tests. Only the transducers located at positions 9 and 10 produced usable data. Figure 17 shows the 0.6 inch nozzle and supply pipe. The nozzle was identical to the 1.0 inch nozzle geometry shown in figure 14. Data were obtained at a height of three nozzle diameters and at velocity ratios of 0.080 to 0.132.

TABLE 1. ONE INCH JET RUN SCHEDULE AND TEST PROGRAM

RUN	Q _m	Q _j	Q _j /Q _m	V _j /V _o	V _e V _m /V _j	V _m
12	2.808	1622.400	577.778	24.037	0.042	48.600
13	3.168	1645.500	519.413	22.791	0.044	51.650
14	2.837	1477.600	520.869	22.823	0.044	48.850
15	3.010	1061.100	352.572	18.777	0.053	50.350
21	4.277	2502.100	585.040	24.188	0.041	59.950
22	4.406	2521.400	572.213	23.921	0.042	60.900
25	7.392	229.600	31.063	5.573	0.179	78.850
26	7.356	236.500	32.153	5.670	0.176	78.650
27	7.439	230.100	30.931	5.562	0.180	79.100
28	7.734	220.000	28.447	5.334	0.187	80.600
29	7.849	878.400	111.906	10.579	0.095	81.250
31	9.567	316.400	33.073	5.751	0.174	89.700
32	9.727	323.800	33.288	5.770	0.173	90.450
40	11.818	339.500	28.727	5.360	0.187	99.700
42	11.818	1536.800	130.038	11.403	0.088	99.700
43	11.949	1490.700	124.754	11.169	0.090	100.250

DATA ANALYSIS

The ground vortex discussed previously in the introduction is formed when the jet strikes the ground and flows forward into the oncoming airstream. The vortex penetration is controlled by the velocity ratio and by the height above the ground. The parameter utilized in this study to define the vortex penetration

characteristics is the ground pressure distribution. The comparison of several references (1 to 7) show, with relatively good agreement, that the vortex boundaries can be determined by the negative ground board pressure area. The references use both ground pressure and flow visualization techniques to map the ground vortex. The vortex penetration is defined as the point at which the negative ground board pressure recovers to ambient.

Pressure Distribution. The ground board pressures were measured by the use of high response pressure transducers located on the ground board surface. The jet was passed over the transducer at the selected velocity. The transducer responded with the pressure change as the jet approached and then moved away from the transducer. The pressure response was initially a small positive pressure as the vortex front approached then a negative pressure as the vortex was over the transducer. The negative pressure was followed by the large positive impact pressure as the jet passed over the transducer that was followed by a negative pressure directly behind the jet. Figure 18 is a sample time history of the pressure variations. For purposes of analysis, the pressures have been converted to pressure coefficient, C_p , and the time has been reduced to nozzle diameter by converting the time parameter to distance utilizing the model speed. Zero distance is considered to be located at the point of maximum positive pressure. This resulted in a small position error as discussed above.

The pressure coefficient results for all data runs for the

one inch nozzle are presented in Appendix A and the data for 0.6 inch nozzle are presented in Appendix B. The position of the pressure instrumentation rows on the ground board does not appear to affect the vortex characteristics. The pressure variation on the ground board appears to be approximately the same at all positions. The knee, the longitudinal point at which the slope ramp and the horizontal section join, does not appear to affect the vortex. The height of the model above all three positions is nearly the same and any effect of the knee is not apparent at position B, ten nozzle diameters downstream of the knee.

Figure 19, 20 and 21 show the ground board pressure distribution of the one inch jet and for the test velocities of $Ve = 0.42$, 0.092 , and 0.17 respectively. The pressure traces along the center of the jet path show the positive pressure from the jet itself to have a larger impact area than expected. The jet appears to be approximately 6 nozzle diameters wide at the ground board for Ve of 0.09 . This spreading is somewhat similar to that experienced with fixed nozzle position testing by Stewart and Kuhn, Reference 1, Colin and Olivari, Reference 6, and others, but is rather greater than seen during a previous test with a 0.6 inch moving model tested by NASA (see Figure 22). The reason for this difference in the apparent spreading can not be isolated from the data. Jet exit profiles taken of both nozzles do not indicate a noticeable difference in jet spreading as will be discussed later in this report. The apparent different spreading may be a different transducer response characteristic caused by a different mounting technique. The

negative pressure indicated for the transducers located on the ramp with the 0.6 inch nozzle appear to be in error and are not included in this analysis.

The time histories of the individual pressure transducers allow the ground pressure distribution of the vortex-jet system to be determined for the various conditions. Figure 23 and 24 show the pressure fields for velocity ratios of 0.042 and 0.09 respectively. Three distinct pressure regions are shown by the results. A negative pressure region is seen in the vicinity of the vortex. This negative pressure region extends ahead of the nozzle and laterally several nozzle diameters. The forward edge of the negative pressure field is the forward extent of the vortex. The forward edge of the vortex is curved aft as the wall jet forward energy decreases as the lateral distance increases. At a V_e of 0.042 the negative pressure field of the ground vortex extends laterally to approximately 18 nozzle diameters while at V_e of 0.09 that distance is reduced to about 10 nozzle diameters.

The area under the jet experiences a positive pressure field due to the impact of the jet on the ground. The positive pressure region is shown to be larger than expected in these data. In fact, along the centerline and at a velocity ratio of 0.09 the vortex is masked by the apparent impact area. The impact area is larger than shown in Reference 3, but, is about the same as shown in Reference 1 and 7. No explanation for the differences between this data and that of Reference 3 can be isolated from the data. It is possible that the flush mounting of the pressure instrumentation for this test allowed the jet

turbulence to mask the vortex pressures and that the Reference 3 instrumentation could have been recessed slightly which would damped the turbulence effects.

Immediately behind the jet a negative pressure field is encountered. This area of negative pressure is the result of the high velocity wall jet and is amplified by the blocking effect of the jet post. The freestream air flow is accelerated around the jet post as it flows into the area behind the post thereby increasing the negative pressure in this area.

Forward Extent. Figure 25 shows the centerline vortex penetration of the one inch jet compared to the 0.6 inch jet and that of Abbott's rotating arm data. The forward penetration of the ground vortex of the one inch jet is the same as that from the earlier test of the 0.6 inch jet, Reference 7. The penetration of the ground vortex from each of the nozzles tested in the NASA moving model facility agree well with that shown by Abbott from the rotating arm rig, Reference 2. Abbott's data were obtained at considerably higher values of V_j/V_o than most of the data base and also higher than the moving jet data. The vortex penetration of the NASA moving model data show a ground vortex to be formed at velocity ratios of 0.042 to 0.092, but, no vortex can be found at the highest velocity ratio tested, $V_e=0.17$. As can also be seen in Figure 26, the vortex penetration of the moving model data show a reduction compared to the stationary model data base of approximately 30 percent.

An extrapolation of the moving model data from the lower

velocities to $Ve=0.17$ would indicate that a vortex at that speed would be expected. The penetration of the ground vortex at $Ve=0.17$ would be expected to be about two nozzle diameters. The ground board pressure for a sample jet pass over the ground at $Ve=0.17$ is shown in Figure 18. As can be seen, the jet width, positive pressure region, is too wide to ascertain the presence of a ground vortex in this case. The vortex may well exist in the region of the positive pressure indicated by the pressure instrumentation, but, in any case would penetrate only a small distance ahead of the jet impact region.

Lateral Shape: The lateral extent of the ground vortex from the moving jet tests can be seen in Figure 27, 28, and 29. The vortex is shown to extend several nozzle diameters to the side of the jet. The data show that the lateral extent of the vortex is approximately 1.5 as much as the forward penetration. The lateral penetration of the jet vortex is the characteristic which is thought to determine the abrupt change in the aerodynamics of the airplane in the presence of the ground. The vortex, if present under a non lifting surface would be expected to show a lift loss equivalent to the negative pressures on the ground which would be reflected back onto the surface. In a case in which the vortex is under a lifting surface, such as the wing, the negative pressures would be felt on the wing also. But, in this case the circulation lift is created by the angle of attack at the wing leading edge of the wing. This angle of attack can be greatly altered by the presence of the ground vortex. With the vortex located aft on the wing a positive angle of attack

will be induced on the wing. As the vortex extent approaches the wing leading edge the wing flow will be disrupted and if the vortex extends forward of the leading edge, the leading edge may be enveloped in a reduced velocity flow field and a significant reduction of the circulation lift may result.

COMPARISON WITH PREVIOUS DATA

The vortex formed by the moving jet differs from that of a stationary jet in both forward penetration and lateral extent and shape. The forward penetration is reduced by approximately 30 percent by the elimination of the ground boundary layer. An even more significant effect can be seen in the lateral penetration of the vortex. The data from the moving jet show the lateral shape of ground vortex to be altered from that occurring under the stationary jet. The shape of the vortex to the side of the jet appears to be swept aft at a greater angle. Figure 30 shows the lateral shape for several vortex conditions of the stationary and moving models. These lateral shapes are correlated in Figure 31 with the parameters discussed previously. The energy factor shown in Figure 31 is $k=1.03$ from Colin and Olivari. The stationary jet data base appears to be well represented by this computation while a much reduced lateral penetration of the moving jet vortex is seen. Figure 32 shows that if $k=0.5$ is used for the moving jet energy ratio a very good agreement can be shown for the comparison. The reduction in the energy factor is consistent with the expected result of the elimination of the ground boundary layer.

The effect of the reduced relative energy described above is reflected in a reduction of the expected lateral extent of the ground vortex. Figure 33 is a comparison of the lateral extent of the vortex formed by the moving jet compared to that formed by a stationary jet. The calculation utilizing the 30 percent reduction in centerline forward penetration and the indicated reduction of 50 percent in the relative energy factor, k , show approximately a 50 percent reduction in the lateral extent of the ground vortex formed by the moving model.

NOZZLE SURVEYS

The ground pressure distribution of the one inch jet is somewhat different from that of the 0.6 inch jet. The positive pressure region created by the impact of the jet on the ground by the one inch jet is approximately twice as large as that from the 0.6 inch jet. These data are recorded for a height of three nozzle diameters above the ground board for each nozzle. Data presented by Stewart and Kuhn, Reference 1, and by Colin and Olivari, Reference 6 appear to verify the larger impact areas. These referenced studies were with a stationary jet over a stationary ground board. The 0.6 inch jet positive pressure field is compressed compared to this other existing data base, but, does appear to be representative of the jet width at the ground height of the current tests.

The jets from the 1.0 and the 0.6 inch nozzles were surveyed at several distances from the jet exit. Surveys were taken by a total pressure survey probe at distances of 0.2, 1.0, 3.0, and

10.0 nozzle diameters from the nozzle exit. The complete data for these surveys are presented in Appendix C. The jet shapes at the ground height of $h/d=3.0$ are presented in figures 34 for the one inch jet and in Figure 35 for the 0.6 inch jet. Figures 34a and 35a present the left one half of the jet and Figures 34b and 35b present the right portion of the jet. The jets from the two nozzles have comparable expansion characteristics at the height shown. Figure 36 shows a comparison of the centerline survey at this height. The jet shapes are essentially the same with the smaller jet showing a slightly greater centerline pressure.

The jet characteristics are summarized in Figures 37, 38, and 39. The comparisons are made for dynamic pressure ratios of 935 psf for the one inch jet and 1054 for the 0.6 inch jet. Figure 37 compares the width of the jets. The data show no consistent differences in the jet width at any height. Figure 38 presents the relative jet pressures along the flow path. The average initial pressure ratio of the 0.6 inch jet is slightly greater due to a slightly skewed pressure distribution at the exit and therefore has a slightly higher velocity along the flow path. Figure 39 shows the jet shape in the longitudinal plane centerline. The spreading rates are consistent with the smaller jet deflected 2 to 3 degrees less than the one inch jet. This greater velocity and the slight under deflection of the jet tend to be compensating in the comparison of the ground vortex penetration.

The flow surveys indicate that the pressure distributions

are relatively unaffected by the jet dynamic pressure, at least at the test conditions. Figures 40 and 41 show the effect of the jet dynamic pressure on the results of for the one inch nozzle. The flows are the same for jet pressures of 265 and 935 psf, but at the lower flows, $q=85$ psf the indicated pressures are less than the calibration would suggest. These lower values are likely the result of the inaccuracies in the calibration at the lower flow rates. The tests were conducted at $q>265$ so the results are not affected by this characteristic.

The surveys of the exit and downstream pressures of the two nozzles show that the jet characteristics are nearly identical at all positions surveyed. The flow characteristics do not show an explanation for the different impact regions discussed earlier. The different impact area seen may be attributed to an instrumentation or to an instrumentation installation discrepancy. The installation of the transducers for the later test of the one inch nozzle covered a larger field with a concentration along three lateral rows. The transducers were installed flush with the ground board. The 0.6 inch test utilized a sparse coverage with instrumentation. The comparison of the one inch results with that of References 1 and 6 indicates that the one inch jet shapes are in better agreement. The comparisons of the vortex penetration of the two jets indicate that the impact area differences are the result of the data acquisition or recording parameters and do not affect the vortex penetration. Until investigated utilizing a common data recording installation, these differences in the impact area will

remain unexplained.

DATA BASE REQUIREMENTS

The development of the aerodynamic characteristics of STOL aircraft which utilize power to augment the lift or to brake the configuration will require additional in ground effect data. The available data have shown that a significant change in the aerodynamic characteristics can be caused by the ground vortex. The positioning of the vortex relative to the lifting surfaces is known to be a critical variable. The effect of the ground boundary layer has been shown by this data to be the critical in controlling both the forward and lateral penetration of the ground vortex. There is no available data to determine the aerodynamic increments on a moving model.

A data base generated using a moving model and containing proper ground pressure measurements to determine the vortex penetration is required. Several test procedures can be utilized to provide this data. The most straight forward would be a test procedure utilizing the setup in the Vortex Research Facility for the vortex penetration study and incorporating a generic model to provide the aerodynamic characteristic measurements. This procedure provides a reasonably adequate measurement of the vortex by the ground pressure surveys and the aerodynamic characteristics by the balance instrumentation. Significant configuration variables are wing position and sweep, longitudinal control surface location, and jet nozzle shape and deflection.

It is recommended that the Vortex Research Facility be used

to provide the extension of the ground effect data base.

CONCLUSIONS

The jet moving over the ground results in a reduced vortex from that created by a stationary jet. Most of the previously existing data base of jets impinging on the ground was dealt with as a stationary jet problem. The known possible source of error was the ground boundary layer created by the tunnel air moving over the ground. It had been expected that with the concentrated jets of consideration this would be a minimum problem. This study utilizing a moving jet over a fixed ground board shows that significant difference can be expected.

The forward penetration is shown to be reduced by as much as 30 percent and the lateral extent can be reduced by approximately 50 percent. The overall effect of these large reductions on configuration aerodynamics can not be predicted without specific planform testing.

It is concluded that additional moving model data with airplane configurations and aerodynamic force instrumentation are required provide data to determine the aerodynamic responses of the configurations.

REFERENCES

1. Stewart, V. R. and Kuhn, R. E.: "A Method for Estimating the Propulsion-Induced Aerodynamic Characteristics of STOL Aircraft in Ground Effect", NADC 80226-60 Aug. 1983

2. Abbott, W. A.: "Studies of Flow Fields Created by Vertical and Inclined Jets Moving over a Horizontal Surface", ACR Cp No. 911, 1967.
3. Schwanties, E.: "The Recirculation Flow Field of a VTOL Lifting Engine", NASA TT F-14912 June 1973.
4. Weber, H. A. and Gay, A.: "VTOL Reingestiom Model Testing of Fountain Control and Wind Effects", AIAA Paper 75-1217, AIAA/SAE Eleventh Propulsion Conference, Sept. 29 to Oct. 1. 1975.
5. Cimbala, J. M., Stinebring, D. R., Treaster, A. L., and Billet, M. L.: "Experimental Investigation of a Jet Impinging on a Ground Plane in the Presence of a Cross Flow", NADC Report 87019-60, March 1987.
6. Colin, P. E. and Olivari, D.: "The Impingement of Circular Jet Normal to a Flat Surface with and without Cross Flow", von Karman Institute for Fluid Dynamics, Rhode-St., Genese, Belgium, Report AD688953, Jan. 1969.
7. Stewart, V. R.: "The Characteristics of the Ground Vortex and its Effect on the Aerodynamics of the STOL Configuration", NASA CP 10008, 1987 Ground Vortex Workshop, pp. 1-38, April 1987.
8. Kemmerly, G. T. and Paulson, J. W. Jr.: "Exploratory Evaluation of a Moving Model Technique For Measurement of Dynamic Ground Effects", AIAA Paper 87-1924, June, 1987.

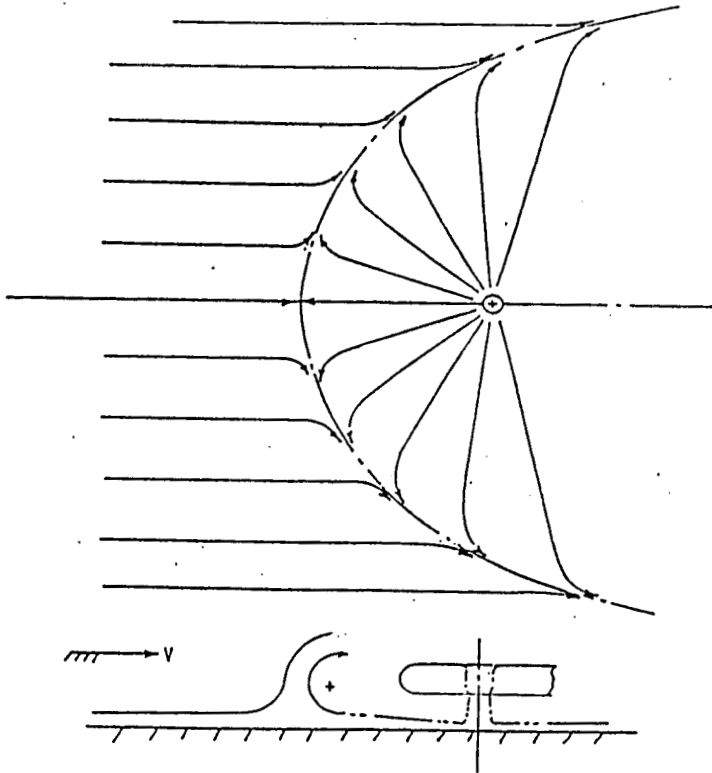


Figure 1. Formation of the Ground Vortex

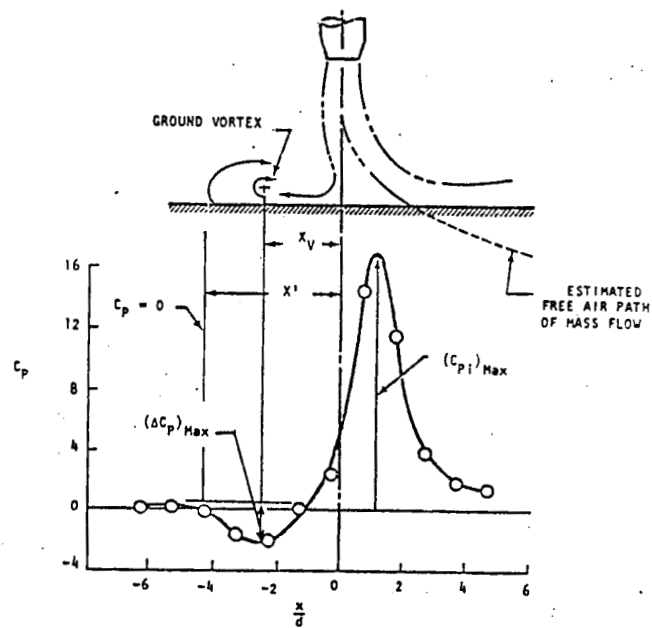


Figure 2. Typical Vortex Ground Pressure Distribution

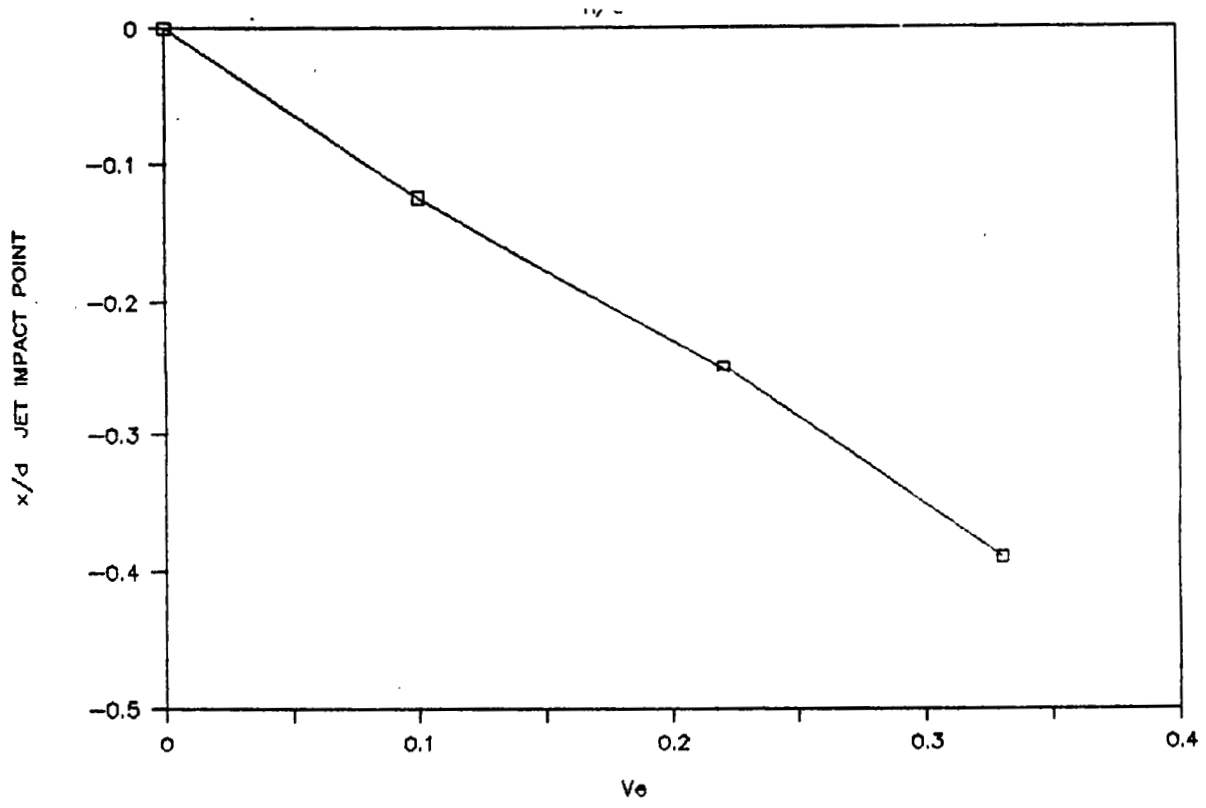


Figure 3. Variation of Jet Free Air Path with velocity Ratio

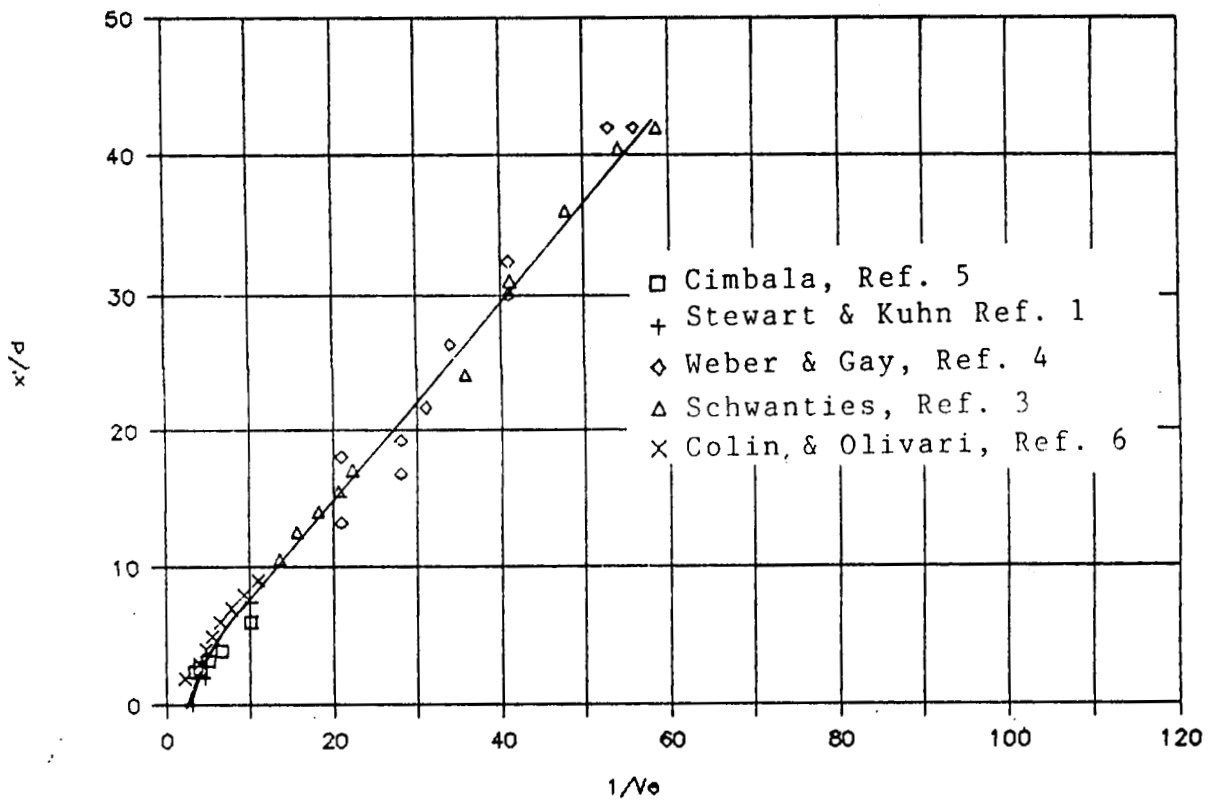


Figure 4. Correlation of the Ground Vortex from Existing Stationary Model Data

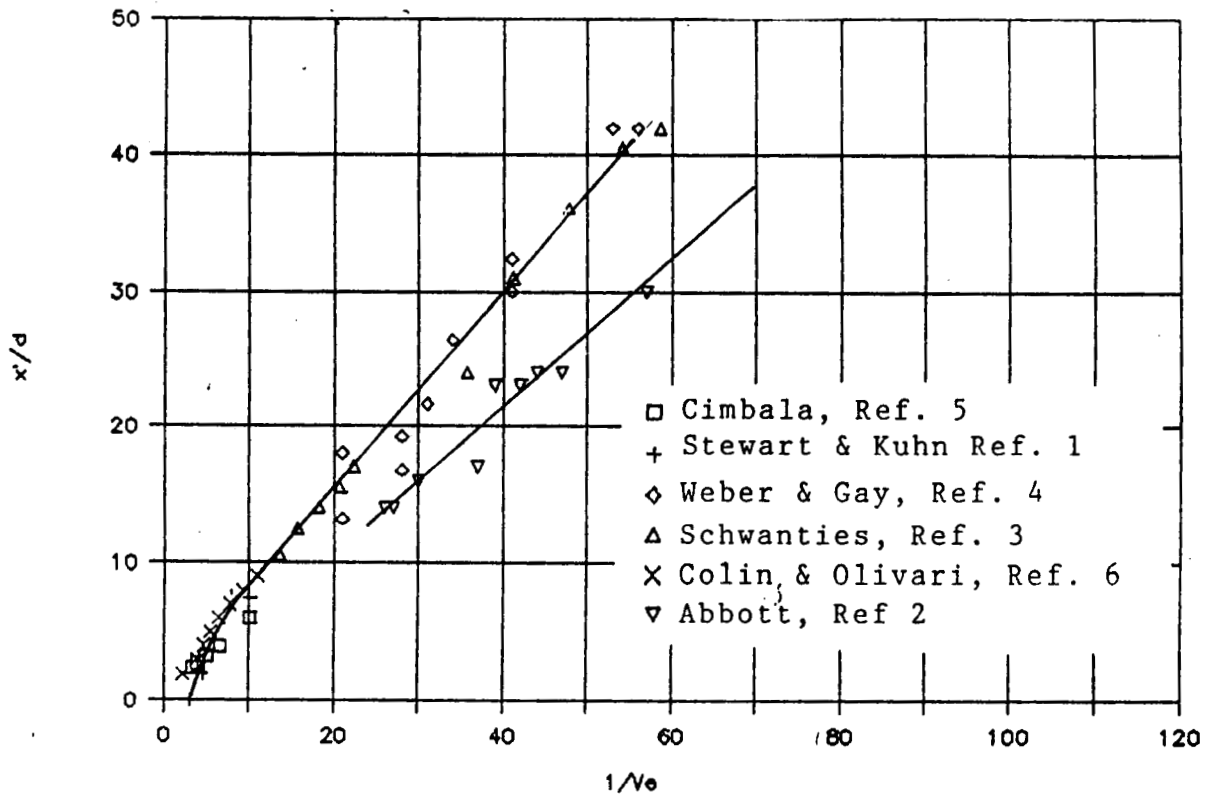


Figure 5. Comparison of Ground Vortex from Existing Stationary and Moving Model Data

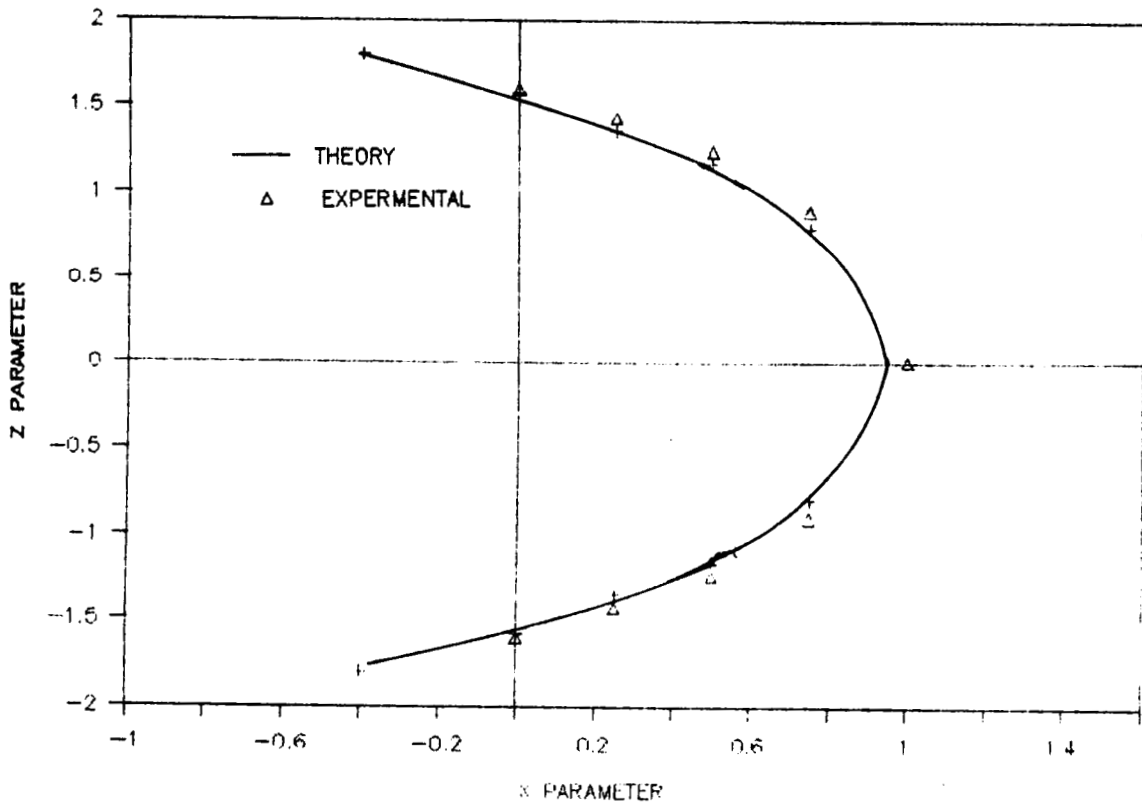


Figure 6. Lateral Ground Vortex Shape, Ref. 6

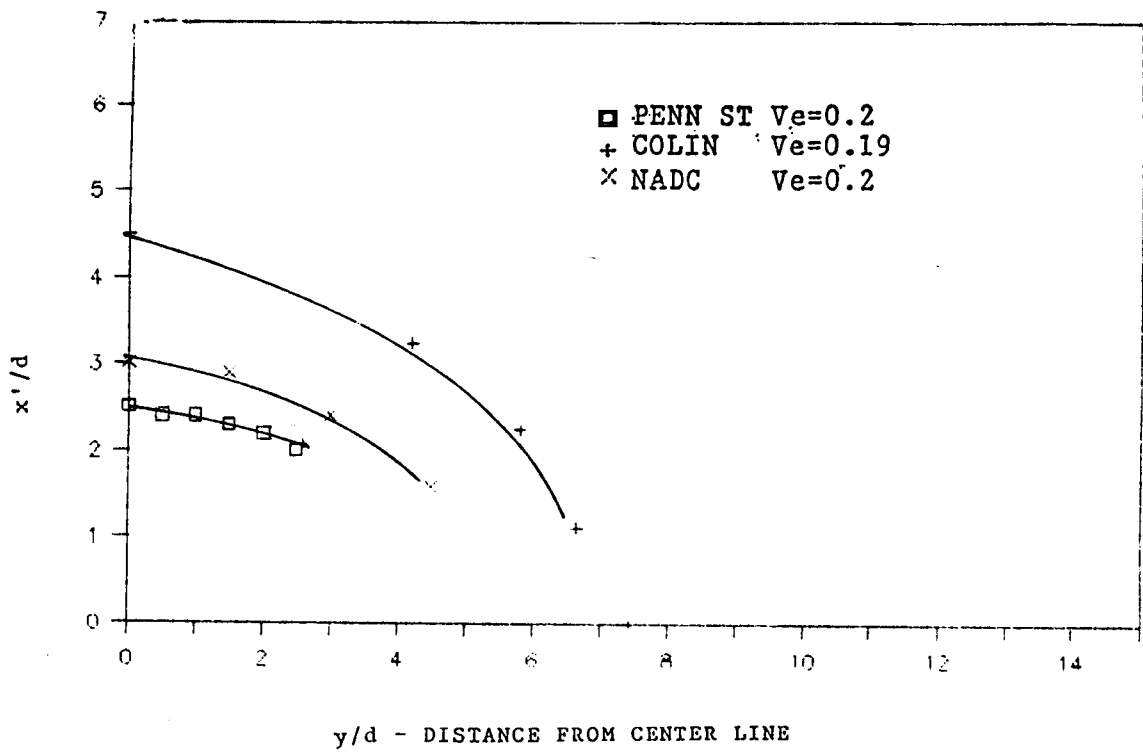


Figure 7. Comparison of Lateral Vortex Shape, Existing Data Base, Refs. 1, 5, and 6

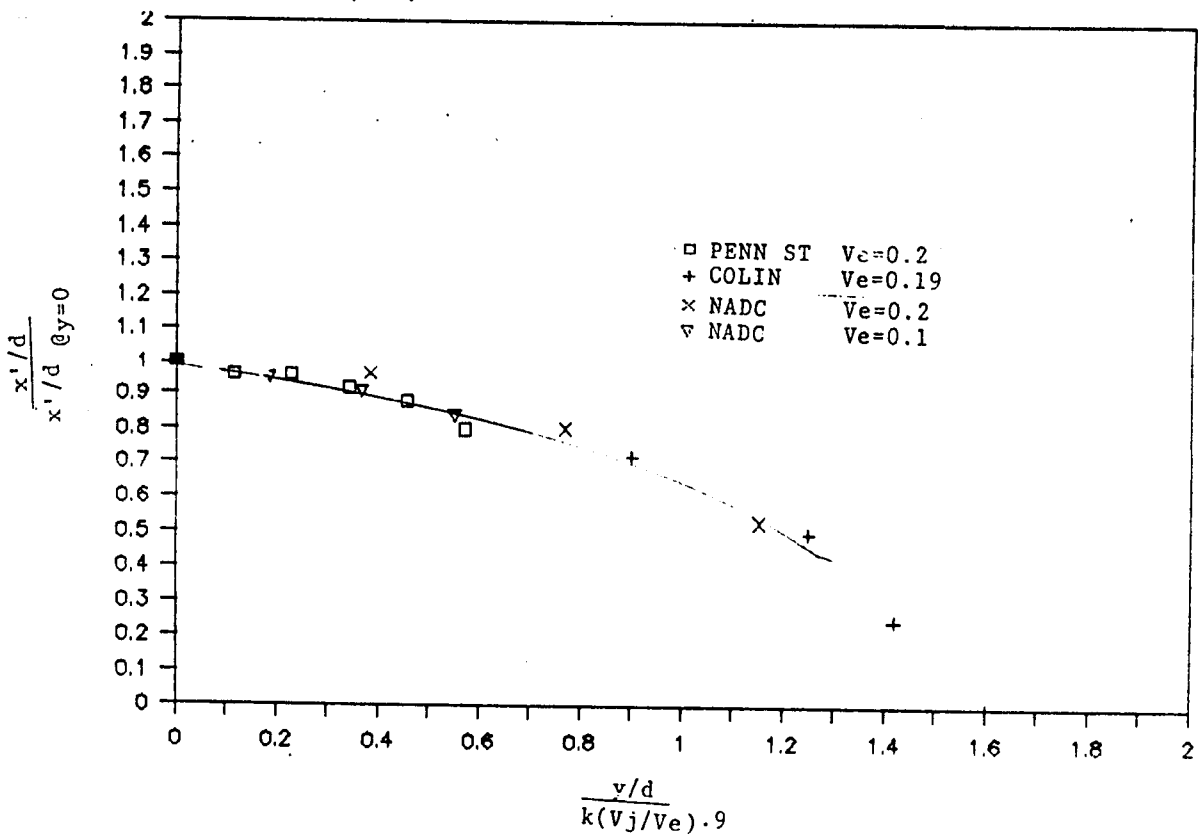
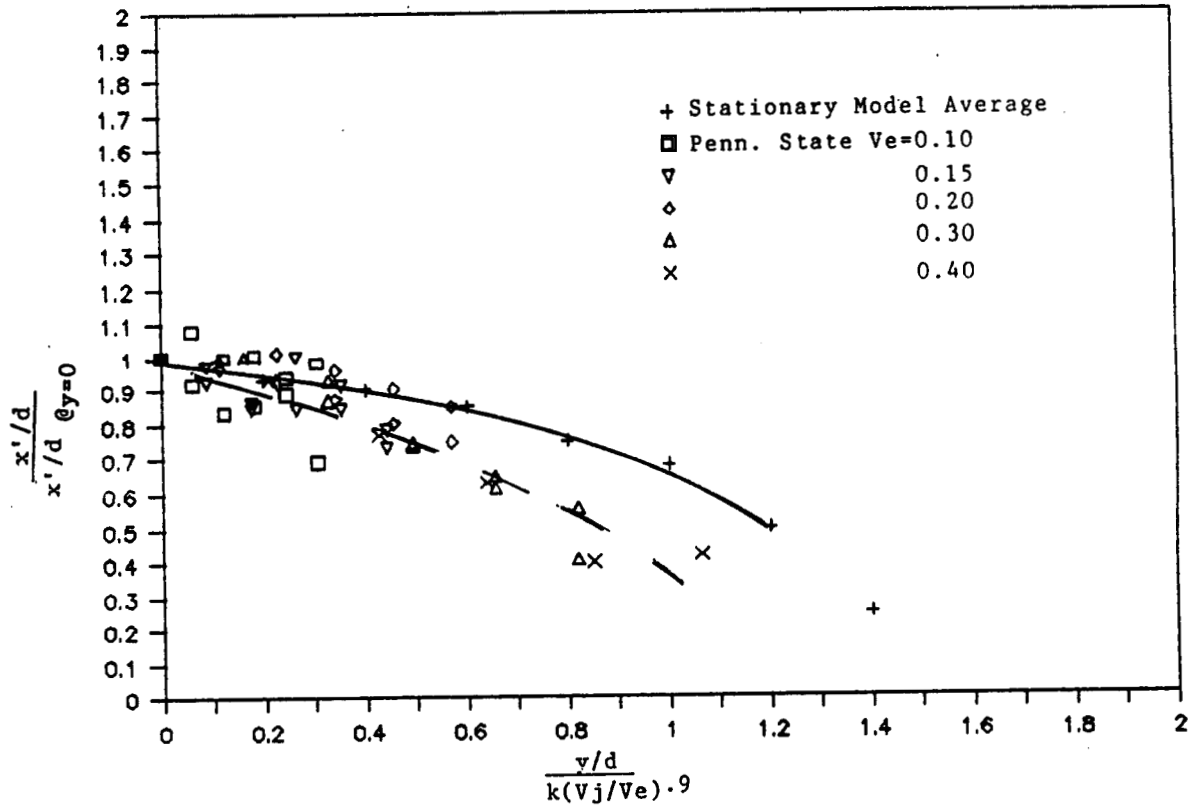
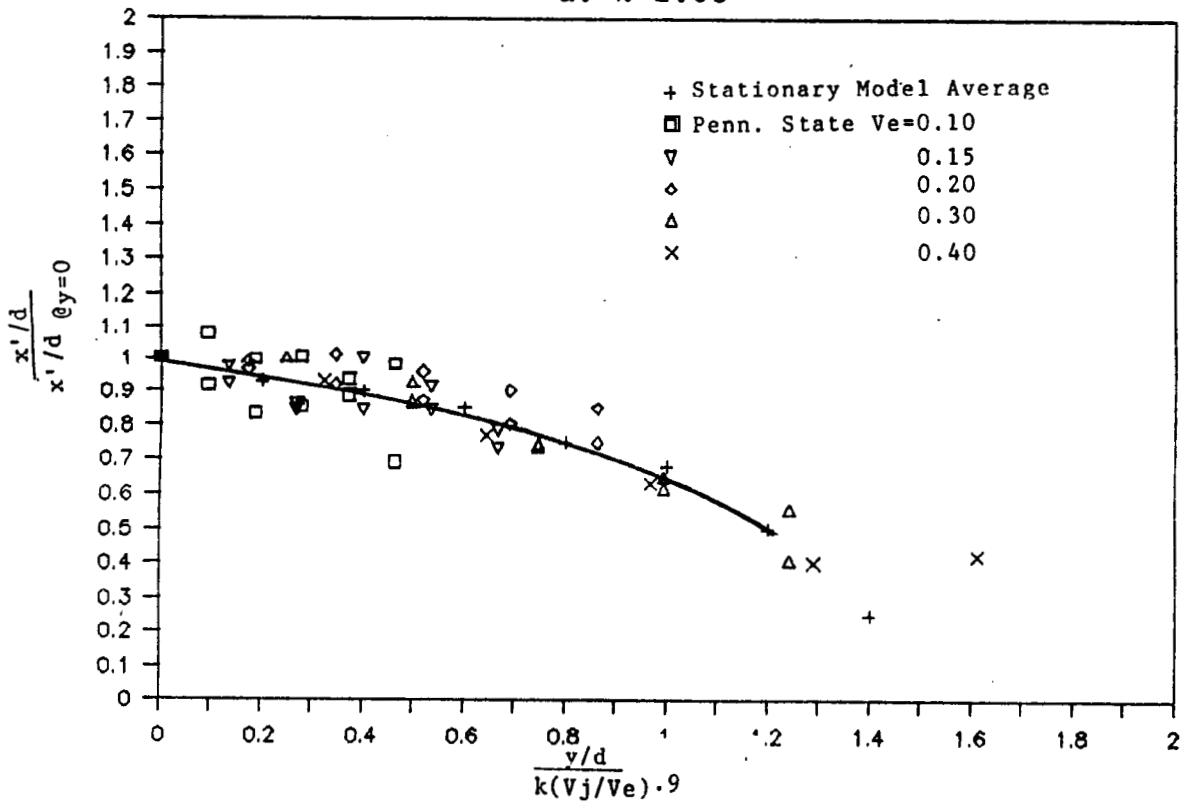


Figure 8. Correlation of Lateral Vortex Shape, Existing Data Base, Refs. 1, 5, and 6



a. $k=1.03$



b. Variable k , $k_s=1.03$, $k_p=.68$

Figure 9. Correlation of Lateral Vortex Shape, Additional Stationary Model Data

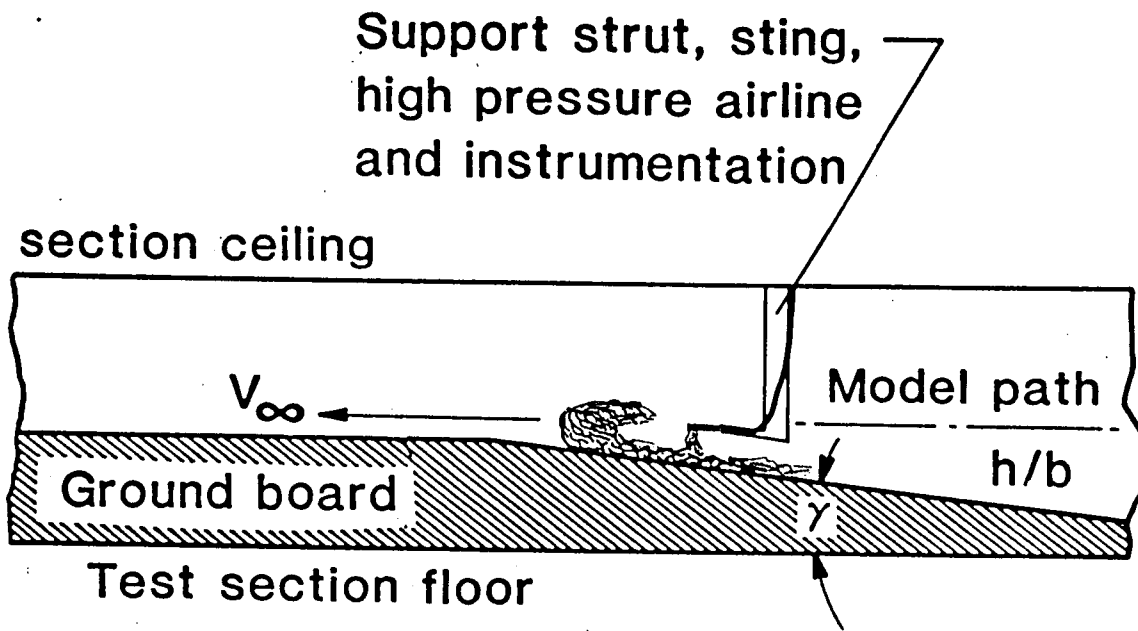
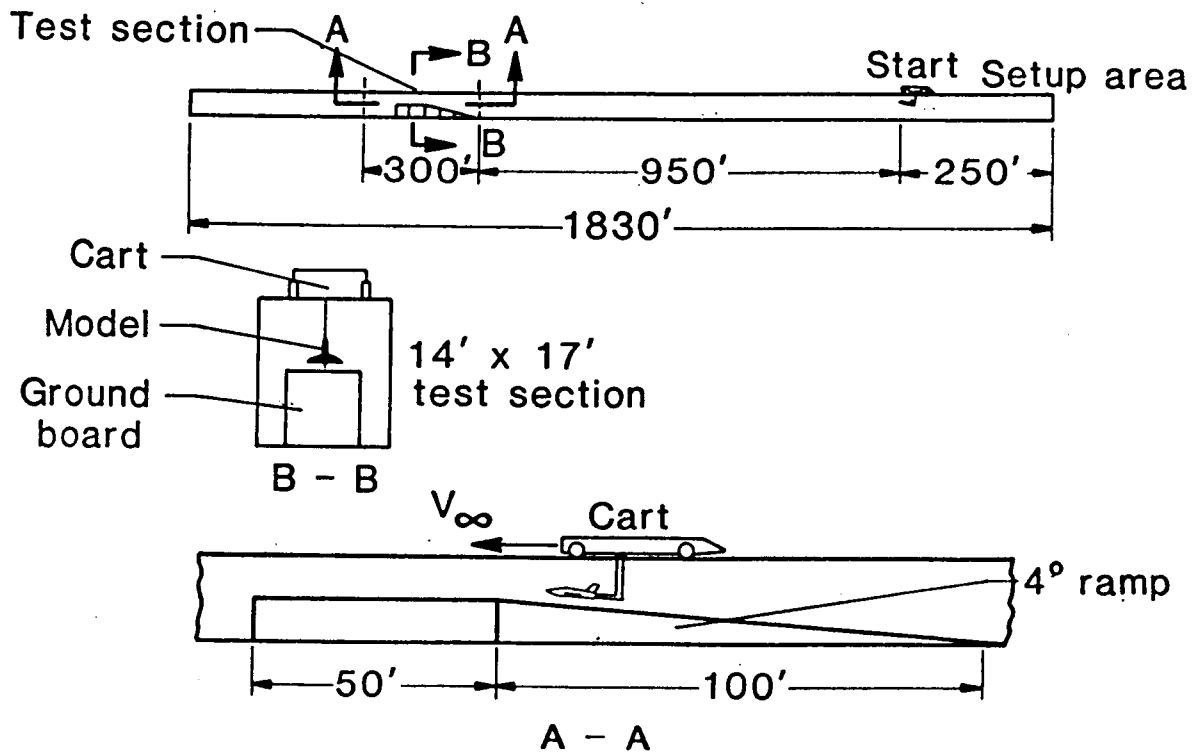


Figure 10. Facility, Model, and Ground Simulation

TAP #	POSITION	X	Y
2	A	-2.5 INCHES	0
4	A	-2.5 inches	5.5 INCHES
5	B	10.0 INCHES	0
6	B	10.0 INCHES	1.5 INCHES
7	B	10.0 INCHES	7.5 INCHES
9	C	25.0 FEET	0
10	C	25.0 FEET	3.0 INCHES
11	C	25.0 FEET	7.0 INCHES
12	C	25.0 FEET	15.0 INCHES

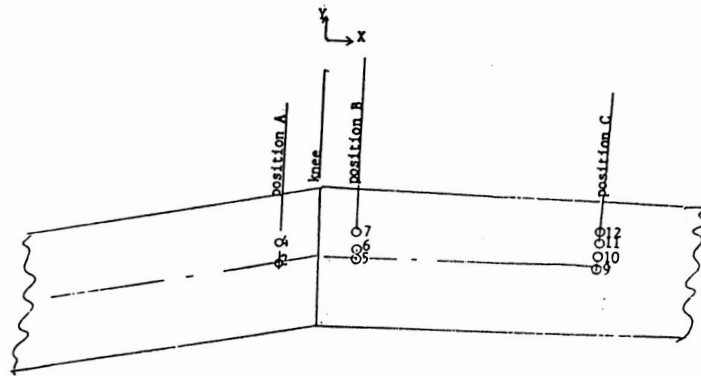


Figure 11. Ground Board Pressure Instrumentation, 1" Jet

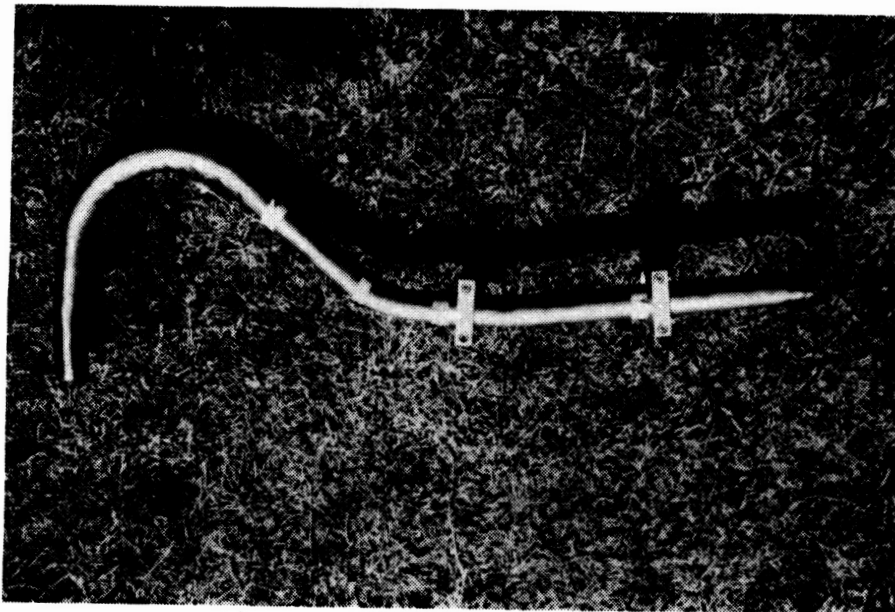


Figure 12. One Inch Jet Nozzle

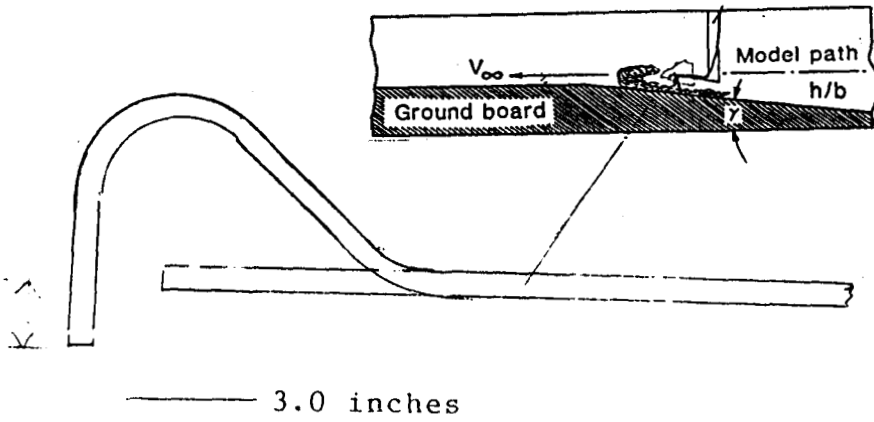


Figure 13. Jet Nozzle Installation

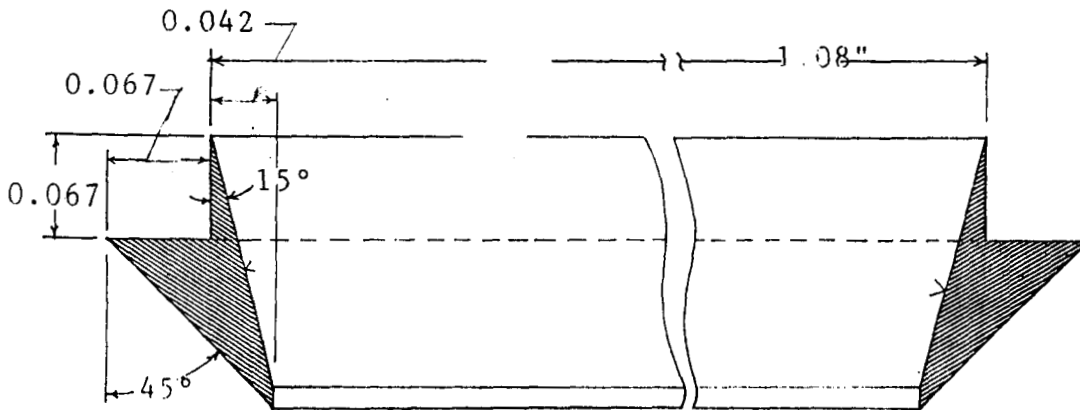


Figure 14. One Inch Jet Nozzle Geometry

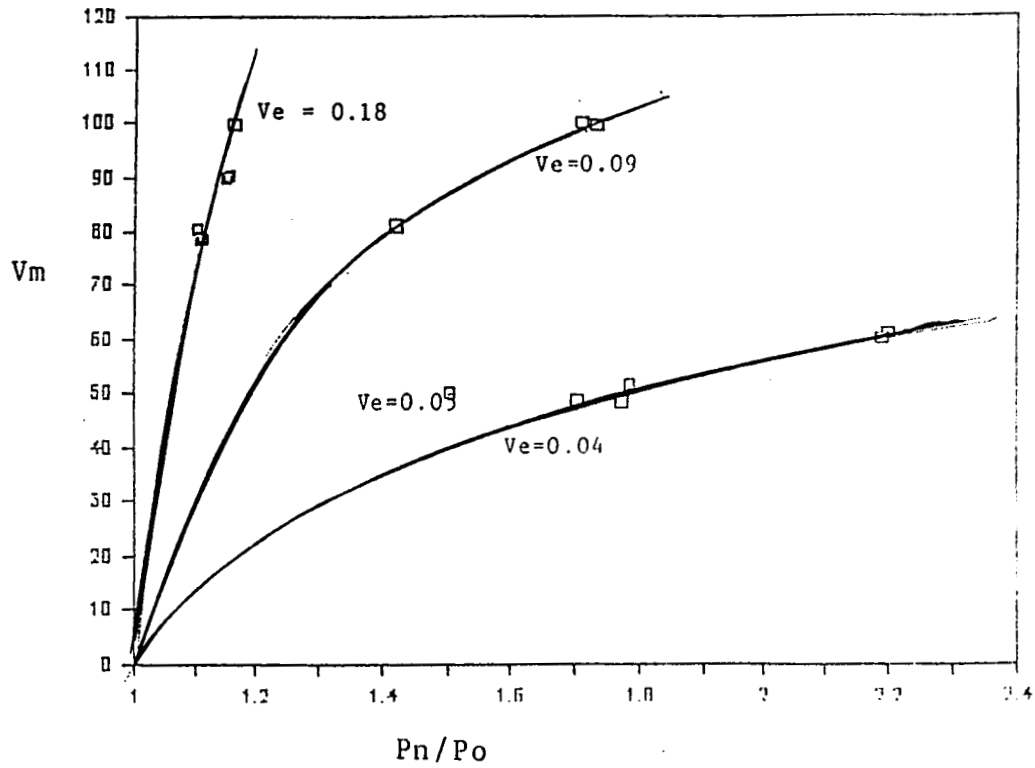
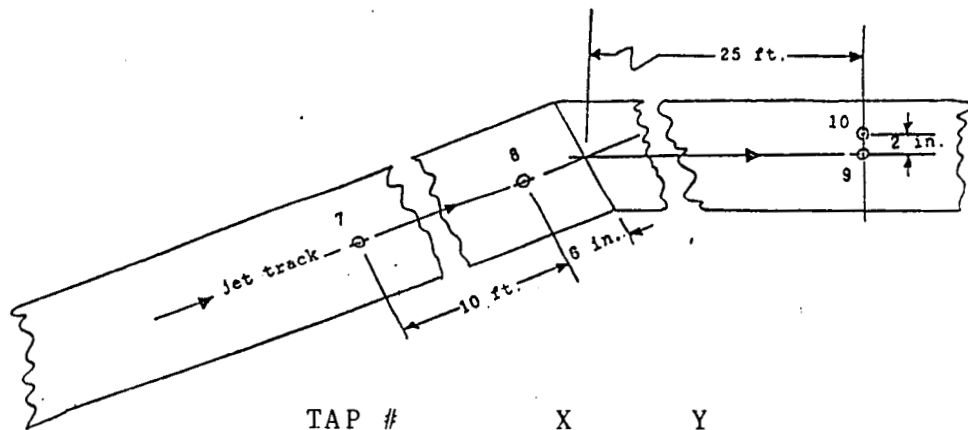


Figure 15. Test Conditions for One inch Nozzle



TAP #	X	Y
7	-10.5 ft.	0 not presented
8	-0.5 ft.	0 not presented
9	25.0 ft.	0
10	25.0 ft.	2 inches

Figure 16. Ground Board Pressure Instrumentation, .6" Jet

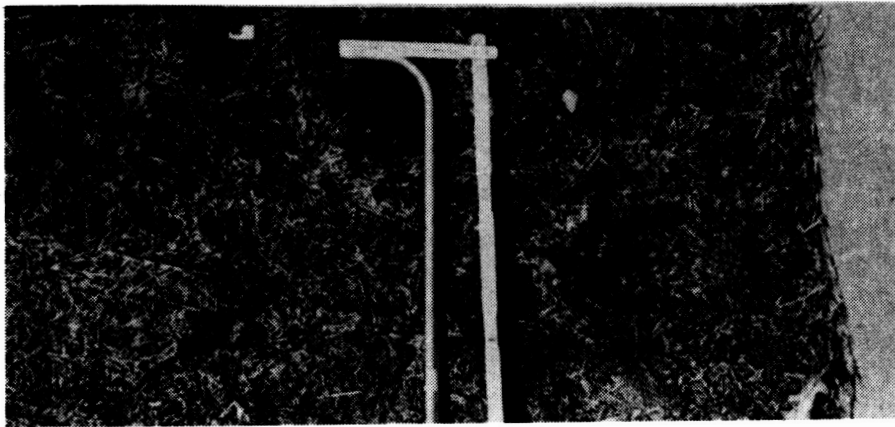


Figure 17. 0.6 Inch Jet Nozzle

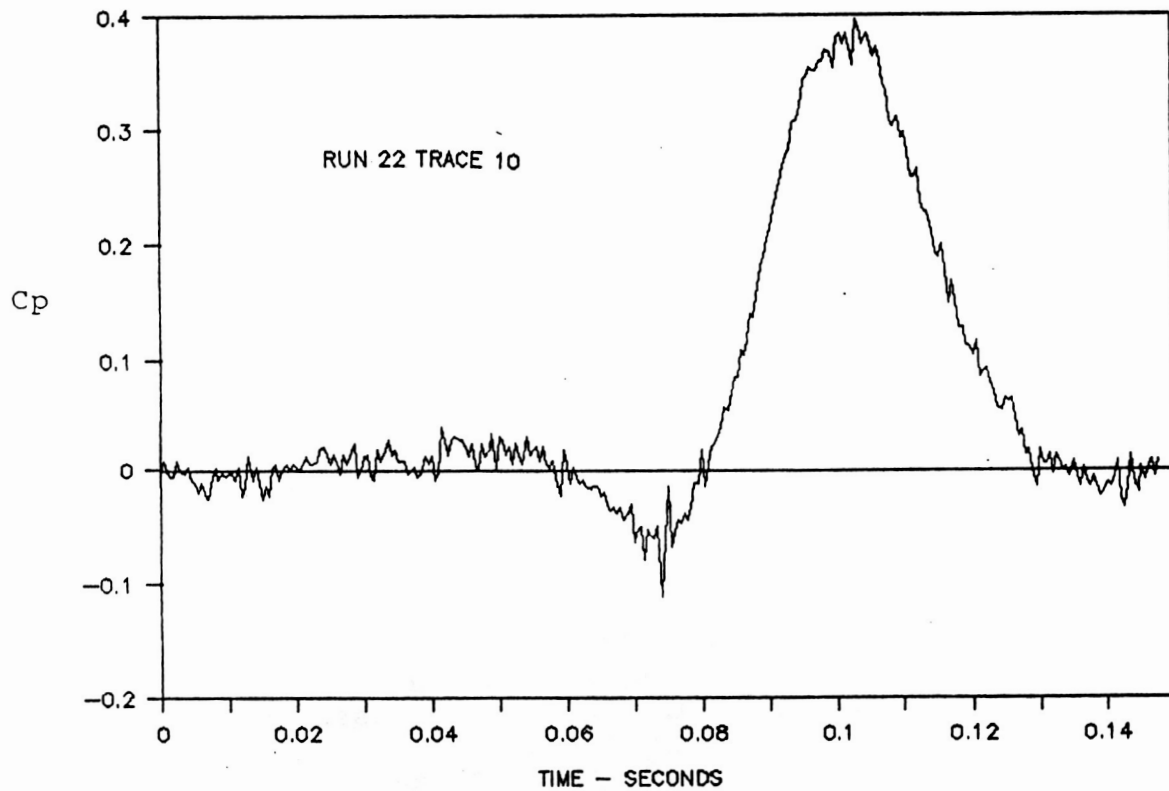


Figure 18. Time History of Ground Board Pressures

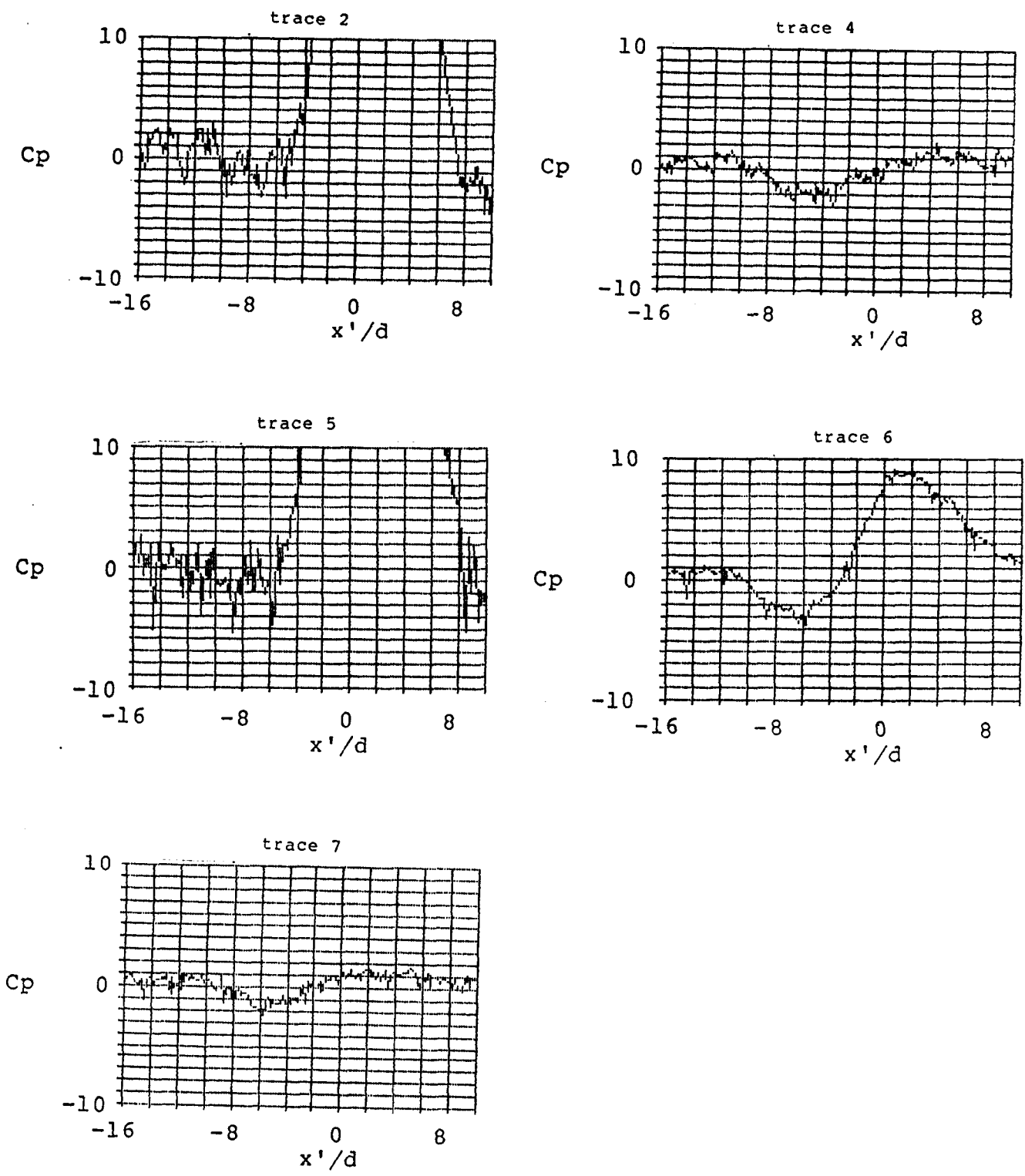


Figure 19. Ground Pressure Distribution, 1.0" Jet, $Ve=0.042$

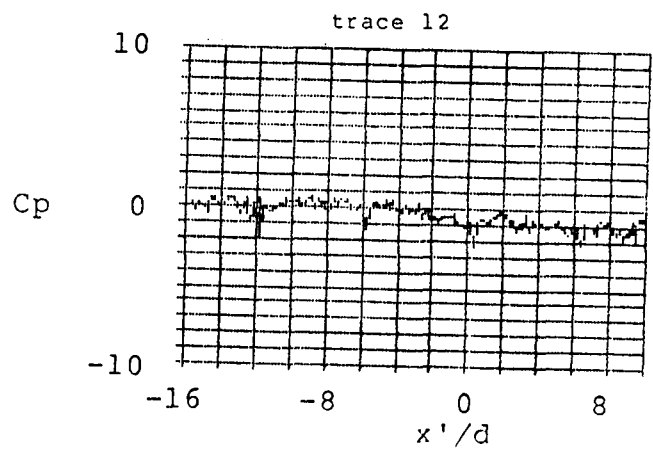
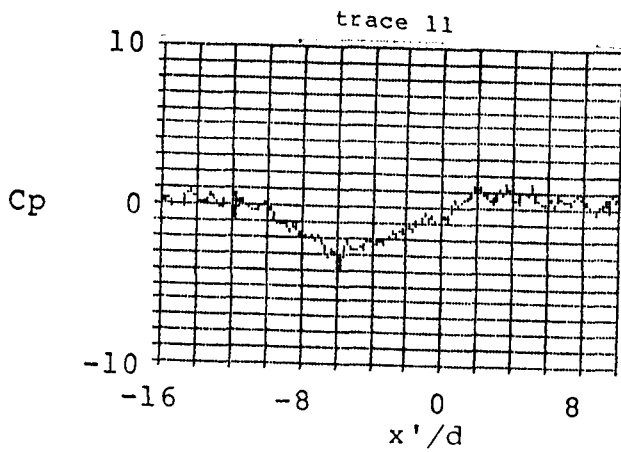
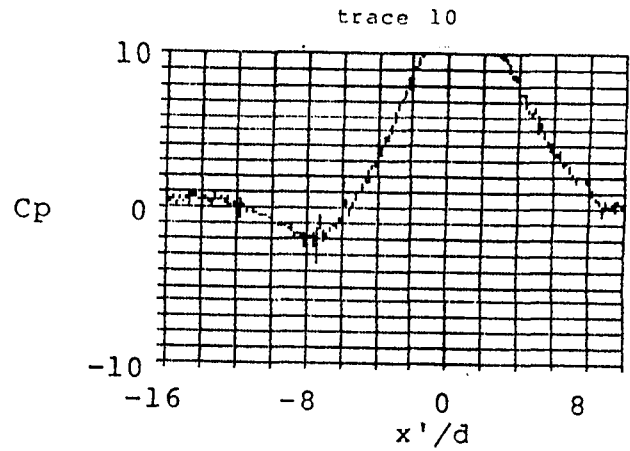
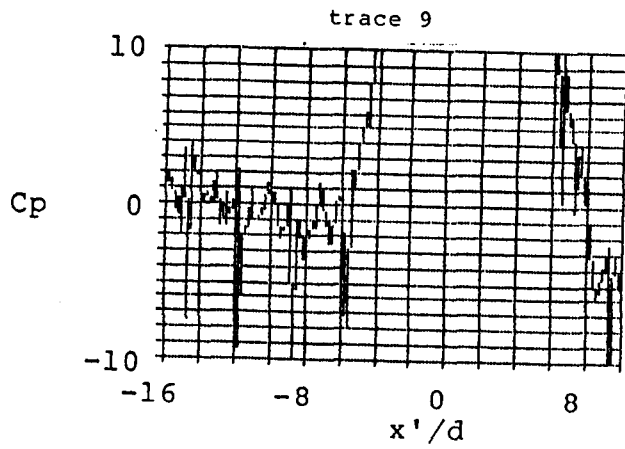


Figure 19 (cont.). Ground Pressure Distribution, 1.0" Jet,
 $Ve=0.042$

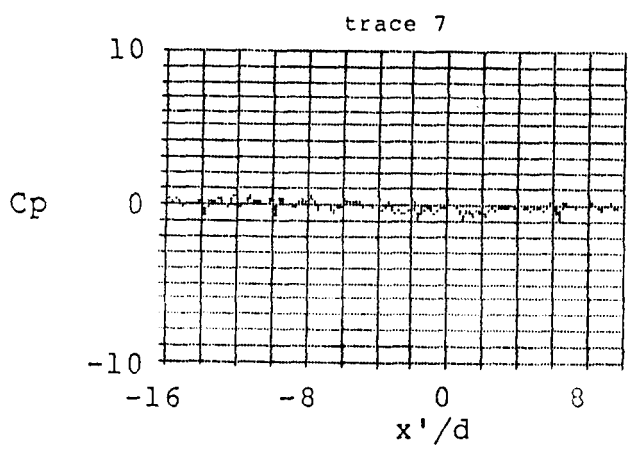
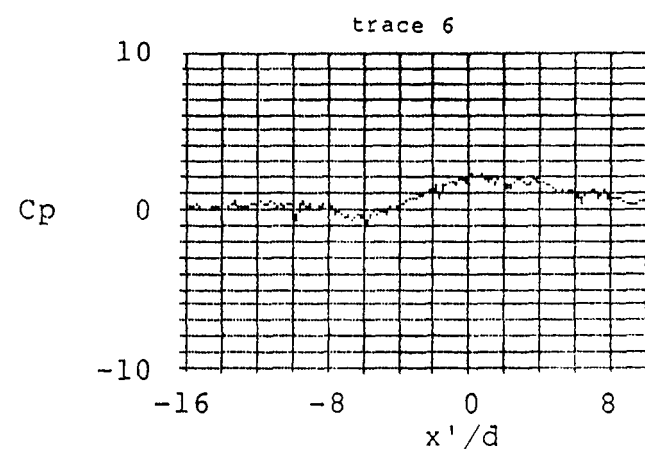
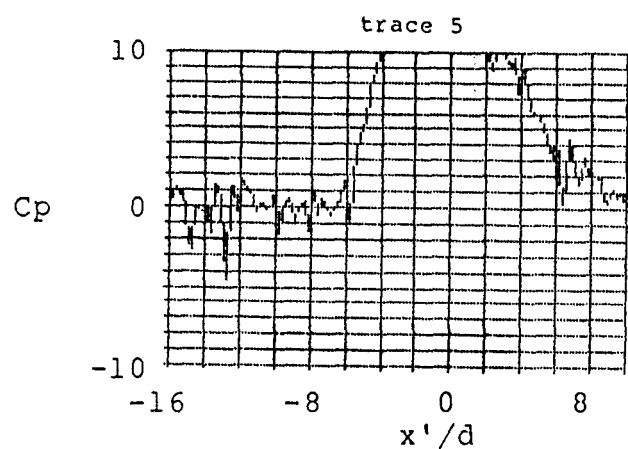
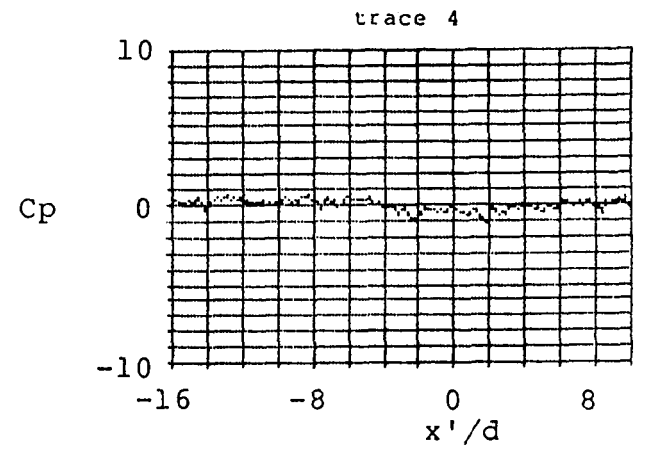
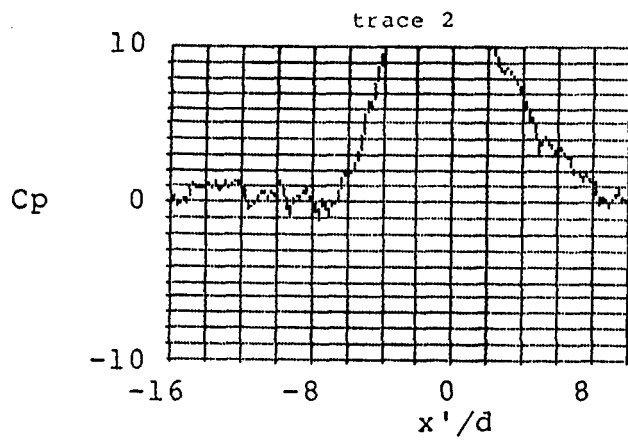


Figure 20. Ground Pressure Distribution, 1.0" Jet, $V_e=0.090$

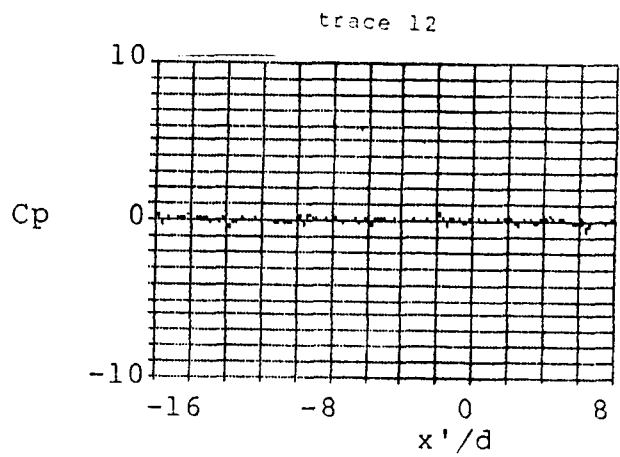
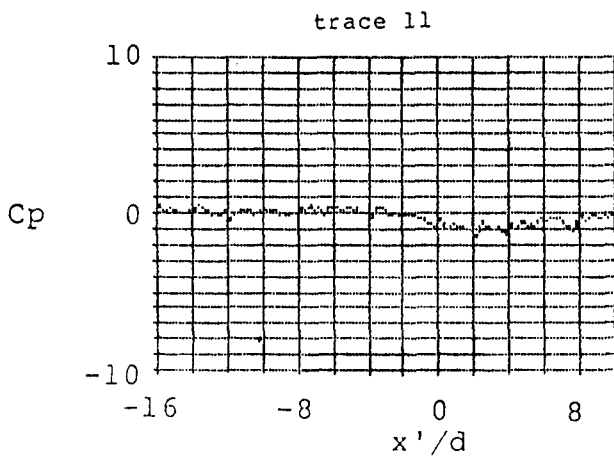
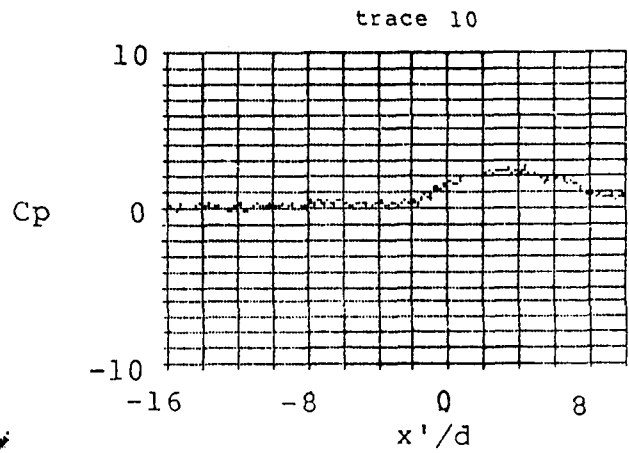
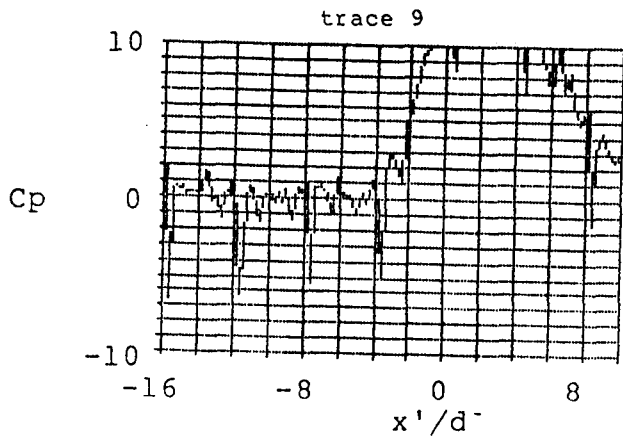


Figure 20 (Cont.). Ground Pressure Distribution, 1.0" Jet,
 $V_e=0.090$

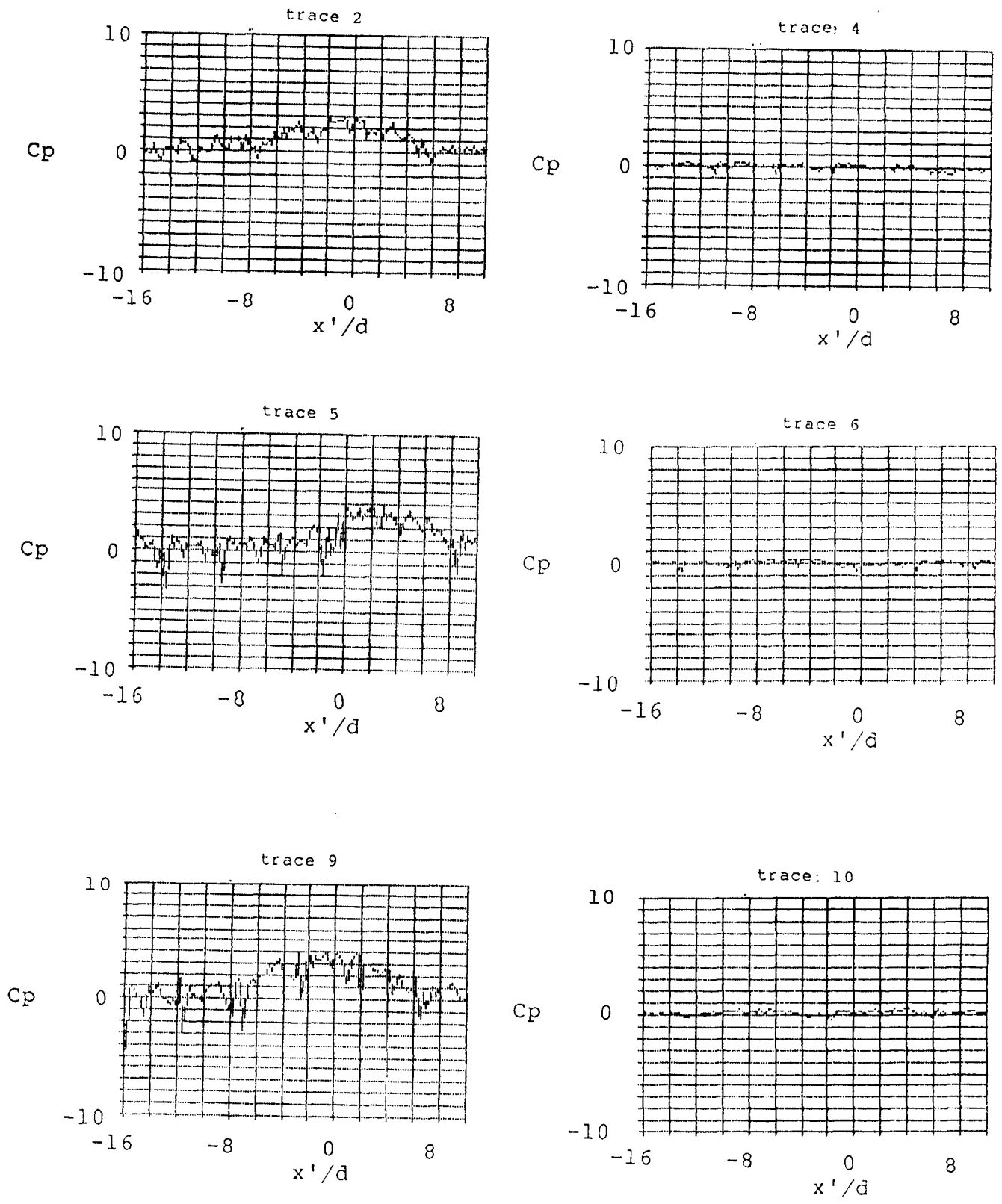
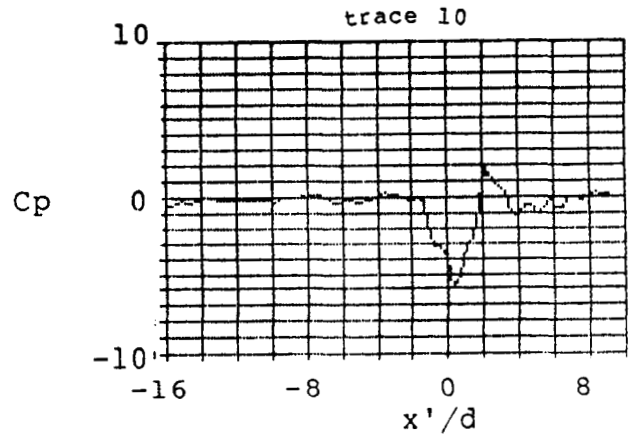
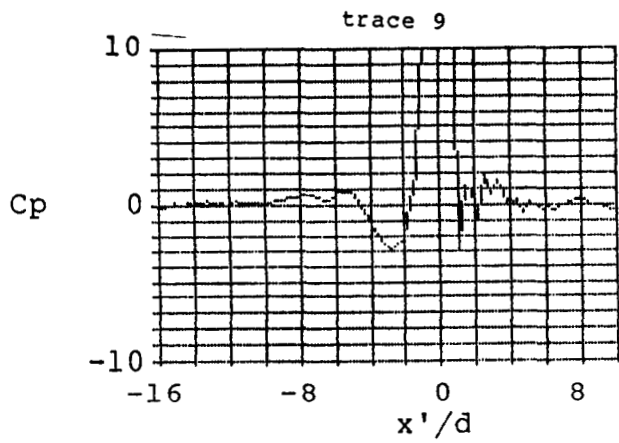
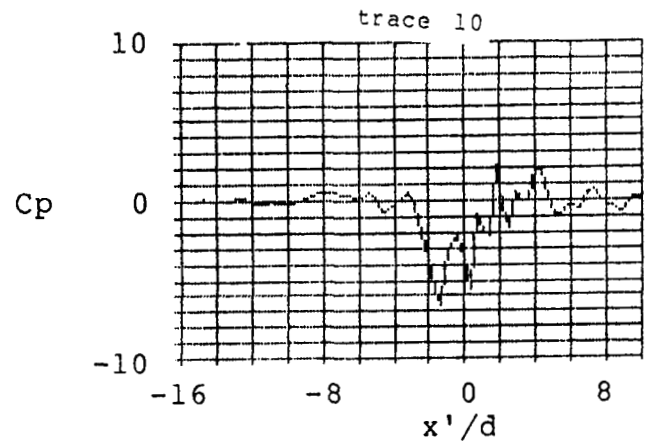
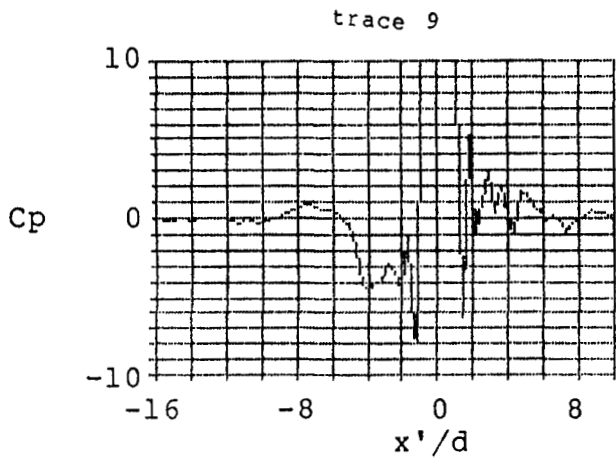


Figure 21. Ground Pressure Distribution, 1.0" Jet, $Ve=0.170$



b. Run 73, $Ve=0.132$



a. Run 74, $Ve=0.093$

Figure 22. Ground Pressure Distribution, 0.6" Jet

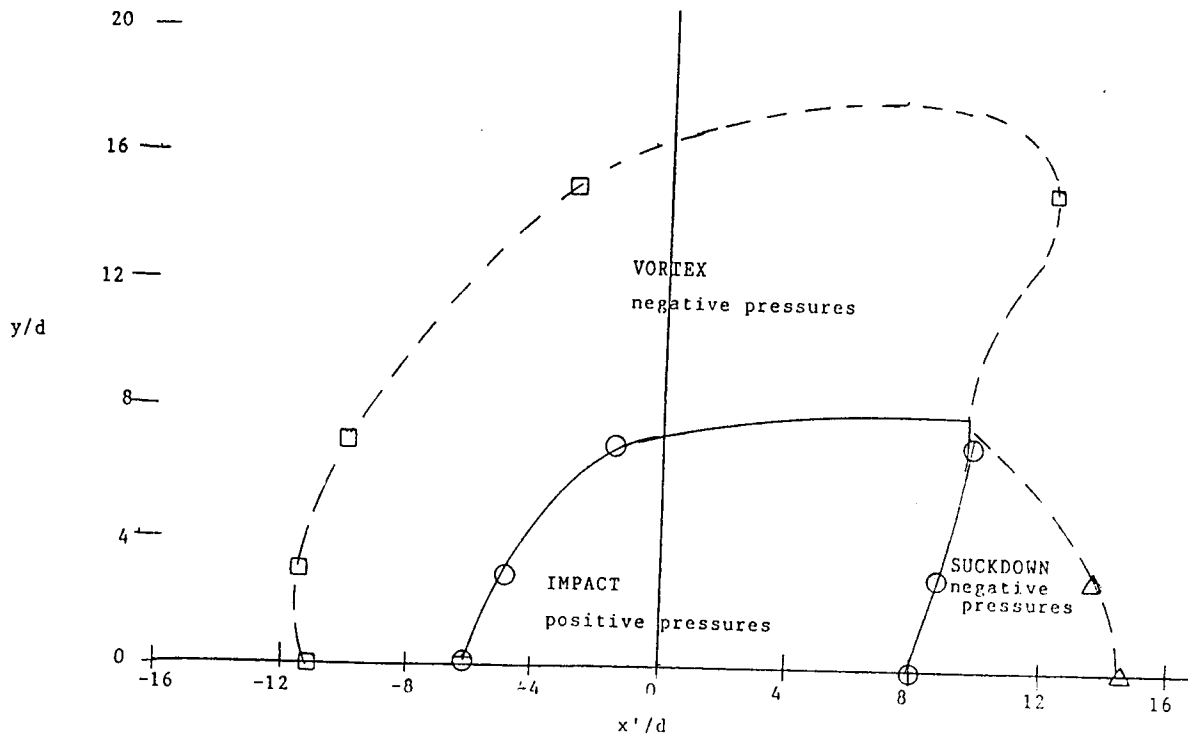


Figure 23. Ground Pressure Field, Position C, Run 22, $V_e = 0.042$

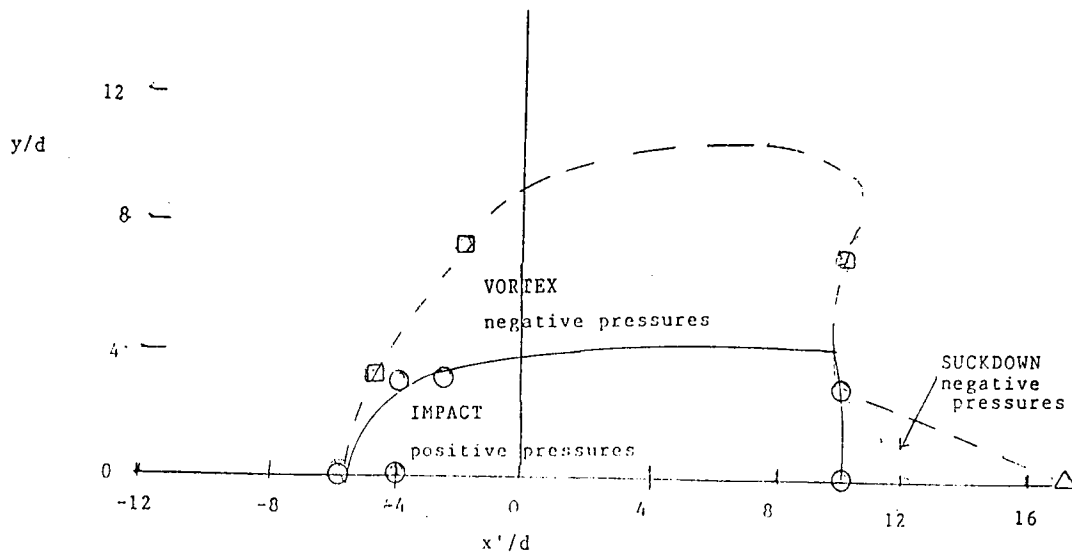


Figure 24. Ground Pressure Field, Position C, $V_e = 0.90$

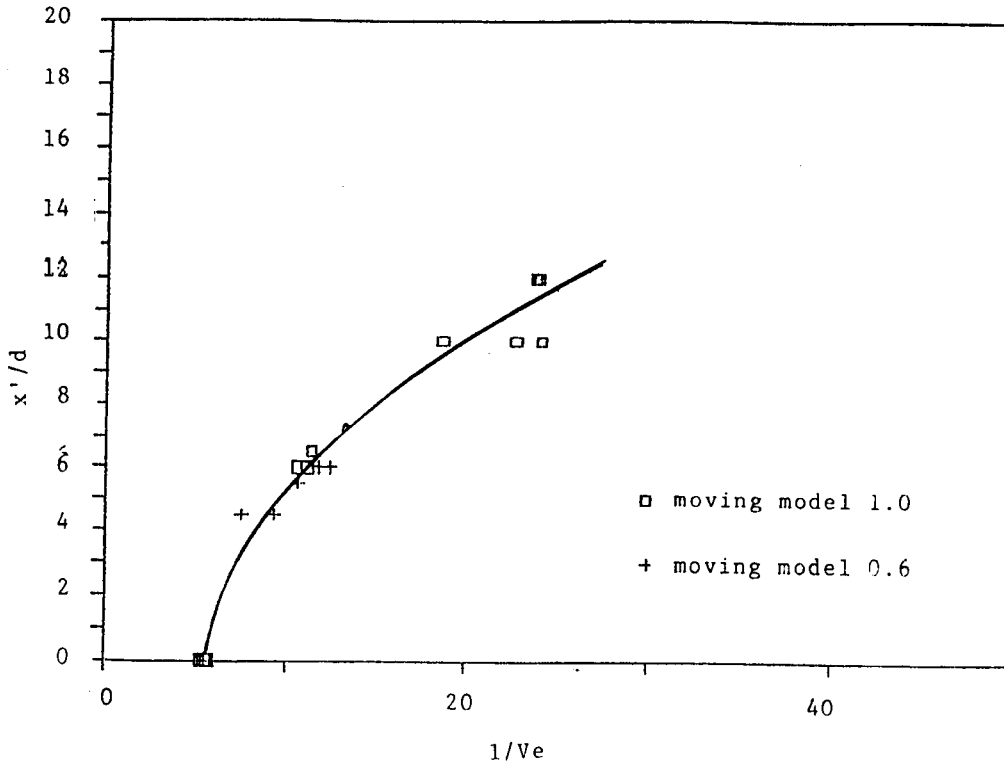


Figure 25. Ground Vortex Forward Penetration, NASA, Moving Model

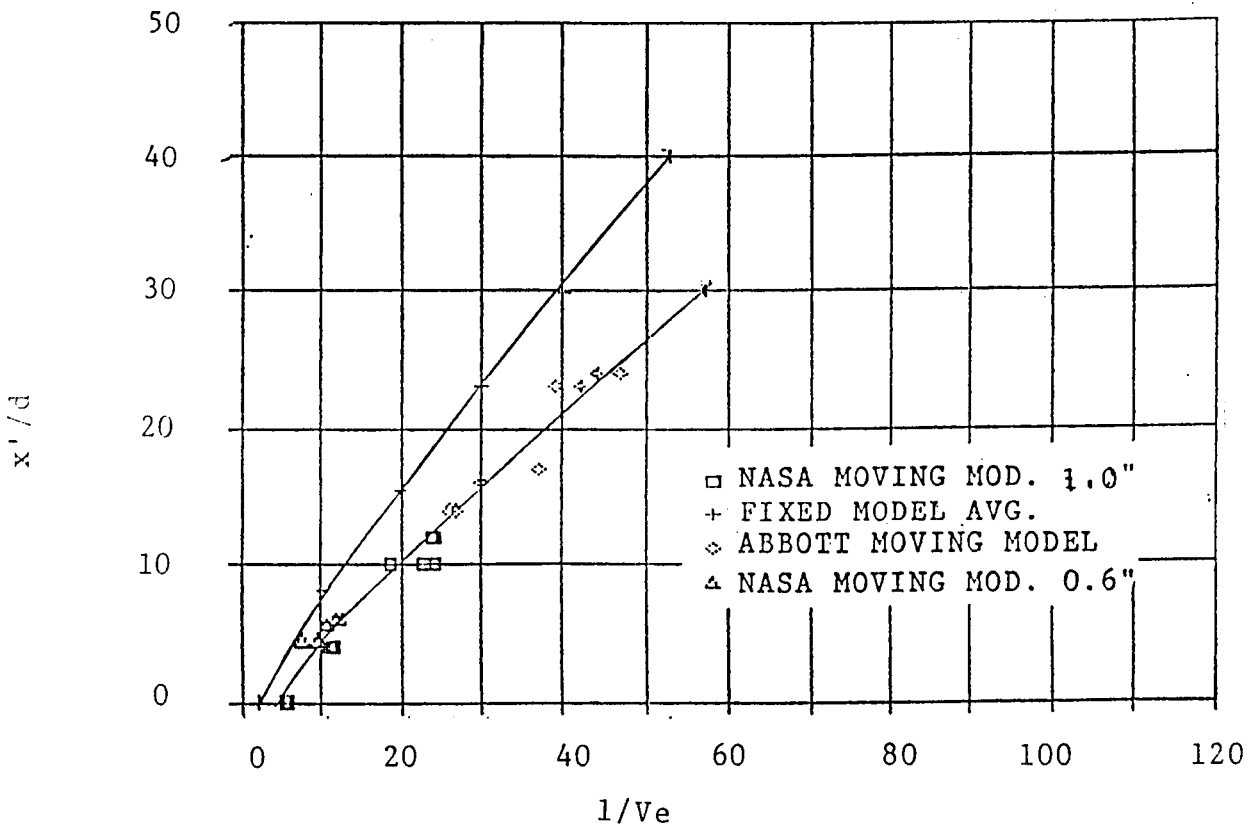


Figure 26. Ground Vortex Forward Penetration, Correlation of Station and Moving Model

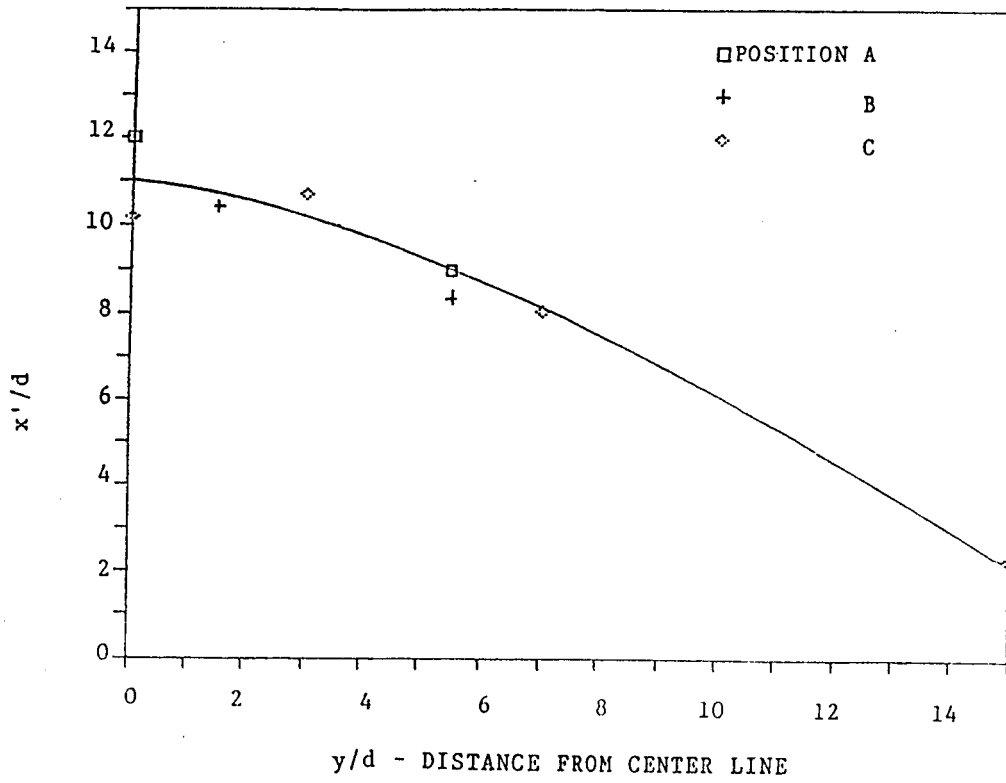


Figure 27. Ground Vortex Lateral Extent, $Ve=0.042$

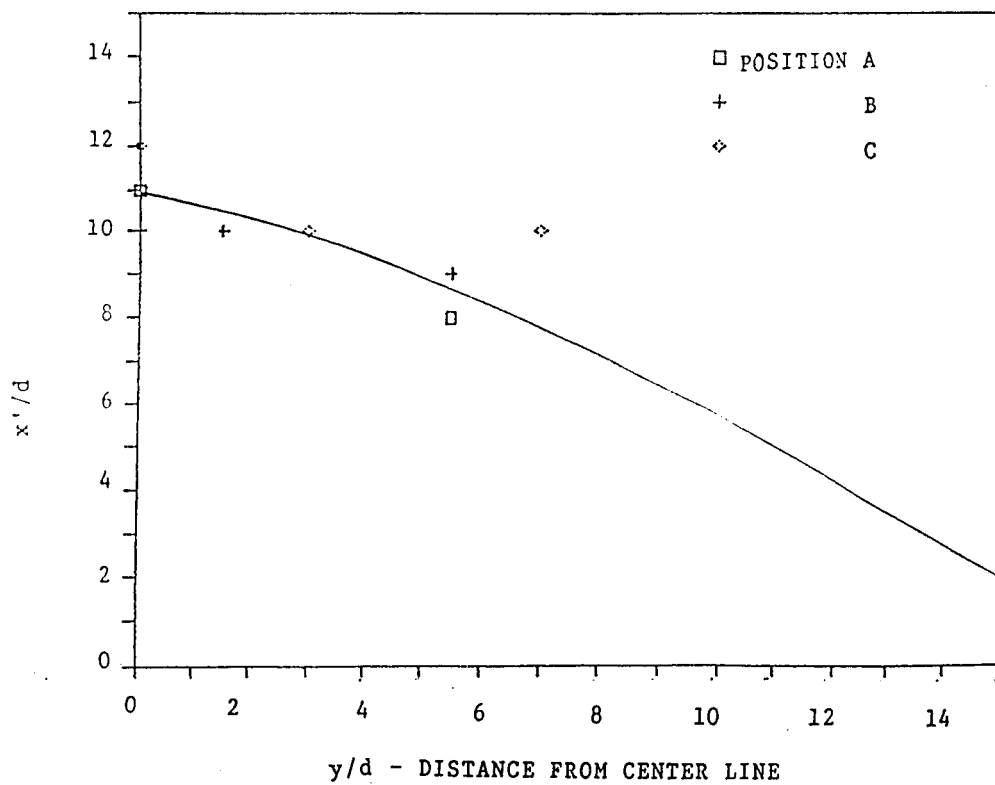


Figure 28. Ground Vortex Lateral Extent, $Ve=0.052$

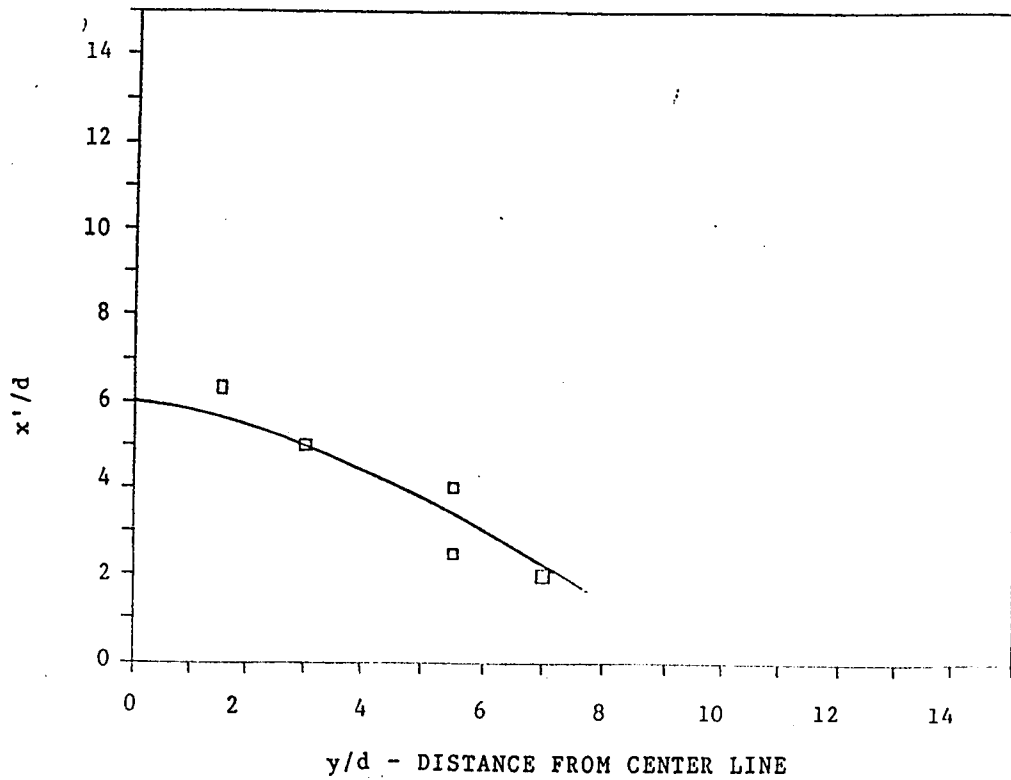


Figure 29. Ground Vortex Lateral Extent, $Ve=0.090$

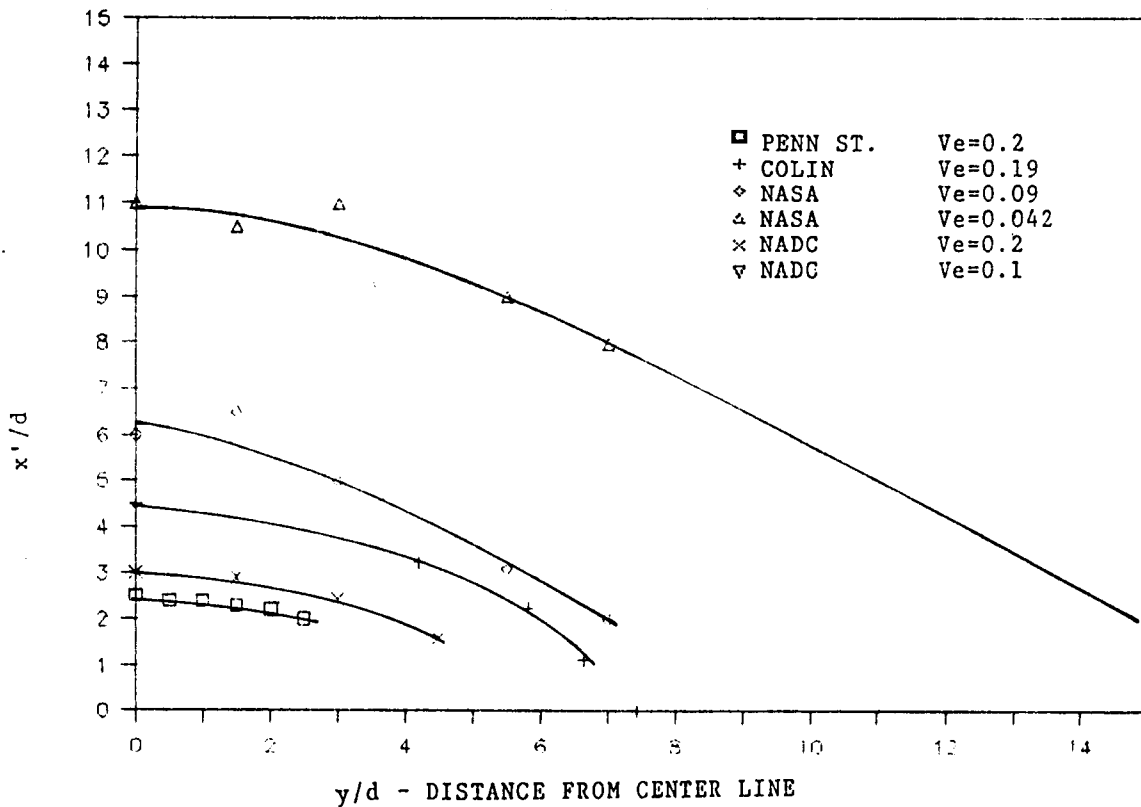


Figure 30. Lateral Shape of the Ground Vortex, Comparison of Stationary and Moving Models

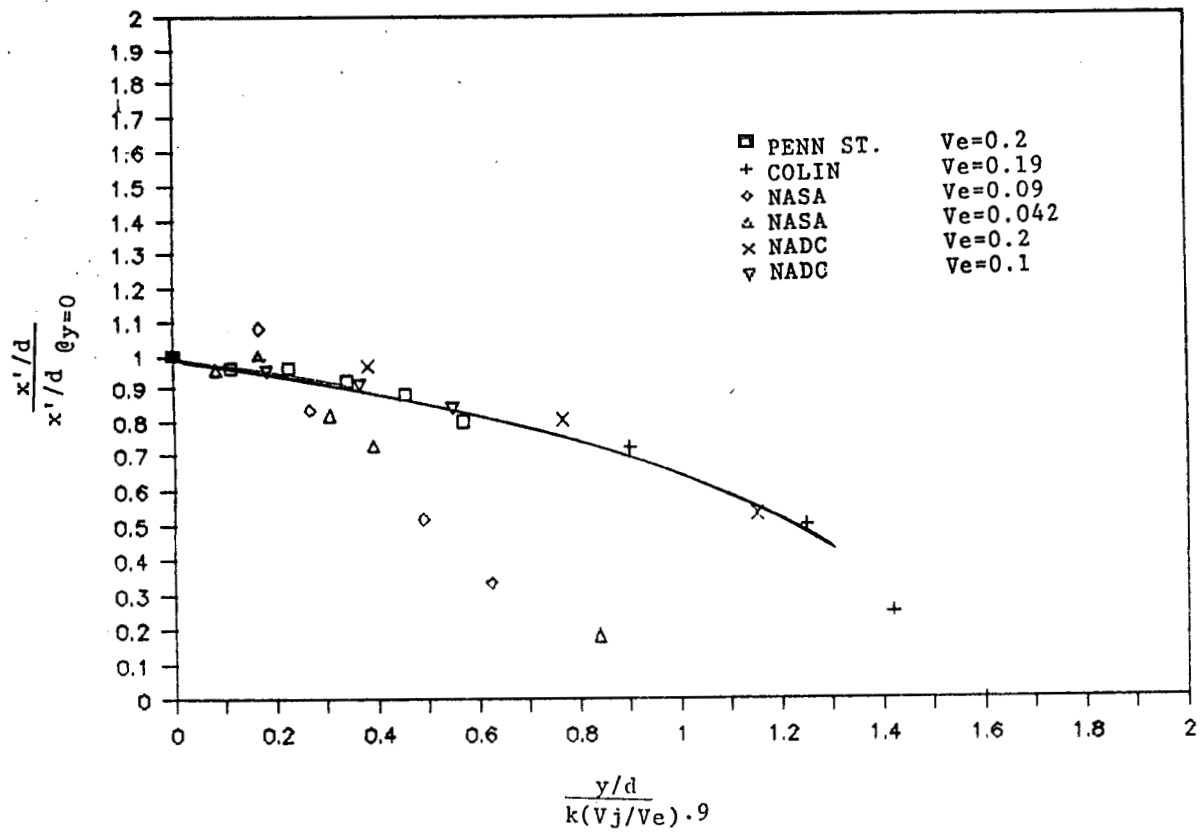


Figure 31. Correlation of Lateral Vortex Shape for Stationary and Moving Jets, $k=1.03$

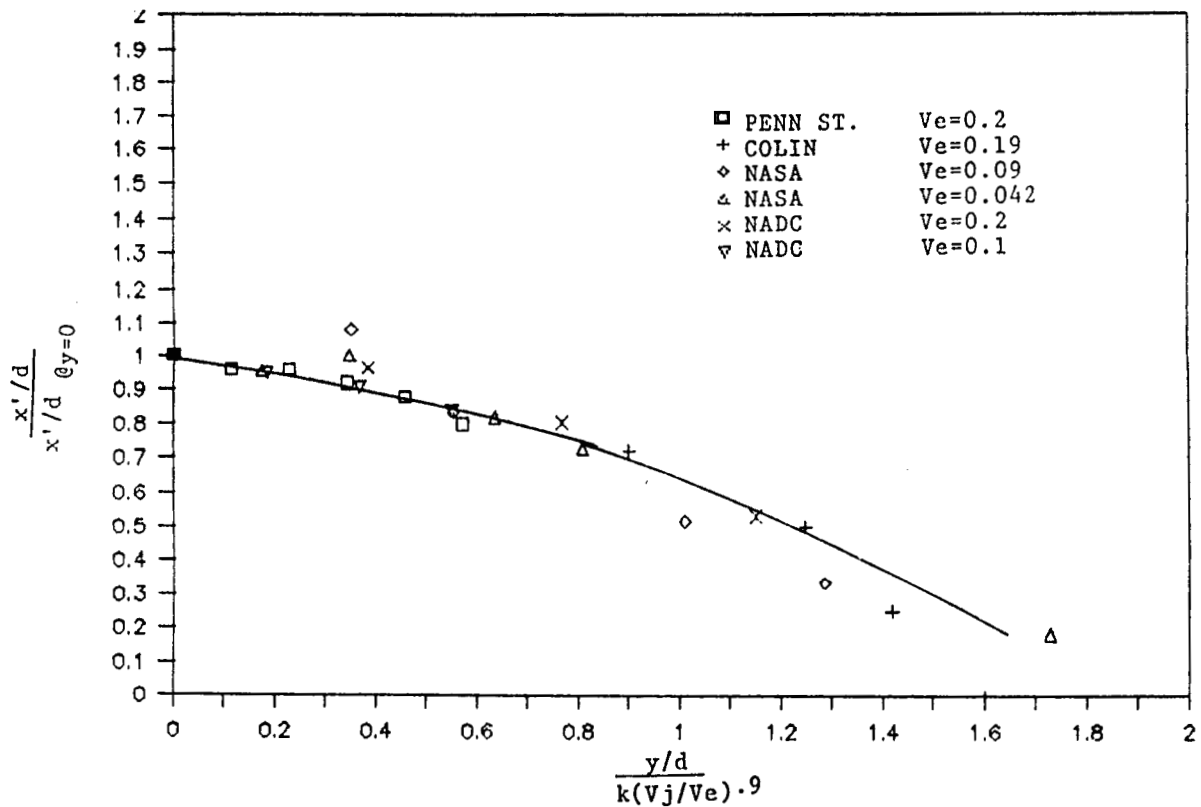


Figure 32. Correlation of Lateral Vortex Shape for Stationary, $k=1.03$, and Moving Jets, $k=0.50$,

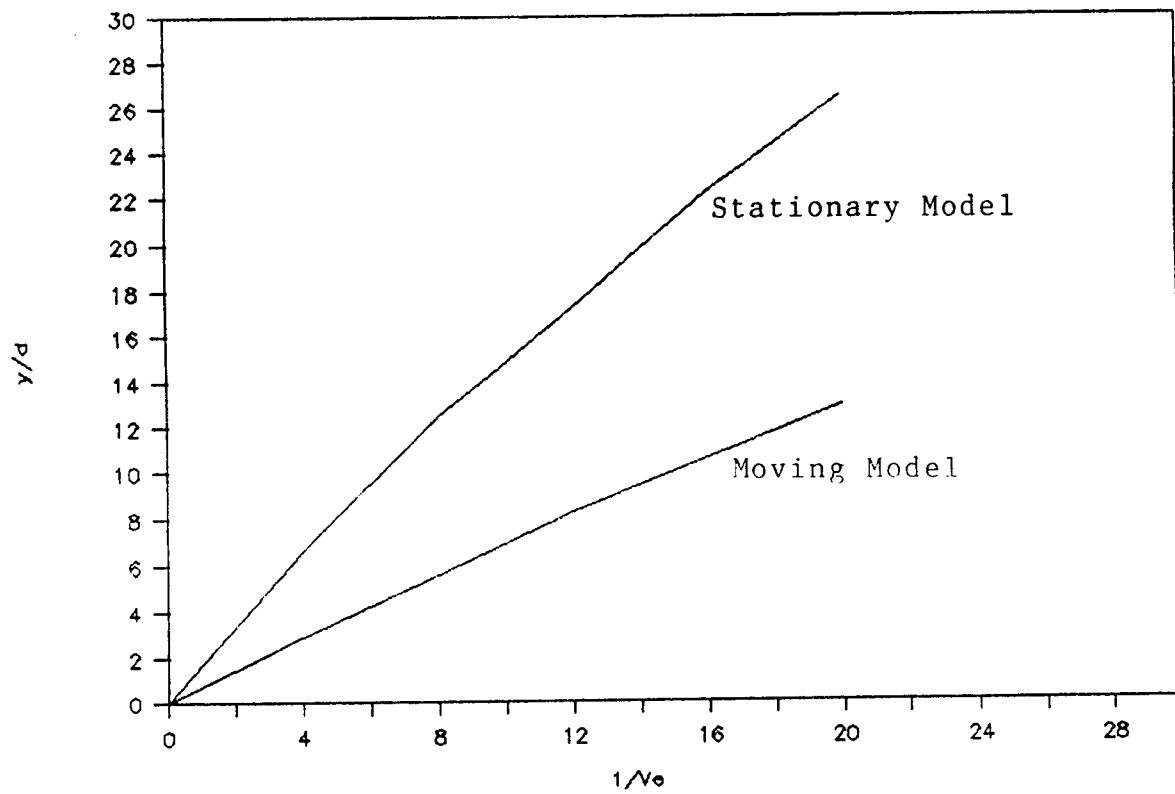


Figure 33. Lateral Penetration of the Ground Vortex
at $x/d = 0.0$

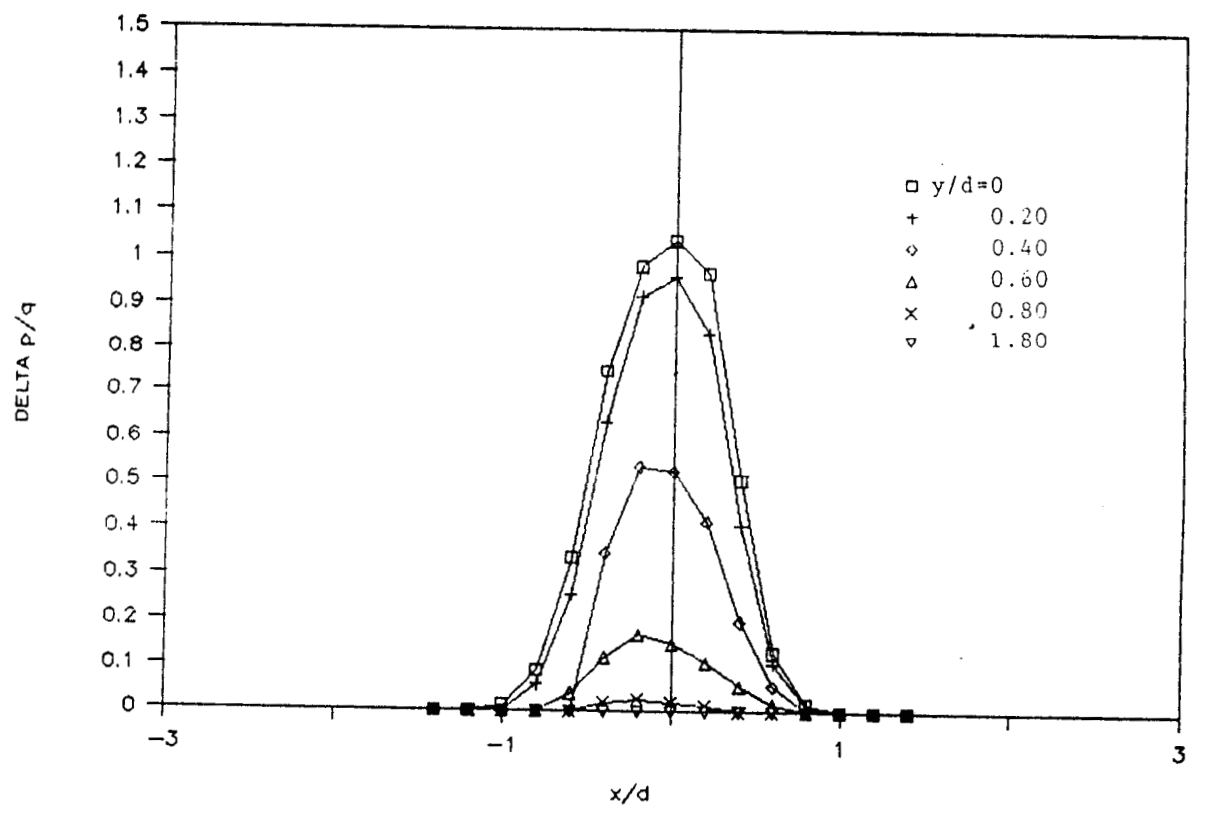
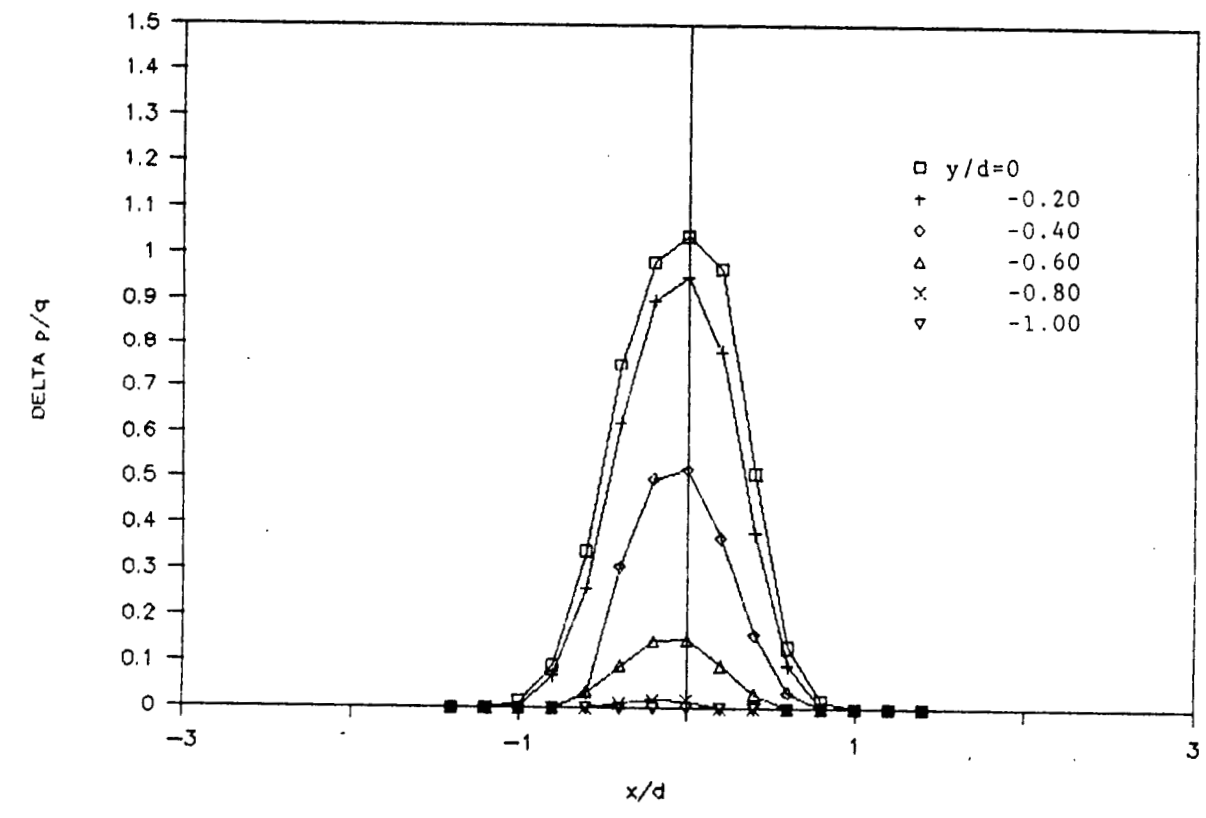


Figure 34. Jet Cross Section Pressure Distribution, $d=1.0''$, $h/d=3.0$, $Q_j = 935$ psf

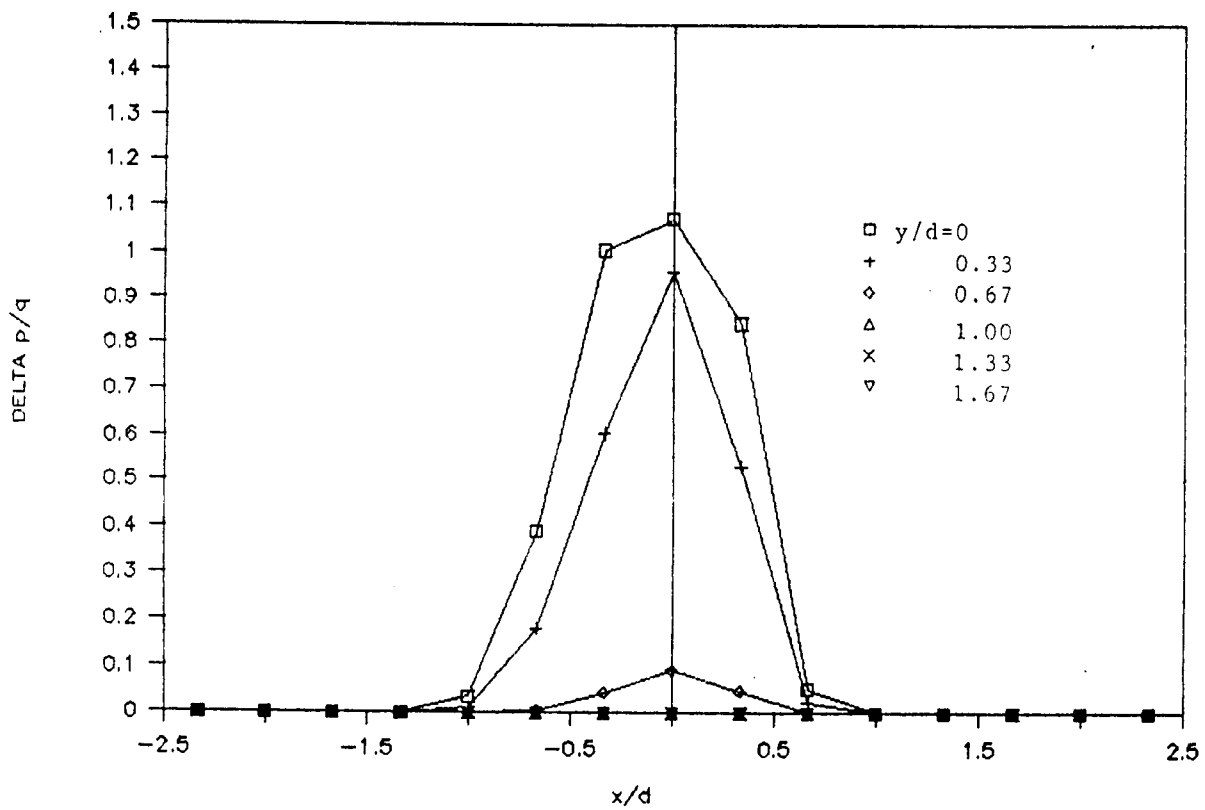
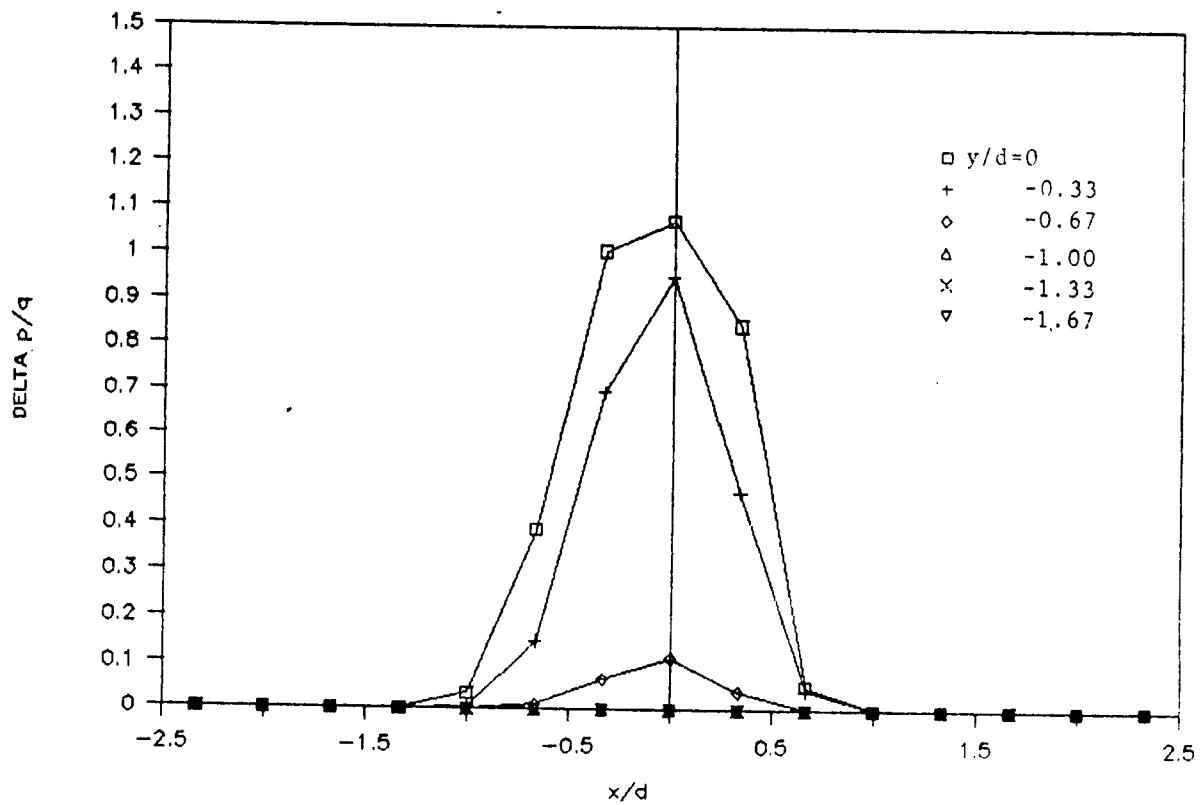


Figure 35. Jet Cross Section Pressure Distribution, $d=0.6''$, $h/d=3.0$, $Q_j = 1054$ psf

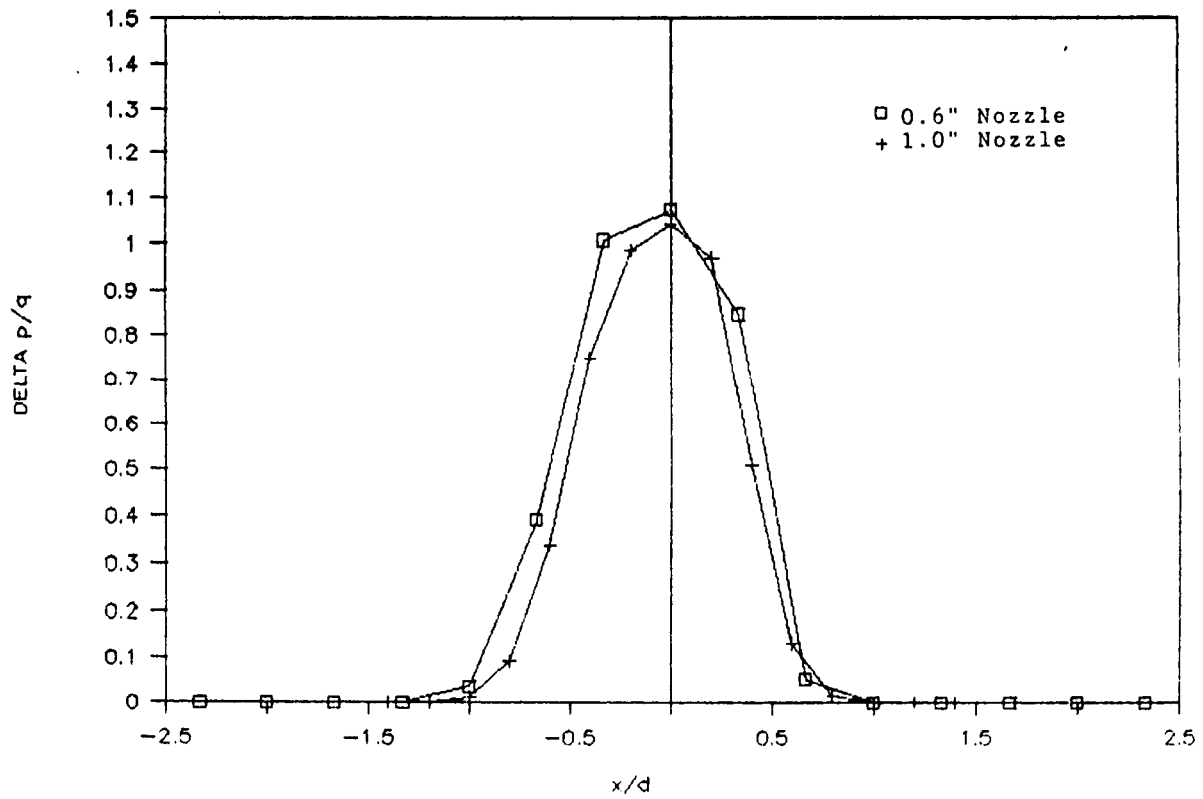


Figure 36. Comparison of Jet Cross Section Pressure Distribution
 $h/d=3.0, y/d=0.0$

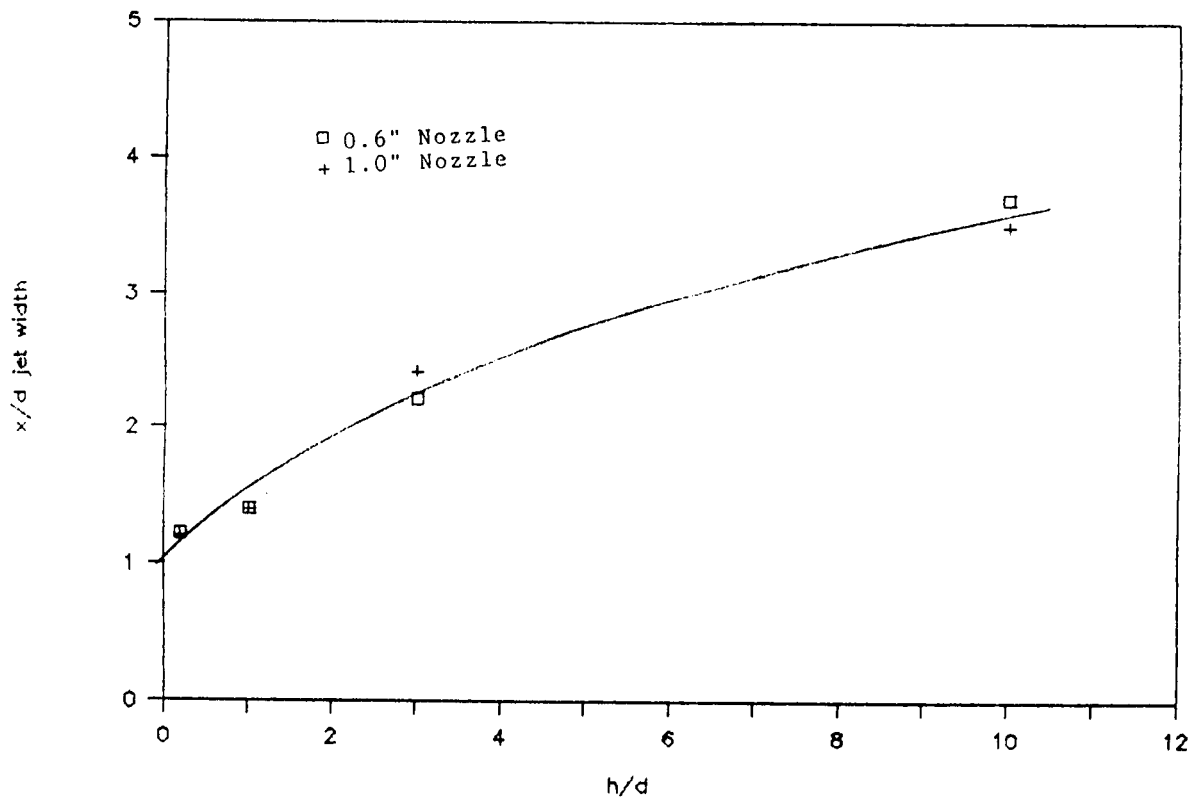


Figure 37. Comparison of Jet Expansion

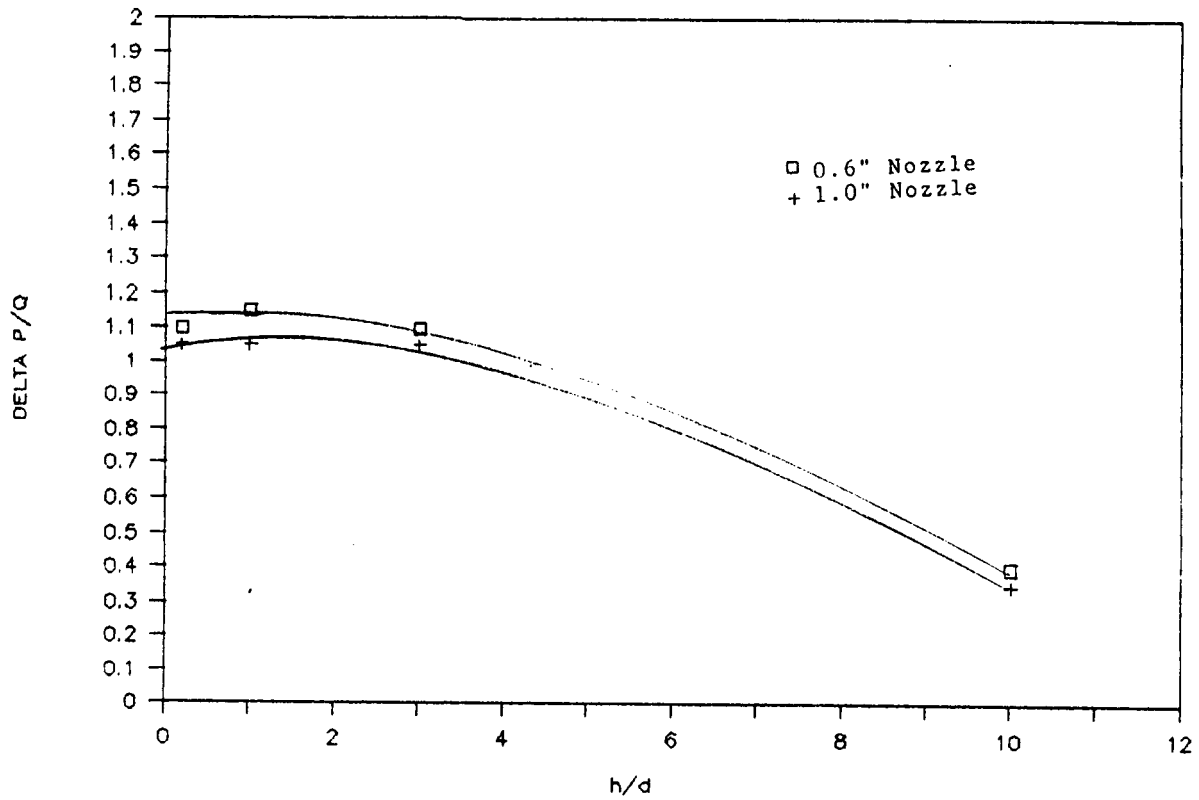


Figure 38. Comparison of Jet Pressure Coefficient Along Jet Centerline

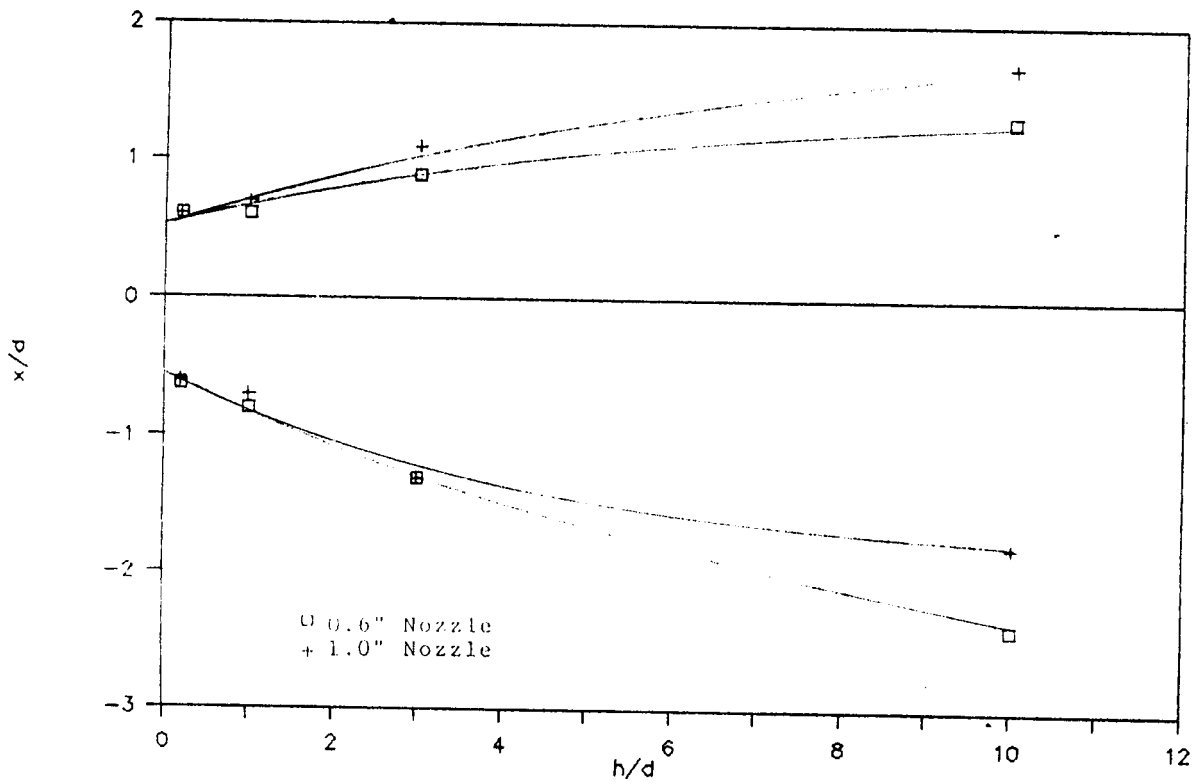


Figure 39. Comparison of Jet Shapes at $y/d=0.0$

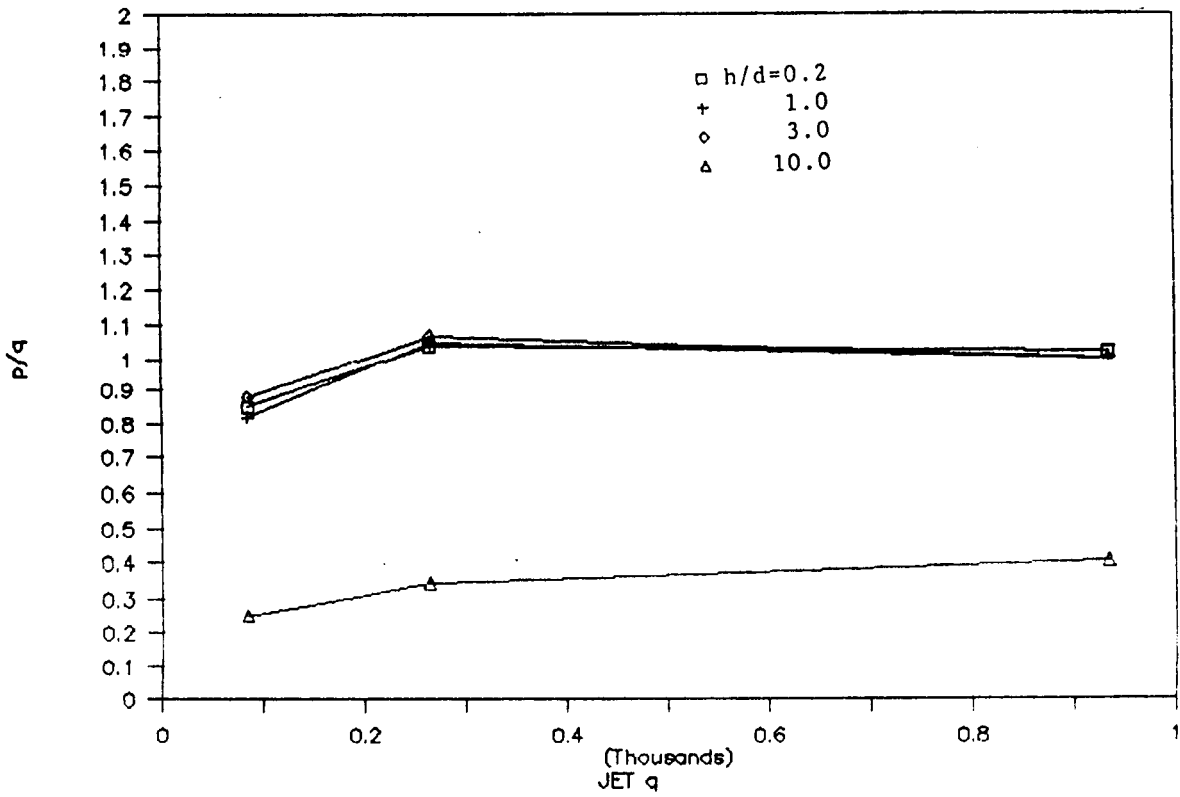


Figure 40. Effect of Jet Dynamic Pressure on Jet Pressure Ratio for the One Inch Jet

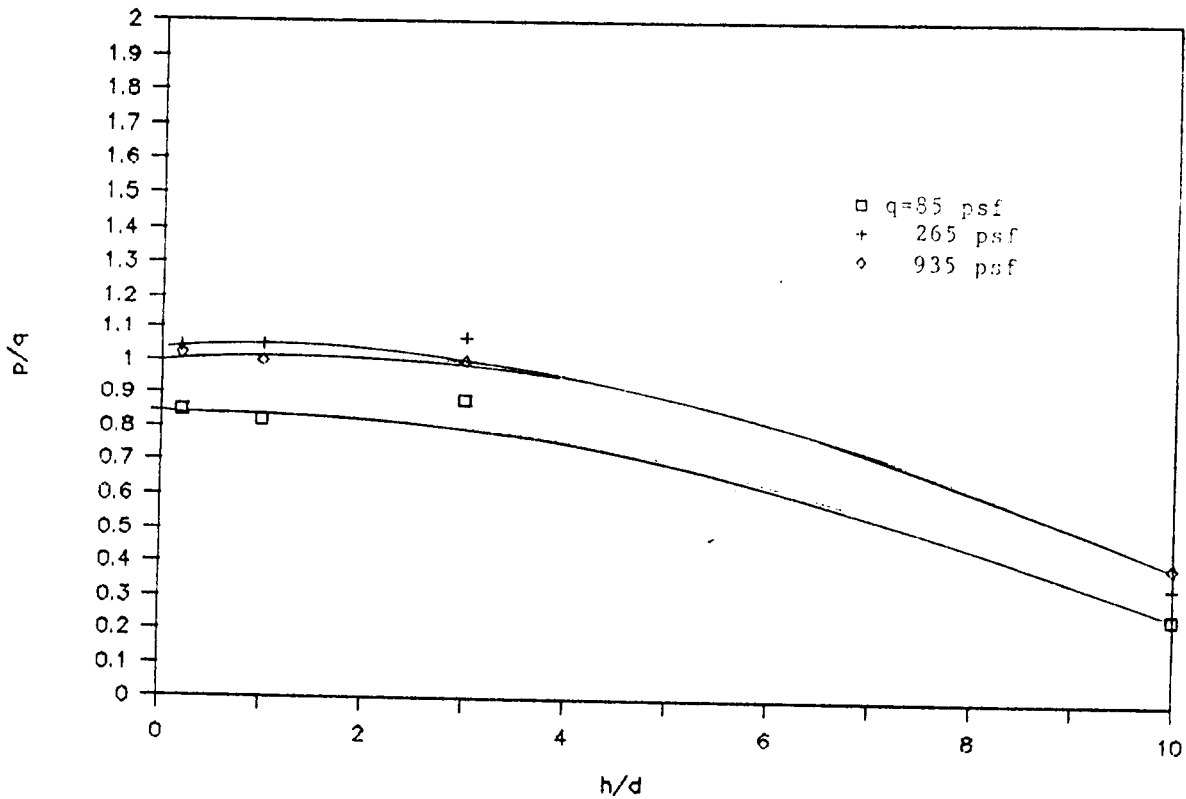


Figure 41. Comparison of One Inch Jet Pressure Ratio at Various Jet Dynamic Pressures

APPENDIX A

BASIC DATA FOR THE 1.0 INCH JET NOZZLE

APPENDIX A

LIST OF FIGURES

FIGURE	TITLE	PAGE
A1	Ground Board Pressure Distribution, Run 12, $V_e=0.042$	A4
A2	Ground Board Pressure Distribution, Run 13, $V_e=0.043$	A6
A3	Ground Board Pressure Distribution, Run 14, $V_e=0.043$	A8
A4	Ground Board Pressure Distribution, Run 15, $V_e=0.053$	A10
A5	Ground Board Pressure Distribution, Run 21, $V_e=0.041$	A12
A6	Ground Board Pressure Distribution, Run 22, $V_e=0.041$	A14
A7	Ground Board Pressure Distribution, Run 25, $V_e=0.168$	A16
A8	Ground Board Pressure Distribution, Run 26, $V_e=0.166$	A17
A9	Ground Board Pressure Distribution, Run 27, $V_e=0.169$	A18
A10	Ground Board Pressure Distribution, Run 28, $V_e=0.187$	A19
A11	Ground Board Pressure Distribution, Run 29, $V_e=0.095$	A20
A12	Ground Board Pressure Distribution, Run 31, $V_e=0.174$	A22
A13	Ground Board Pressure Distribution, Run 32, $V_e=0.173$	A23
A14	Ground Board Pressure Distribution, Run 40, $V_e=0.187$	A24
A15	Ground Board Pressure Distribution, Run 42 $V_e=0.088$	A25

LIST OF FIGURES (CONT.)

FIGURE	TITLE	PAGE
A16	Ground Board Pressure Distribution, Run 43, $V_e=0.090$	A27

LIST OF TABLES

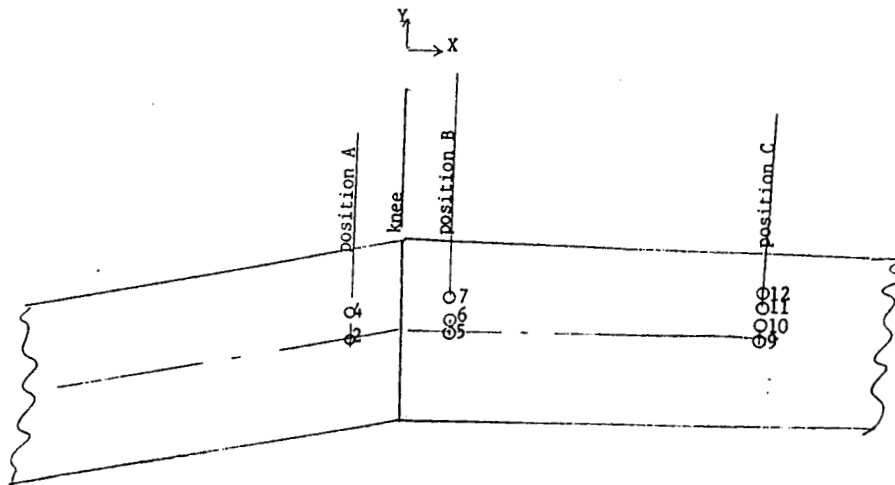
TABLE	TITLE	PAGE
A1	RUN SCHEDULE AND TEST CONDITIONS	A3
A2	INSTRUMENTATION LOCATION	A3

TABLE A1. RUN SCHEDULE AND TEST CONDITIONS

RUN	Qm	Qm	Qj	Qj/Qm	Vj/V	V/Vj
12	0.0195	2.808	1622.4	577.7777	24.03700	0.041602
13	0.022	3.168	1715.5	541.5088	23.27034	0.042973
14	0.0197	2.8368	1477.6	520.8685	22.82254	0.043816
15	0.0209	3.0096	1061.1	352.5717	18.77689	0.053256
21	0.0297	4.2768	2502.1	585.0402	24.18760	0.041343
22	0.0306	4.4064	2601.1	590.3004	24.29609	0.041158
25	0.05133	7.39152	259.3	35.08074	5.922899	0.168836
26	0.05108	7.35552	267.2	36.32645	6.027143	0.165916
27	0.05166	7.43904	259.8	34.92386	5.909641	0.169215
28	0.053706	7.733664	220	28.44705	5.333578	0.187491
29	0.05451	7.84944	878.4	111.9060	10.57856	0.094530
31	0.066436	9.566784	316.4	33.07276	5.750892	0.173886
32	0.06755	9.7272	323.8	33.28809	5.769583	0.173322
40	0.08207	11.81808	339.5	28.72717	5.359773	0.186575
42	0.08207	11.81808	1536.8	130.0380	11.40342	0.087692
43	0.08298	11.94912	1490.7	124.7539	11.16933	0.089530

TABLE A2. INSTRUMENTATION LOCATION

TAP #	POSITION	X	Y
2	A	-2.5 INCHES	0
4	A	-2.5 inches	5.5 INCHES
5	B	10.0 INCHES	0
6	B	10.0 INCHES	1.5 INCHES
7	B	10.0 INCHES	7.5 INCHES
9	C	25.0 FEET	0
10	C	25.0 FEET	3.0 INCHES
11	C	25.0 FEET	7.0 INCHES
12	C	25.0 FEET	15.0 INCHES



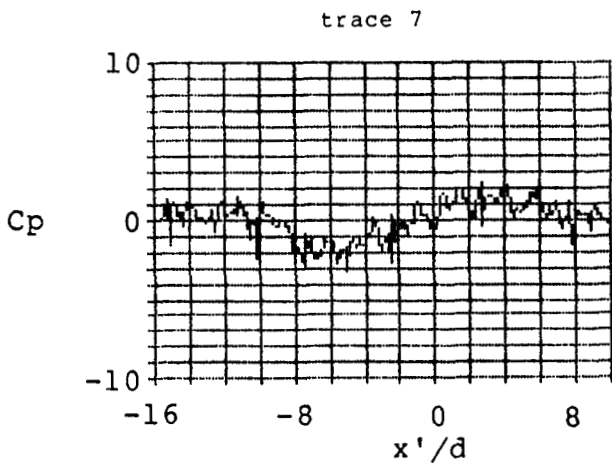
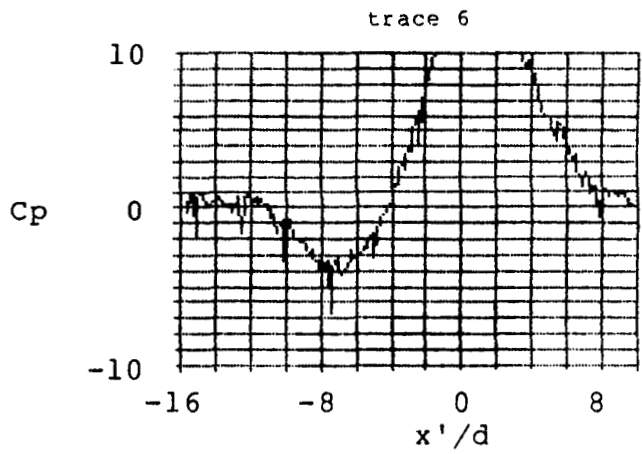
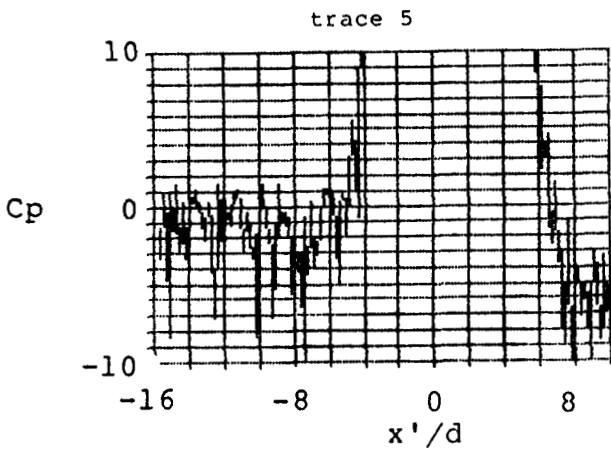
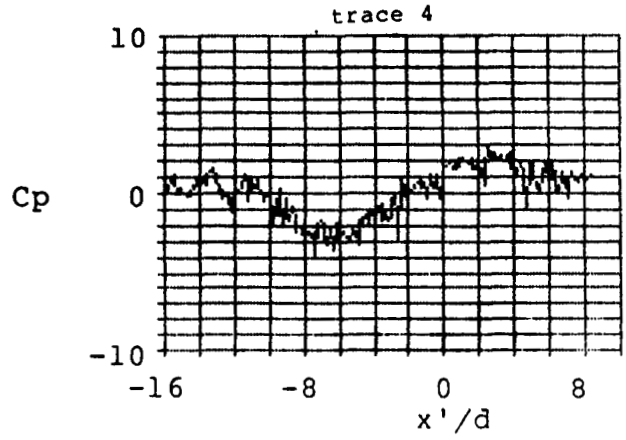
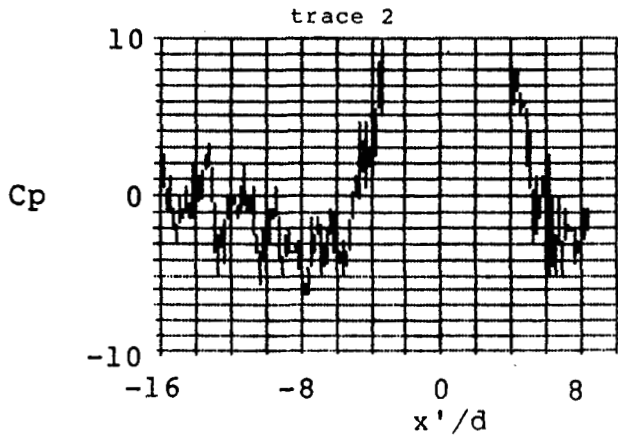


Figure A1 . Ground Board Pressure Distribution, Run 12 , $Ve = .042$

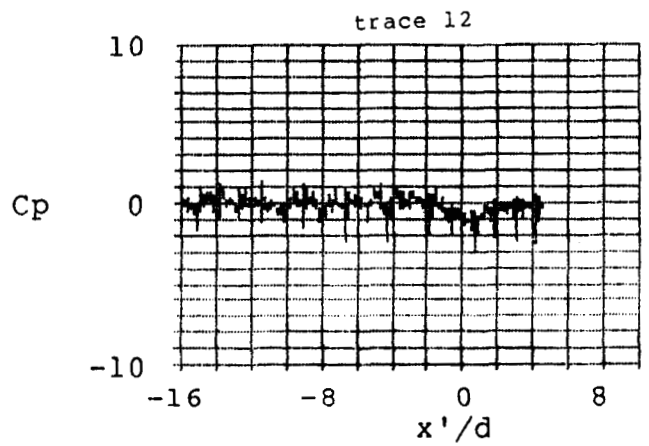
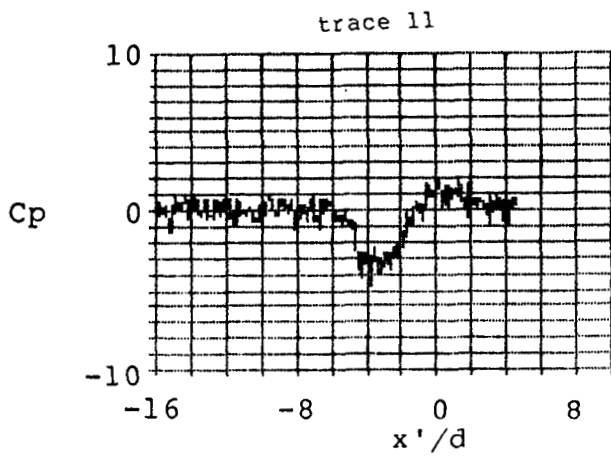
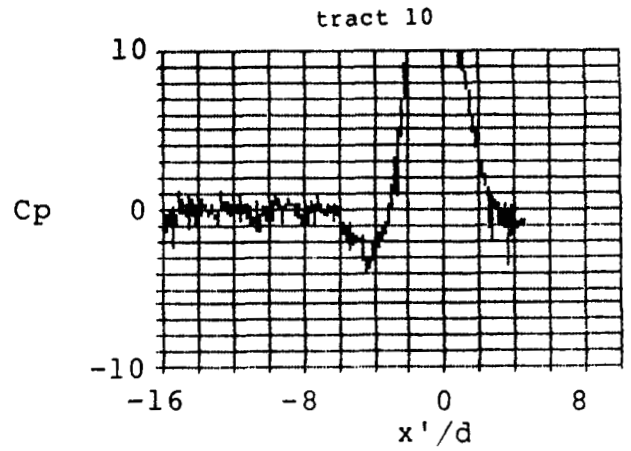
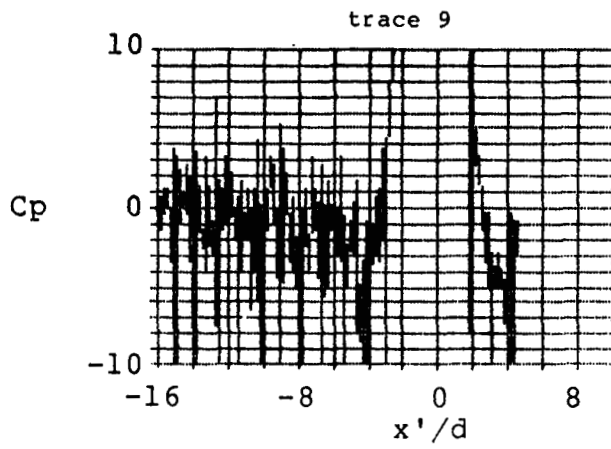


Figure A1 . Ground Board Pressure Distribution, Run 12 , $Ve=.042$

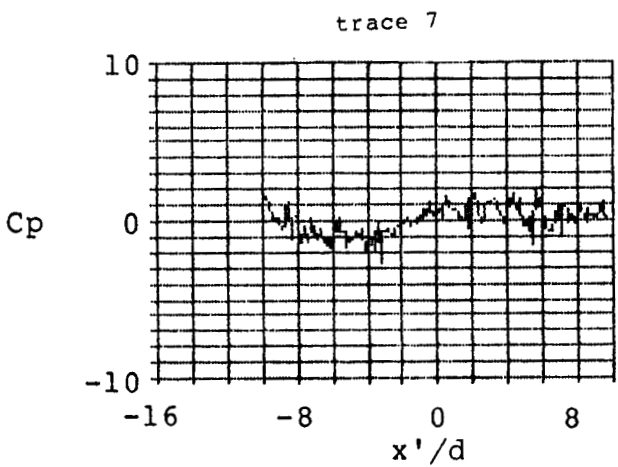
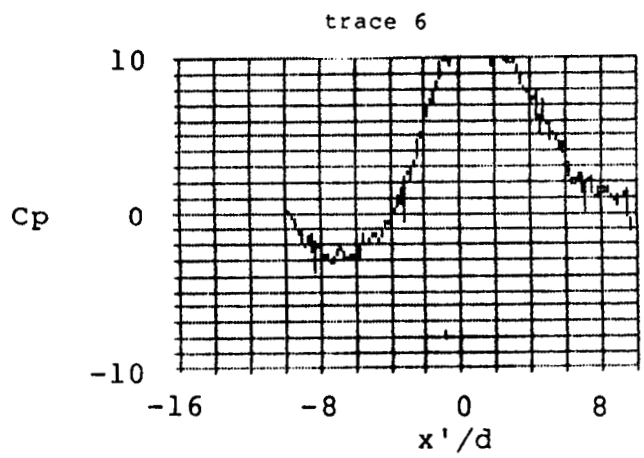
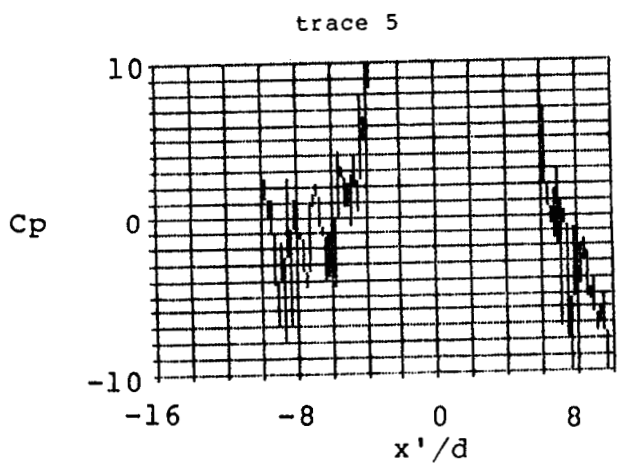
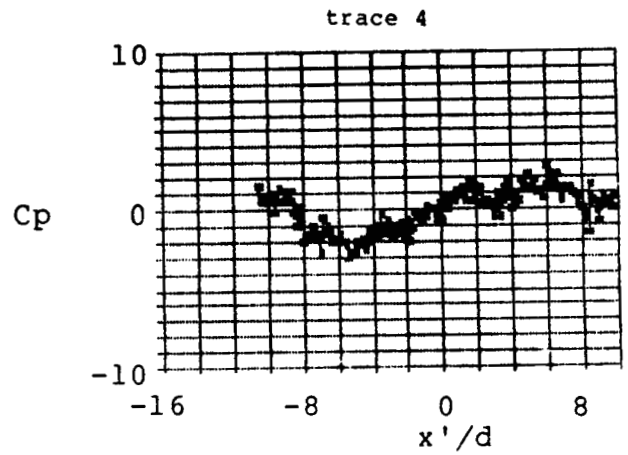
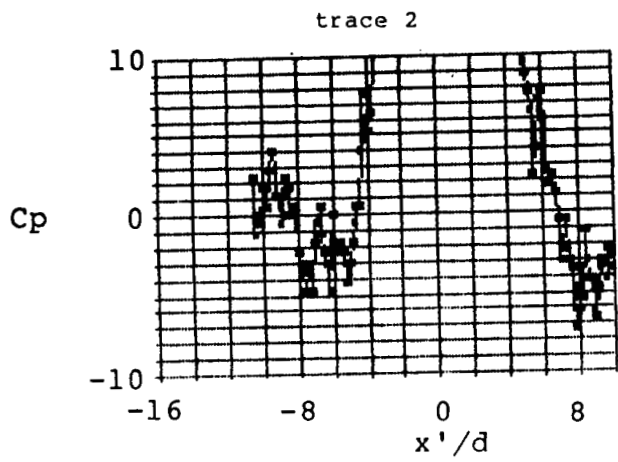


Figure A2 . Ground Board Pressure Distribution, Run 13 , $Ve = .043$

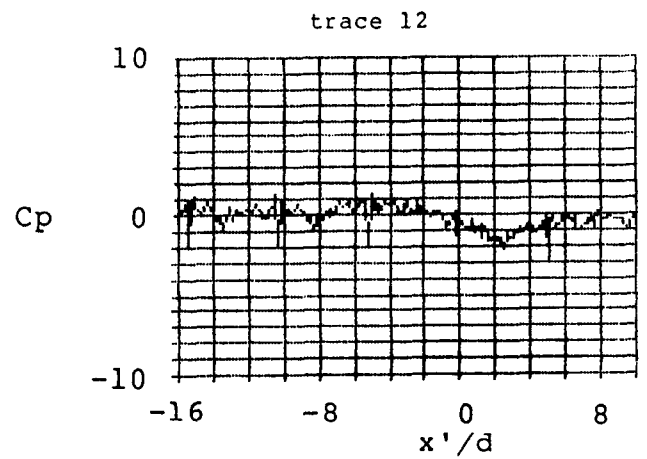
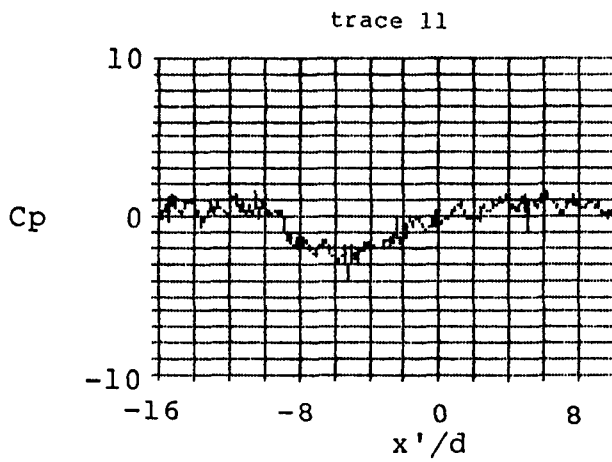
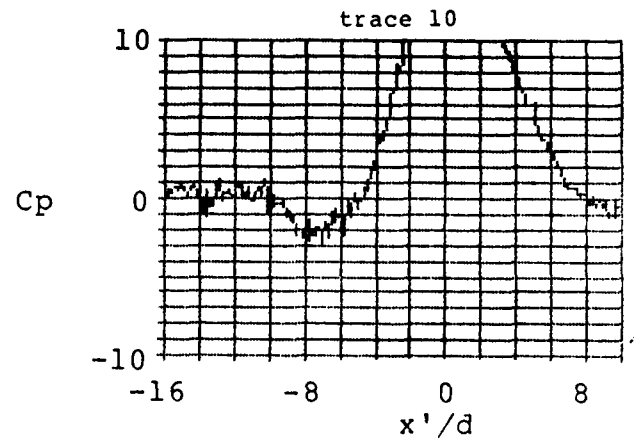
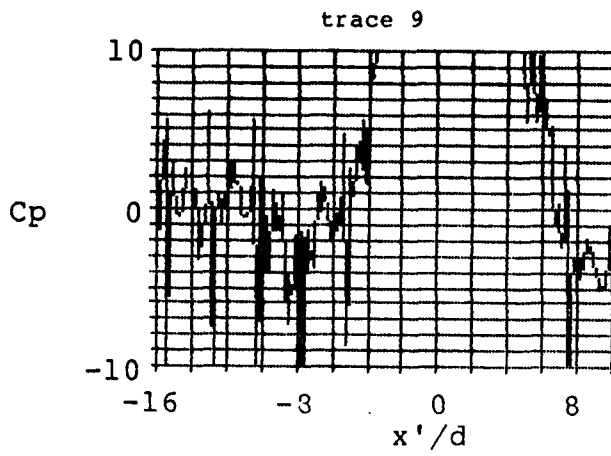


Figure A2 . Ground Board Pressure Distribution, Run 13, $Ve = .043$

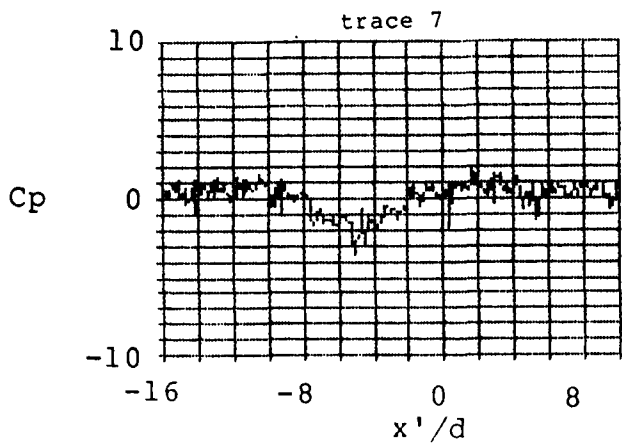
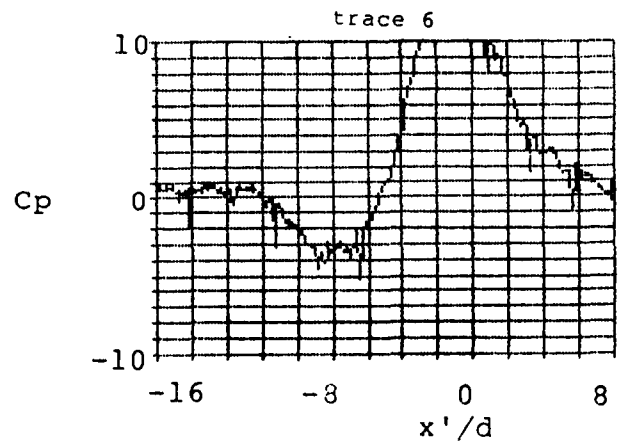
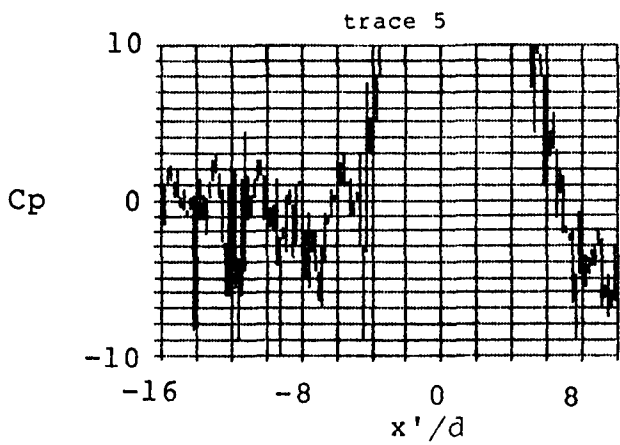
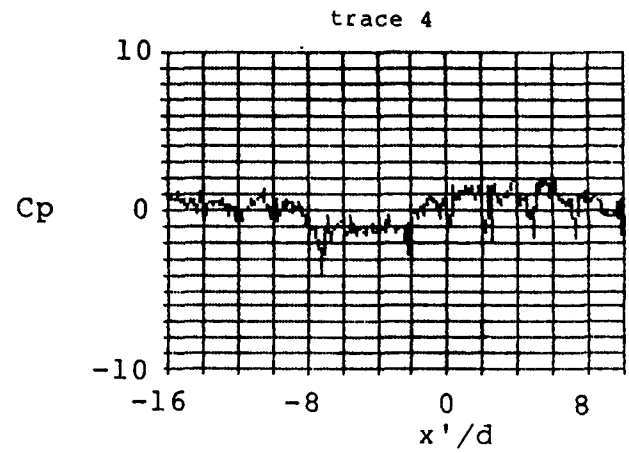
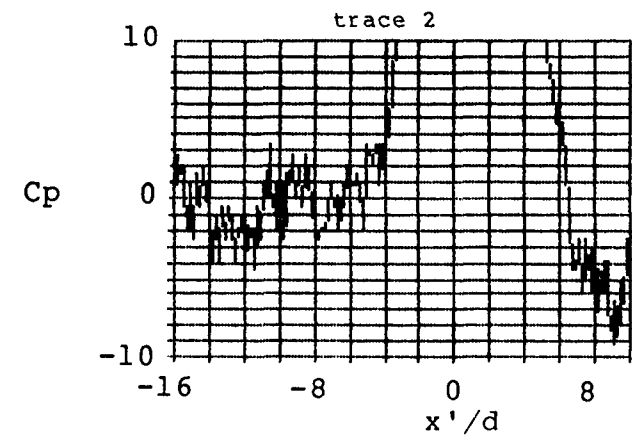


Figure A3 . Ground Board Pressure Distribution, Run 14 , $Ve = .044$

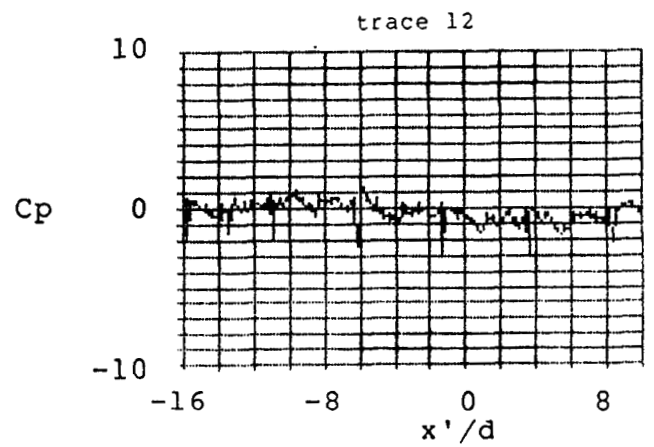
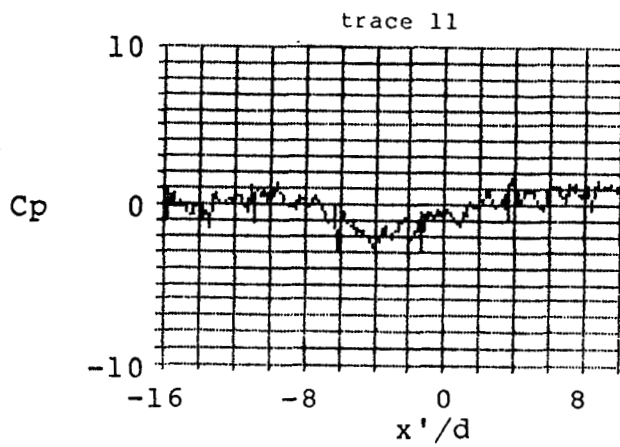
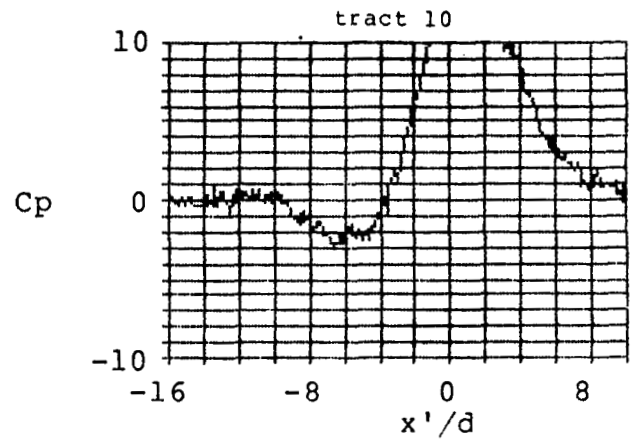
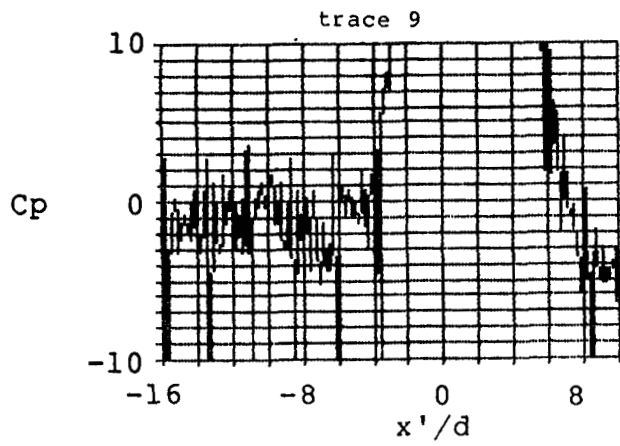


Figure A3 . Ground Board Pressure Distribution, Run 14 , $Ve = .044$

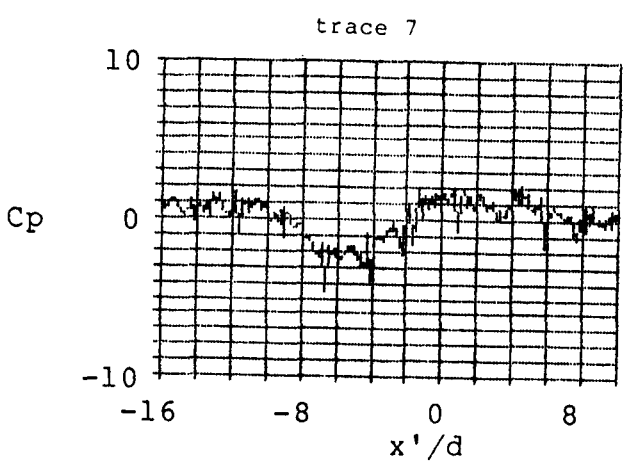
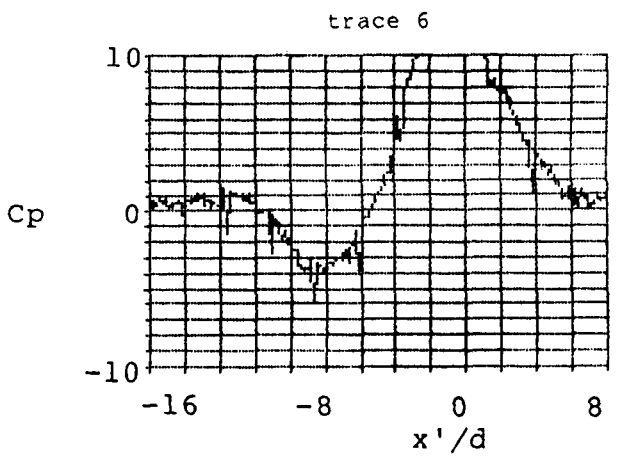
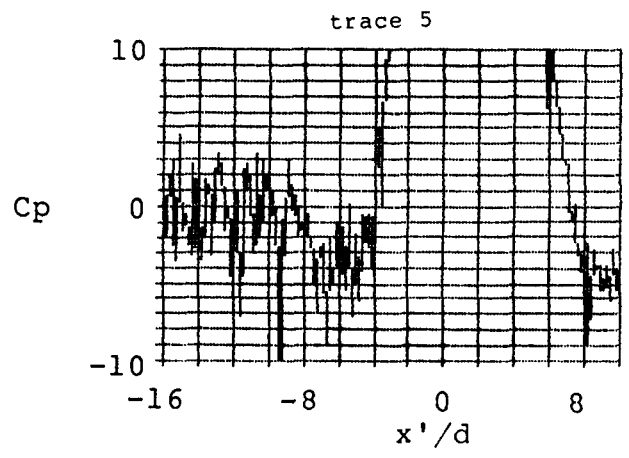
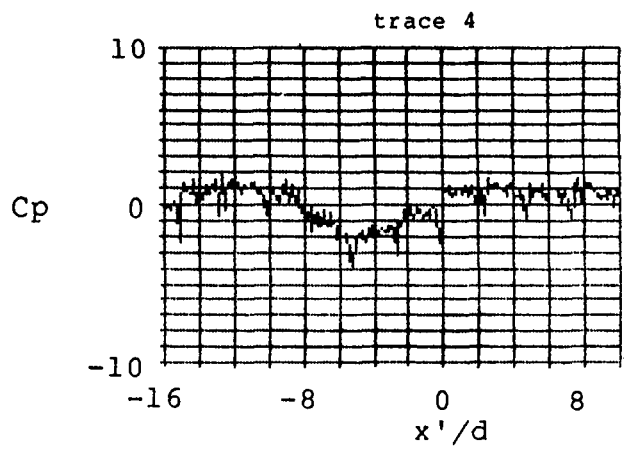
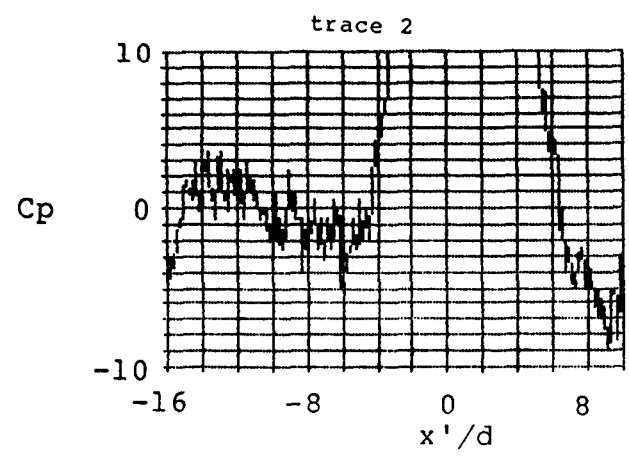


Figure A4 . Ground Board Pressure Distribution, Run 15 , $Ve = .053$

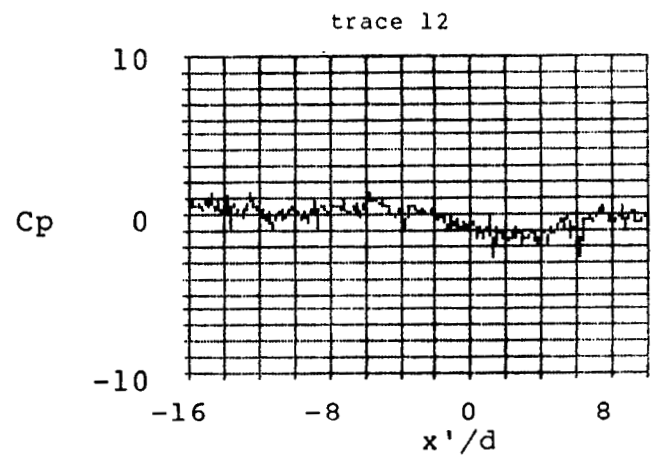
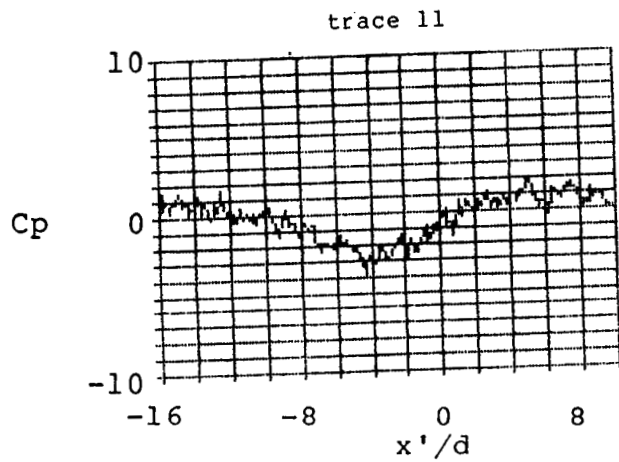
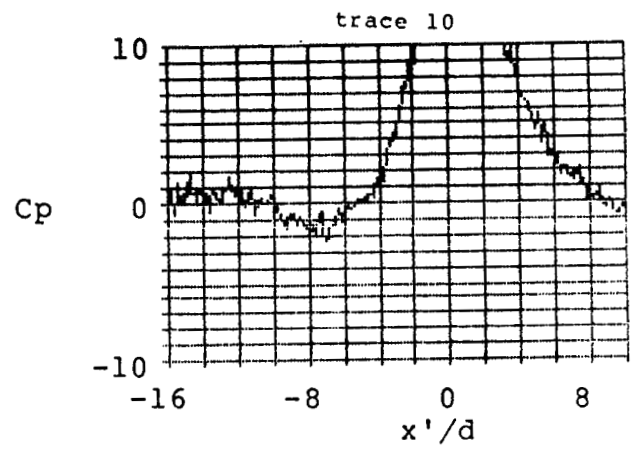
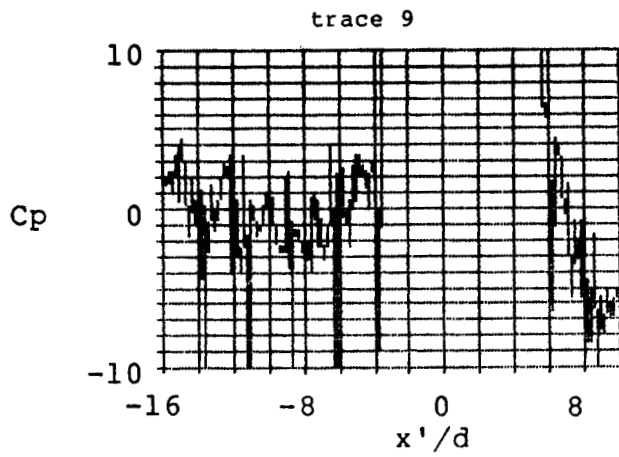


Figure A4 . Ground Board Pressure Distribution, Run 15 , $Ve=.053$

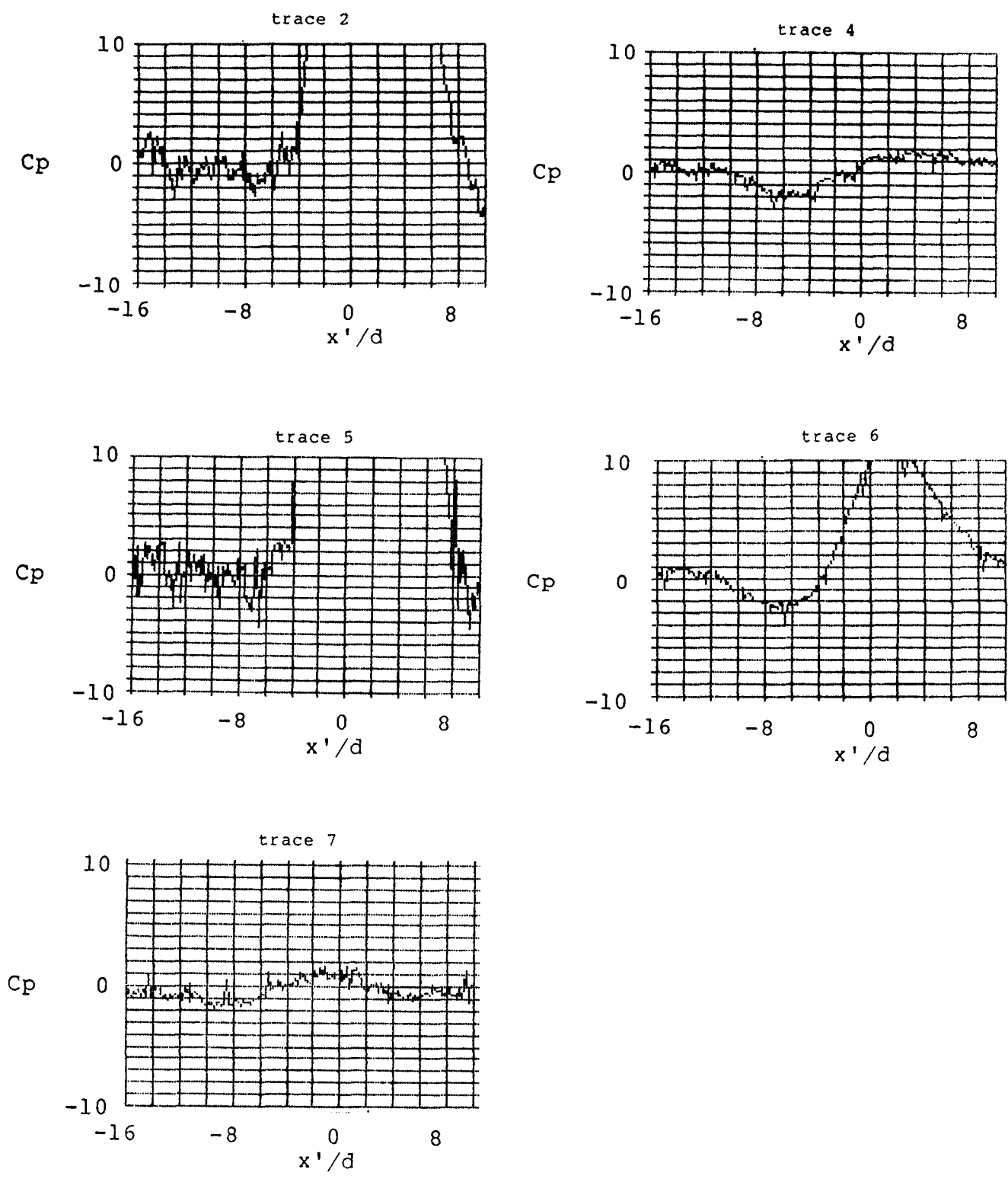


Figure A5 . Ground Board Pressure Distribution, Run 21, $Ve = .041$

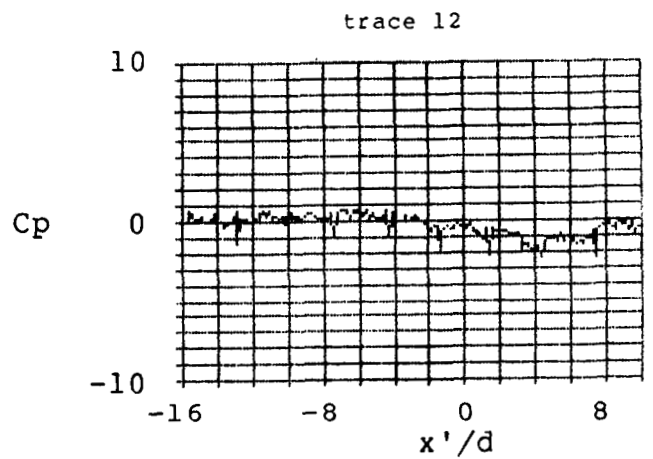
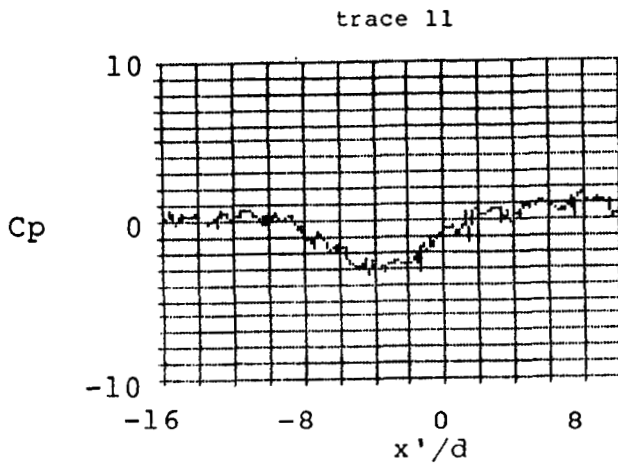
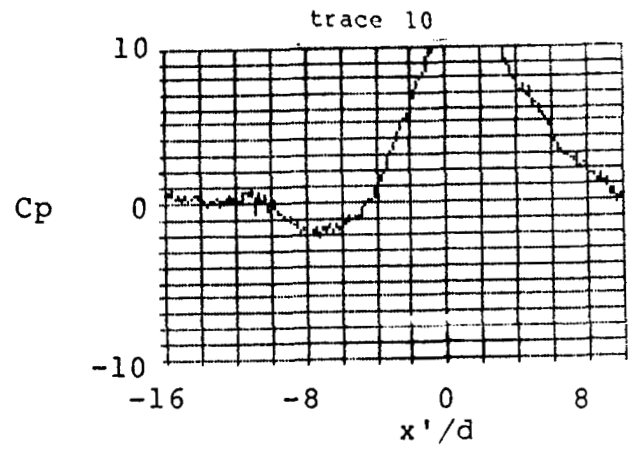
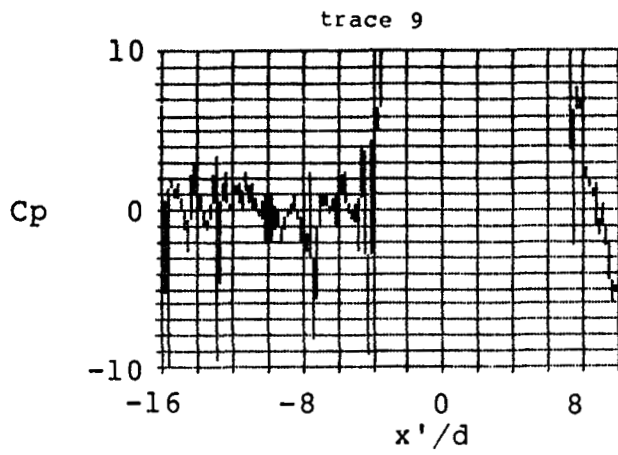


Figure A5 . Ground Board Pressure Distribution, Run 21 , $Ve = .041$

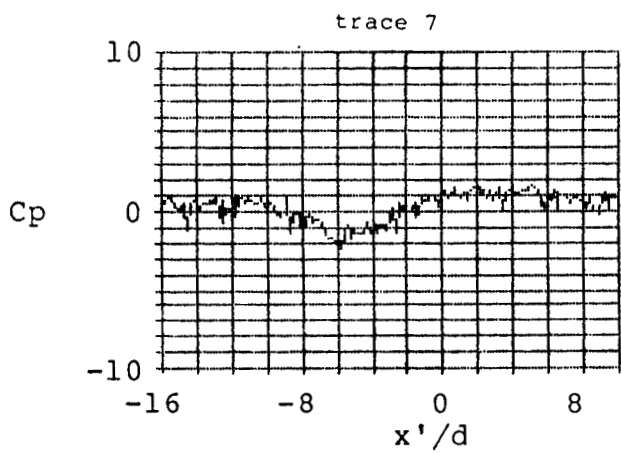
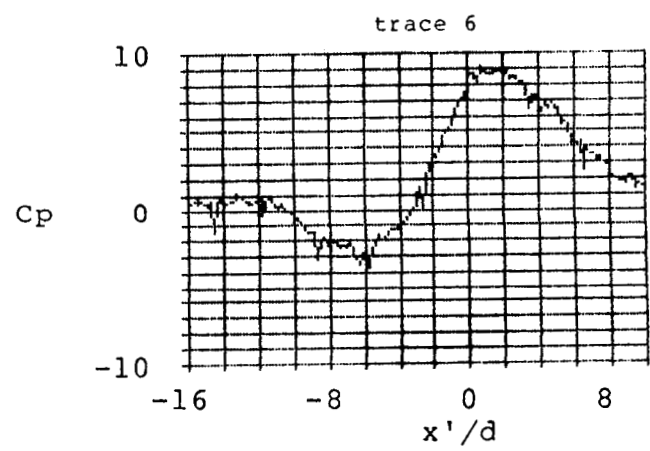
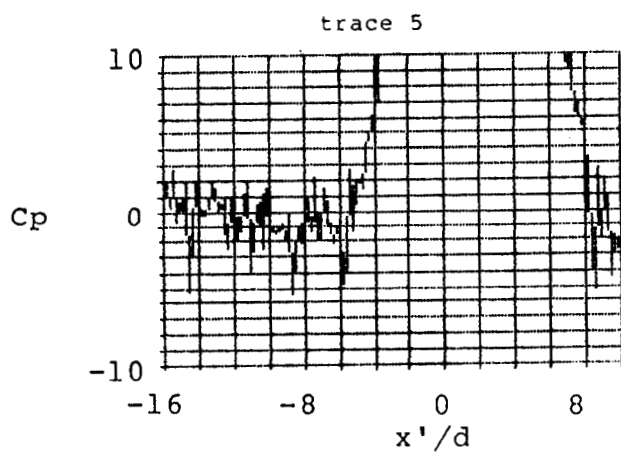
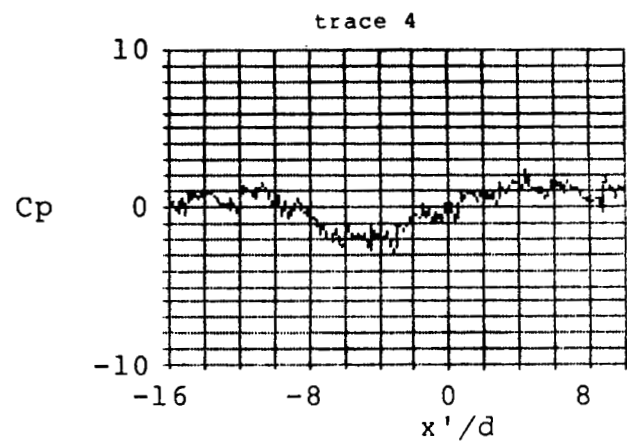
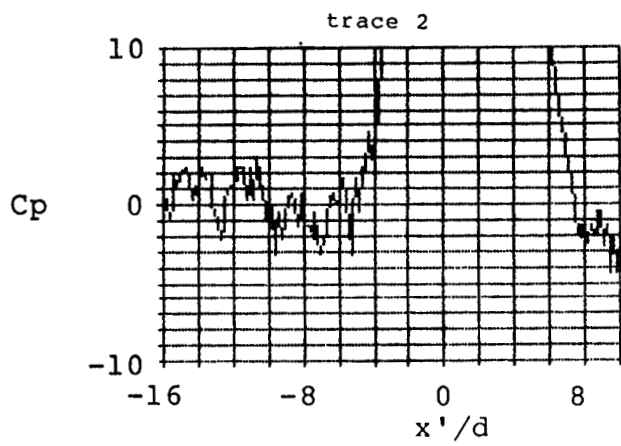


Figure A6 . Ground Board Pressure Distribution, Run 22 , $Ve = .041$

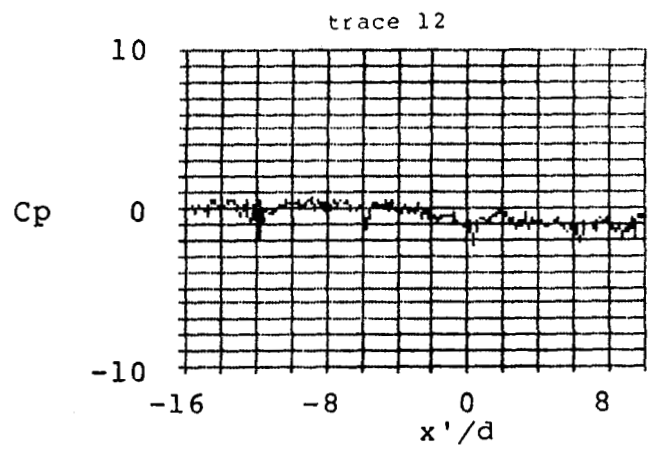
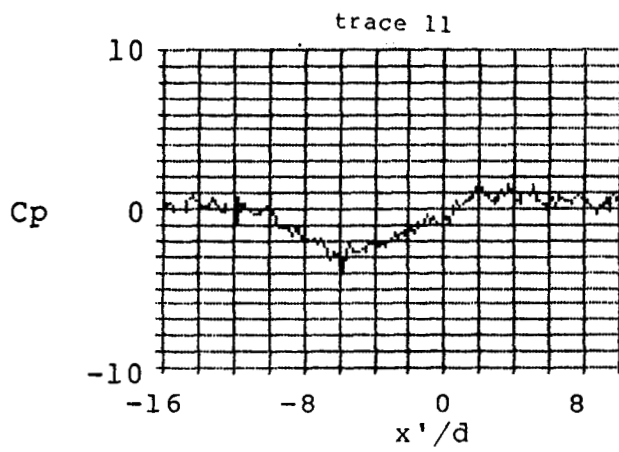
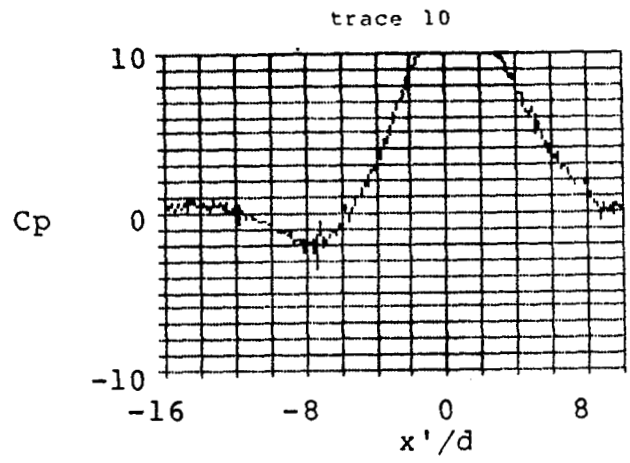
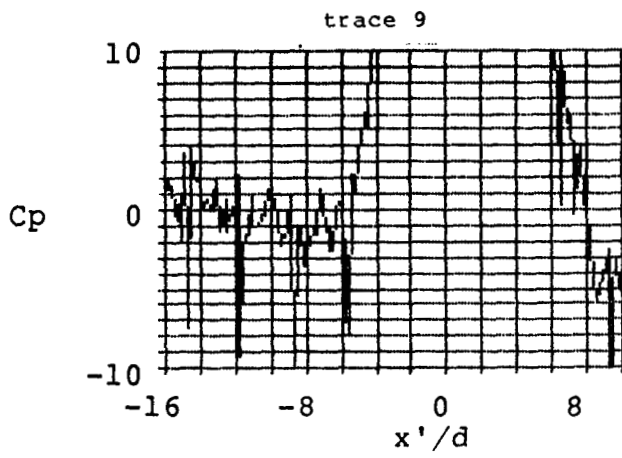


Figure A6 . Ground Board Pressure Distribution, Run 22 , $Ve = .041$

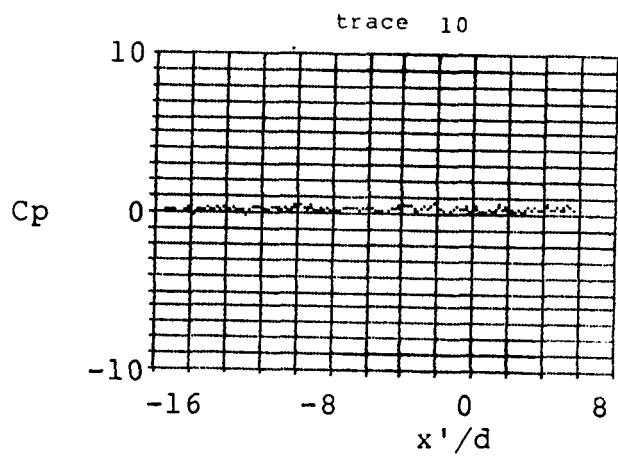
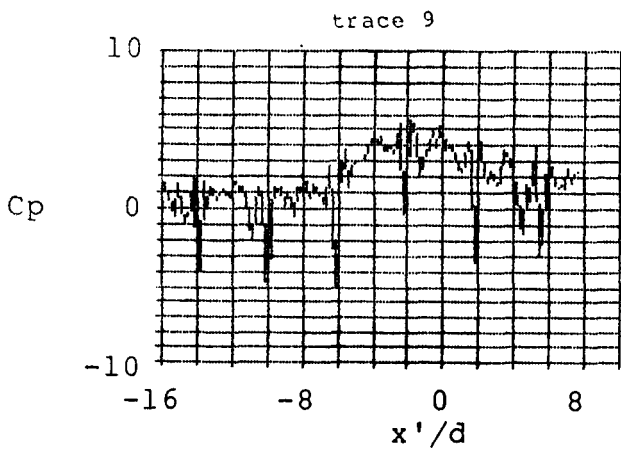
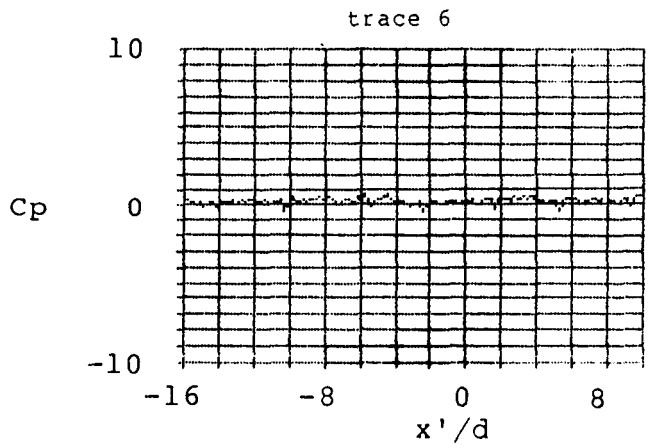
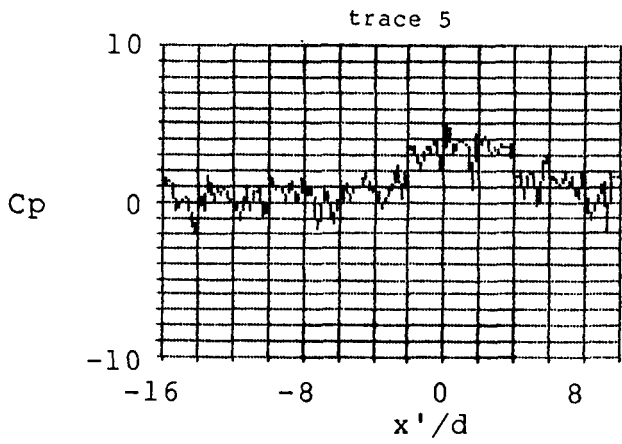
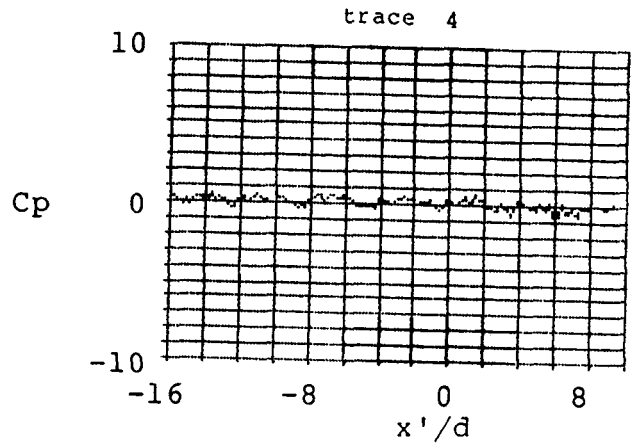
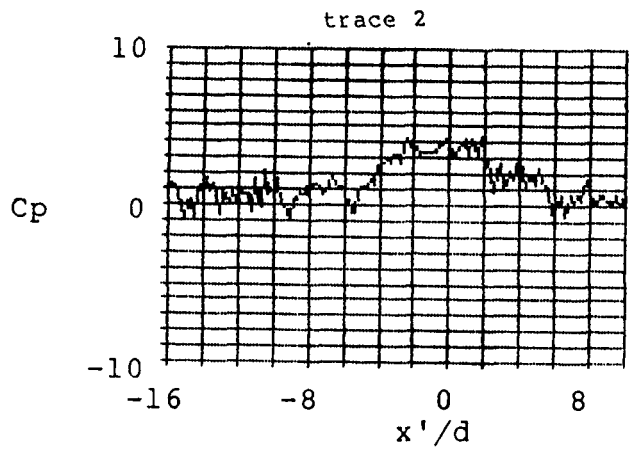


Figure A7 . Ground Board Pressure Distribution, Run 25 , $Ve=.169$

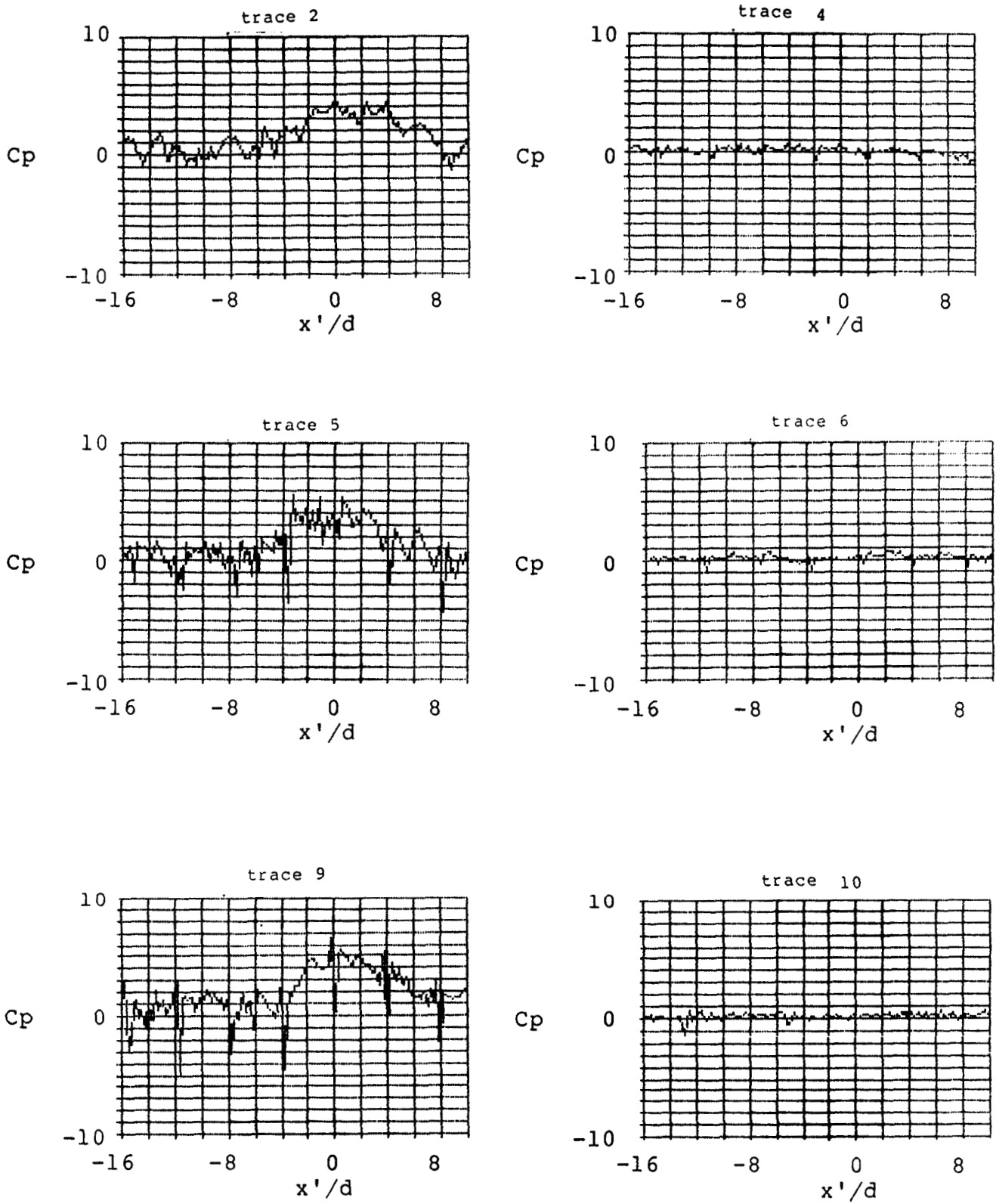


Figure A8 . Ground Board Pressure Distribution, Run 26 , $Ve = .166$

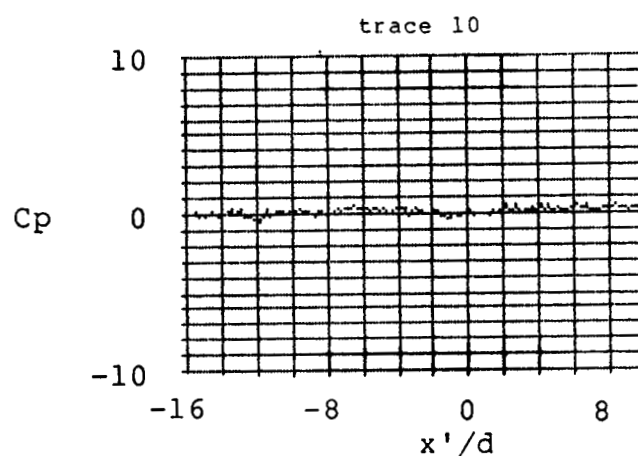
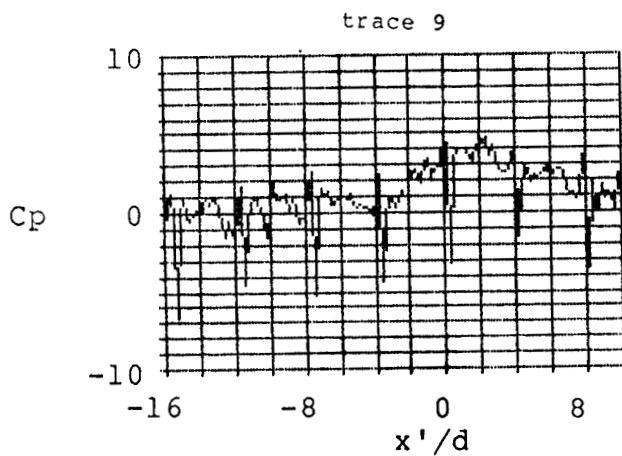
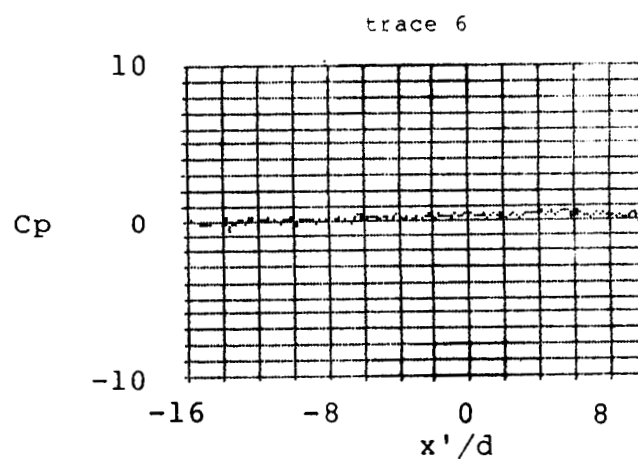
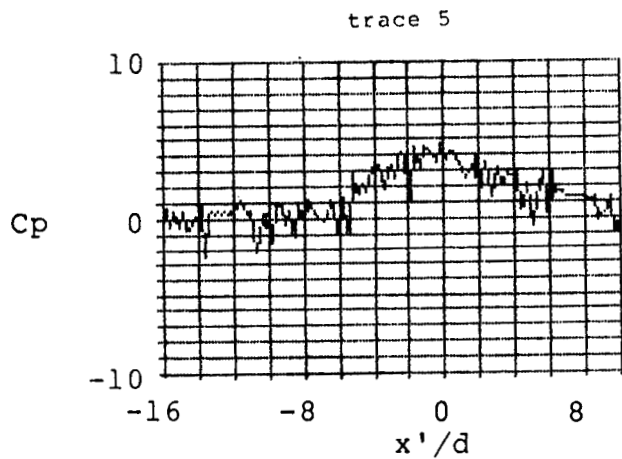
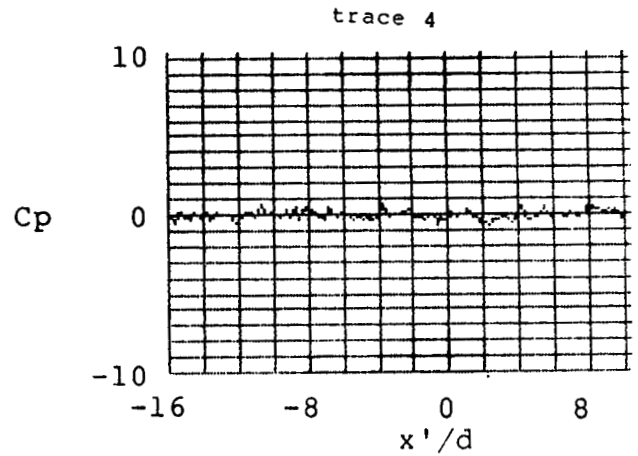
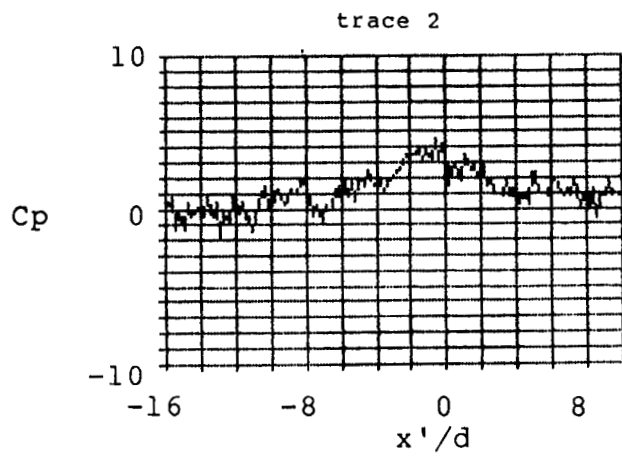


Figure A9 . Ground Board Pressure Distribution, Run 27 , $Ve=.169$

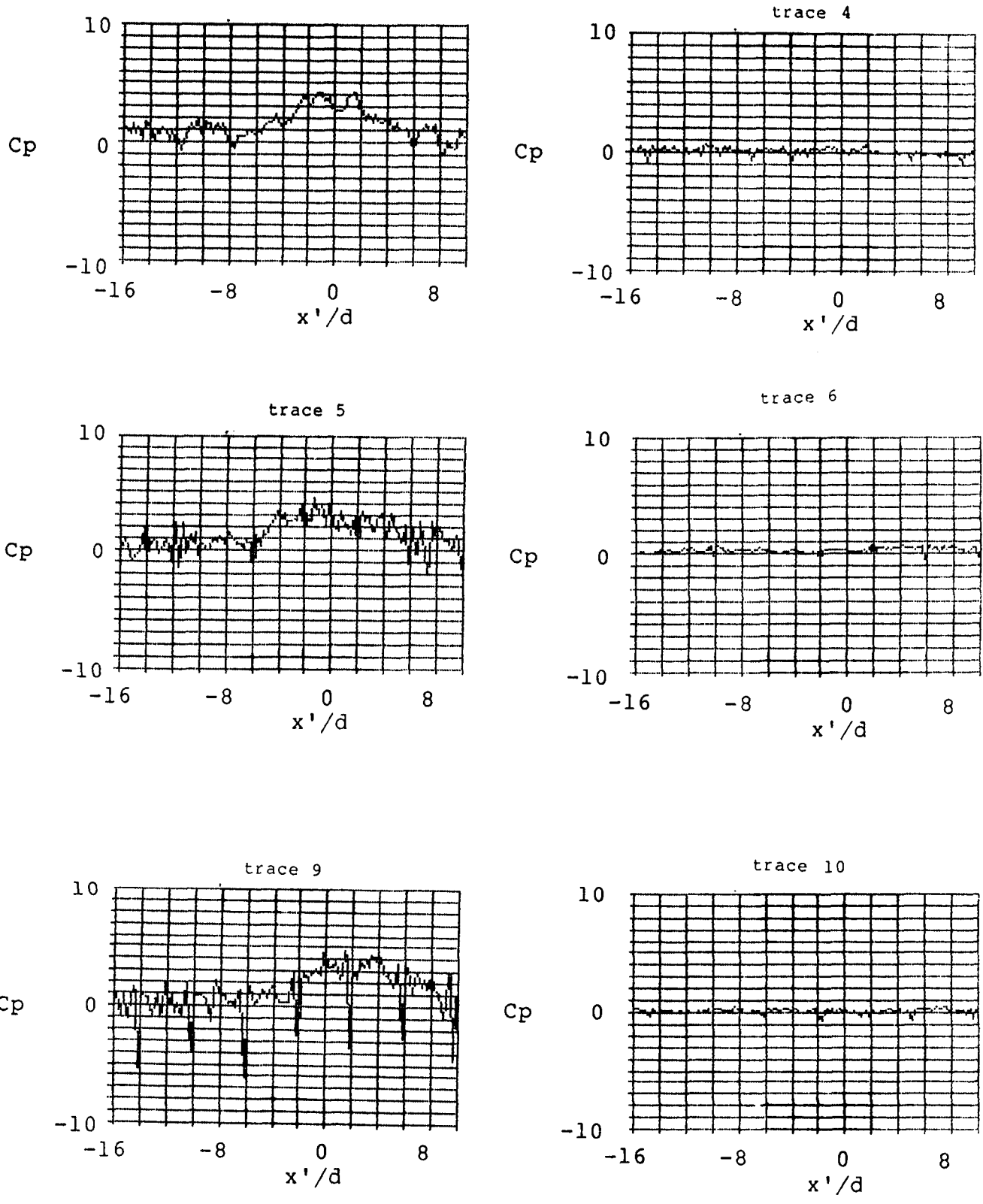


Figure A10 . Ground Board Pressure Distribution, Run 28 , $Ve=.187$

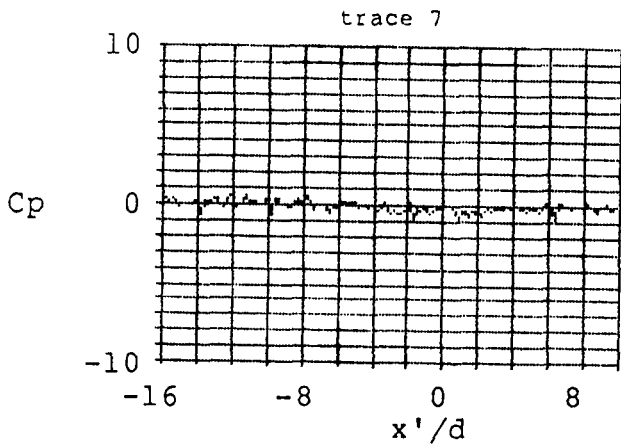
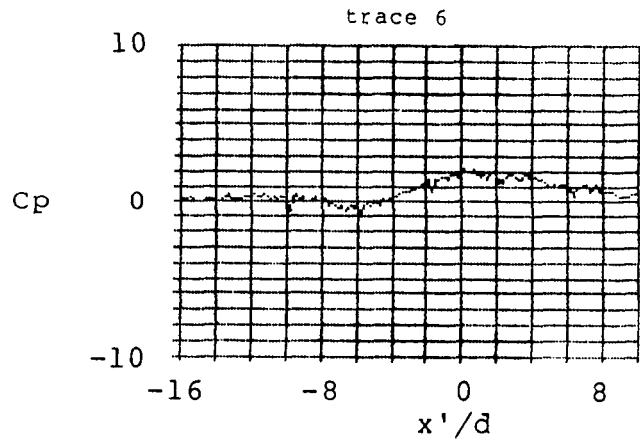
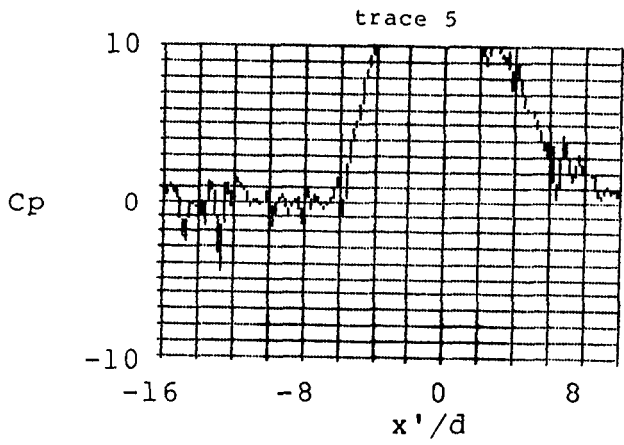
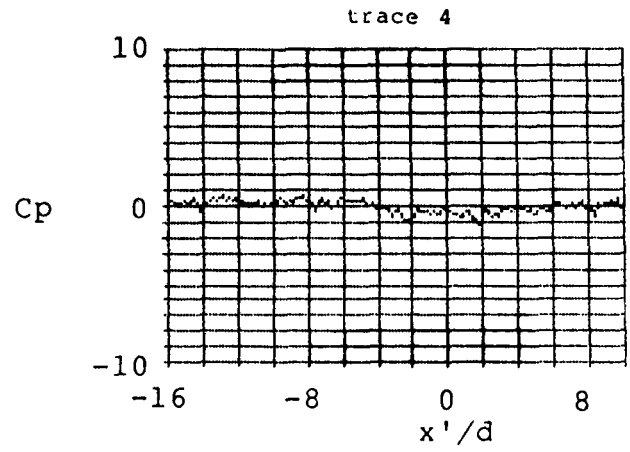
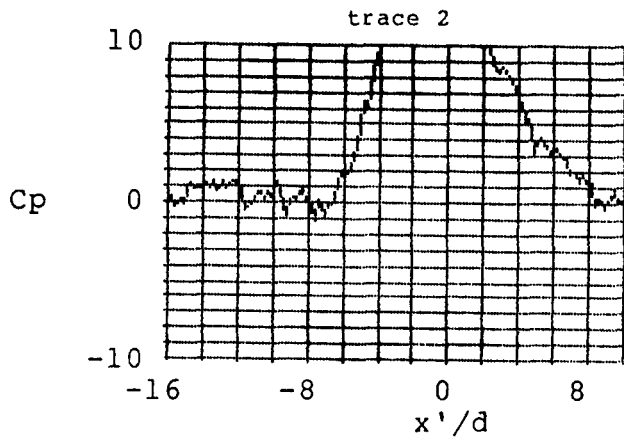


Figure All . Ground Board Pressure Distribution, Run 29 , $Ve = .095$

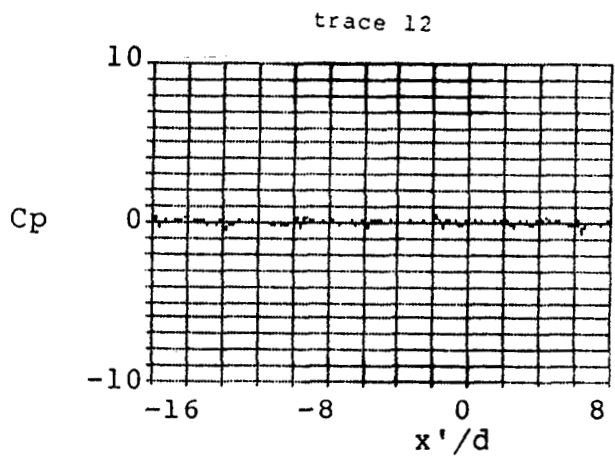
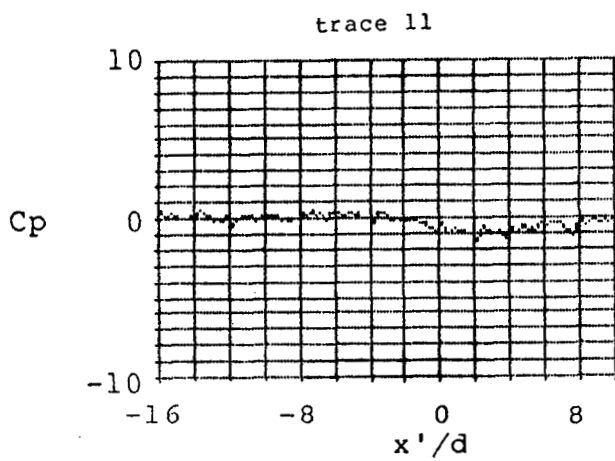
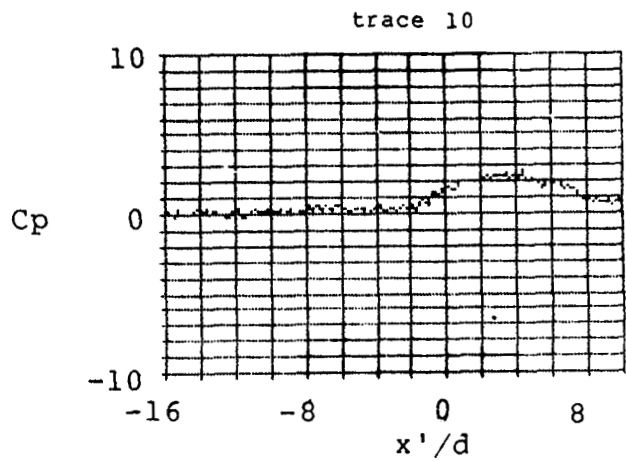
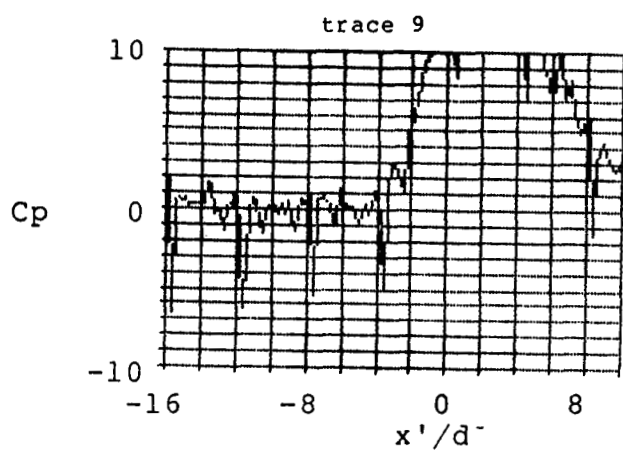


Figure A11 . Ground Board Pressure Distribution, Run 29 , $Ve = .095$

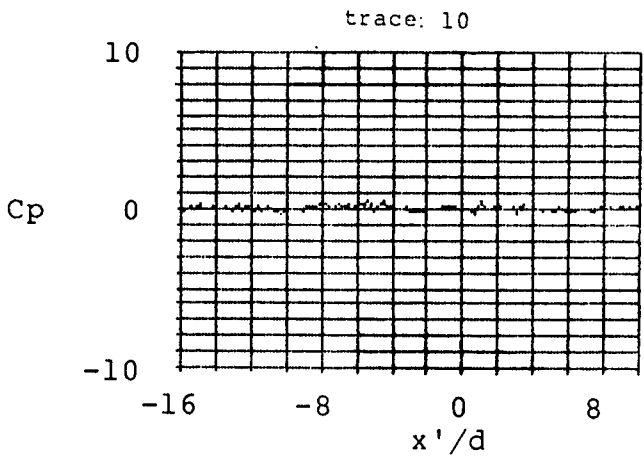
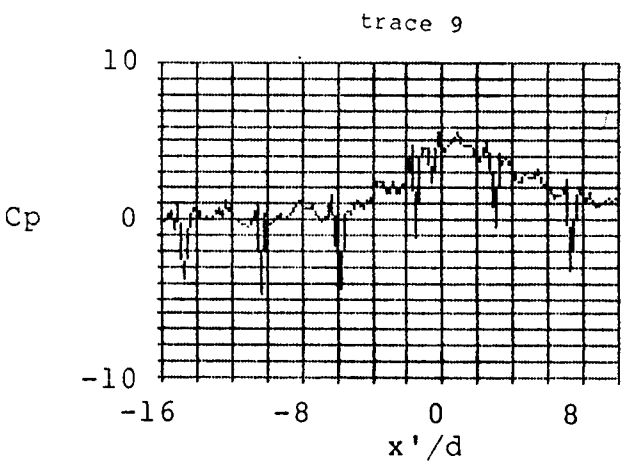
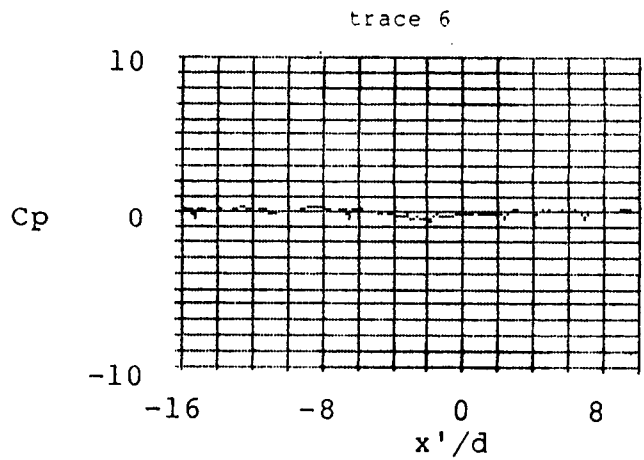
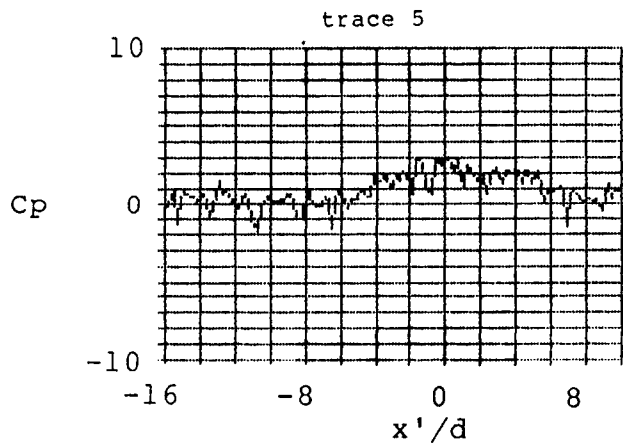
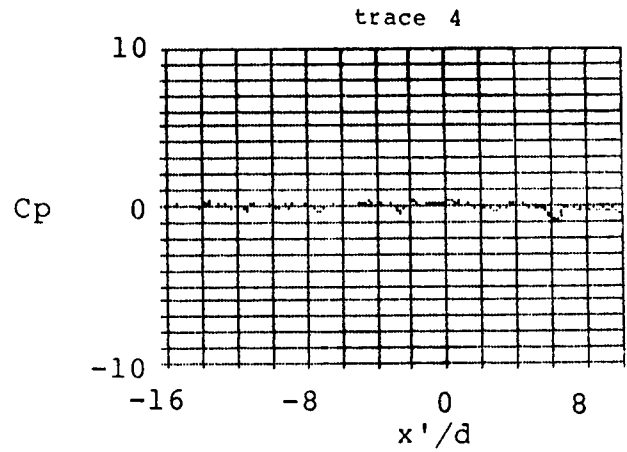
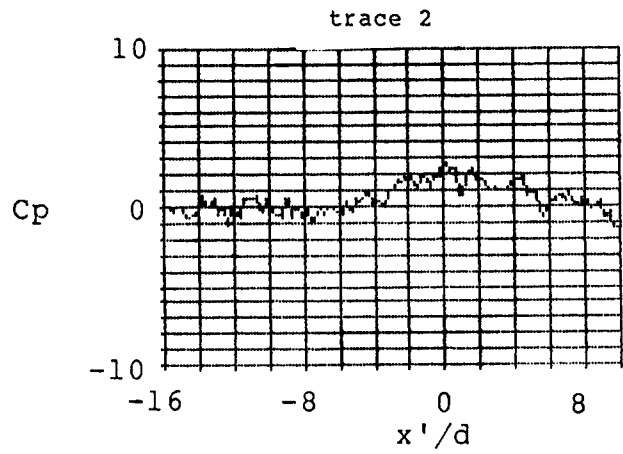


Figure A12 . Ground Board Pressure Distribution, Run 31 , $V_e = .174$

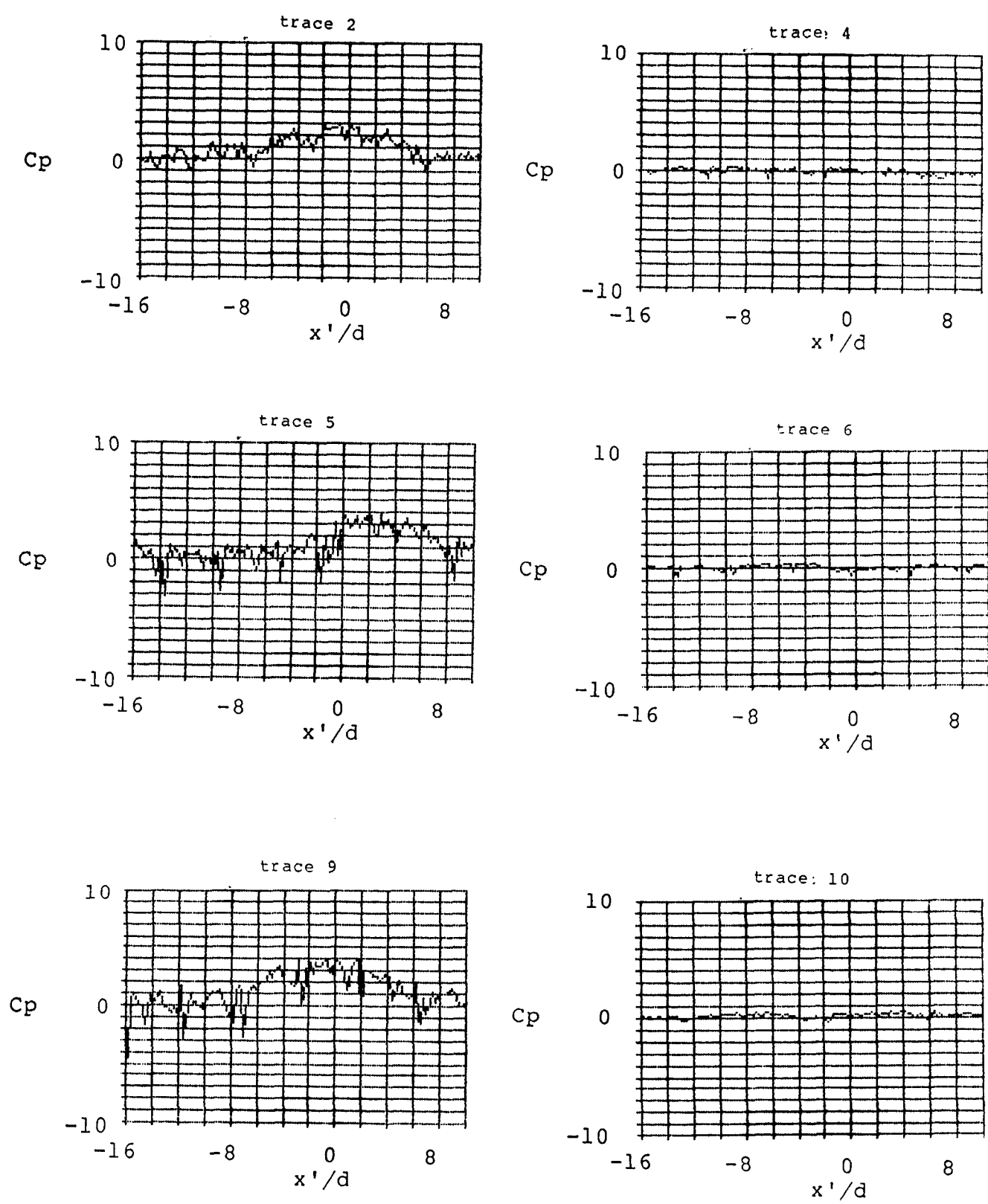


Figure A13. Ground Board Pressure Distribution, Run 32 , $Ve = .173$

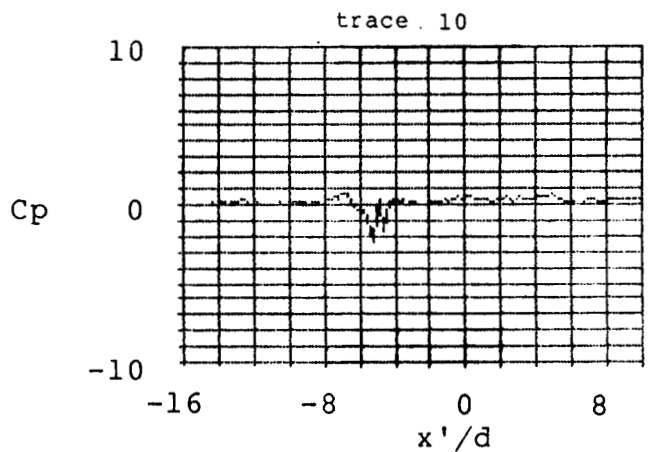
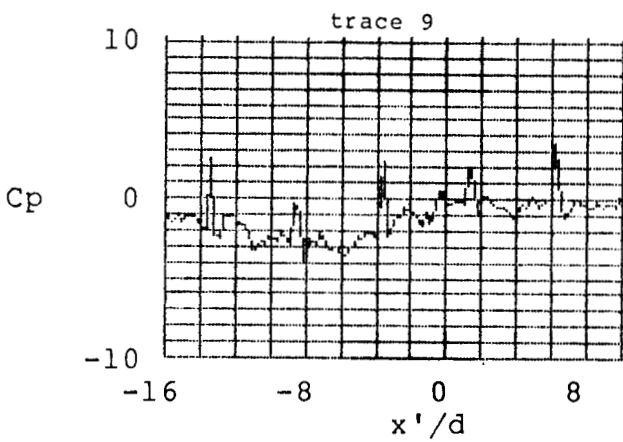
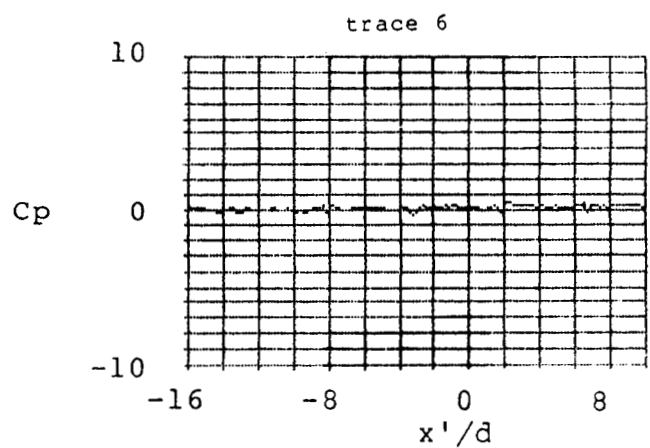
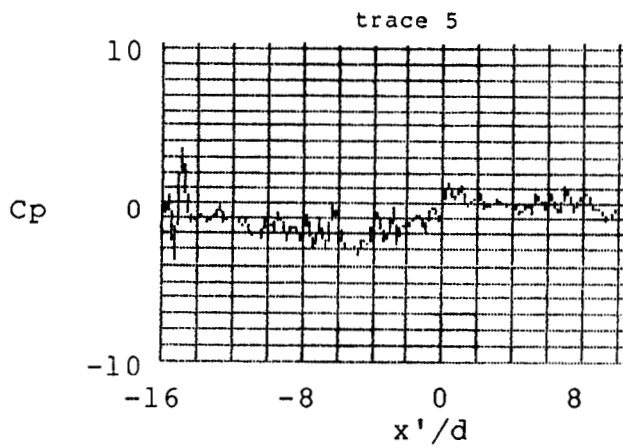
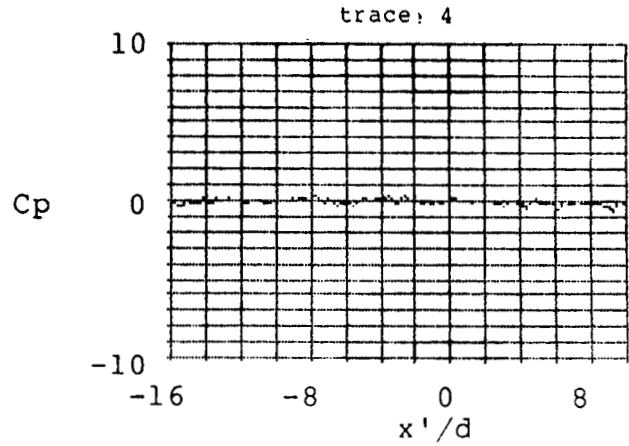
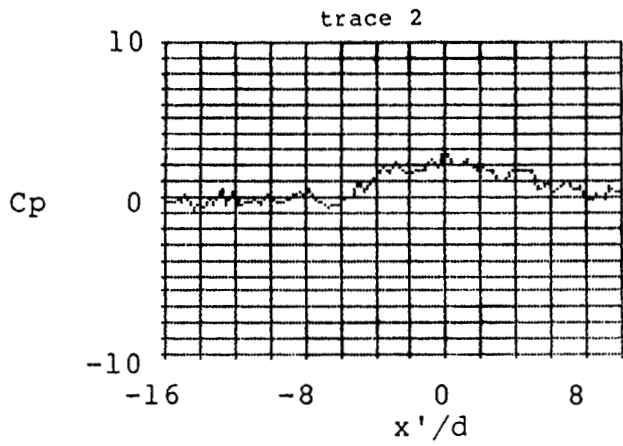


Figure A14 . Ground Board Pressure Distribution, Run 40 , $Ve = .187$

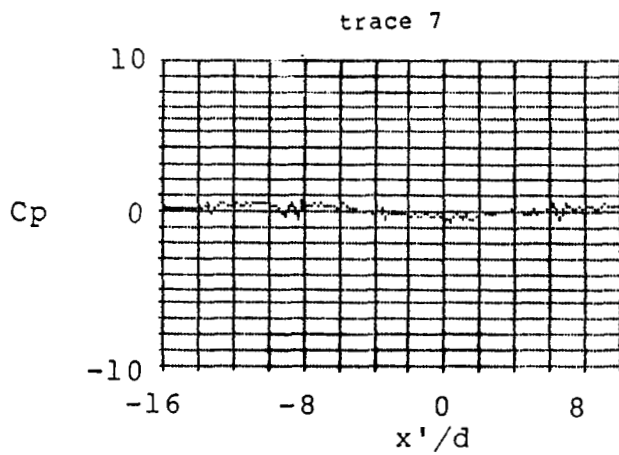
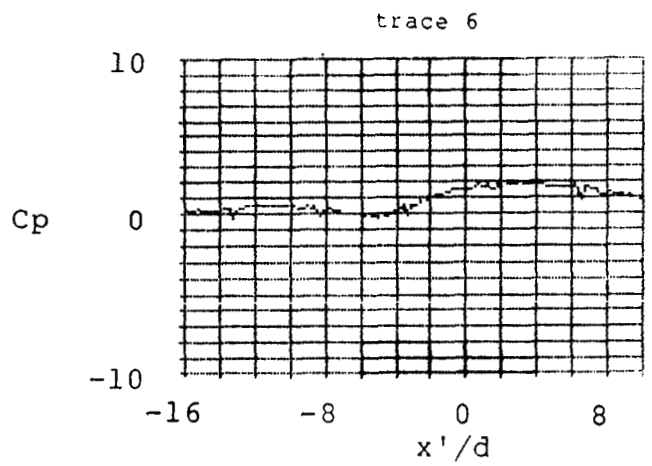
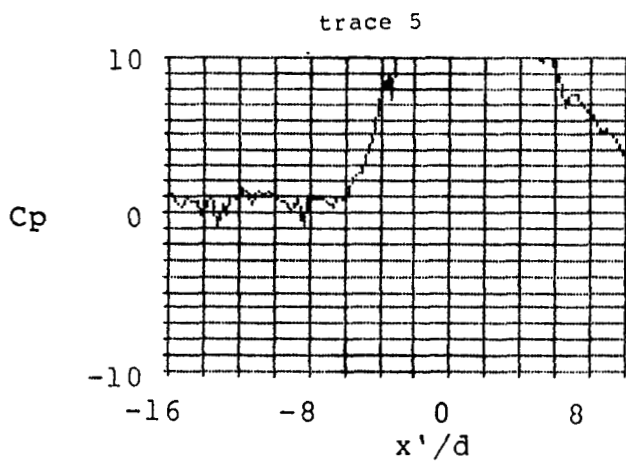
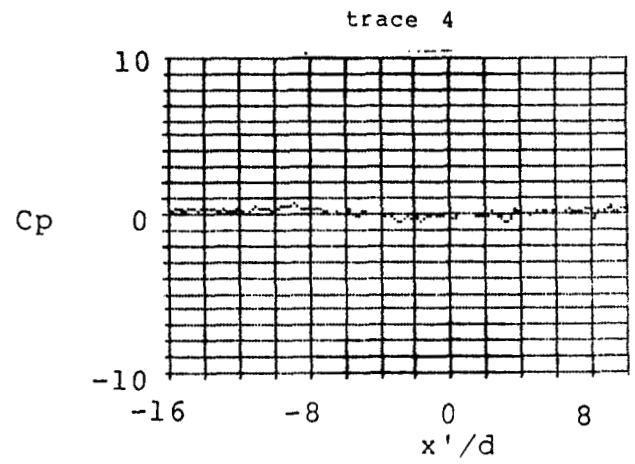
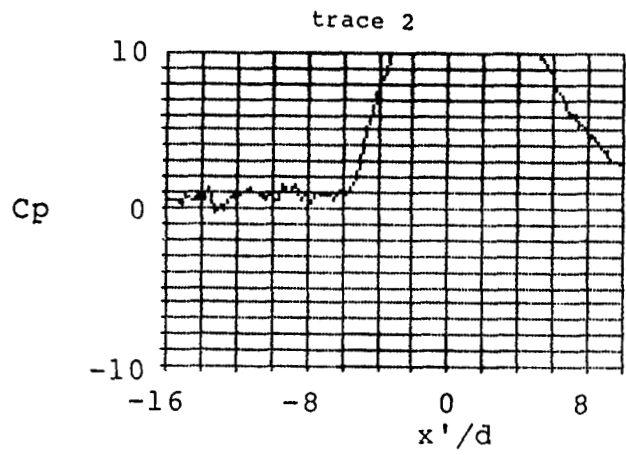


Figure A15. Ground Board Pressure Distribution, Run 42 , $Ve=.088$

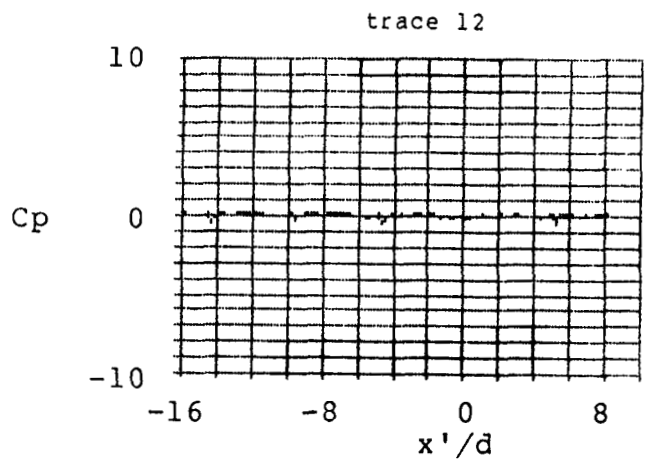
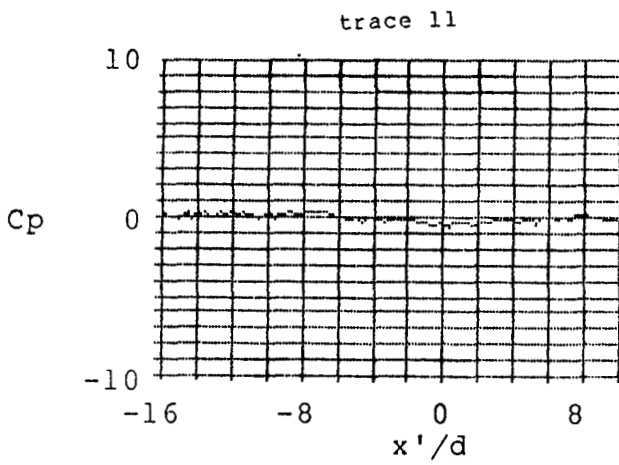
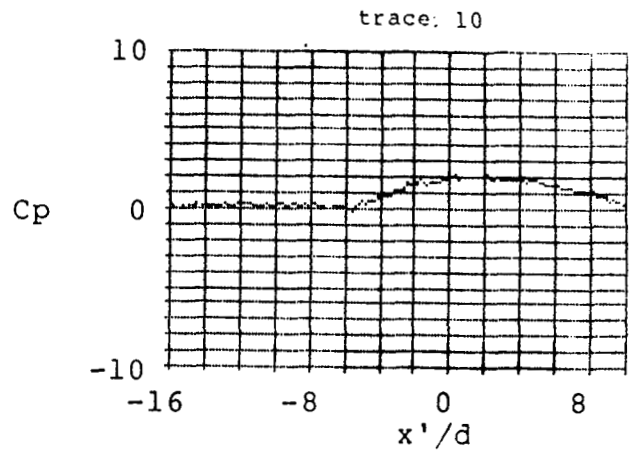
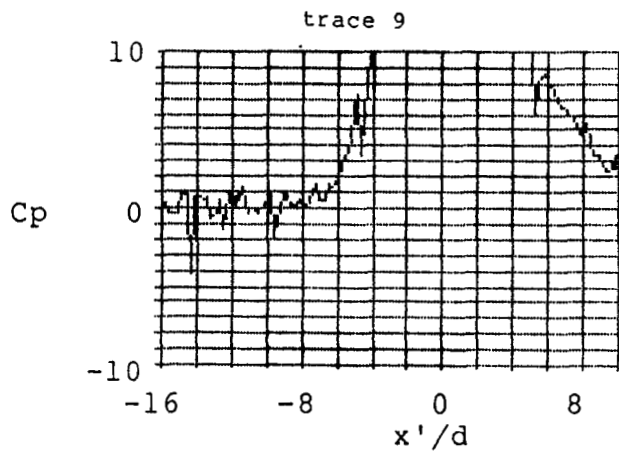


Figure A15. Ground Board Pressure Distribution, Run 42 , $Ve=.088$

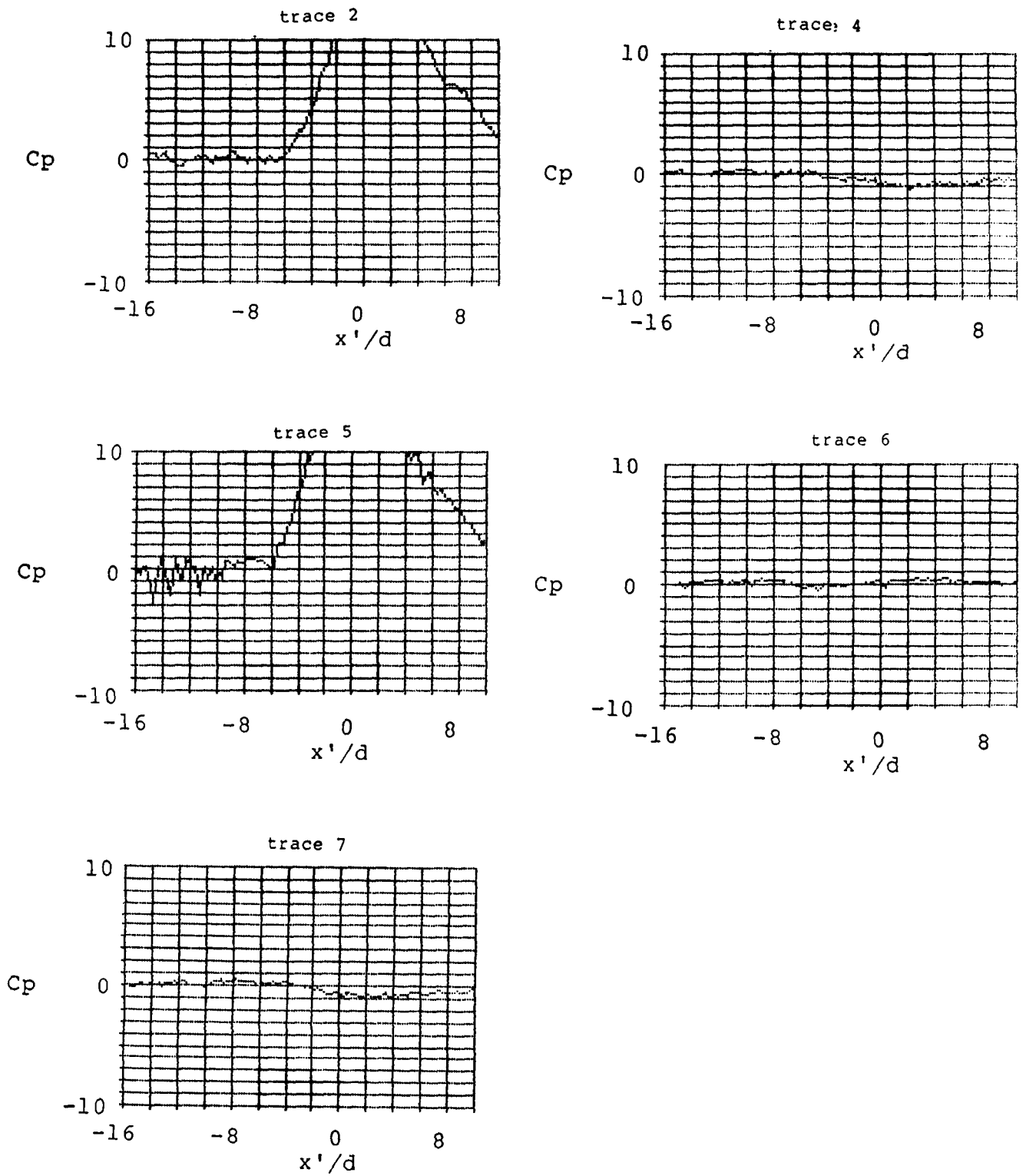


Figure A16. Ground Board Pressure Distribution, Run 43 , $Ve=.090$

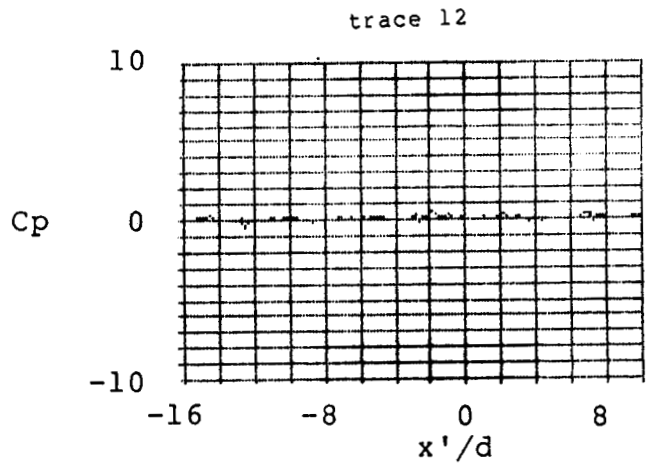
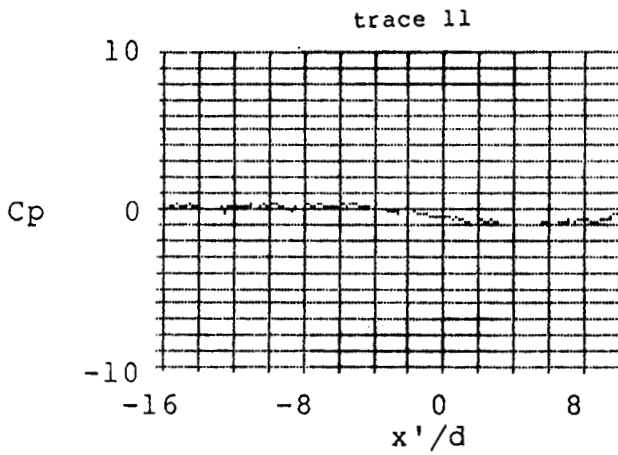
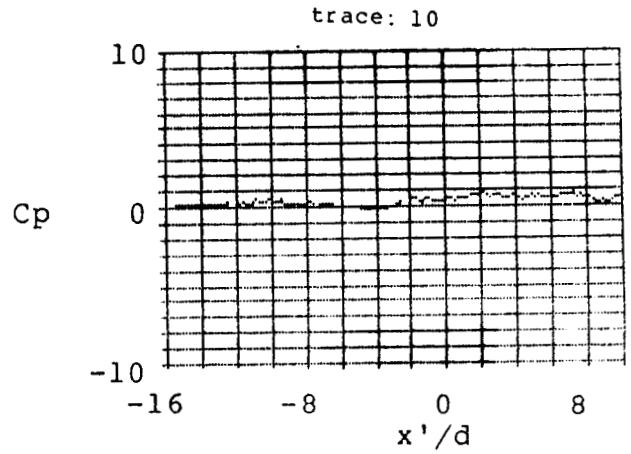
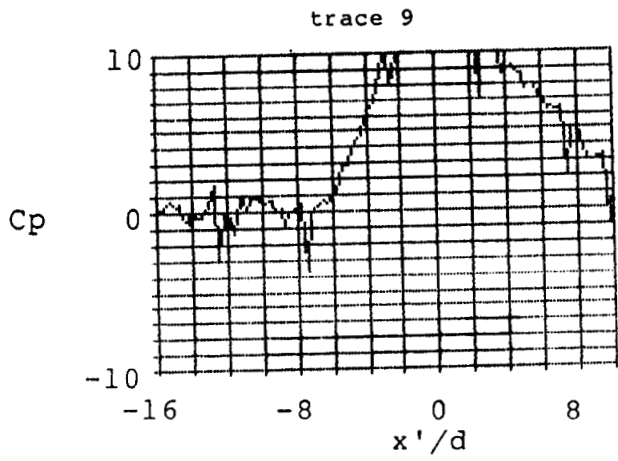


Figure A16. Ground Board Pressure Distribution, Run 43 , $Ve = .090$

APPENDIX B

BASIC DATA FOR THE 0.6 INCH NOZZLE CONFIGURATION

APPENDIX B

LIST OF FIGURES

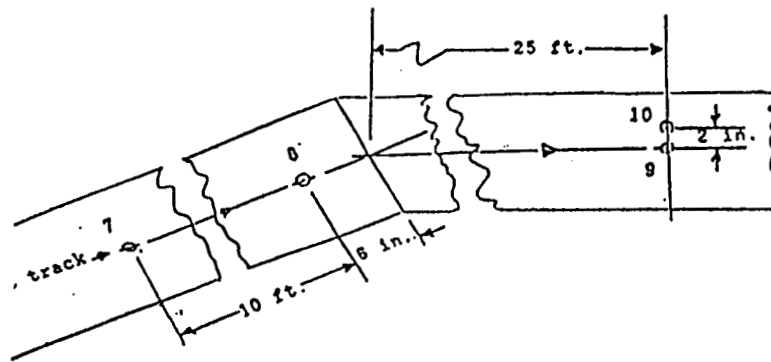
FIGURE	TITLE	PAGE
B1.	Ground Board Pressure Distribution, Run 66, $V_e=0.080$.	B3
B2.	Ground Board Pressure Distribution, Run 67, $V_e=0.084$.	B3
B3.	Ground Board Pressure Distribution, Run 69, $V_e=0.107$.	B3
B4.	Ground Board Pressure Distribution, Run 73, $V_e=0.132$.	B4
B5.	Ground Board Pressure Distribution, Run 74, $V_e=0.093$.	B4

LIST OF TABLES

TABLE	TITLE	PAGE
B1	INSTRUMENTATION LOCATION	B2

TABLE B1. INSTRUMENTATION LOCATION

TAP #	X	Y
7	-10.5 FEET	0 NOT AVAILABLE
8	-0.5 FEET	0 NOT AVAILABLE
9	25.0 FEET	0
10	25.0 FEET	2.0 INCHES



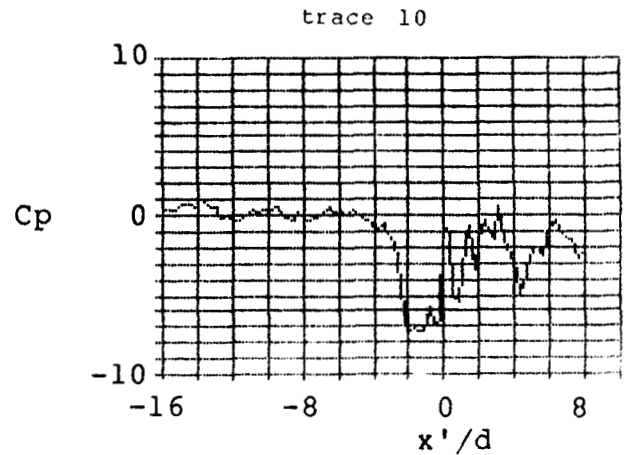
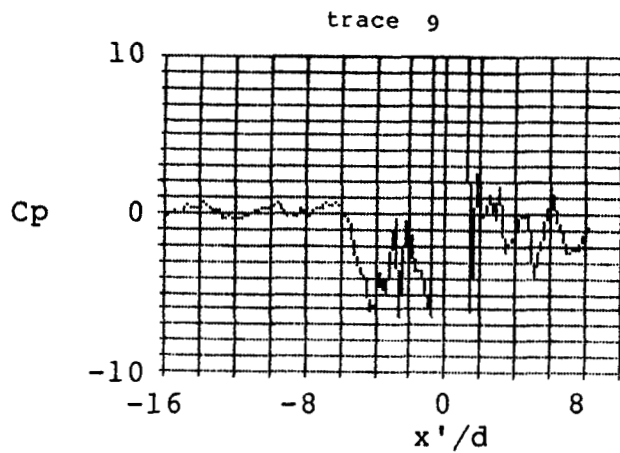


Figure B1. Ground Board Pressure Distribution, Run 66, $Ve=0.080$.

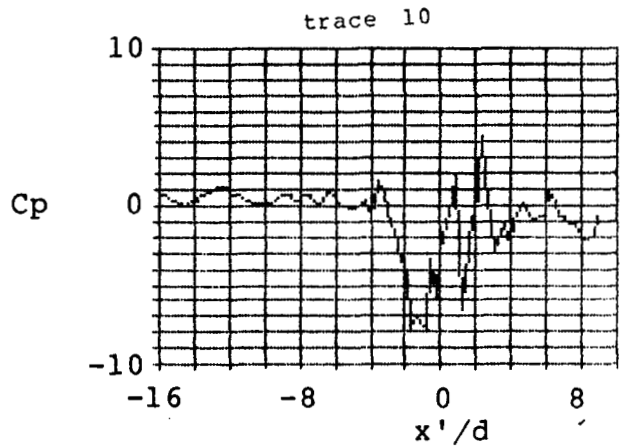
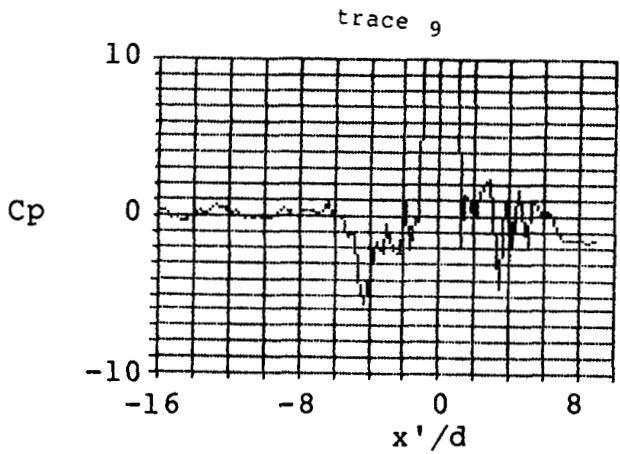


Figure B2. Ground Board Pressure Distribution, Run 67, $Ve=0.084$.

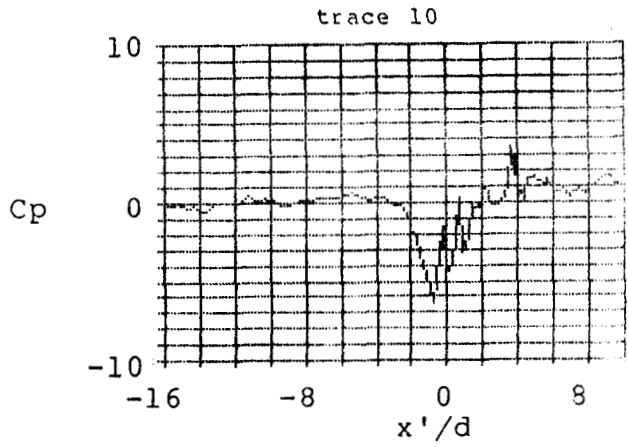
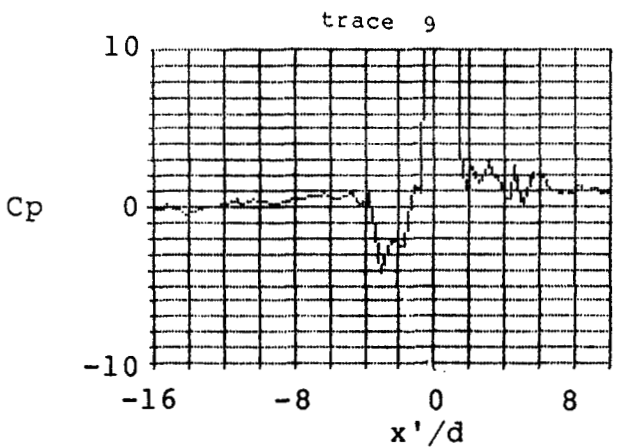


Figure B3. Ground Board Pressure Distribution, Run 69, $Ve=0.107$.

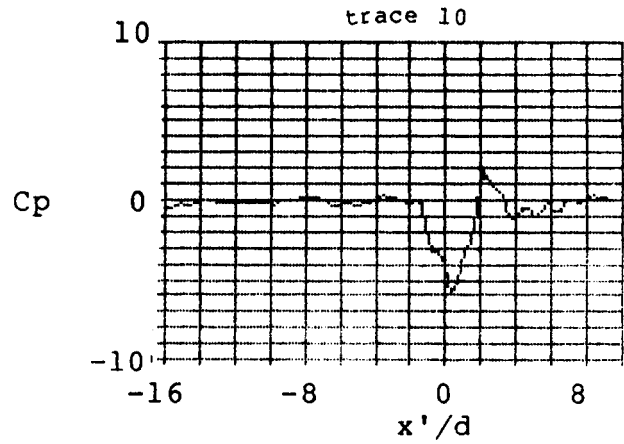
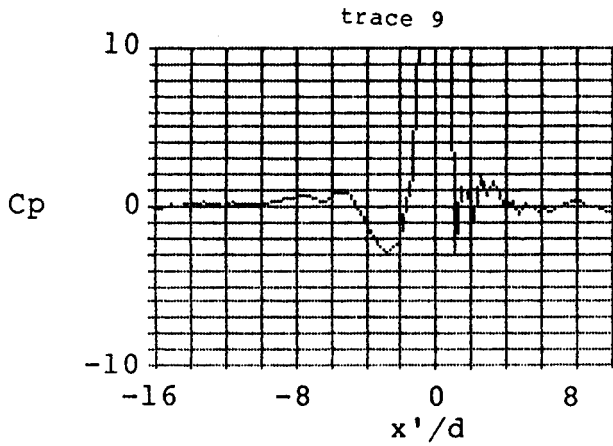


Figure B4. Ground Board Pressure Distribution, Run 73, $Ve=0.132$.

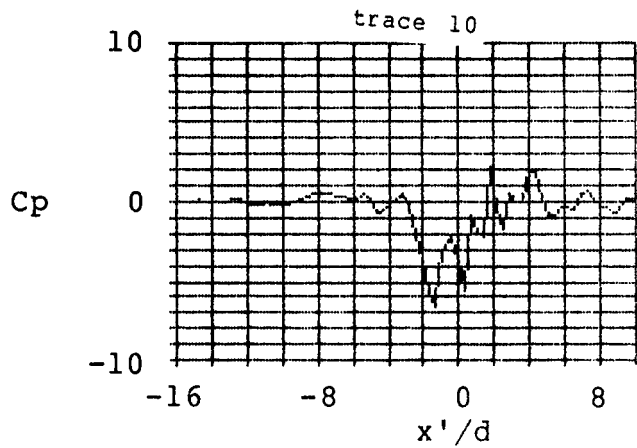
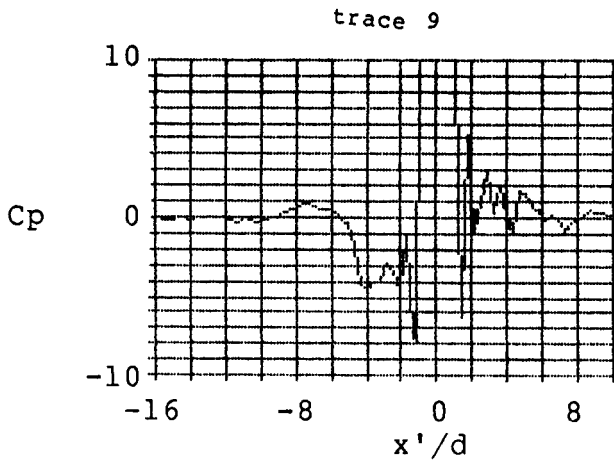


Figure B5. Ground Board Pressure Distribution, Run 74, $Ve=0.093$.

APPENDIX C
NOZZLE SURVEY DATA

APPENDIX C

LIST OF FIGURES

FIGURE	TITLE	PAGE
C1	Nozzle Exit Pressure Survey, 0.6", h/d=0.2 Q jet=634	C2
C2	Nozzle Exit Pressure Survey, 0.6", h/d=0.2 Q jet=1054	C3
C3	Nozzle Exit Pressure Survey, 0.6", h/d=0.2 Q jet=1337	C4
C4	Nozzle Exit Pressure Survey, 0.6", h/d=1.0 Q jet=634	C5
C5	Nozzle Exit Pressure Survey, 0.6", h/d=1.0 Q jet=1054	C6
C6	Nozzle Exit Pressure Survey, 0.6", h/d=1.0 Q jet=1337	C7
C7	Nozzle Exit Pressure Survey, 0.6", h/d=3.0 Q jet=634	C8
C8	Nozzle Exit Pressure Survey, 0.6", h/d=3.0 Q jet=1054	C9
C9	Nozzle Exit Pressure Survey, 0.6", h/d=3.0 Q jet=1337	C10
C10	Nozzle Exit Pressure Survey, 0.6", h/d=10.0 Q jet=634	C11
C11	Nozzle Exit Pressure Survey, 0.6", h/d=10.0 Q jet=1054	C12
C12	Nozzle Exit Pressure Survey, 0.6", h/d=10.0 Q jet=1337	C13
C13	Nozzle Exit Pressure Survey, 1.0", h/d=0.2 Q jet=85	C14
C14	Nozzle Exit Pressure Survey, 1.0", h/d=0.2 Q jet=265	C15
C15	Nozzle Exit Pressure Survey, 1.0", h/d=0.2 Q jet=935	C16
C16	Nozzle Exit Pressure Survey, 1.0", h/d=1.0 Q jet=85	C17
C17	Nozzle Exit Pressure Survey, 1.0", h/d=1.0 Q jet=265	C18
C18	Nozzle Exit Pressure Survey, 1.0", h/d=1.0 Q jet=935	C19
C19	Nozzle Exit Pressure Survey, 1.0, h/d=3.0 Q jet=85	C20
C20	Nozzle Exit Pressure Survey, 1.0, h/d=3.0 Q jet=265	C21
C21	Nozzle Exit Pressure Survey, 1.0, h/d=3.0 Q jet=935	C22
C22	Nozzle Exit Pressure Survey, 1.0", h/d=10.0 Q jet=85	C23
C23	Nozzle Exit Pressure Survey, 1.0", h/d=10.0 Q jet=265	C24
C24	Nozzle Exit Pressure Survey, 1.0", h/d=10.0 Q jet=935	C26

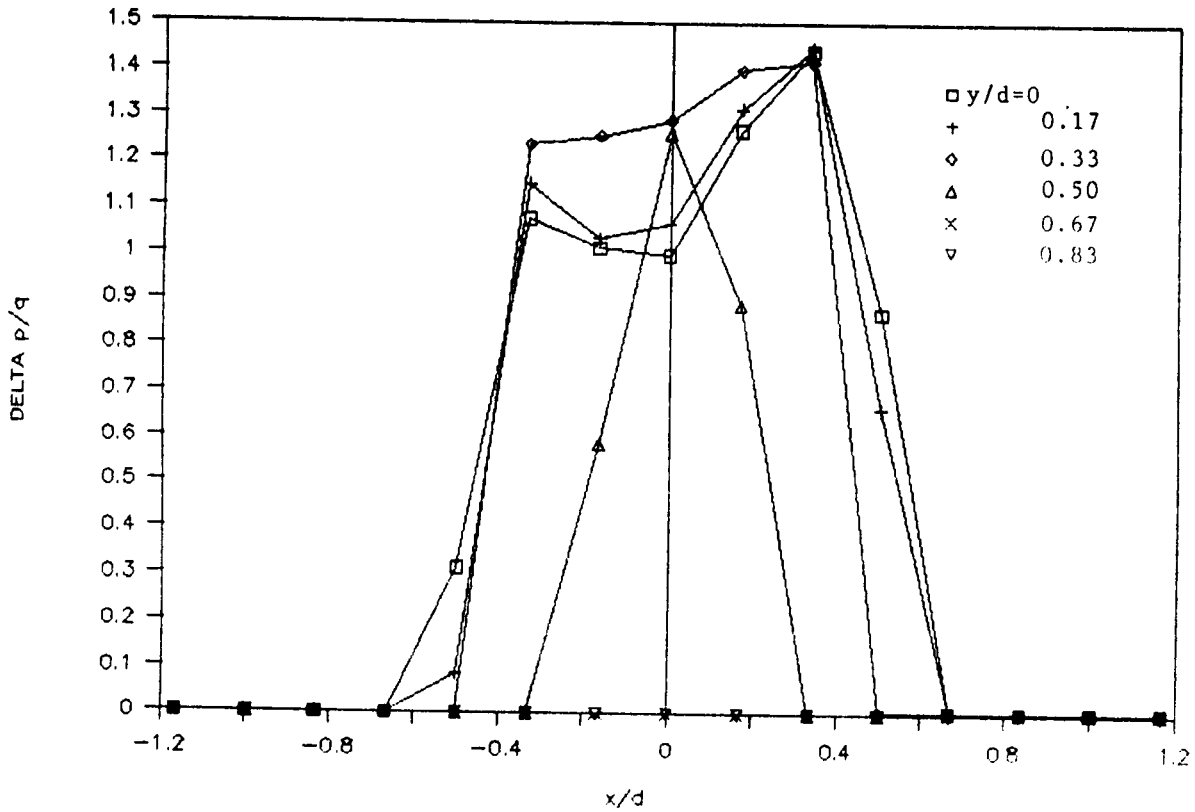
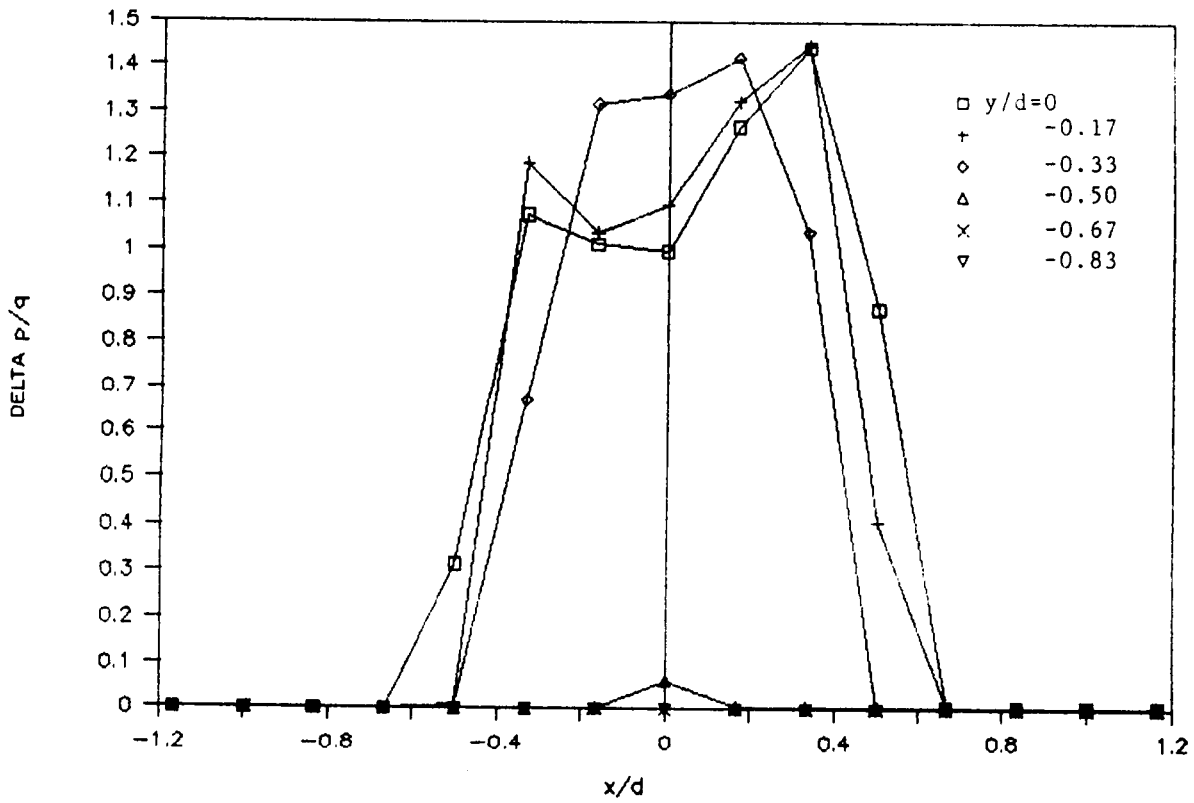


Figure C1. Nozzle Exit Pressure Survey, 0.6", h/d=0.2
Q jet=634

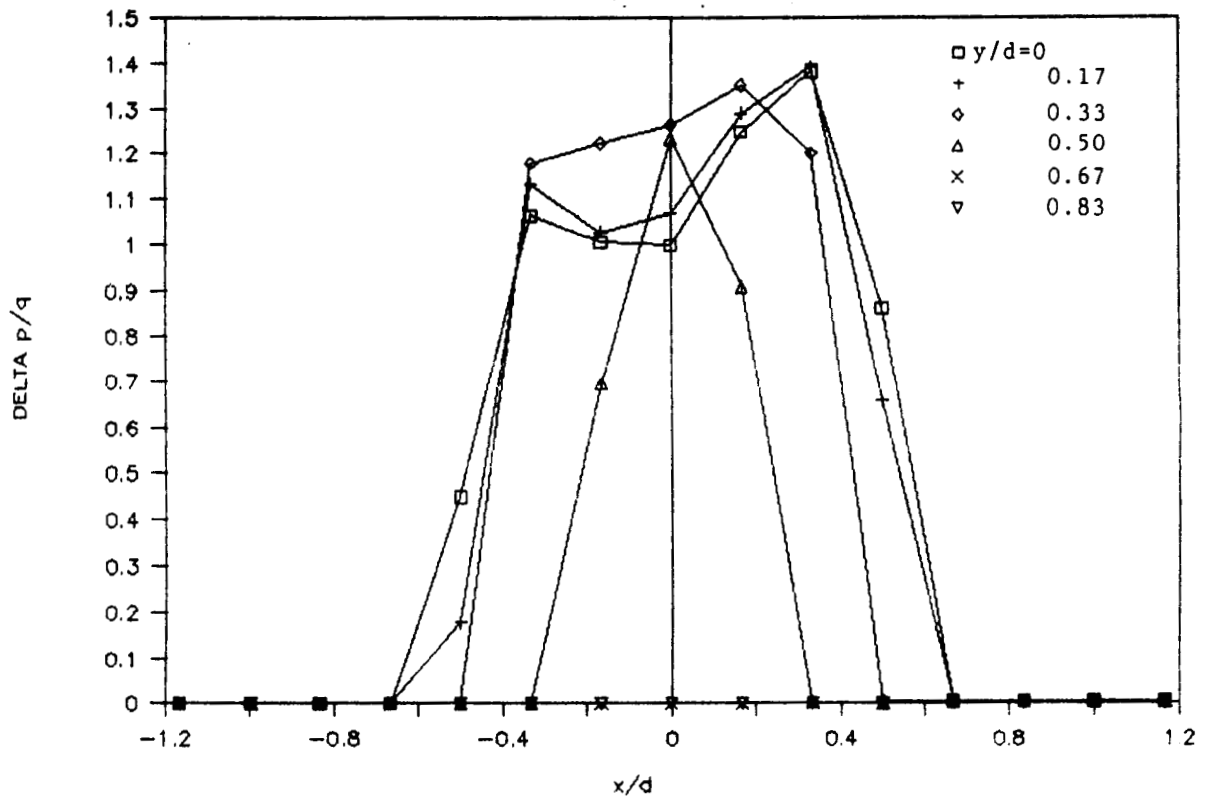
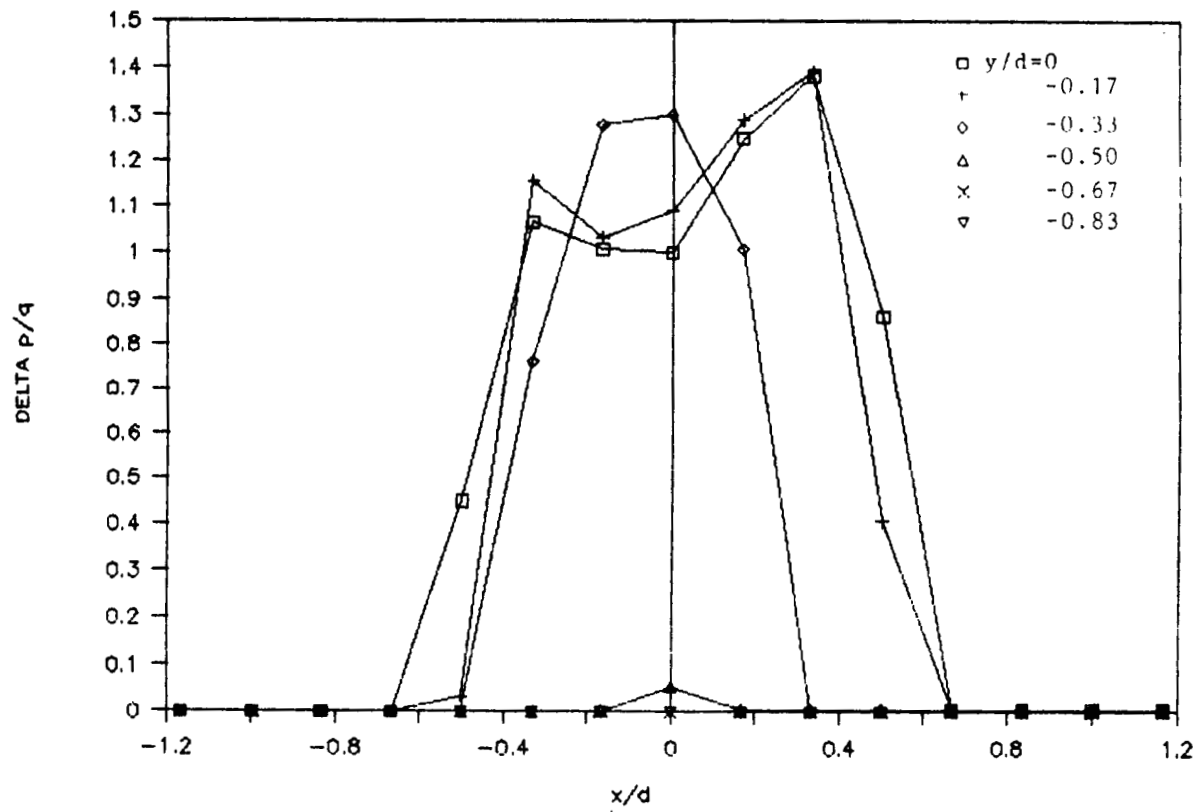


Figure C2. Nozzle Exit Pressure Survey, 0.6", h/d=0.2
 Q jet=1054

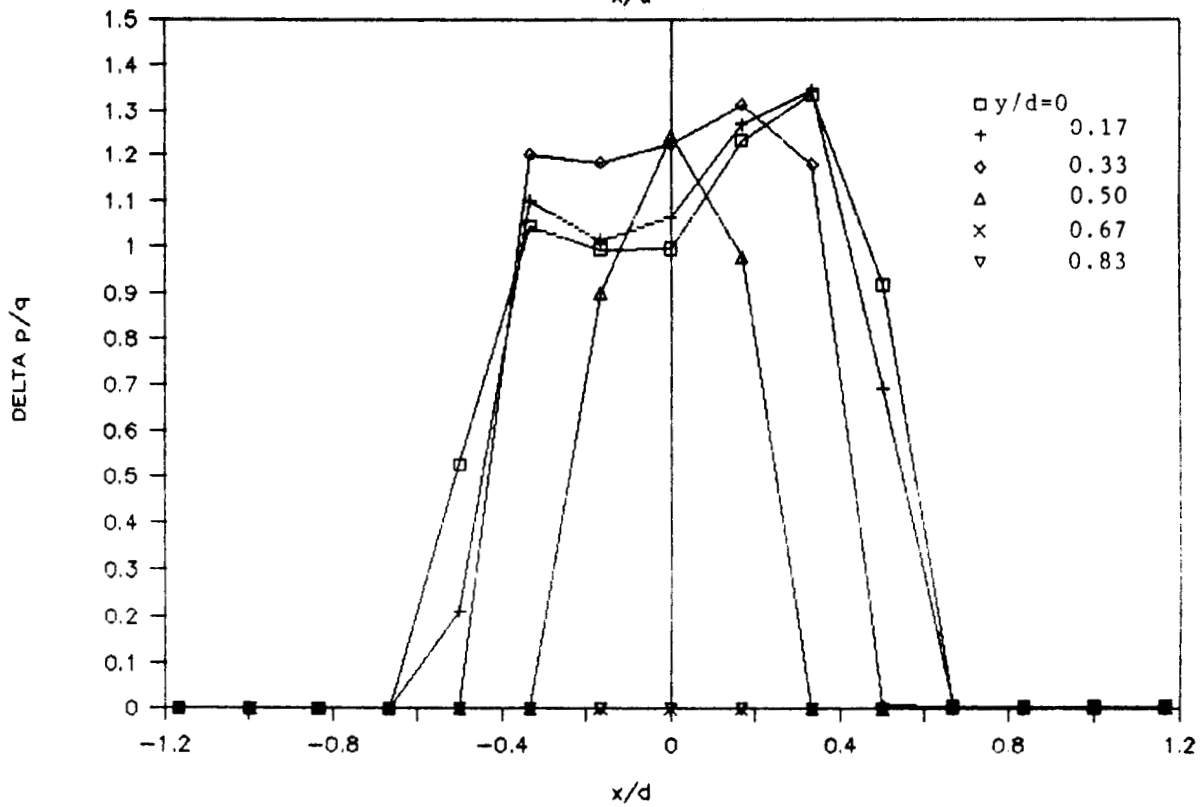
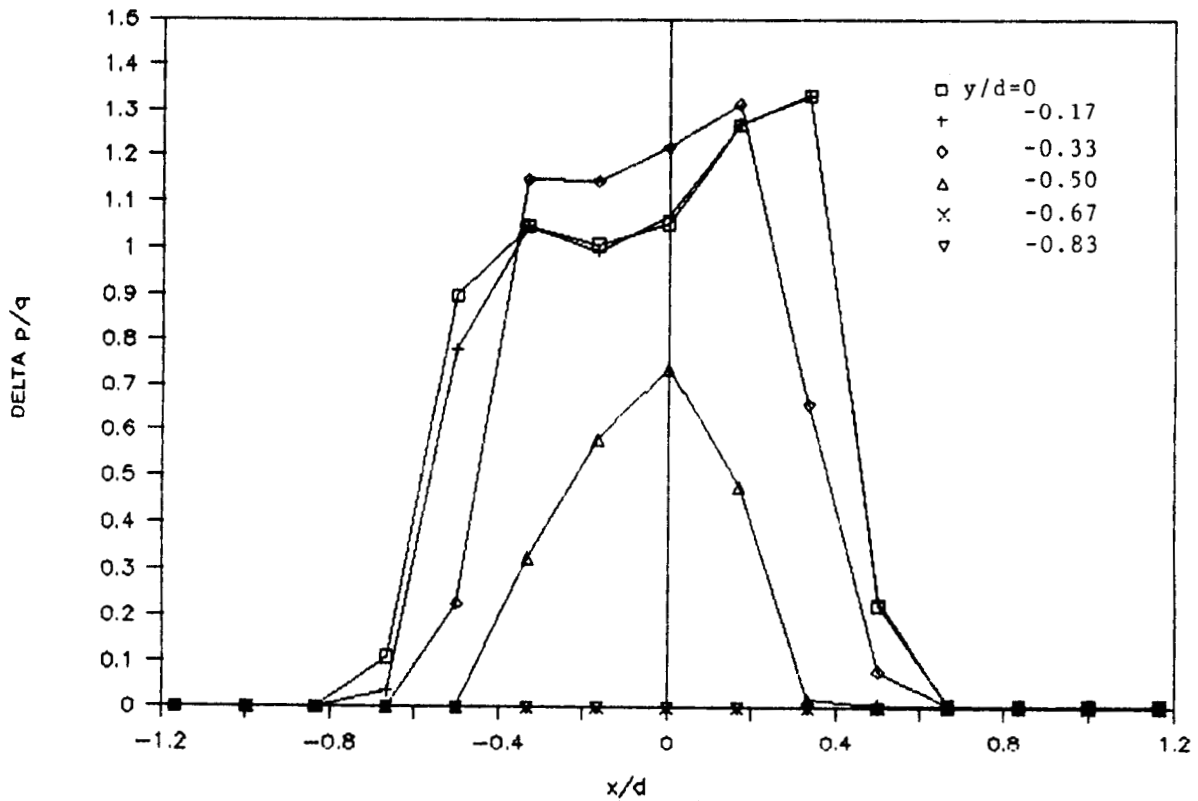


Figure C3. Nozzle Exit Pressure Survey, 0.6", $h/d=0.2$
 $Q_{jet}=1337$

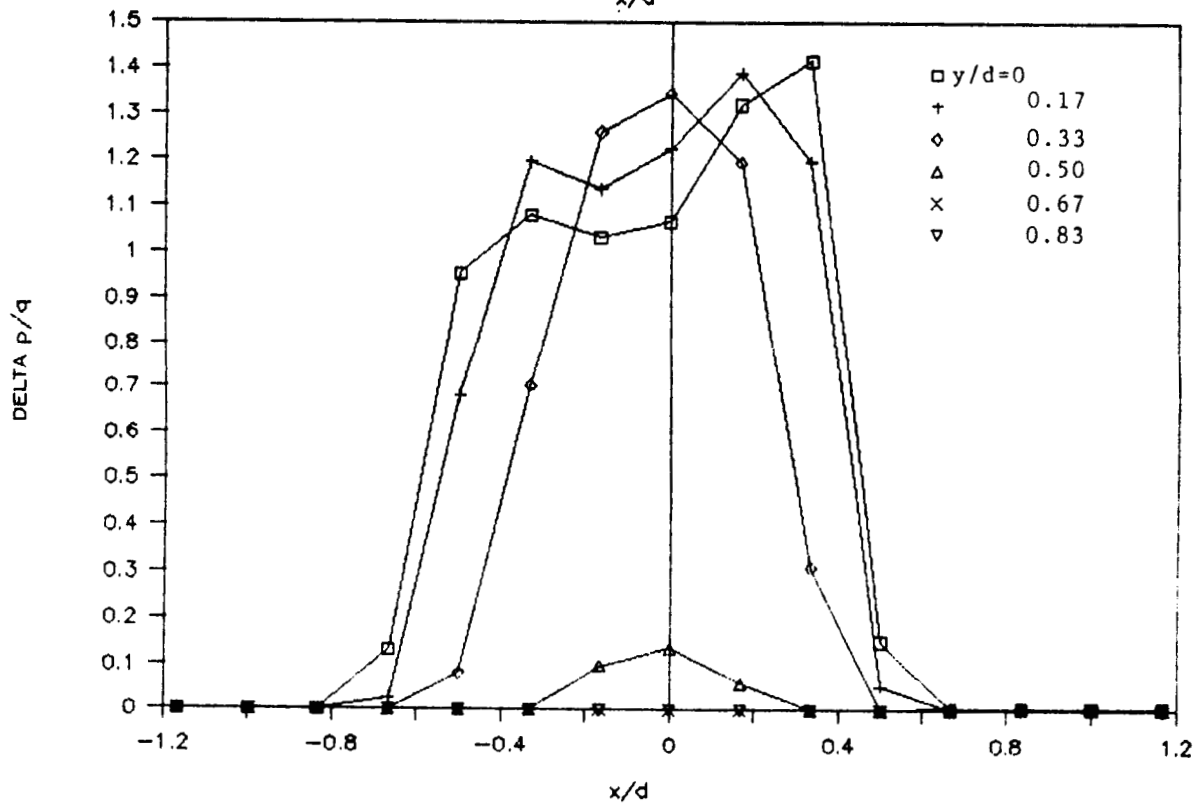
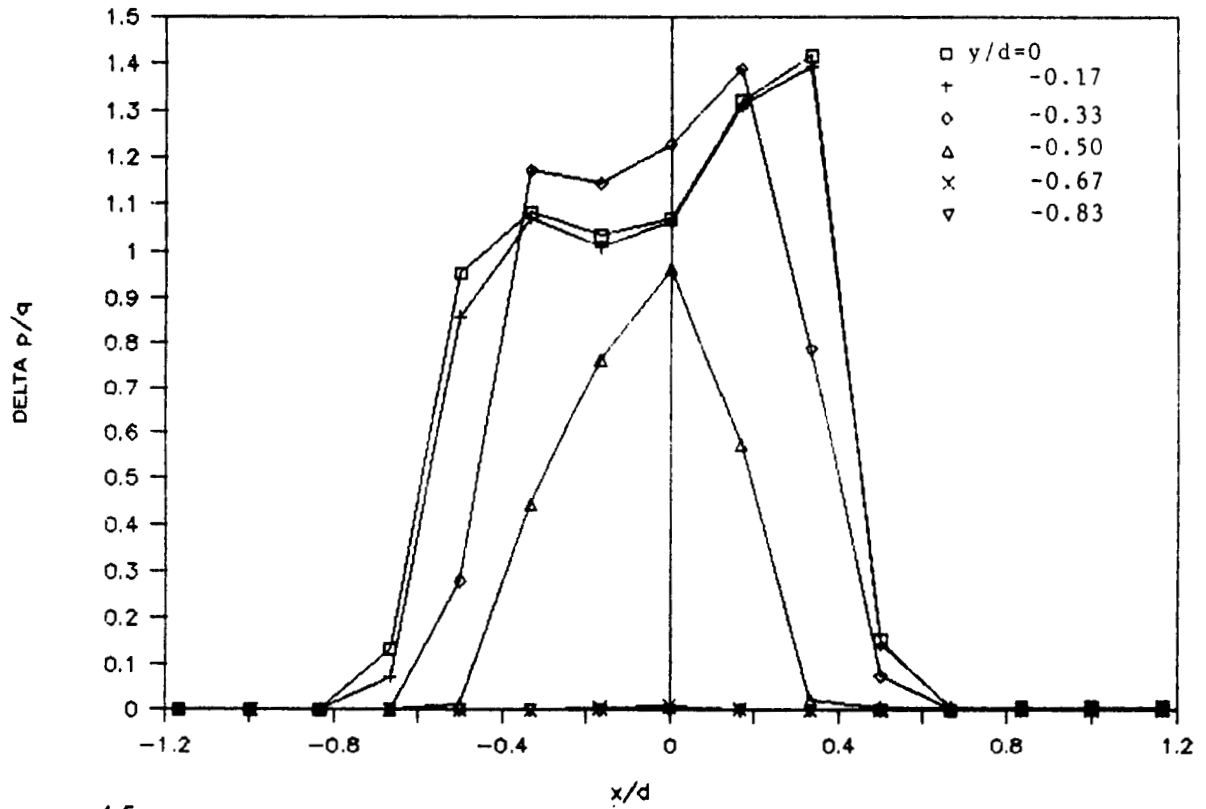


Figure C4. Nozzle Exit Pressure Survey, 0.6", h/d=1.0
Q jet=634

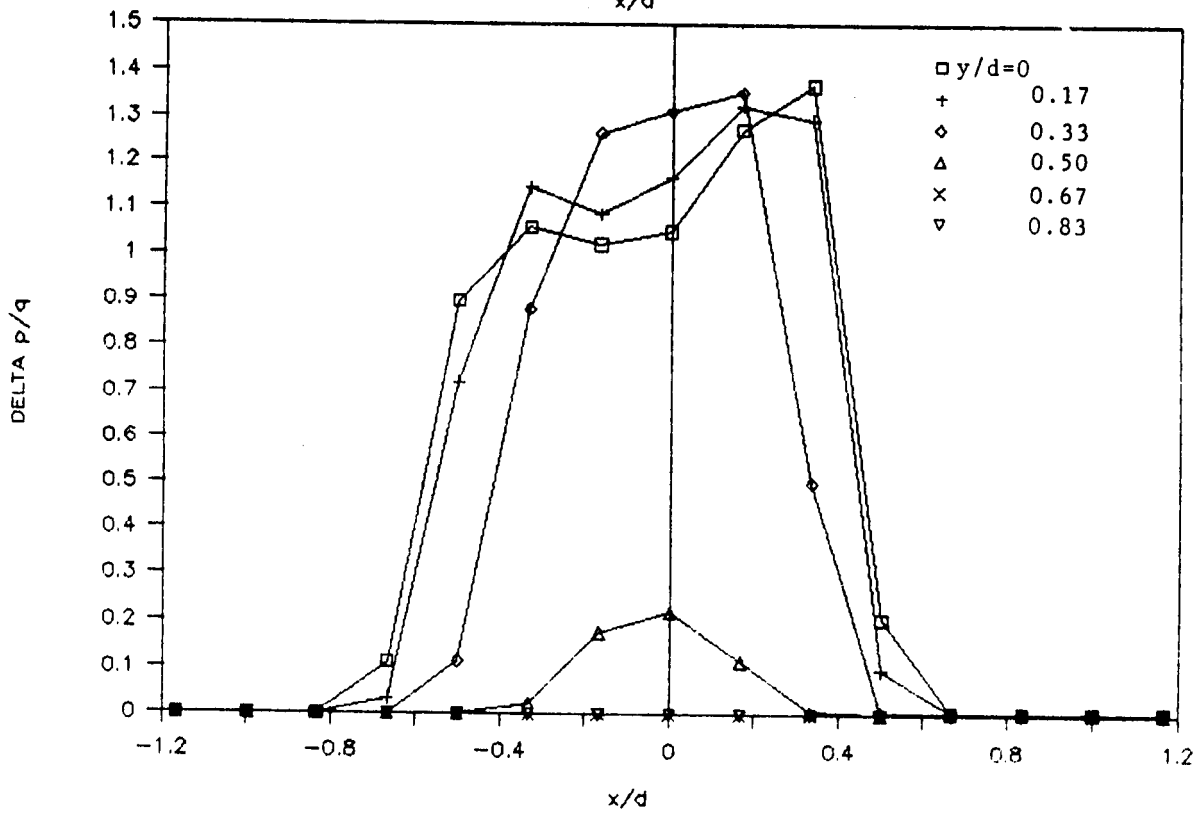
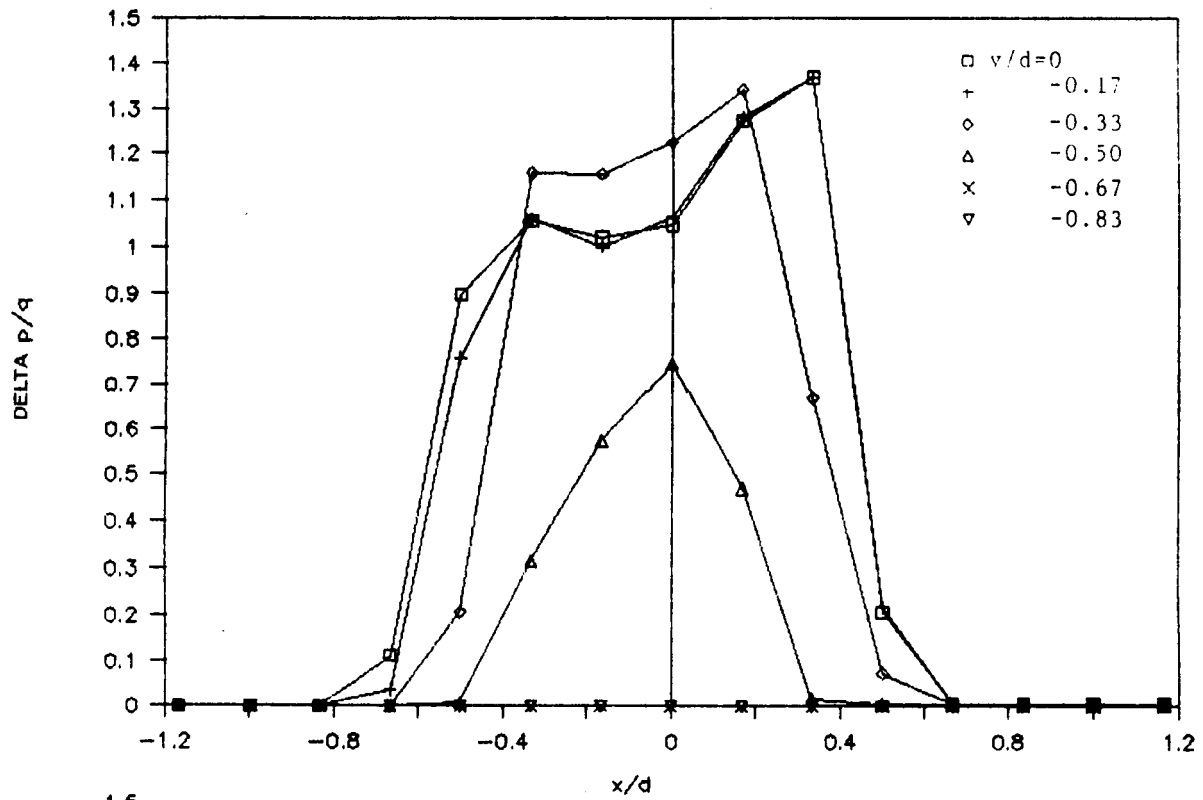


Figure C5; Nozzle Exit Pressure Survey, 0.6", $h/d=1.0$
 $Q_{jet}=1054$

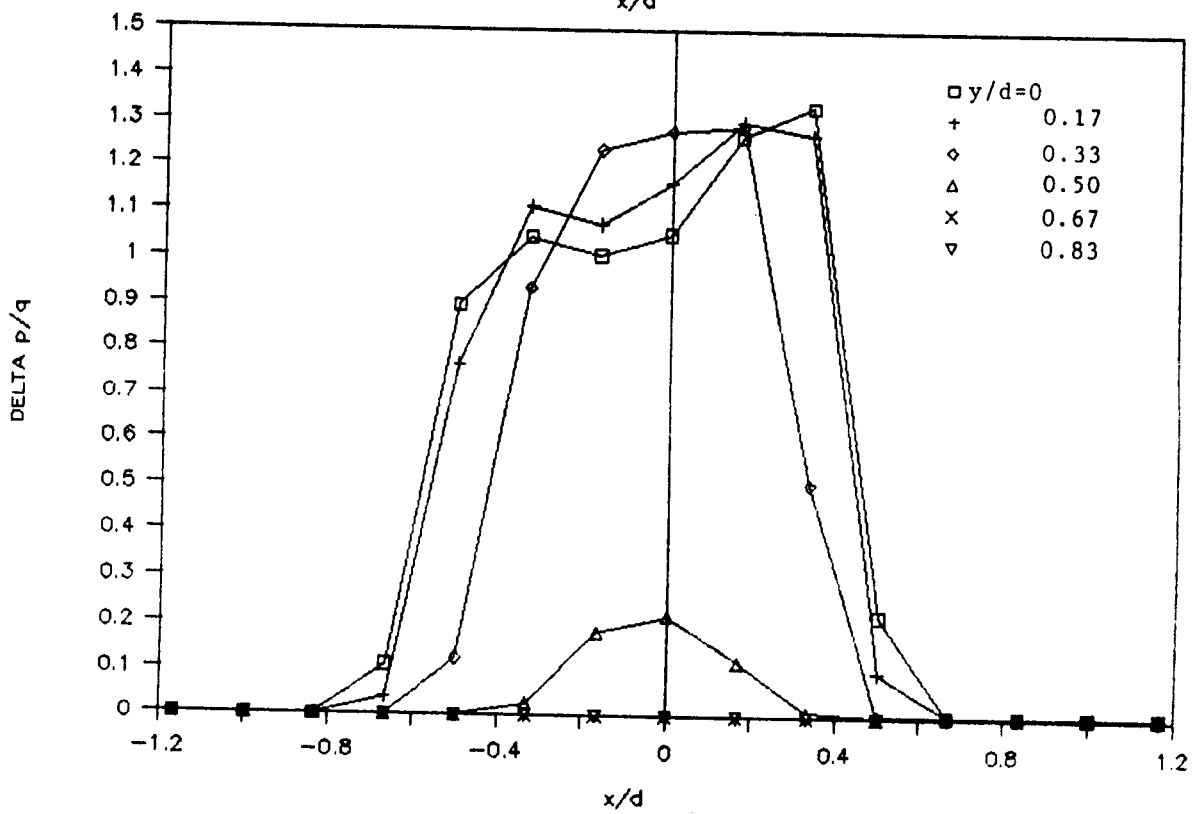
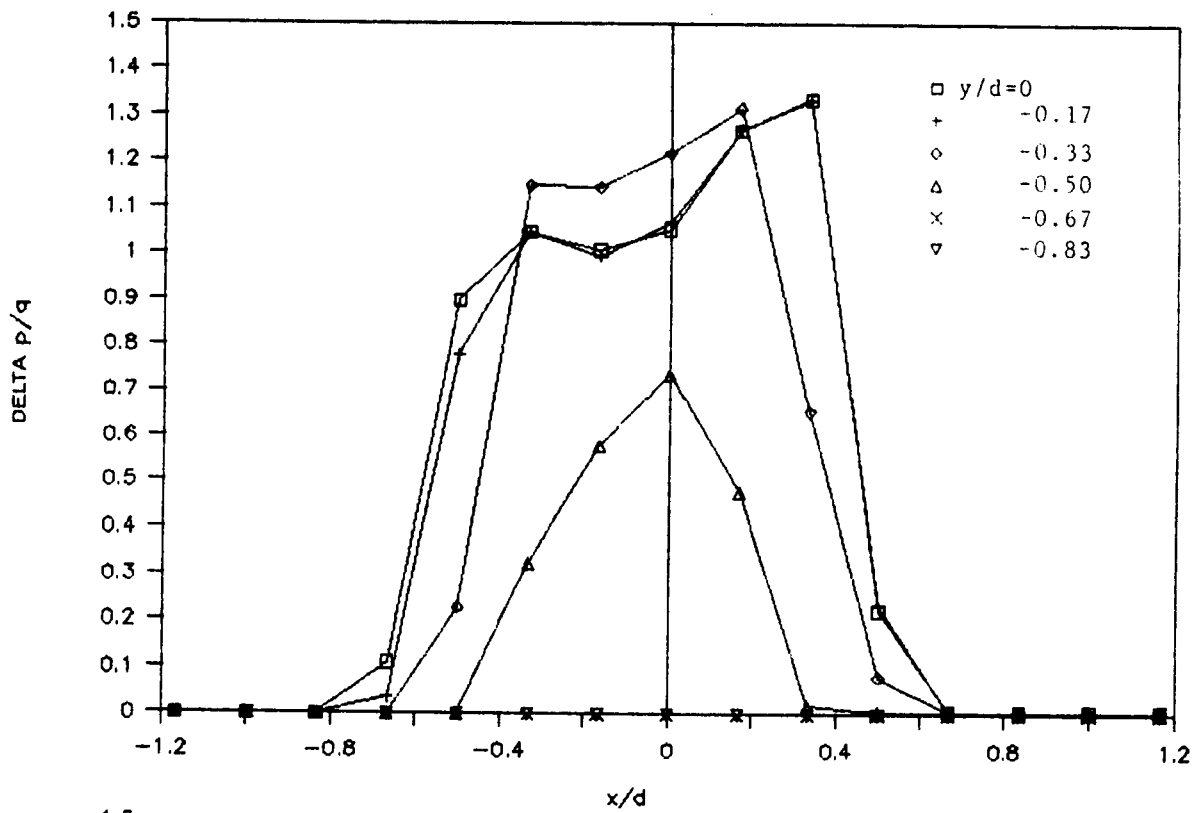


Figure C6; Nozzle Exit Pressure Survey, 0.6", $h/d=1.0$
 $Q_{jet}=1337$

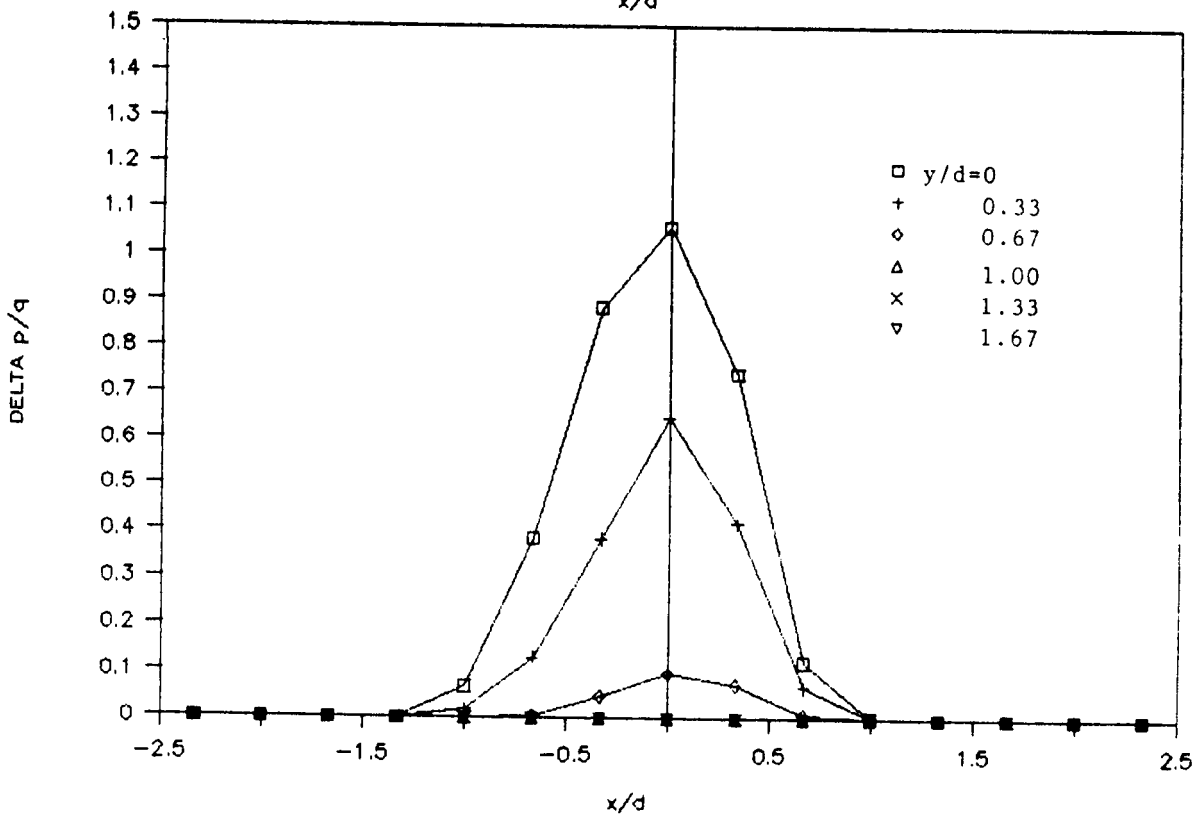
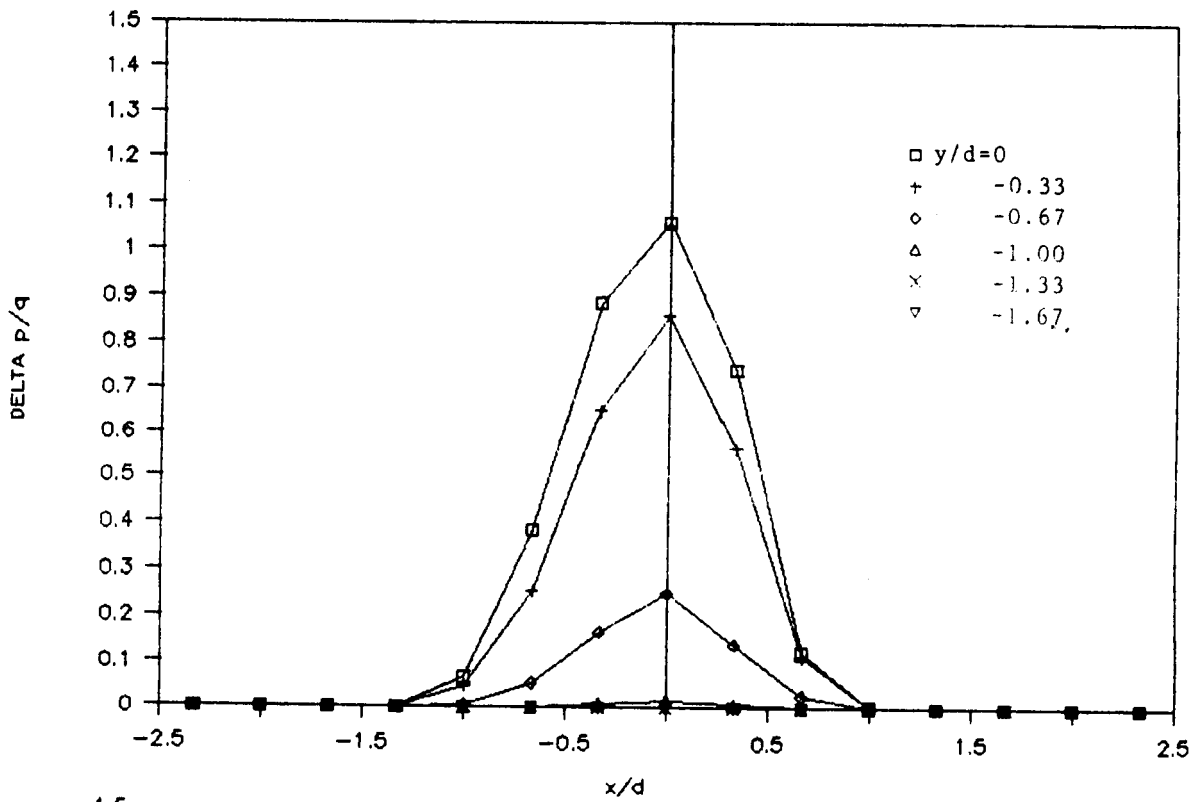


Figure C7; Nozzle Exit Pressure Survey, 0.6", h/d=3.0
Q jet=634

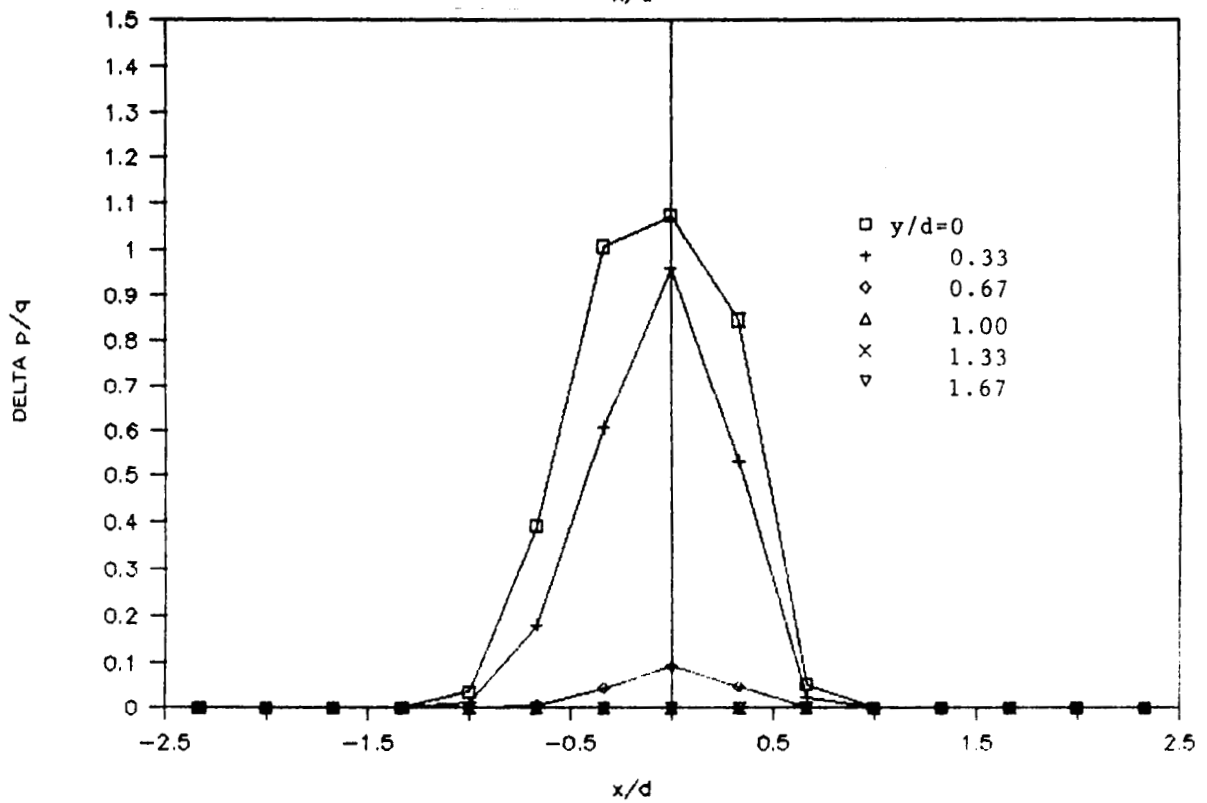
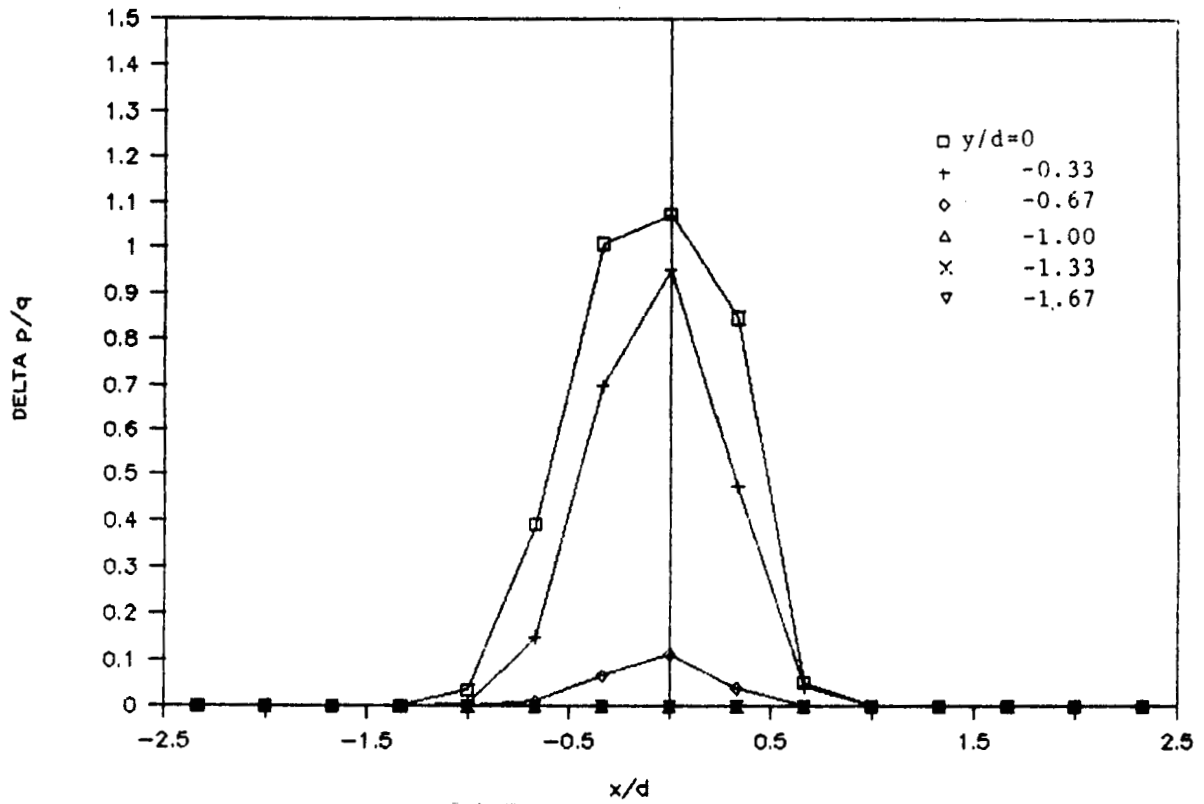


Figure C8; Nozzle Exit Pressure Survey, 0.6", h/d=3.0
Q jet=1054

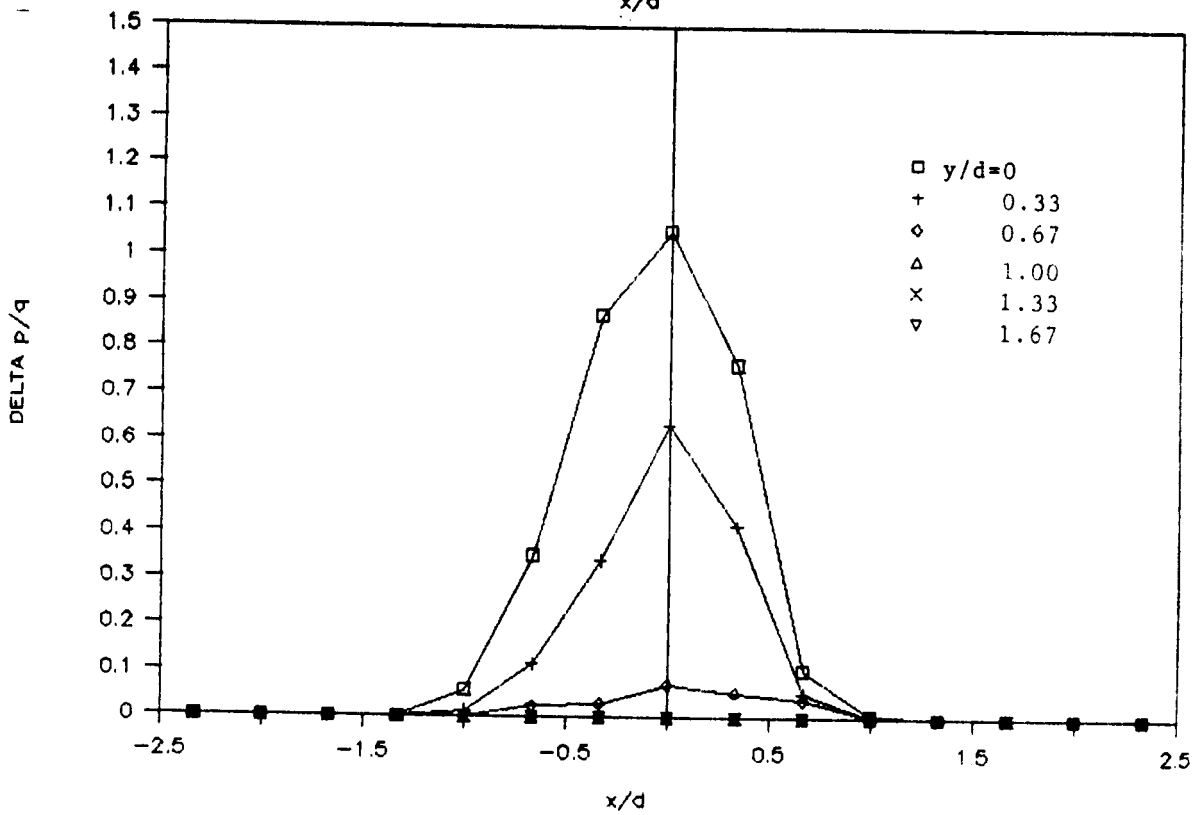
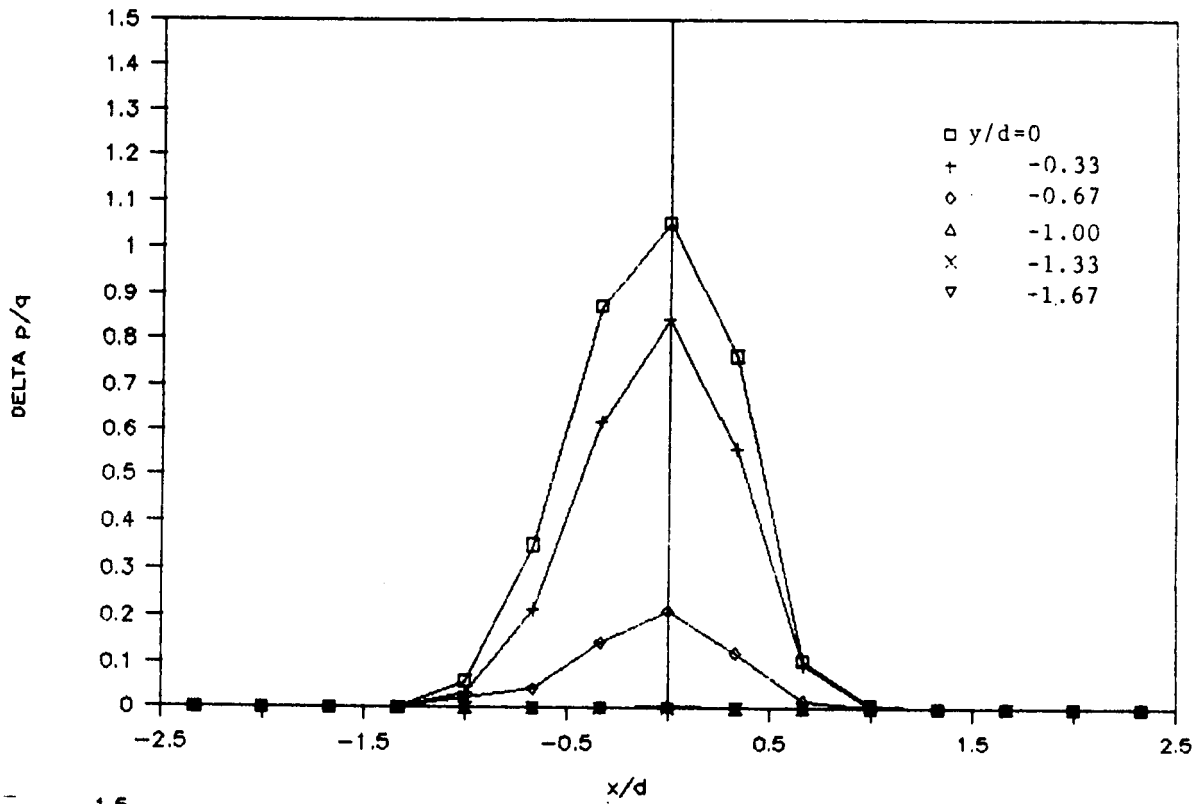


Figure C9; Nozzle Exit Pressure Survey, 0.6", h/d=3.0
Q jet=1337

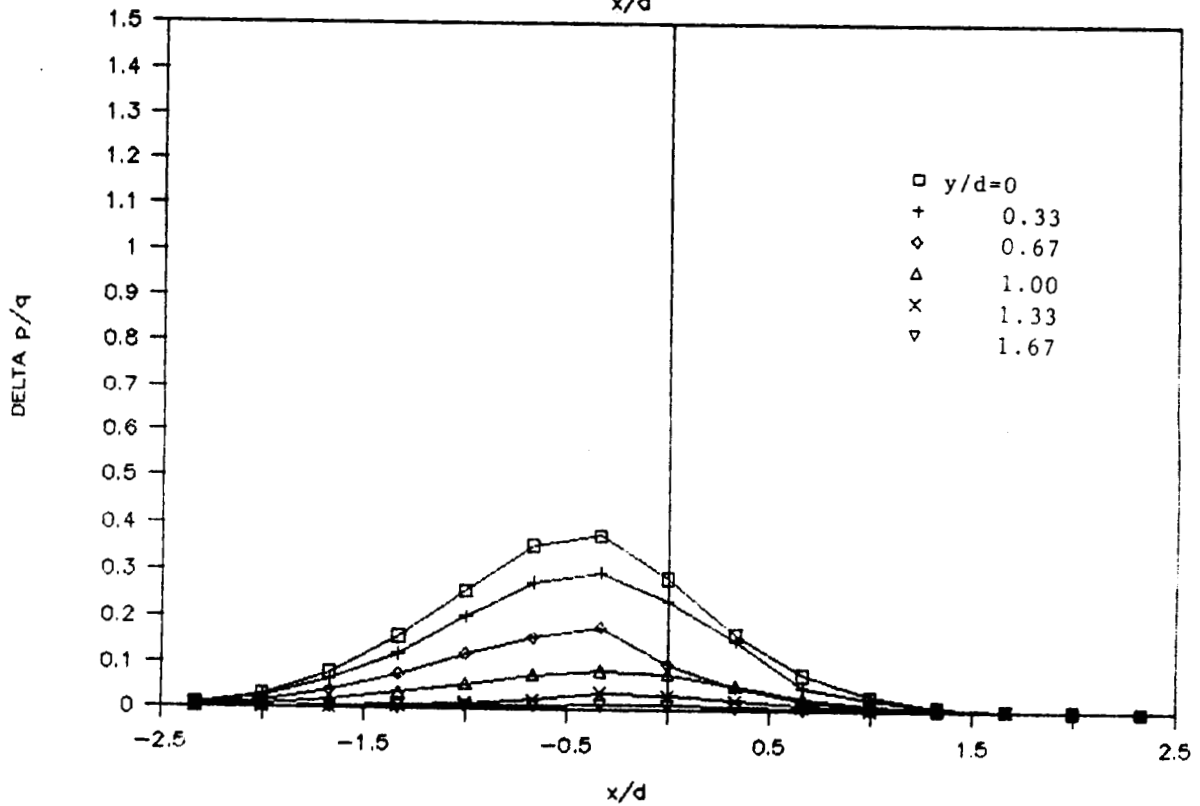
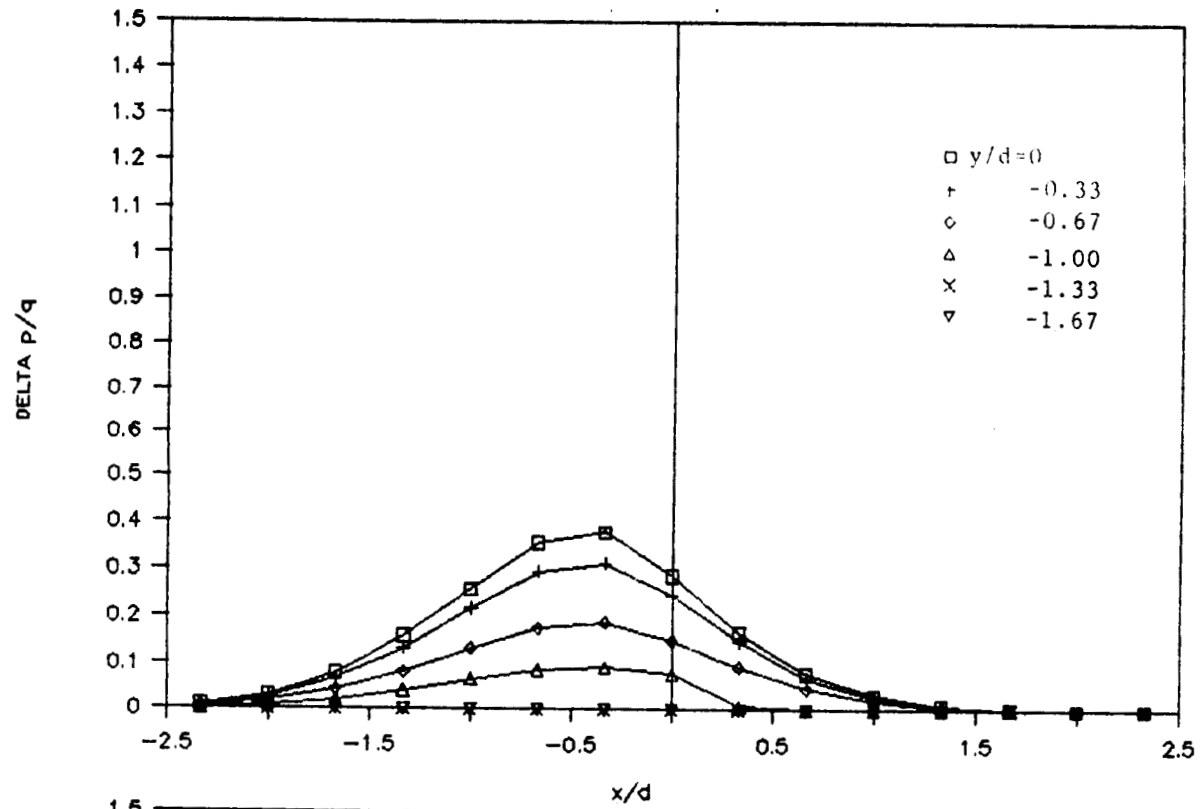


Figure C10; Nozzle Exit Pressure Survey, 0.6", $h/d=10.0$
 $Q_{jet}=634$

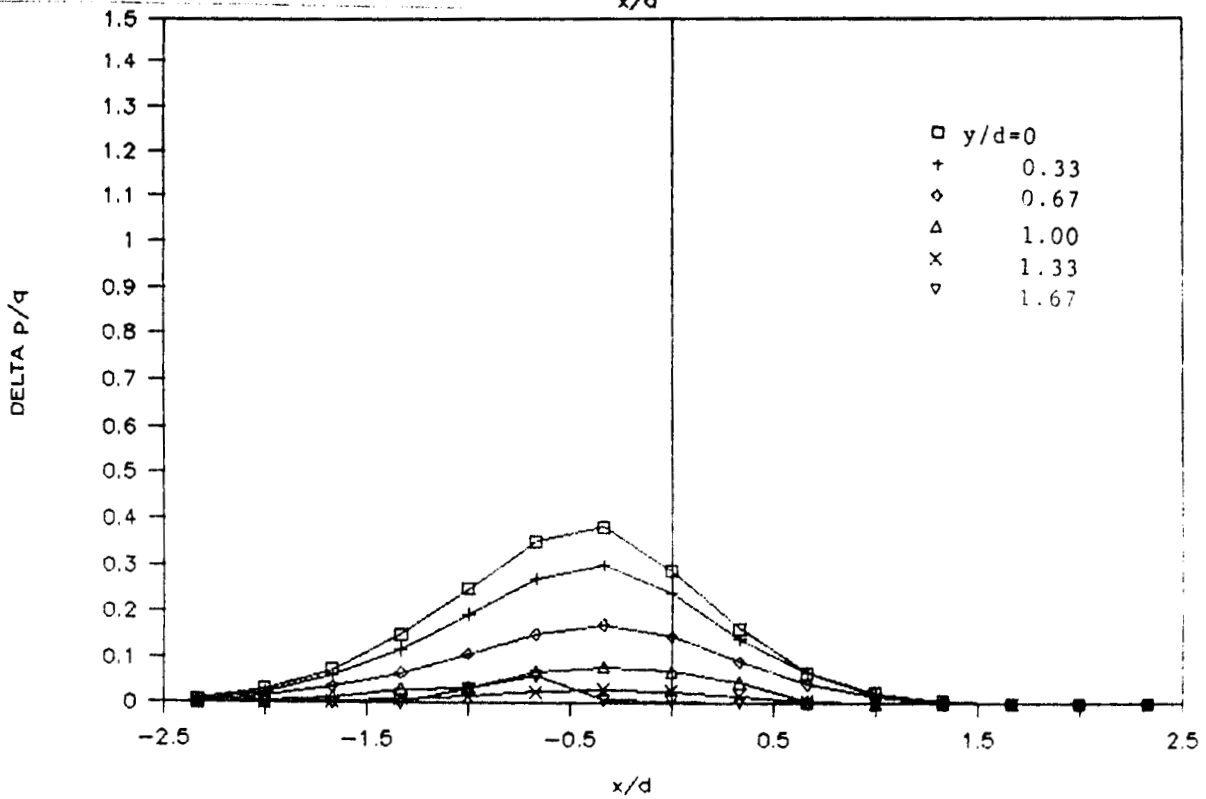
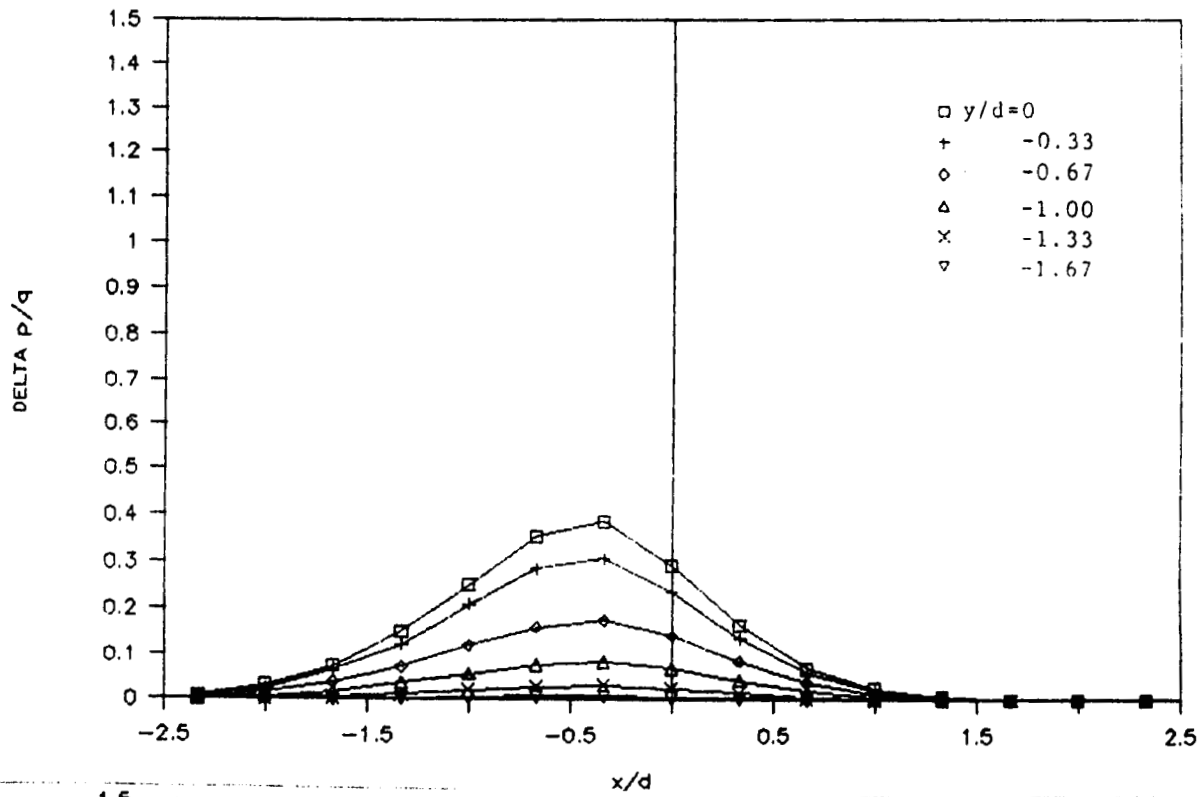


Figure C11; Nozzle Exit Pressure Survey, 0.6", $h/d=10.0$
 $Q_{jet}=1054$

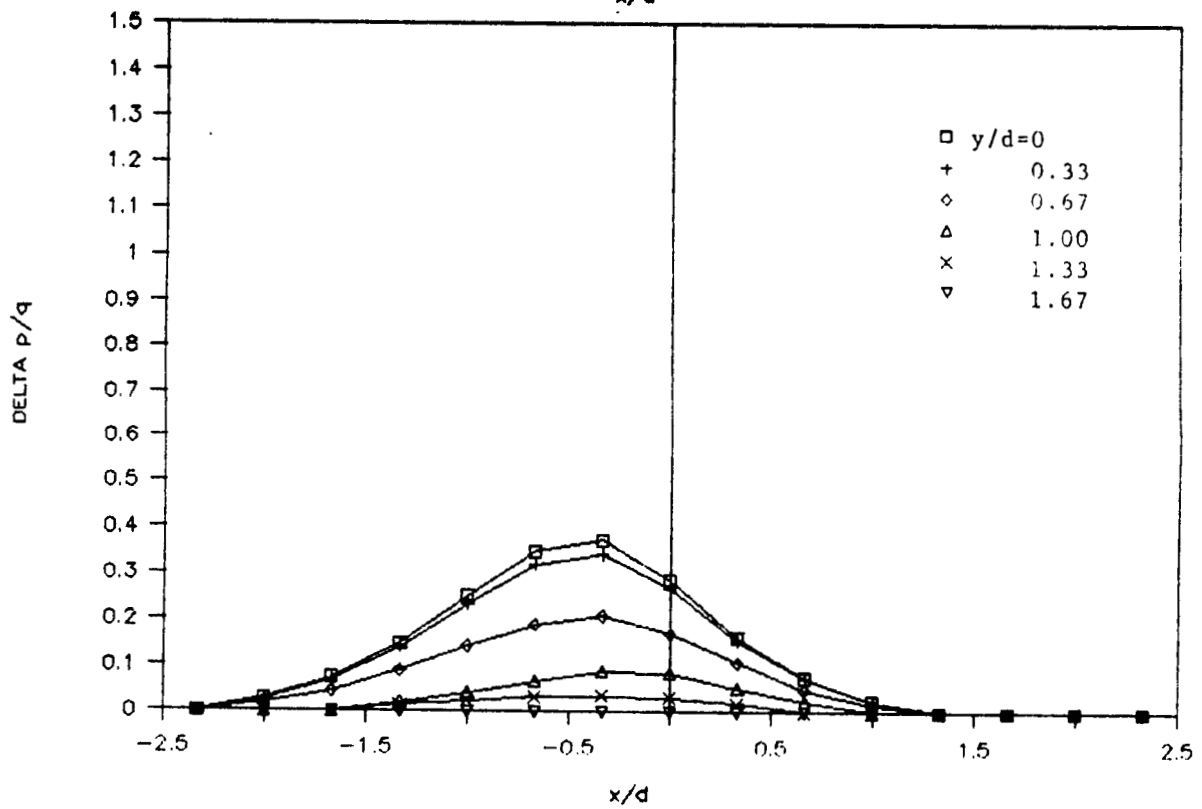
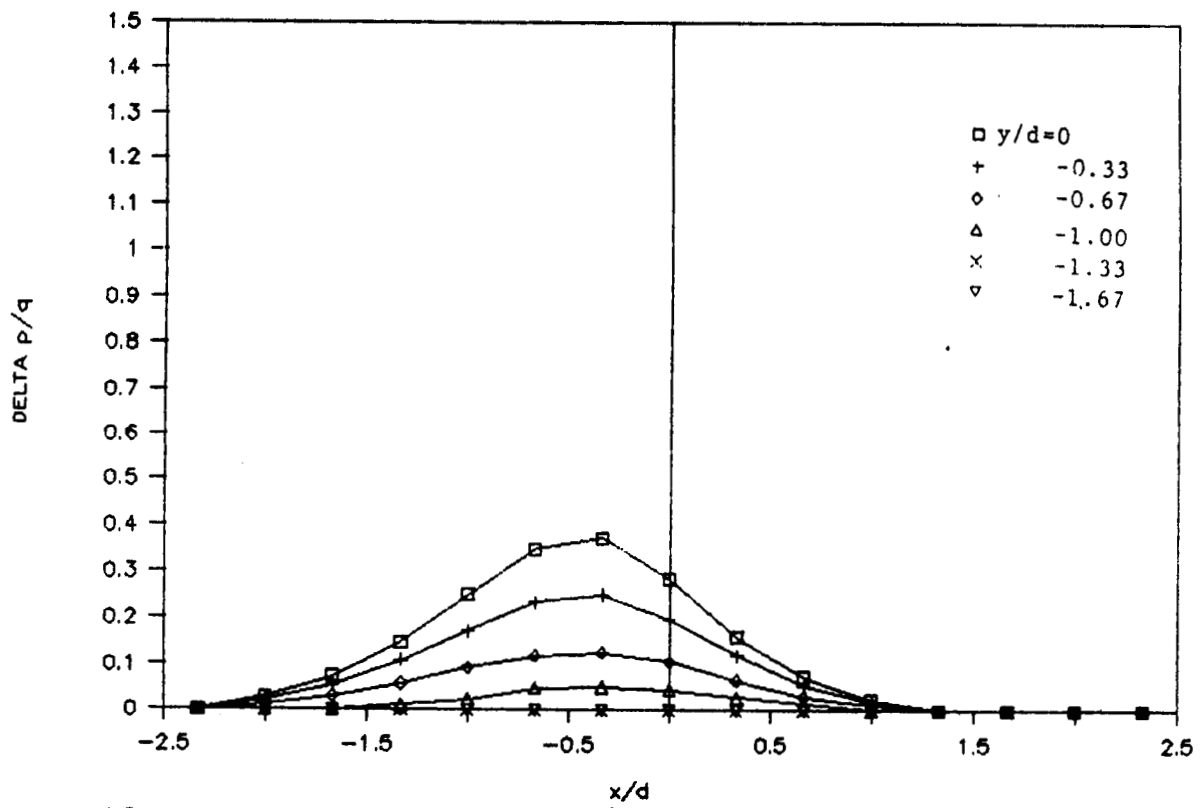


Figure C12; Nozzle Exit Pressure Survey, 0.6", $h/d=10.0$
 $Q_{jet}=1337$

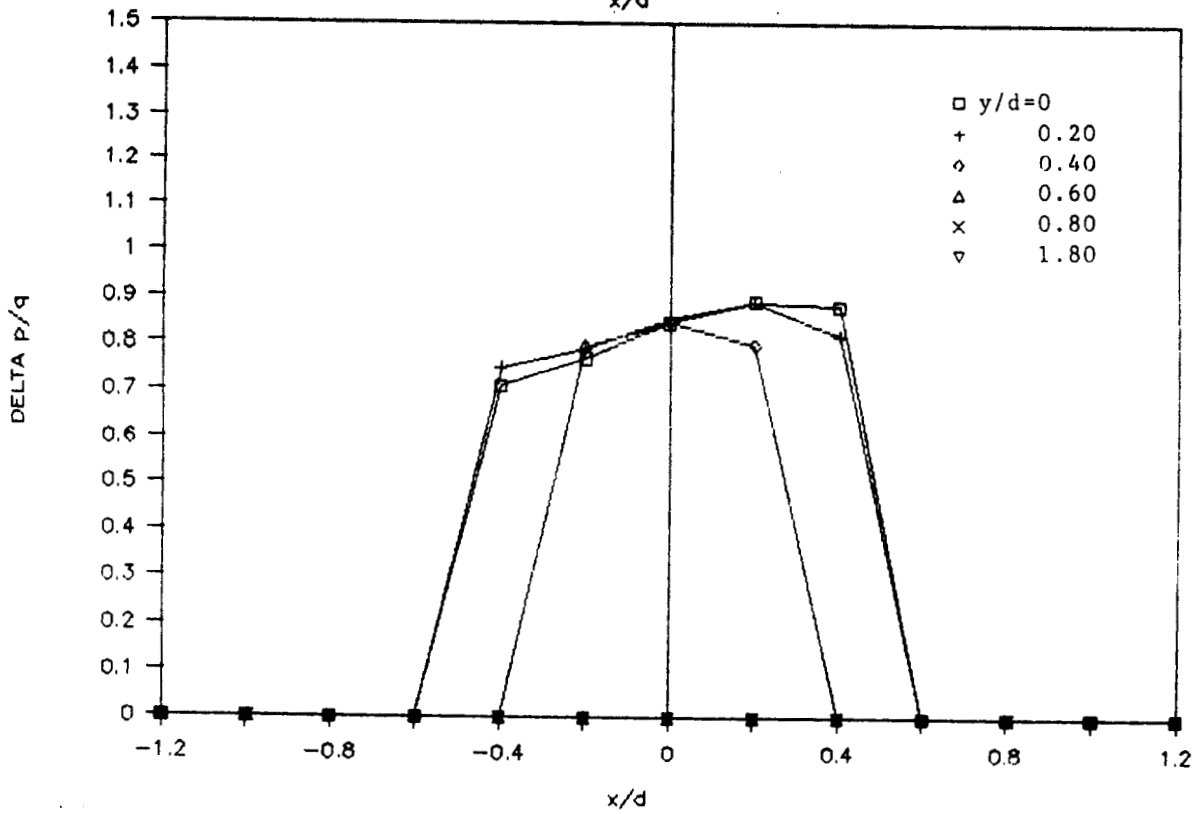
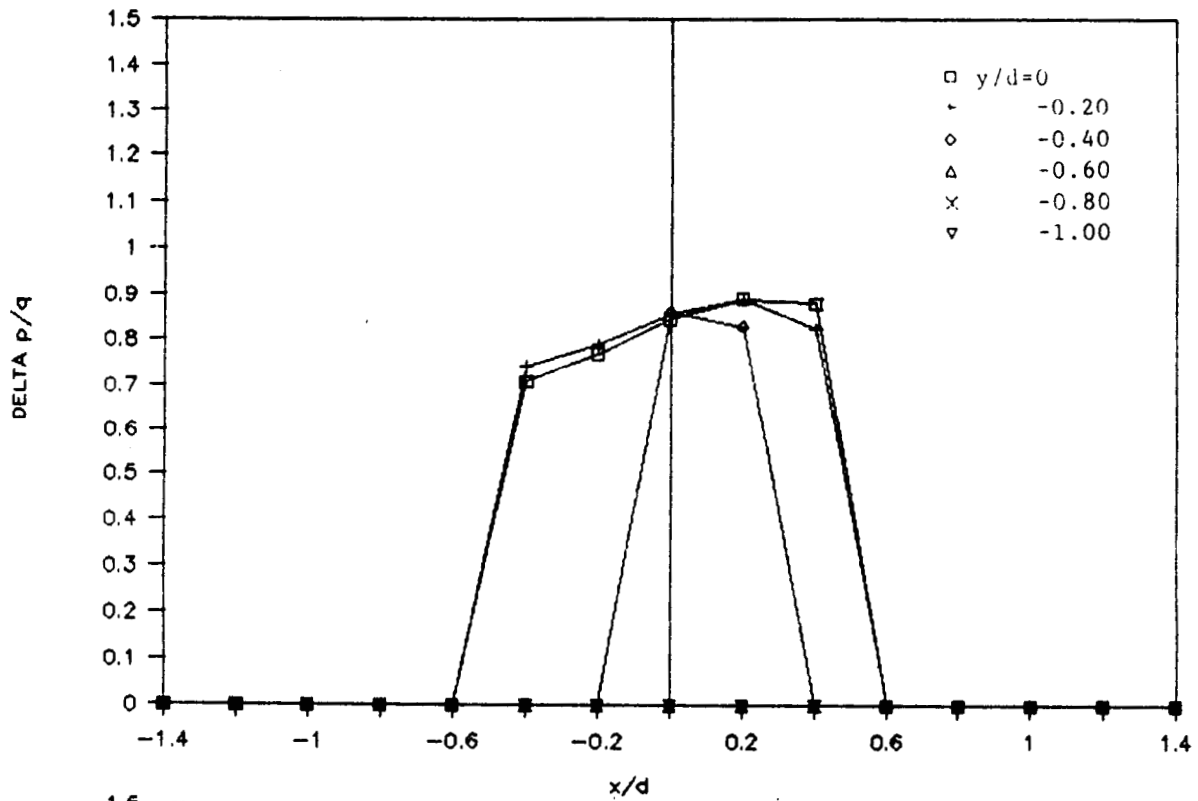


Figure C13; Nozzle Exit Pressure Survey, 1.0", h/d=0.2
 Q jet=85

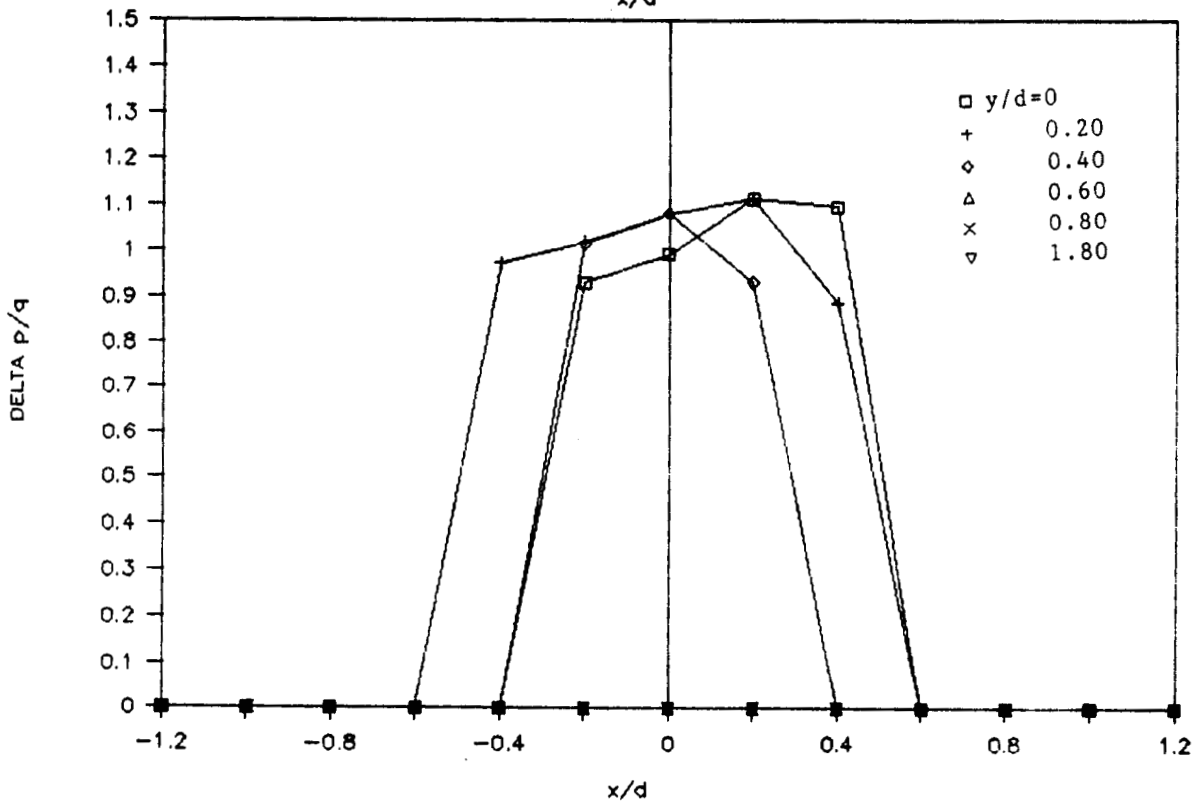
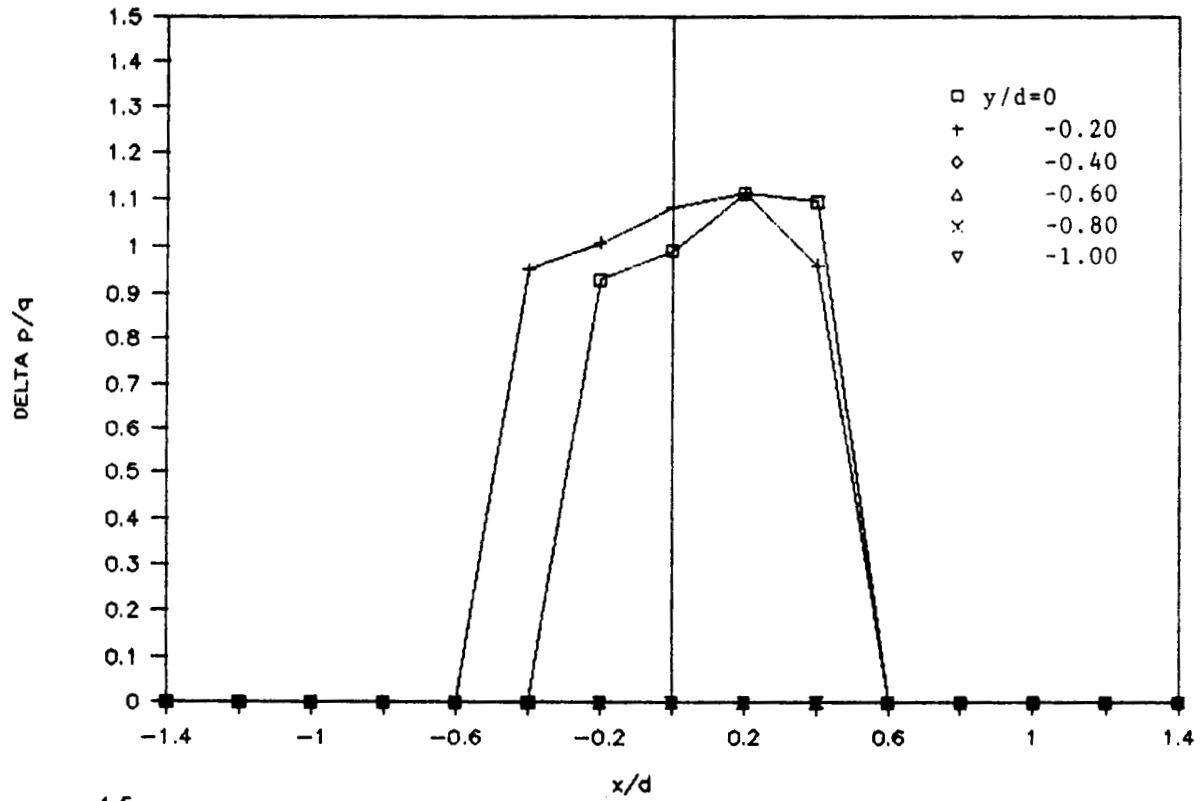


Figure C14; Nozzle Exit Pressure Survey, 1.0", $h/d=0.2$
 $Q_{jet}=265$

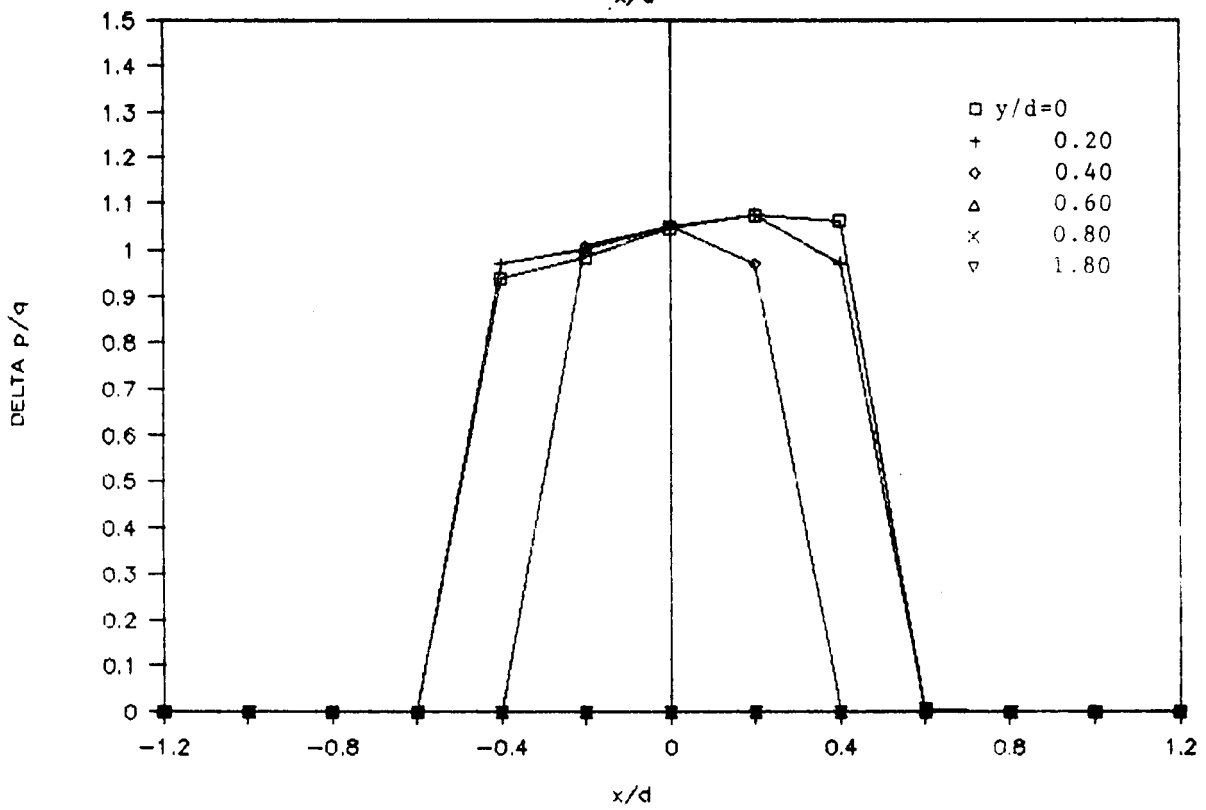
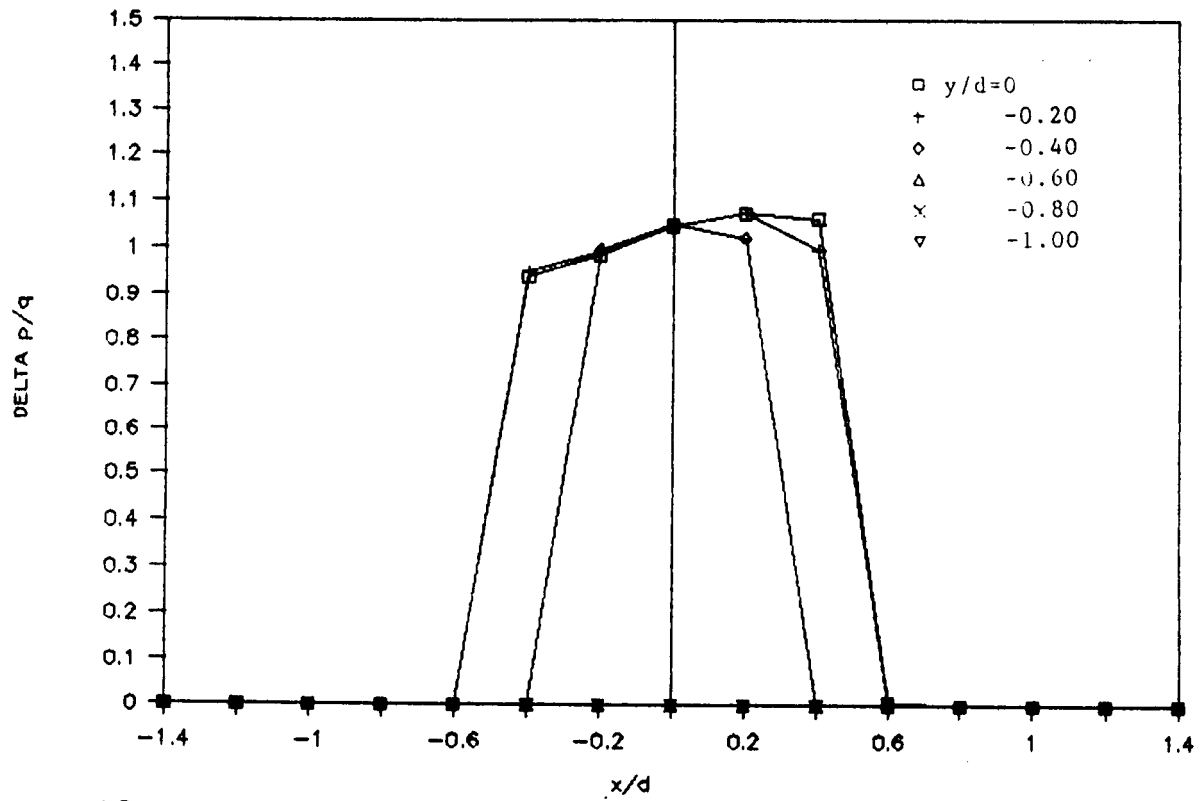


Figure C15; Nozzle Exit Pressure Survey, 1.0", $h/d=0.2$
 $Q_{jet}=935$

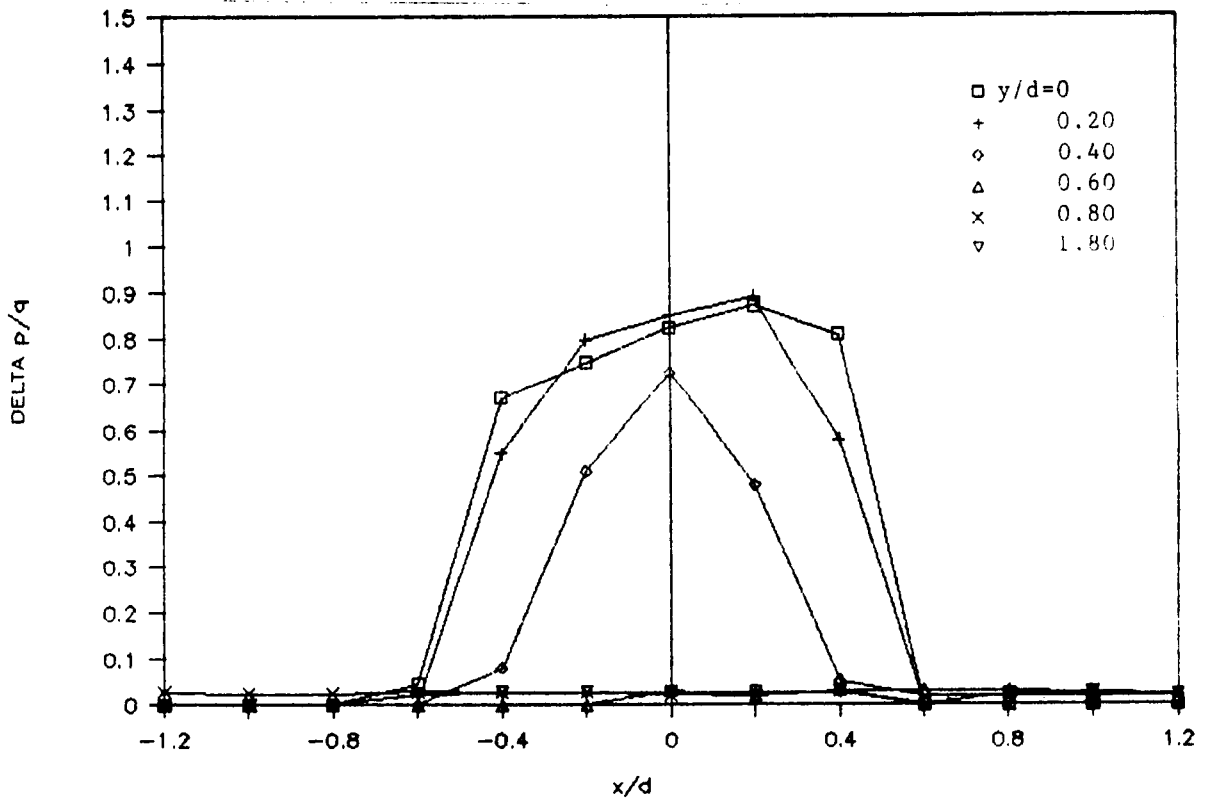
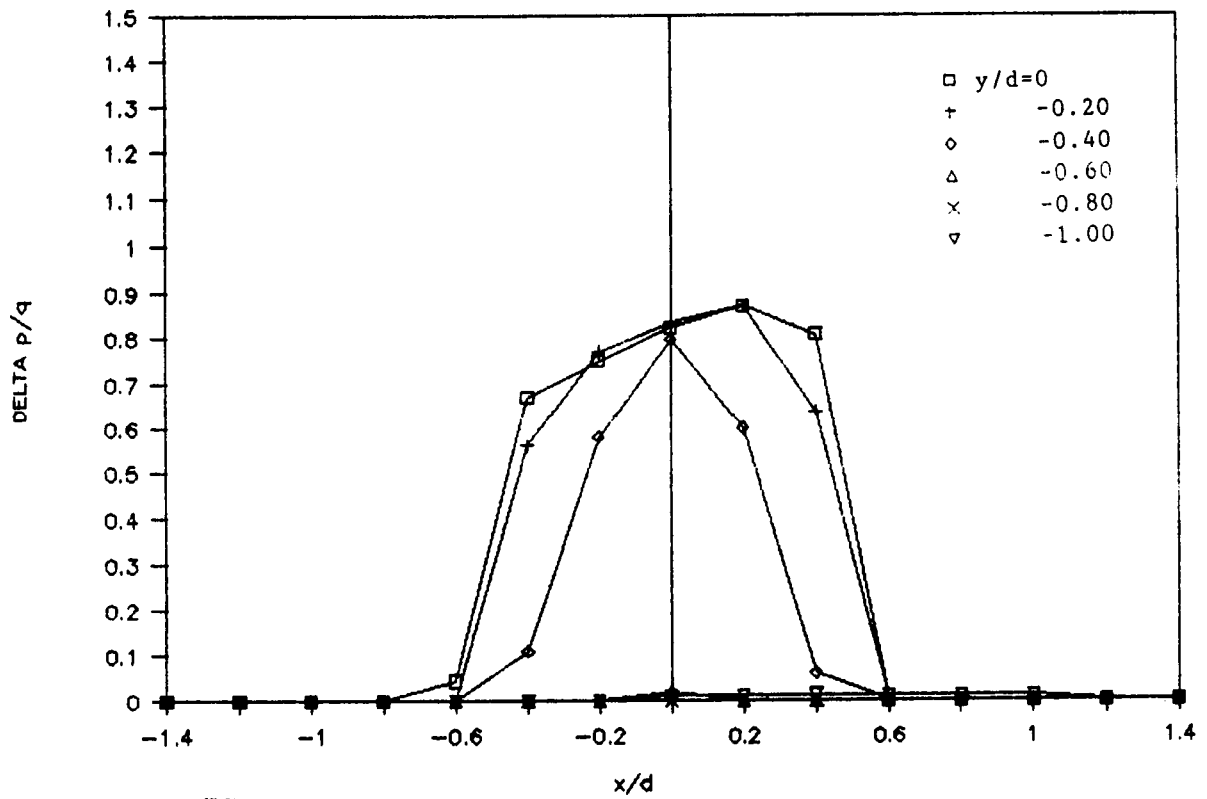


Figure C16; Nozzle Exit Pressure Survey, 1.0", $h/d=1.0$
 $Q_{jet}=85$

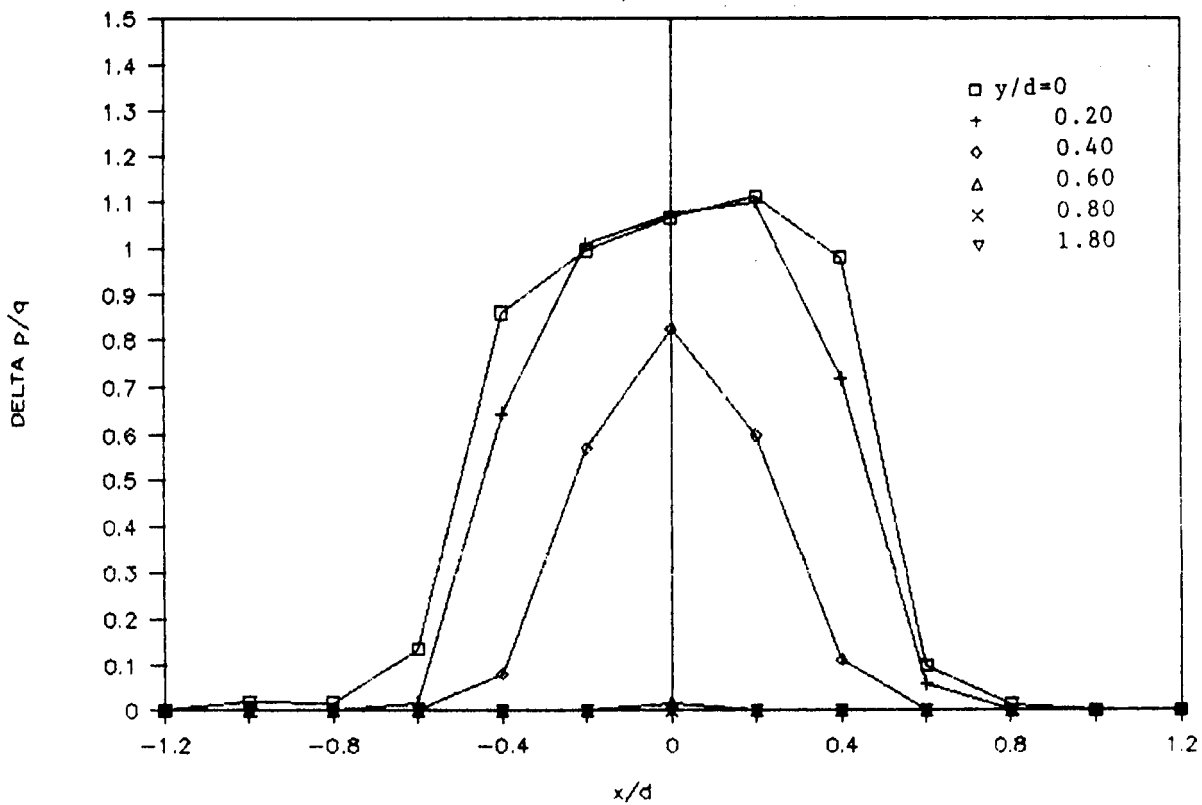
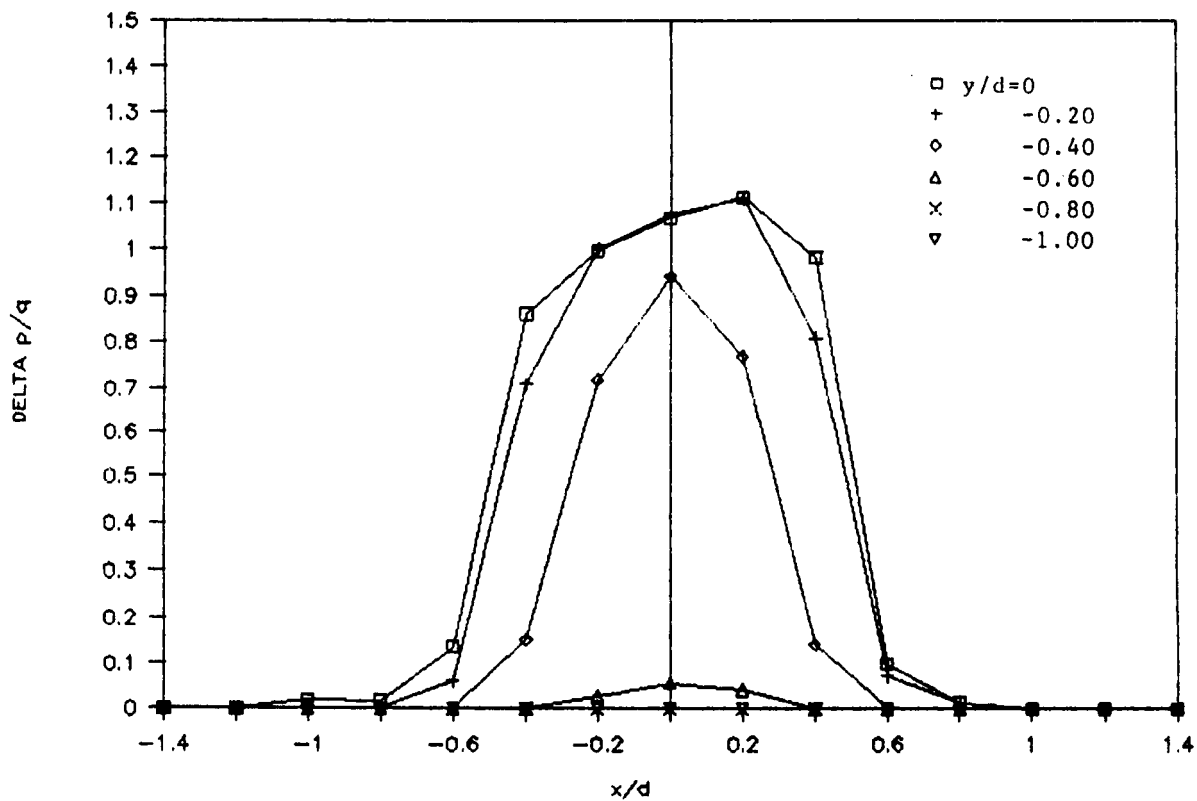


Figure C17; Nozzle Exit Pressure Survey, 1.0", h/d=1.0
jet=265

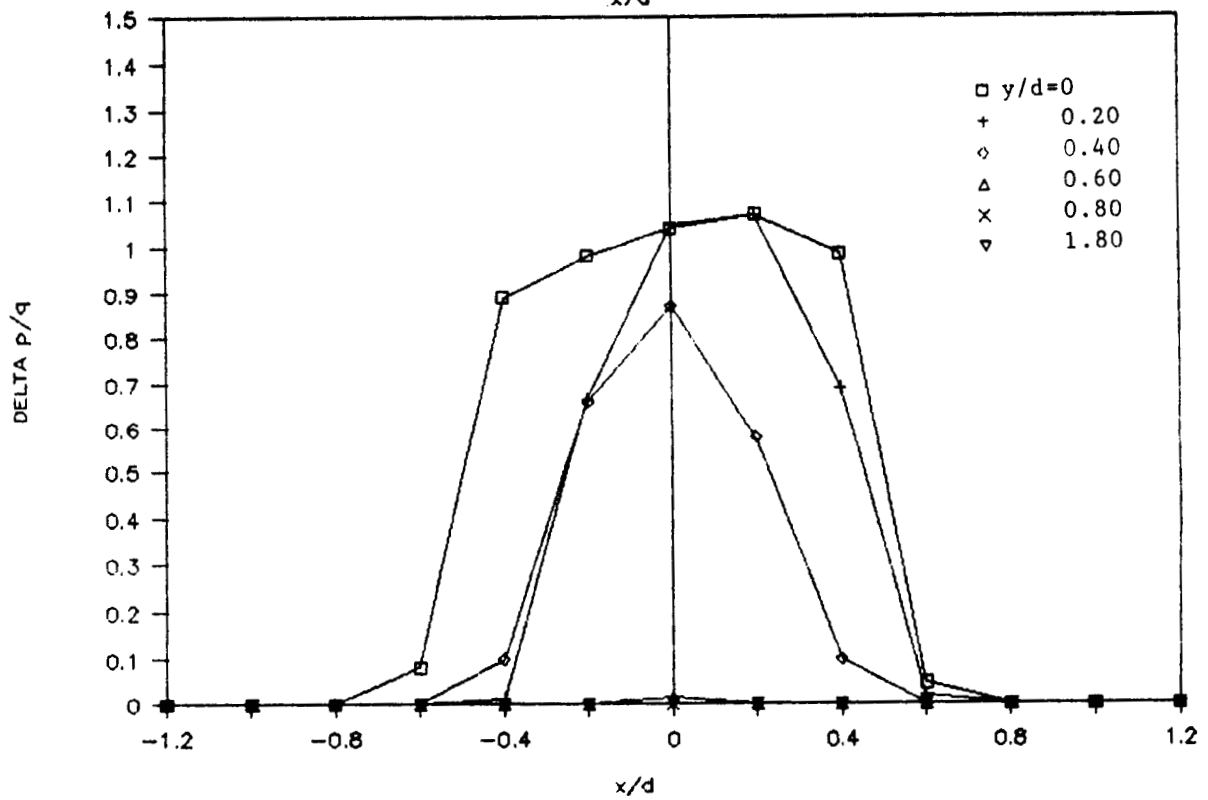
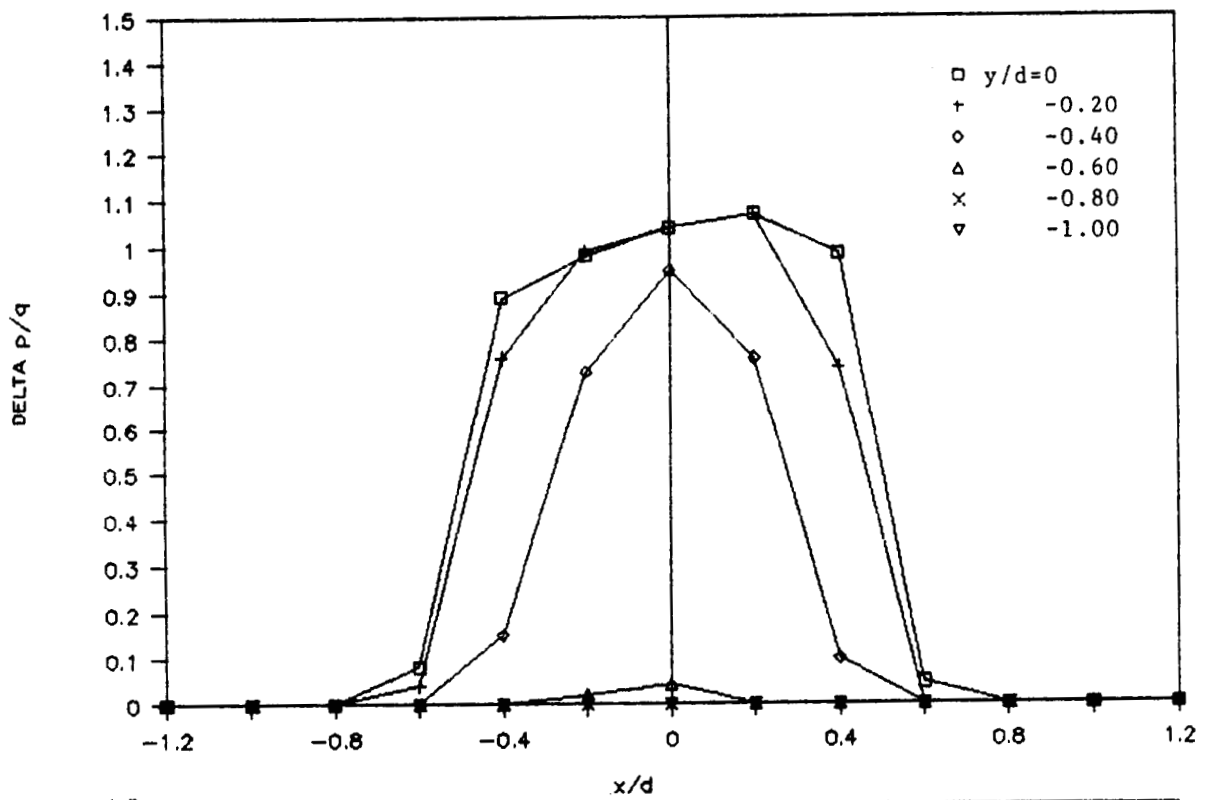


Figure C18; Nozzle Exit Pressure Survey, 1.0", h/d=1.0
Q jet=935

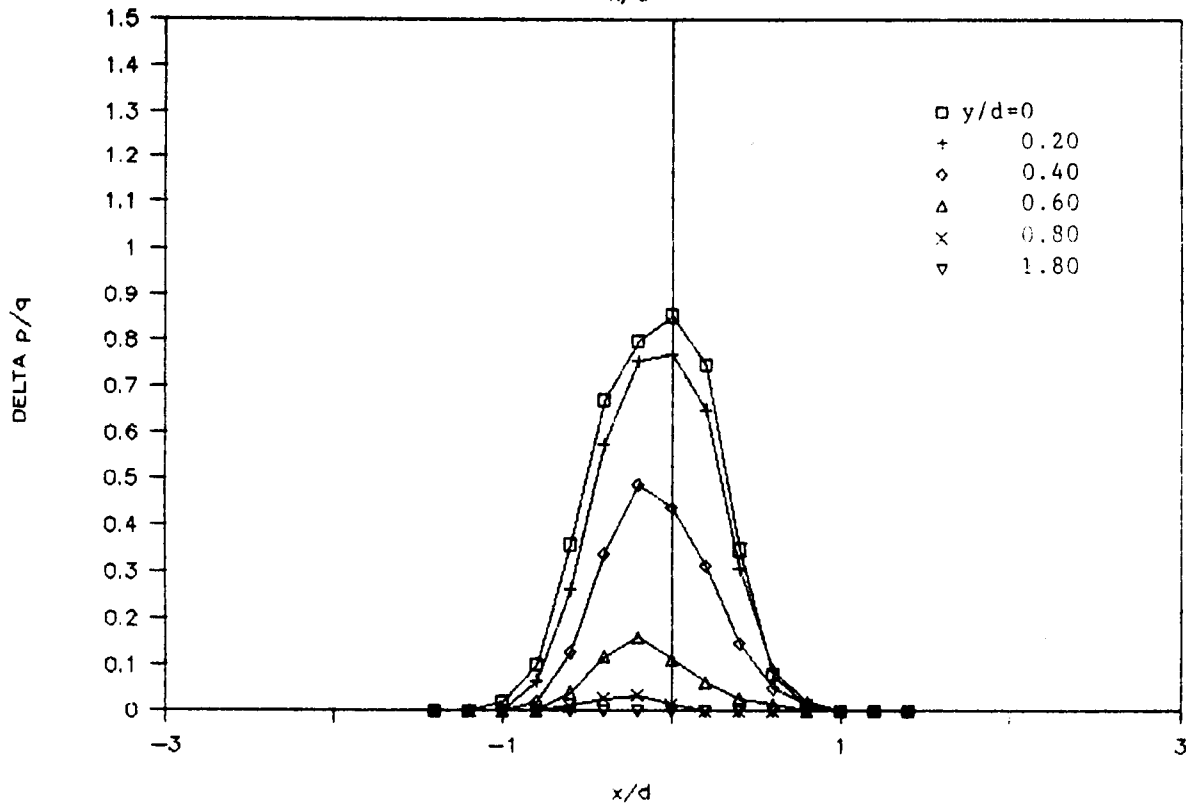
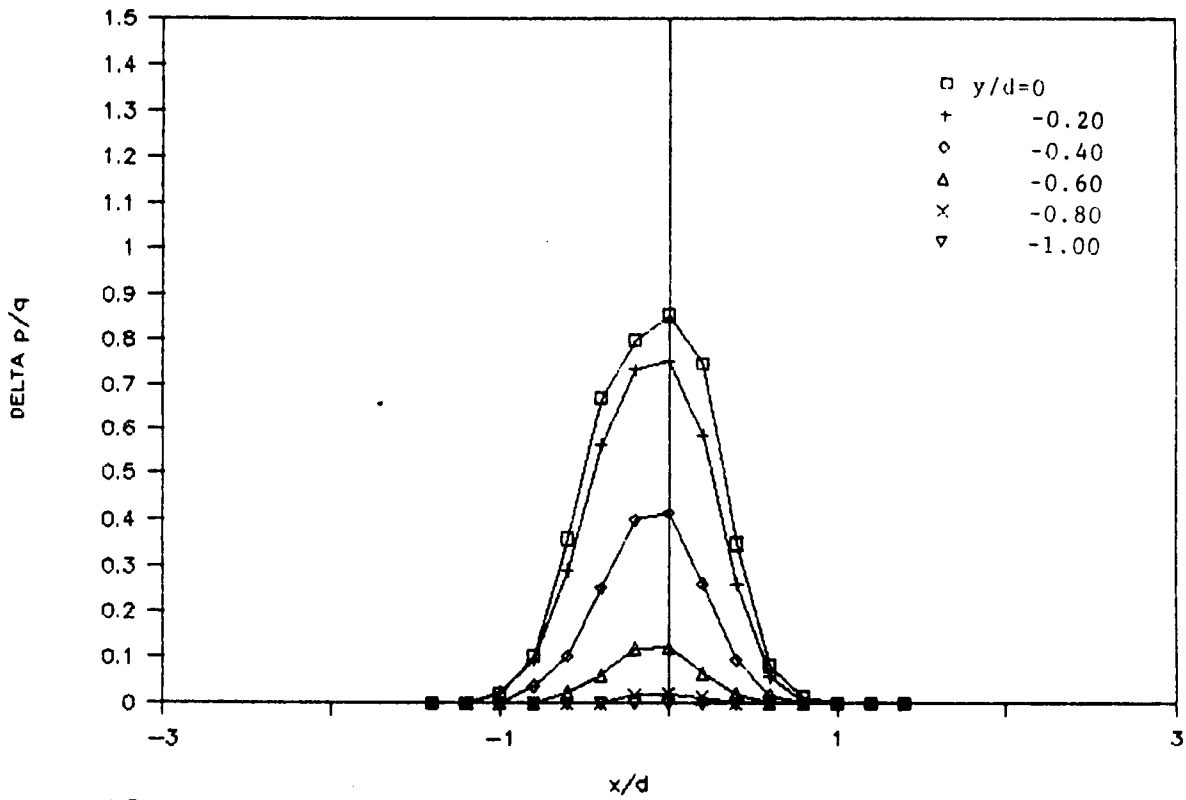


Figure C19; Nozzle Exit Pressure Survey, 1.0, h/d=3.0
Q jet=85

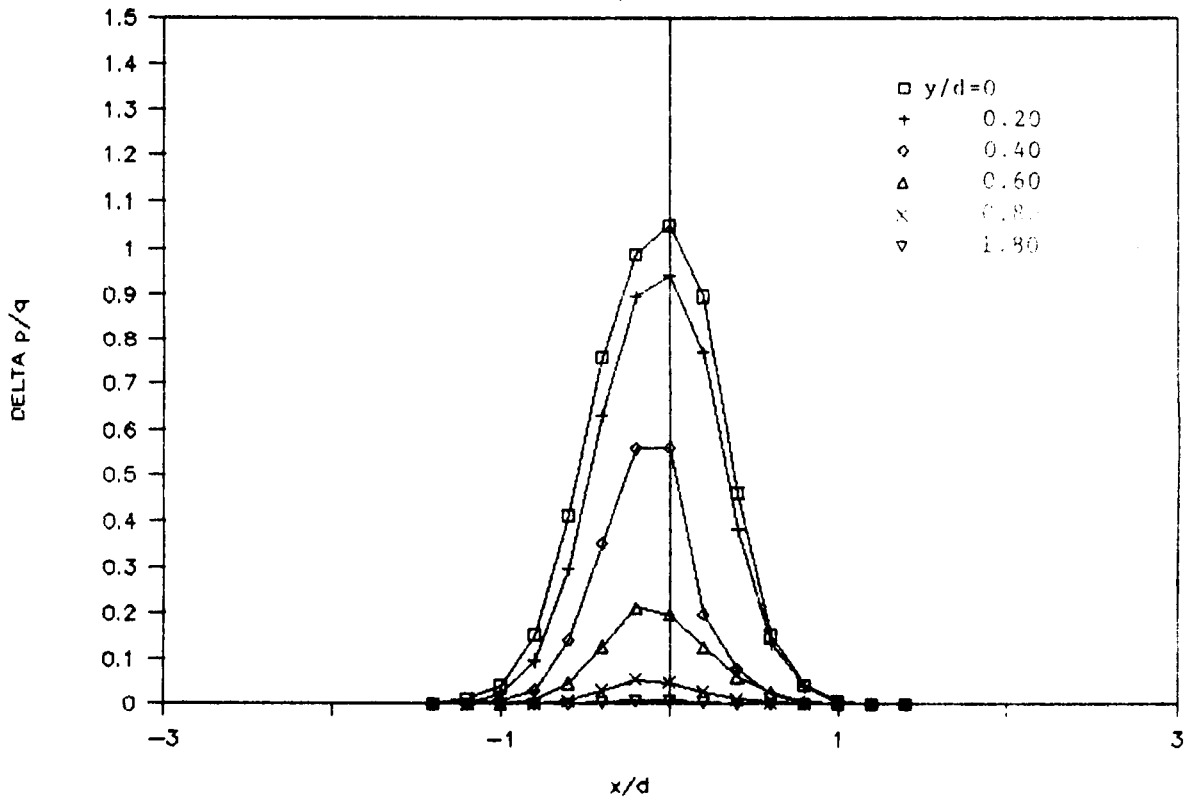
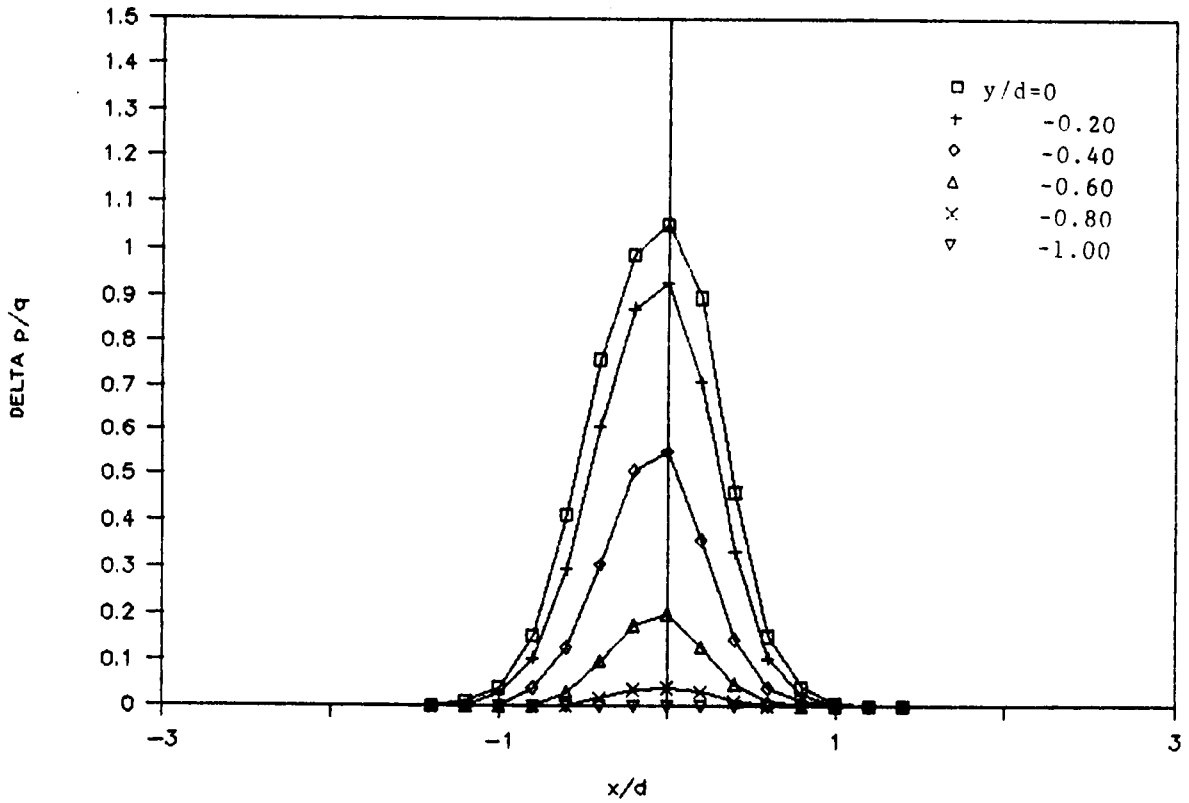


Figure C20; Nozzle Exit Pressure Survey, 1.0, h/d=3.0
Q jet=265

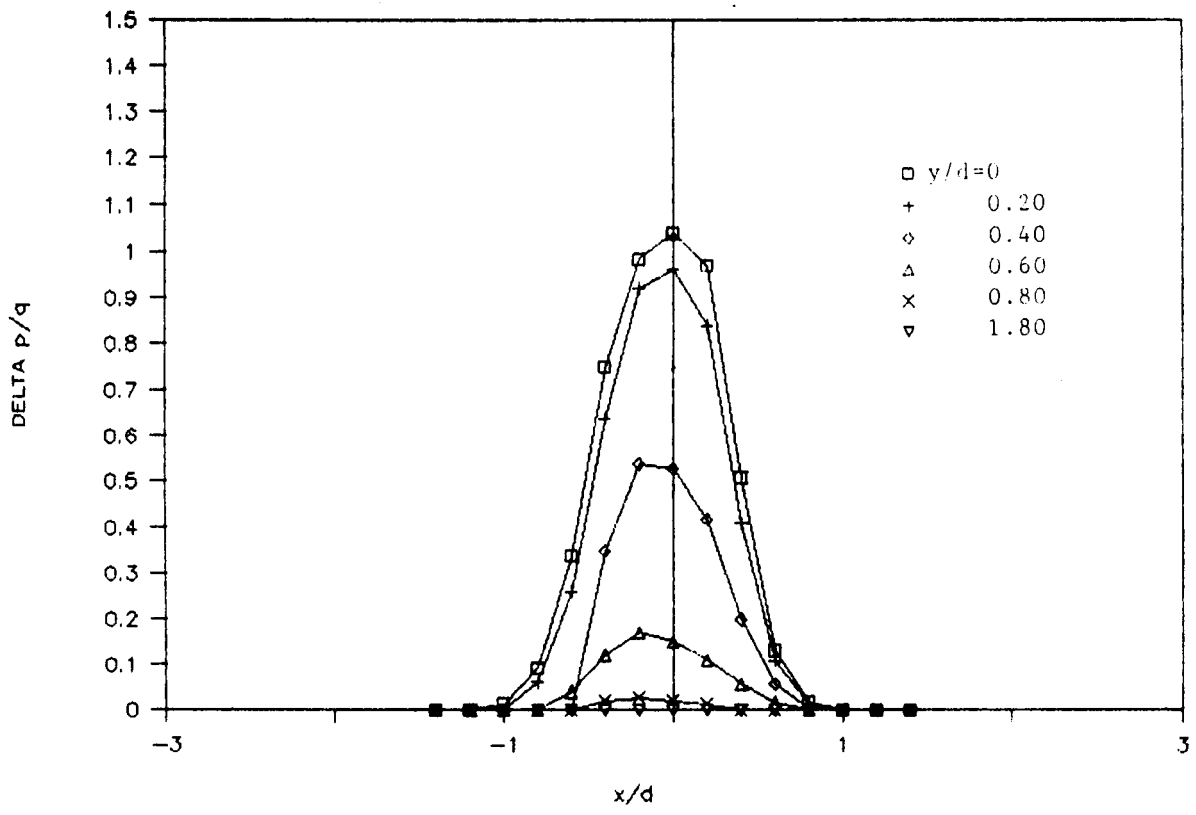
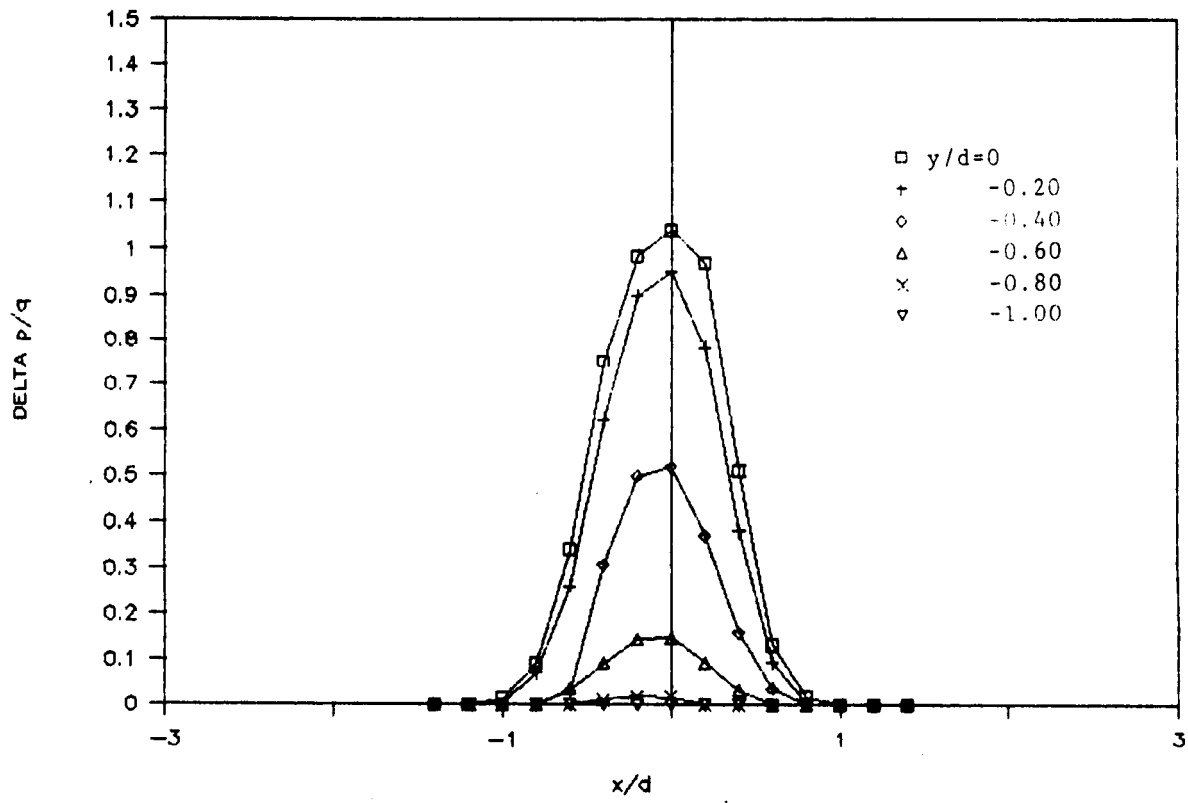


Figure C21; Nozzle Exit Pressure Survey, 1.0, h/d=3.0
Q jet=935

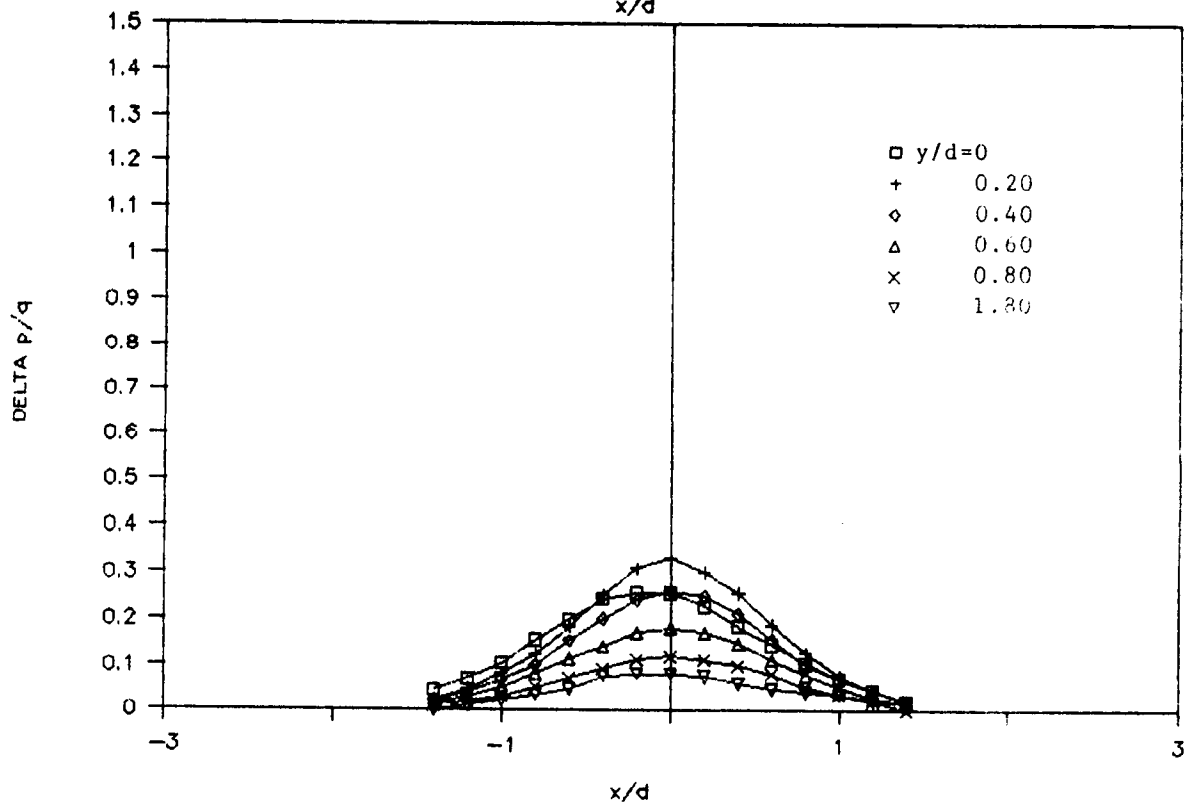
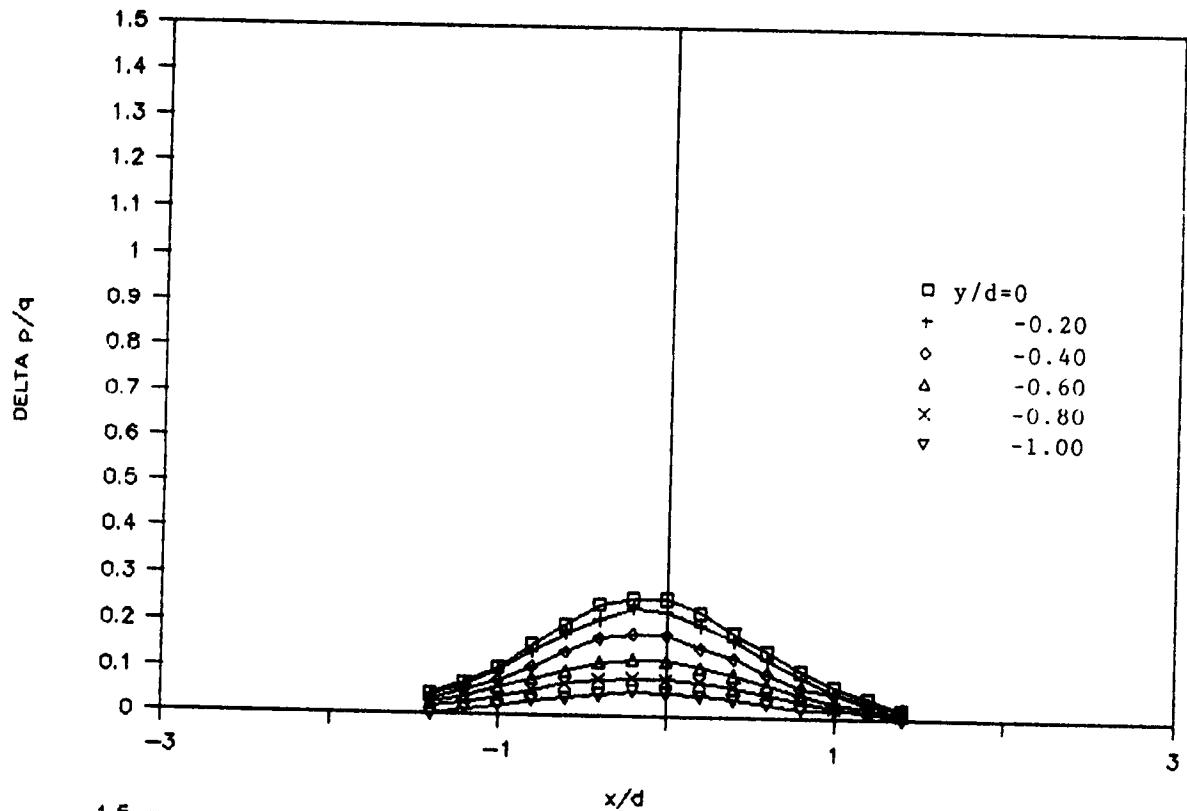


Figure C22; Nozzle Exit Pressure Survey, 1.0", h/d=10.0
Q jet=85

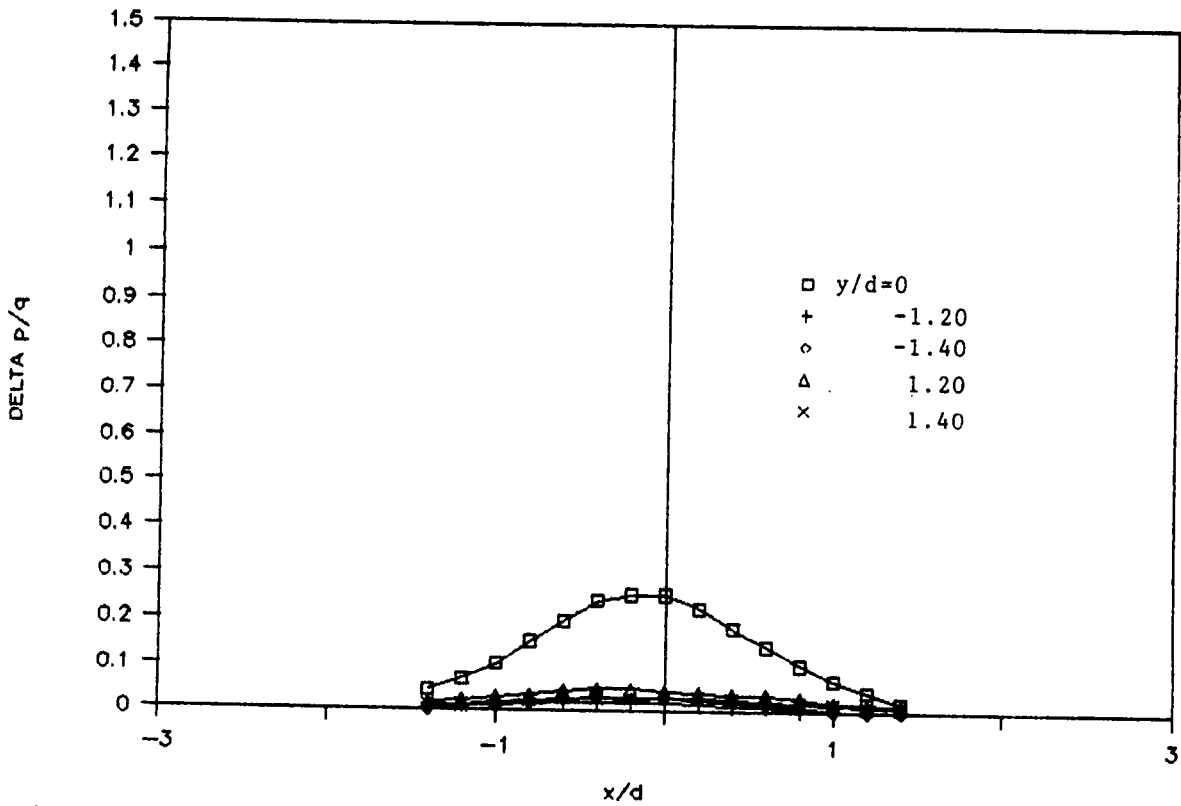


Figure C22; Nozzle Exit Pressure Survey, 1.0", $h/d=10.0$
 $Q_{jet}=85$ (Cont.)

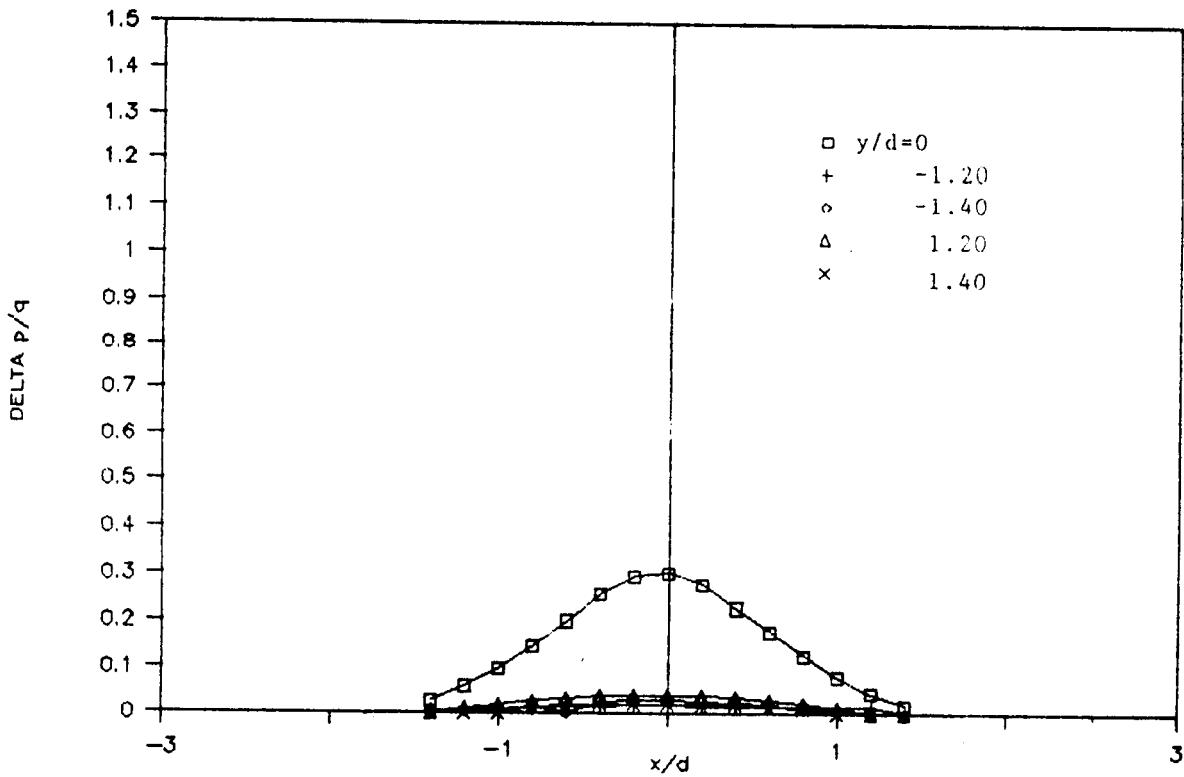


Figure C23; Nozzle Exit Pressure Survey, 1.0", $h/d=10.0$
 $Q_{jet}=265$

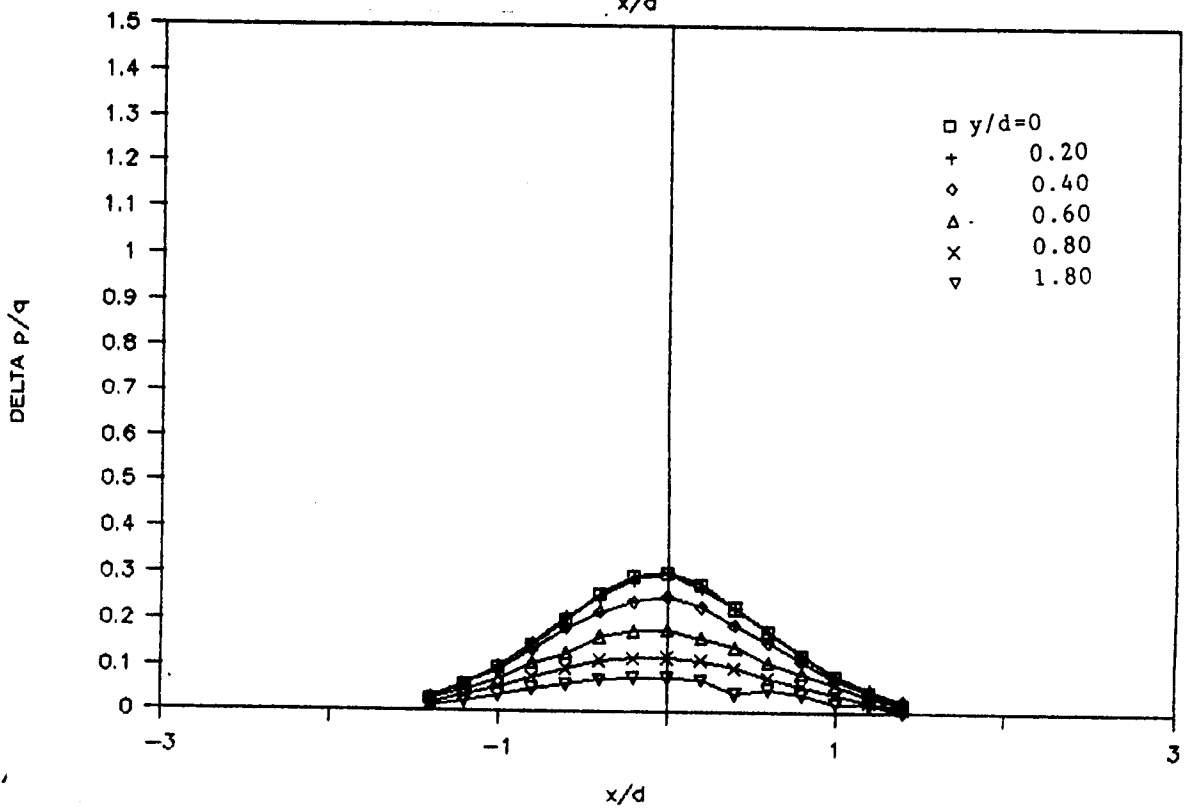
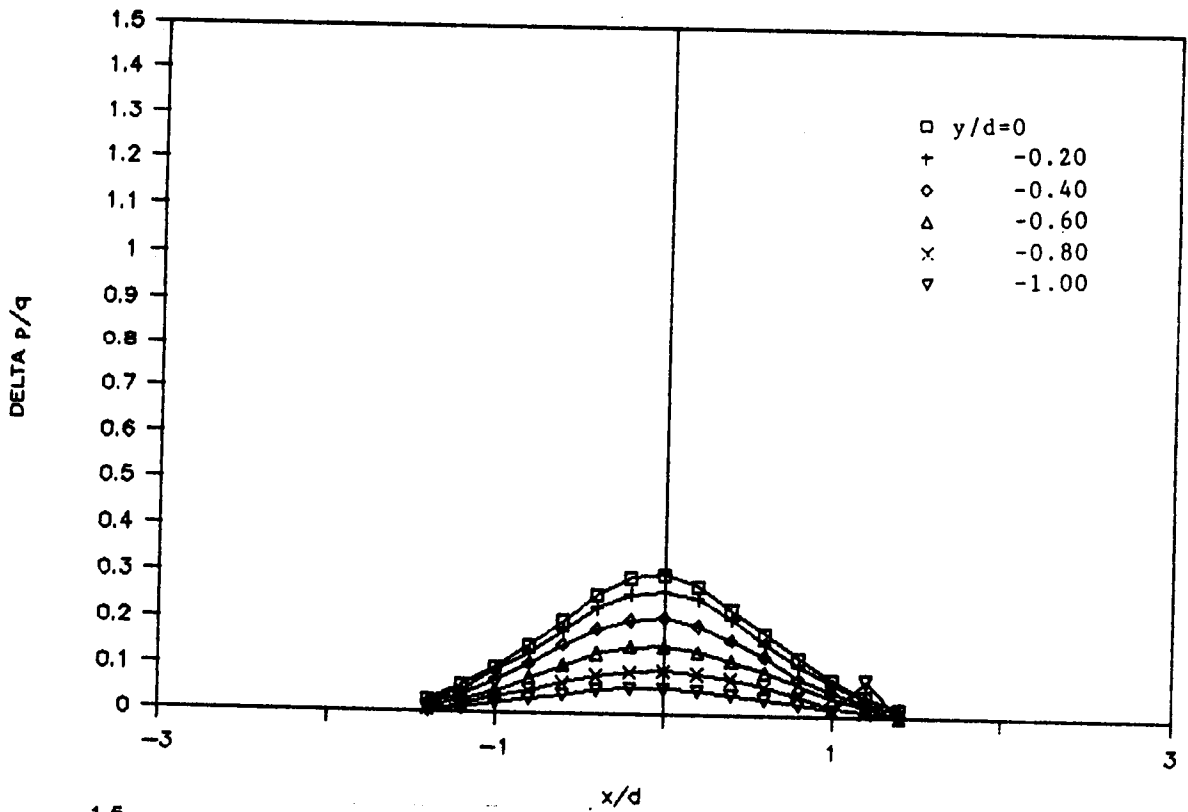


Figure C23; Nozzle Exit Pressure Survey, 1.0", h/d=10.0
Q jet=265 (Cont.)

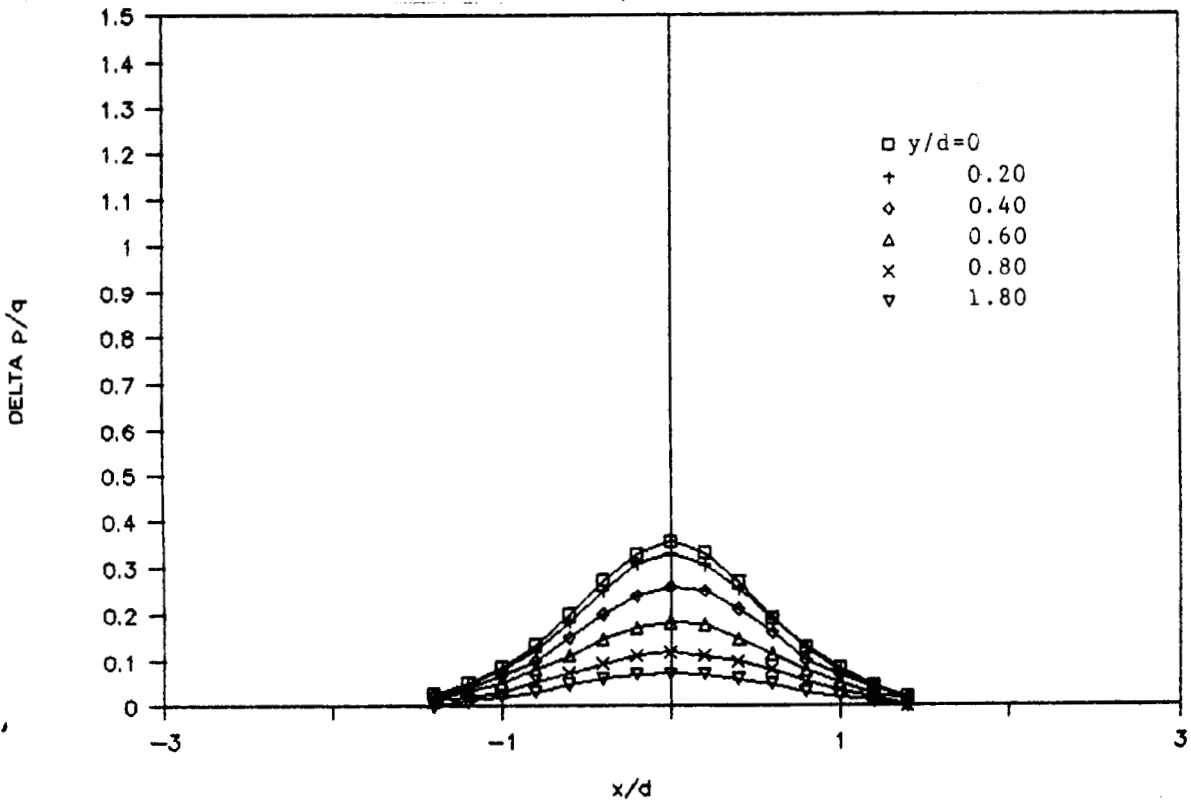
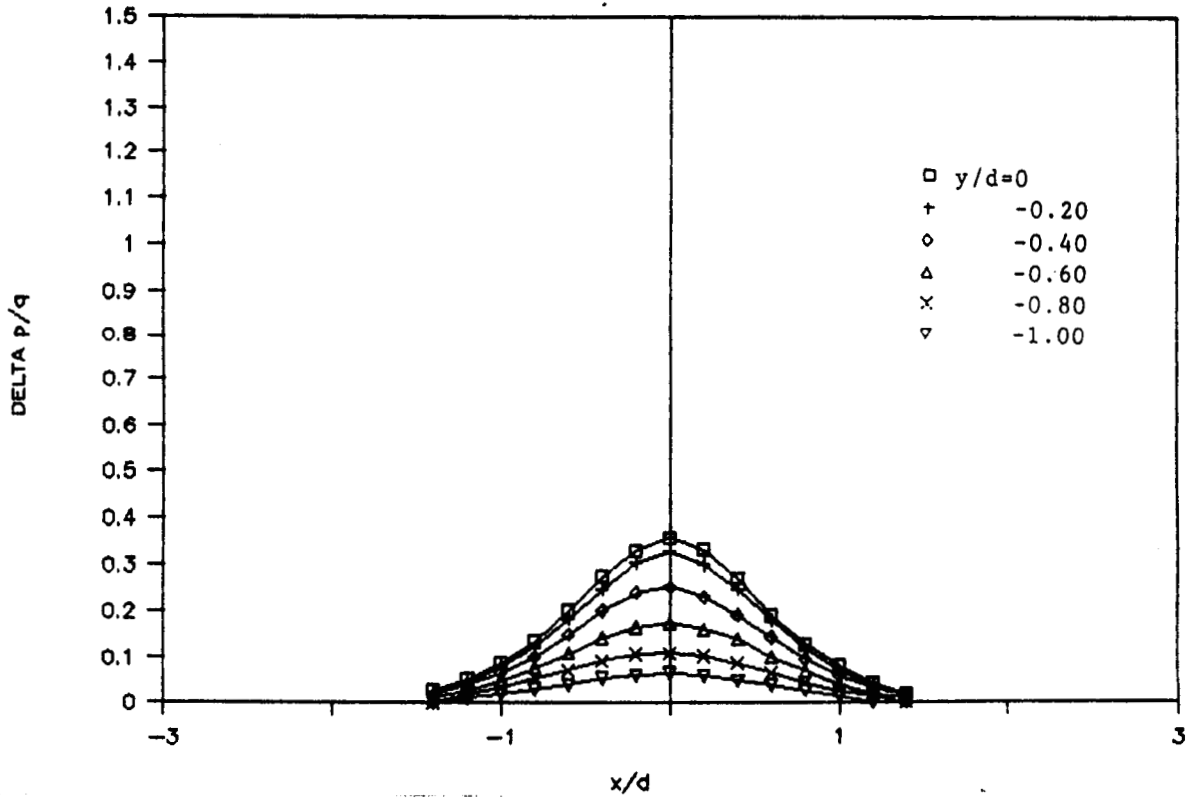


Figure C24; Nozzle Exit Pressure Survey, 1.0", h/d=10.0
Q jet=935

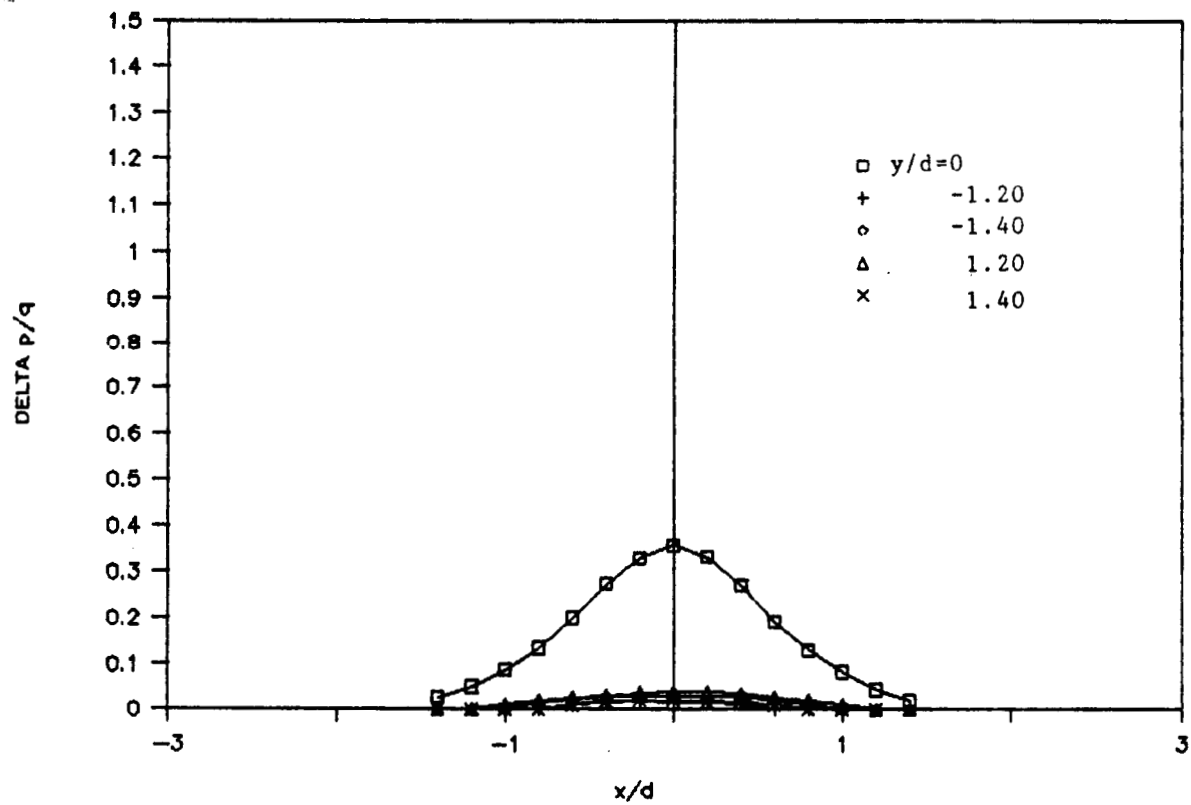


Figure C24; Nozzle Exit Pressure Survey, 1.0", $h/d=10.0$
 $Q_{jet}=935$ (Cont.)



Report Documentation Page

1. Report No. NASA CR-181841	2. Government Accession No.	3. Recipient's Catalog No.	
4. Title and Subtitle An Experimental Investigation of the Ground Vortex Created by a Moving Jet		5. Report Date July 1989	
		6. Performing Organization Code	
7. Author(s) V. R. Stewart		8. Performing Organization Report No. VS 1-88	
		10. Work Unit No. 505-61-71-02	
9. Performing Organization Name and Address V. R. Stewart, Consultant 5689 Plum Orchard Drive Columbus, OH 43213		11. Contract or Grant No. L-29341C	
		13. Type of Report and Period Covered Contractor Report	
12. Sponsoring Agency Name and Address National Aeronautics and Space Administration Langley Research Center Hampton, VA 23665-5225		14. Sponsoring Agency Code	
		15. Supplementary Notes Langley Technical Monitor: G. T. Kemmerly	
16. Abstract An experimental investigation of a 1 inch circular jet moving over a fixed ground board has been conducted in the NASA Langley Research Center Vortex Research Center. The jet passing over the ground board at a height of three nozzle diameters creates a ground vortex which was measured by a pattern of Endevco high response pressure transducers. The results are compared to existing data to determine the effect of the ground boundary eliminated by the moving jet. The penetration of the vortex both forward of and latterly to the impact point of the jet on the ground. The resulting ground vortex penetration forward of the impact point is reduced by approximately 30 percent and the lateral penetration is reduced by 50 percent over that experienced from a stationary jet over a stationary ground board with a free stream velocity.			
17. Key Words (Suggested by Author(s)) Ground Effect Ground Vortex Moving Jet Dynamic Variations of Pressure		18. Distribution Statement Unclassified--Unlimited Subject Category 02	
19. Security Classif. (of this report) Unclassified	20. Security Classif. (of this page) Unclassified	21. No. of pages 128	22. Price A07